Natural Fiber Densification for Sustainable Composite Manufacturing

by

Gulzeb Khan Khakwani

A thesis

presented to the University of Waterloo

in fulfillment of the

thesis requirement for the degree of

Master of Applied Science

in

Chemical Engineering

Waterloo, Ontario, Canada, 2023

© Gulzeb Khan Khakwani 2023

AUTHOR'S DECLARATION

I hereby declare that I am the sole author of this thesis. This is a true copy of the thesis, including any required final revisions, as accepted by my examiners.

I understand that my thesis may be made electronically available to the public.

ABSTRACT

The need for inexpensive, sustainable, and environmentally friendly materials has significantly increased in recent years as a result of rising environmental awareness. Given the widespread usage of petrochemical plastics, which are frequently reinforced with synthetic fibers to improve their functionality, there is a noteworthy potential for natural fibers to be employed as a feasible substitute in reinforcement applications. When incorporated into a thermoplastic matrix, natural fibers present a structural material that possesses not only strength and other mechanical properties but also demonstrates environmental friendliness due to its renewability. Within the wide range of natural fibers, industrial hemp fiber distinguishes itself as a highly robust and rigid alternative. Hemp fibers provide composite materials with distinct characteristics that are comparable to those exhibited by conventional synthetic fiber composites.

This research focused on developing hemp fiber-reinforced polypropylene composite materials. The pelletization of hemp fibers was a crucial step in this research, which aimed to improve their ease of handling, storage, and feeding in extruders along with polypropylene pellets. The present research also extensively investigated the impact of different variables on the mechanical properties of hemp pellets and the subsequent composites. These variables included the use of different particle sizes, the use of additives to enhance fiber dispersion in composites, the application of coupling agents, the alkali treatment of hemp fibers, different composition mixes of bast and hurd fibers, and a comparative analysis of composites prepared with hemp fibers obtained from different suppliers from different countries such as USA, Canada, and Paraguay.

The research revealed a noteworthy correlation between the size of fibers and the overall performance of the composite material. The flexural modulus exhibited a steady upward trend as the size of fibers increased from 1 mm to 3 mm, whereas the tensile modulus reached its highest point with a 1.5 mm fiber size. The use of wax additives did not yield any significant impact on the mechanical properties of the composites. Moreover, by performing NaOH treatment of hemp fibers, the moisture absorbance of fibers was reduced and composites with NaOH-treated fiber demonstrated enhanced mechanical properties in comparison to composites with untreated fibers. However, composites with MAPP coupling agent exhibited better properties than NaOH-treated fiber composites. A comparison of different proportions of bast and hurd fibers in the pellets and

composites showed that an increase in bast fiber concentration correlated with an increase in mechanical properties.

These above-mentioned findings function as a guiding principle for customizing polypropylene composites reinforced with hemp fiber to meet specific performance requirements. Lastly, a comparison between glass fiber and hemp fiber reinforced polypropylene composite was made and it was found that composites reinforced with 20% hemp fiber exhibited superior flexural and tensile properties than 10% glass fiber reinforced composites.

ACKNOWLEDGEMENTS

First and foremost, I want to express my sincere gratitude to the Almighty, Allah, the Most High, for granting me strength, perseverance, and guidance throughout my academic journey.

I express profound gratitude towards my committed and encouraging supervisor, Professor Dr. Leonardo Simon, for his invaluable mentorship and guidance. His profound knowledge and extensive experience have played a crucial role in shaping the course of this research.

I would also like to express my sincere appreciation to Douglas Casetta and Dr. Franciele Turbiani for their invaluable support and unwavering motivation throughout this research.

In addition, I want to express my gratitude to Professor Dr. Mario Ioannidis and Professor Dr. Ting Tsui, who agreed to read and assess my thesis.

I also want to extend my heartfelt appreciation to PhD student James Kim and research assistants, Dr. Chong Meng, and Sarah Jankhani, for their time, assistance, and profound insights.

I would like to thank my fellow lab mates Yasaman Yasoubi, and Rageswari Sen and co-op students, Aknan Ali and Ahreum Kim, for their support and precious friendship.

I would also like to express my profound appreciation to all the teachers who have played a pivotal role in my academic journey. Their unwavering commitment and ceaseless efforts have shaped my educational path, and I am genuinely grateful for their invaluable contributions.

Lastly, I would like to thank Mitacs and Tangho Green Canada for their generous funding of this project. I also want to express my gratitude to the individuals at Tangho, Marco, Edson, Nina, and David for their support.

DEDICATION

I want to dedicate this thesis to my parents, Muhammad Asif Khan Khakwani and Anjum Afshan Asif; my siblings, Shahrukh, Shahzeb, Humayun, Taimoor, and Maria; and my nephews, Zaid, Hashir, and Ali. Without their encouragement and support, I would never have reached this far. I am forever grateful to them.

TABLE OF CONTENTS

AUTHOR'S DECLARATION ..... *ii*
ABSTRACT ..... *iii*
ACKNOWLEDGEMENTS ..... *v*
DEDICATION ..... *vi*
LIST OF FIGURES ..... *x*
LIST OF TABLES ..... *xvi*
LIST OF ABBREVIATIONS ..... *xviii*
CHAPTER 1: INTRODUCTION *1*
1.1 Background and Motivation: **1**
1.2 Research Objectives: **4**
1.3 Project Outline: **4**
CHAPTER 2: LITERATURE REVIEW *6*
2.1 Composites: **6**
2.1.1 Composites in nature: 7
2.1.2 Man-Made Composites: 9
2.2 Polypropylene **15**
2.3 Processing Techniques of Polypropylene **16**
2.3.1 Extrusion 16
2.3.2 Injection Molding 18
2.4 Thermoplastics in automotive application **19**
2.5 Glass Fiber Reinforced Thermoplastic Composites **21**
2.6 Natural Fiber-Reinforced Thermoplastic Composites **23**
2.6.1 Chemical Treatments 24
2.6.2 Coupling Agent 27
2.7 Industrial Hemp **28**
2.8 Particle Size Enlargement **32**
2.8.1 Overview 32
2.8.2 Mechanisms of Size Enlargement 34
2.8.2.1 Binding Mechanisms 34
2.8.2.2 Compaction Mechanism 35
2.8.3 Extrusion Presses 37
2.8.3.1 Roll-type extrusion presses (Pellet mill): 37
2.8.4 Characterization of Pellets 39
2.8.4.1 Compressive Resistance 39
2.8.4.2 Durability 39
2.8.5 Factors Affecting Pellet Quality 41
2.8.5.1 Effect of Moisture Content of Feed on Strength of Pellets 41
2.8.5.2 Effect of Particle Size of Feed 42
2.8.5.3 Effect of Additives or Binders 43
2.8.5.4: Effect of Temperature 45

CHAPTER 3: MATERIALS AND METHODS *46*
3.1 MATERIALS **46**
3.1.1 Hemp Fibers 46
3.1.2 Surfactant 46
3.1.3 Polypropylene 47
3.1.4 Compatibilizer 47
3.1.5 Chemical Treatment 47
3.2 METHODS **47**
3.2.1 Processing Methods 47
3.2.1.1 Size Reduction Equipment (Knife Mill): 47
3.2.1.2 Size Enlargement Process (Pelletization): 49
3.2.1.3 Melt Compounding via Twin Screw Extruder 50
3.2.1.4 Injection Molding 51
3.2.2 Characterization 52
3.2.2.1 Size Analysis Equipment 52
3.2.2.2 Scanning Electron Microscope 53
3.2.2.3 Moisture Content 54
3.2.3 Pellet Mechanical Properties 54
3.2.3.1 Pellet Durability Index (PDI): 54
3.2.3.2 Specific Compression Strength 55
3.2.3.3 Pellets Bulk Density 56
3.2.4 Composite Mechanical Properties 56
3.2.4.1 Flexural Properties 56
3.2.4.2 Tensile Properties 57
3.2.4.3 Impact Strength 58
3.2.4.4 Melt Flow Index (MFI): 58
3.2.4.5 Composite Specific Density 58
CHAPTER 4: HEMP PELLETIZATION *60*
RESULTS AND DISCUSSION *60*
4.1 INTRODUCTION: **60**
4.2 CHARACTERIZATION OF HEMP FIBERS **62**
4.2.1 Particle size analysis 63
4.3 HEMP PELLETS WITH DIFFERENT FIBER SIZE AND WITH OR WITHOUT WAX. **67**
4.3.1 Specific compressive strength 69
4.3.2 Pellet Bulk Density 70
4.3.3 Pellet Durability Index (PDI): 72
4.4 HEMP HURD PELLETS **73**
4.4.1 Specific Compressive Strength 75
4.4.2 Pellet Bulk Density 76
4.4.3 Pellet Durability Index (PDI): 77
4.5 HEMP PELLETS WITH DIFFERENT COMPOSITIONS OF HEMP BAST AND HURD FIBERS **80**
4.5.1 Specific Compressive Strength 81
4.5.2 Pellet Bulk Density 82
4.5.3 Pellet Durability Index 84
4.6 PELLETIZING OF WHOLE HEMP FIBERS TREATED WITH NAOH **87**
4.7 CHANGE IN FIBER SIZE AFTER PELLETIZATION **92**
CHAPTER 5: COMPOSITES *98*

RESULTS AND DISCUSSION *98*
5.1 INTRODUCTION: **98**
5.2: EFFECT OF CHEMICALLY TREATED FIBER AND COUPLING AGENT ON MECHANICAL PROPERTIES OF COMPOSITES **99**
5.2.1 Flexural Properties 100
5.2.2 Tensile Properties 101
5.2.3 Impact Strength 103
5.2.4 Melt Flow Index 104
5.2.5 Specific Flexural Modulus (SFM): 105
5.2.6 Scanning Electron Microscopy (SEM): 106
5.3: EFFECT OF FIBER LENGTH AND USE OF WAX ON MECHANICAL PROPERTIES OF COMPOSITES **110**
5.3.1 Flexural Properties 112
5.3.2 Tensile Properties 114
5.3.3 Impact strength 116
5.3.4 Melt Flow Index 116
5.3.5: Specific Flexural Modulus 117
5.4 EFFECT OF HEMP BAST AND HURD FIBERS OF DIFFERENT SIZES ON THE MECHANICAL PROPERTIES OF COMPOSITES **119**
5.4.1 Flexural Properties 121
5.4.2 Tensile Properties 123
5.4.3 Impact Strength 125
5.4.4 Melt Flow Index 126
5.4.5 Specific Flexural Modulus 126
5.4.6 Scanning Electron Microscope (SEM): 127
5.5 COMPOSITES CONTAINING HEMP PELLETS WITH DIFFERENT COMPOSITIONS OF HURD AND BAST FIBER FROM DIFFERENT SUPPLIERS **130**
5.5.1 Flexural Properties 132
5.5.2 Tensile Properties 133
5.5.3 Impact Strength 135
5.5.5 Melt Flow Index 135
5.5.5 Specific Flexural Modulus 136
5.6 EFFECT OF HEMP FIBER FROM DIFFERENT COUNTRIES ON THE MECHANICAL PROPERTIES OF THE COMPOSITES **138**
5.6.1: Flexural Properties 140
5.6.2: Tensile Properties 143
5.6.3 Impact strength 146
5.6.4 Melt Flow Index 148
5.6.5: Specific Flexural Modulus 149
5.7 COMPARISON BETWEEN COMPOSITE WITH FIBER AND PELLET **151**
CHAPTER 6: CONCLUSION AND RECOMMENDATIONS *154*
LETTER OF COPYRIGHT PERMISSION *157*
REFERENCES *162*

LIST OF FIGURES

Figure 1.1 US$ 742 million revenue generated in 2016 by the use of natural fiber composites in different applications (Elseify et al., 2021). 2
Figure 1.2 Different car parts made with natural fiber reinforced polymer composites, a) Tesla S P100D race car representing a body made from natural fiber, b) McLaren F1 seat reinforced with natural fiber (Bcomp powerRibs), c) Porsche Motorsport 718 Cayman GT4 CS MR equipped with natural fiber body kit, adapted from (Elseify et al., 2021). 3
Figure 1.3 Project outline. 5
Figure 2.1 Different geometrical and spatial aspects of particles in the dispersed phase that may affect the properties of composites are illustrated schematically: (a) concentration, (b) size, (c) shape, (d) distribution, and (e) orientation, adapted from (Callister, 2007) under John Wiley And Sons License. 6
Figure 2.2 Illustration of assembling of three polypeptide chains containing α chains in a triple-helix structure forming a tropocollagen. Cross-linking of tropocollagen to form collagen fibrils with gaps called D-period. Formation of hydroxyapatite mineral in between gaps and around collagen fibrils and formation of collagen fibers by stacking together hydroxyapatite mineralized collagen fibrils, adapted from (Rosa et al., 2022) under the terms of the Creative Commons Attribution 3.0 License. 8
Figure 2.3 Classification of composites, adapted from (Callister, 2007) under John Wiley And Sons License. 9
Figure 2.4 Illustration of fiber-reinforced composites (a) continuous and aligned (b) discontinuous and aligned (c) discontinuous and randomly oriented, adapted from (Egbo, 2021) under the terms of the Creative Commons Attribution 4.0 License 11
Figure 2.5 Stress-strain curve of fiber, continuously aligned fiber-reinforced composite, and matrix, adapted from (Egbo, 2021) under the terms of the Creative Commons Attribution 4.0 License. 13
Figure 2.6 Classification of composites based on matrix materials, image by author. 14
Figure 2.7 Structure of Polypropylene. 15
Figure 2.8 Schematics of twin screw extruder adapted from (P Chinna et al., 2011), under the terms of the Creative Commons Attribution 3.0 License. 17

Figure 2.9 Schematic diagram of injection molding machine adapted from (Svečko et al., 2013), under the terms of the Creative Commons Attribution 3.0 License. 19
Figure 2.10 SEM analysis of abaca fiber, a) untreated fibers, b-d) fiber treated with 5, 10, and 15 wt.% NaOH, adapted from (Cai et al., 2016), under Elsevier license. 26
Figure 2.11 Structure of hemp stem and fiber, a) longitudinal hemp stem section, b) hemp fiber bundle morphology, c) depiction of hemp bast fiber, adapted from (Manaia et al., 2019) under the terms of the Creative Commons Attribution 3.0 License. 29
Figure 2.12 Different saturation states of liquid-bound granules, adapted from (Green and Southard, 2019)..... 35
Figure 3.1 Thomas Wiley Mill Model 4, image from (labwrench.com). 48
Figure 3.2 Sieves used to mill, image by author. 48
Figure 3.3 a) CMO ECO-3 flat die pellet mill, b) roller and flat die setup, image by author. 49
Figure 3.4 Flat die with 4 mm diameter holes in hexagonal geometry, image by author. 50
Figure 3.5 a) Haake Minilab Microcompunder, b) conical screws, image by author. 51
Figure 3.6 Flexural, tensile, and impact test specimen of pure PP, PP/GF, and PP/HF composites, image by author. 52
Figure 3.7 RO-TAP Sieve shaker with ten sieves, image by author. 53
Figure 3.8 Pellet tumbling machine, image by author. 55
Figure 4.1 Comparison between space occupied by 200 grams of hemp bast fibers (left) and 200 grams of hemp bast pellets (right). 60
Figure 4.2 Flow diagram of hemp fiber pelletization process. 61
Figure 4.3 Visual representation of hemp bast and hemp hurd fiber milled in 1 mm, 1.5 mm, and 3 mm sizes. 62
Figure 4.4 Sieve shaker analysis results of 1 mm, 1.5 mm, and 3 mm milled hemp bast and Hurd fibers. 64
Figure 4.5 Cake-like formation of 3 mm milled bast fibers in sieve shaker. 64
Figure 4.6 Visual appearance of bast and hurd fiber milled in 1-, 1.5- and 3-mm size under an optical microscope. 66
Figure 4.7 Optical microscope analysis results of hemp bast and hurd fibers milled in 1-, 1.5- and 3-mm sizes. 66

Figure 4.8 Specific compressive strength of whole hemp pellets with different fiber sizes and with and without wax. 70
Figure 4.9 Bulk density of whole hemp pellets with different fiber sizes and with and without wax. 71
Figure 4.10 PDI of whole hemp pellets with different fiber sizes and with and without wax. 72
Figure 4.11 Hurd Pellets, a) 100% Hurd fiber pellets (H1), b) 85/15% Hurd and bast fiber pellets (H3). 75
Figure 4.12 Specific compressive strength of hurd pellets. 76
Figure 4.13 Bulk density of hurd pellets. 77
Figure 4.14 PDI of Hurd pellets. 78
Figure 4.15 Visual appearance of hurd pellets at different temperature ranges. 79
Figure 4.16 Specific compressive strength of pellets with different compositions of hemp bast and hurd fibers. 82
Figure 4.17 Bulk density of pellets with different compositions of hemp bast and hurd fibers. .. 83
Figure 4.18 Visual appearance of whole hemp, bast, and hurd pellets. 83
Figure 4.19 PDI of pellets with different compositions of hemp bast and hurd fibers. 84
Figure 4.20 a) 1 mm bast fiber pellet, b) 1 mm hurd fiber pellet. 85
Figure 4.21: 3 mm bast fiber stuck between roller and hopper preventing the roller from moving. 86
Figure 4.22 SEM analysis of hemp fibers at 1000X magnification a) untreated TwH fiber, b) 5 wt.% NaOH treated TwH fiber. 88
Figure 4.23 FTIR spectrum of untreated TwH and 5 wt.% NaOH TwH fibers. 89
Figure 4.24 Change in color in NaOH treated (1) and untreated (2) hemp fibers. 89
Figure 4.25 Cake-like agglomerates of NaOH-treated TwH fibers formed in between pellet mill die and rollers. 91
Figure 4.26 Appearance of 1 mm milled bast and hurd fiber before and after pelletization. 93
Figure 4.27 Bast fiber lengths a) before pelletization, b) after pelletization. 94
Figure 4.28 Bast fiber aspect ratio a) before pelletization, b) after pelletization. 95
Figure 4.29 Hurd fiber lengths a) before pelletization, b) after pelletization. 96
Figure 4.30 Hurd fiber aspect ratio a) before pelletization, b) after pelletization. 97
Figure 5 Flow chart of the composite-making process. 98

Figure 5.1 Flexural modulus of composites with NaOH-treated fibers and MAPP. 100
Figure 5.2 Flexural Strength of composites with NaOH treated fibers and MAPP. 101
Figure 5.3 Tensile modulus of composites with NaOH-treated fibers and MAPP. 102
Figure 5.4 Tensile strength of composites with NaOH-treated fibers and MAPP. 102
Figure 5.5 Tensile strength of composites with NaOH-treated fibers and MAPP. 104
Figure 5.6 Melt flow index (MFI) of composites with NaOH-treated fibers and MAPP. 105
Figure 5.7 Specific Flexural Modulus (SFM) of composites with NaOH-treated fibers and MAPP. 106
Figure 5.8 SEM of 20TwH composite (1000X). 107
Figure 5.9 SEM of 20TwH-5Na composite (1000X). 107
Figure 5.10 SEM of 20TwH+0.5MA composite (1000X). 108
Figure 5.11 SEM of 20TwH-5Na+0.5MA composite (1000X). 108
Figure 5.12 Flexural modulus of composites with hemp pellets of different fiber sizes and with and without wax. 113
Figure 5.13 Flexural strength of composites with hemp pellets of different fiber sizes and with and without wax. 114
Figure 5.14 Tensile modulus of composites with hemp pellets of different fiber sizes and with and without wax. 115
Figure 5.15 Tensile strength of composites with hemp pellets of different fiber sizes and with and without wax. 115
Figure 5.16 Impact strength of composites with hemp pellets of different fiber sizes and with and without wax. 116
Figure 5.17 Melt flow index of composites with hemp pellets of different fiber sizes and with and without wax. 117
Figure 5.18 SFM of composites with hemp pellets of different fiber sizes and with and without wax. 118
Figure 5.19 Flexural modulus of composites with hemp bast, hurd, and glass fiber. 122
Figure 5.20 Flexural strength of composites with hemp bast, hurd, and glass fiber. 122
Figure 5.21 Tensile modulus of composites with hemp bast, hurd, and glass fiber. 124
Figure 5.22 Tensile strength of composites with hemp bast, hurd, and glass fiber. 124
Figure 5.23 Impact strength of composites with hemp bast, hurd, and glass fiber. 125

Figure 5.24 Melt flow index of composites with hemp bast, hurd, and glass fiber. 126
Figure 5.25 Specific flexural modulus of composites with hemp bast, hurd, and glass fiber. ... 127
Figure 5.26 SEM of 20F-U.B composite (500X). 128
Figure 5.27 SEM of 20F-VB.H composite (500X). 128
Figure 5.28 SEM of 10GF composite (500X). 129
Figure 5.29 Flexural modulus of composites with hemp pellets of different compositions of bast and hurd fiber from different suppliers. 132
Figure 5.30 Flexural strength of composites with hemp pellets of different compositions of bast and hurd fiber from different suppliers. 133
Figure 5.31 Tensile modulus of composites with hemp pellets of different compositions of bast and hurd fiber from different suppliers. 134
Figure 5.32 Tensile strength of composites with hemp pellets of different compositions of bast and hurd fiber from different suppliers. 134
Figure 5.33 Impact strength of composites with hemp pellets of different compositions of bast and hurd fiber from different suppliers. 135
Figure 5.34 Melt flow index of composites with hemp pellets of different compositions of bast and hurd fiber from different suppliers. 136
Figure 5.35 Specific flexural modulus of composites with hemp pellets of different compositions of bast and hurd fiber from different suppliers. 137
Figure 5.36 Flexural Modulus of composites with a) different whole hemp fiber pellets, b) different bast fiber pellets, and c) different hurd fiber pellets. 141
Figure 5.37 Flexural Strength of composites with a) different whole hemp fiber pellets, b) different bast fiber pellets, and c) different hurd fiber pellets. 142
Figure 5.38 Tensile Modulus of composites with a) different whole hemp fiber pellets, b) different bast fiber pellets, and c) different hurd fiber pellets. 144
Figure 5.39 Tensile modulus of composites with a) different whole hemp fiber pellets, b) different bast fiber pellets, and c) different hurd fiber pellets. 145
Figure 5.40 Impact strength of composites with a) different whole hemp fiber pellets, b) different bast fiber pellets, and c) different hurd fiber pellets. 147
Figure 5.41 Melt flow index of composites with a) different whole hemp fiber pellets, b) different bast fiber pellets, and c) different hurd fiber pellets. 148

Figure 5.42 Specific flexural modulus of composites with a) different whole hemp fiber pellets, b) different bast fiber pellets, and c) different hurd fiber pellets. 150
Figure 5.43 Pre extrusion mix a) hemp fiber and PP milled, b) hemp and PP pellets. 152
Figure 5.44 Mechanical properties of composites with hemp fiber and pellets, a) Flexural Modulus, b) Flexural Strength, c) Tensile Modulus, d) Tensile Strength, e) Impact strength, f) Melt flow index, g) Specific flexural modulus. 153

LIST OF TABLES

Table 1.1 Common commercially available natural fibers and their world production adapted from (Mohammed et al., 2015). 2
Table 2.1 Thermoplastics and their applications in automotive, data from (Patil et al., 2017). ... 20
Table 2.2 List of different chemical treatments employed to process natural fibers adapted from (Sun, 2018), under the terms of the Creative Commons Attribution 3.0 License. 25
Table 2.3 Chemical composition of different plant fibers and mechanical properties of plant fibers and glass fibers. Data from (Manaia et al., 2019) 31
Table 2.4 Advantages and disadvantages of hemp over other natural fibers, data from (Sen and Reddy, 2011). 31
Table 2.5 Equations used to represent powder compression, adapted from (Capes, 2013). 36
Table 3.1 Different Hemp Fiber Description. 46
Table 4.1 Sieve shaker sieves size and corresponding particle size range. 63
Table 4.2 Formulation and mechanical properties of whole hemp pellets with different fiber sizes and with and without wax. 68
Table 4.3 Hurd pellets formulations and mechanical properties. 74
Table 4.4 Formulation and mechanical properties of hemp pellets with different compositions of bast and hurd fibers. 81
Table 5.1 Formulation of composites with NaOH-treated fibers and MAPP. 99
Table 5.2 Mechanical properties of composites with NaOH-treated fibers and MAPP. 99
Table 5.3 Formulation of composites with Hemp pellets of different fiber sizes and with and without wax. 111
Table 5.4 Mechanical properties of composites with Hemp pellets of different fiber sizes and with and without wax. 112
Table 5.5 Formulation of composites with hemp bast, hurd, and glass fiber. 120
Table 5.6 Mechanical properties of composites with hemp bast, hurd, and glass fiber. 120
Table 5.7 Formulation of composites with hemp pellets of different compositions of bast and hurd fiber from different suppliers. 130
Table 5.8 Mechanical properties of composites with hemp pellets of different compositions of bast and hurd fiber from different suppliers. 131

Table 5.9 Formulation of composites with pellets of whole hemp fiber, bast fiber, and hurd fiber provided by different suppliers. 138
Table 5.10 Mechanical properties of composites with pellets of whole hemp fiber, bast fiber, and hurd fiber provided by different suppliers. 139
Table 5.11 Formulation and mechanical properties of composites with hemp fiber and pellets. 152

LIST OF ABBREVIATIONS

%	Percentage
ε	Strain
°	Degree
°C	Degree Celsius
α	Alpha
β	Beta
μm	Micrometer
ρ	Density
σ	Stress
ρ_{bulk}	Bulk density
ASTM	American standard for testing of materials
ABS	Acrylonitrile/Butadiene/Styrene
ASABE	American Society of Agricultural and Biological Engineers
cm	Centimeter
CF	Carbon fiber
cP	Centipoise
d	Diameter
E	Young's Modulus or Modulus of Elasticity
F	Force
FTIR	Fourier Transform Infrared Spectroscopy.
ft	Feet
g	Gram
GFRPC	Glass Fiber Reinforced Polypropylene Composites
GF	Glass Fiber
GPa	Giga Pascal
hr	Hour
HF	Hemp Fiber
IRI	Impact Resistance Index
ISO	International Organization for Standardization

J	Joules
kg	Kilogram
k	kelvin
KOH	Potassium Hydroxide
l_c	Critical length
l	Length
min	Minute
m	Meter
nm	Nanometer
mm	Millimetre
m	Matrix
MAPP	Maleic Anhydride Grafted Polypropylene
MFI	Melt Flow Index
MPa	Mega Pascal
mg	Milligram
m_c	Moisture Content
MFR	melt flow rate
MA	Maleic Anhydride
NFRPC	Natural Fiber Reinforced Polypropylene Composites
N	Newton
NaOH	Sodium Hydroxide
PP	Polypropylene
PE	Polyethylene
Psi	Pound per square inch
PDI	Pellet Durability Index
r	Reinforcement
Rpm	Revolutions Per Minute
s	Second
Sp gr	Specific Gravity
SEM	Scanning Electron Microscope

SFM	Specific Flexural Modulus
T_g	Glass Transition Temperature
T_m	Melting Temperature
T	Time
THC	Tetrahydrocannabinol
V	Volume fraction
Wt.	Weight
W_a	Water Absorption

CHAPTER 1: INTRODUCTION

1.1 Background and Motivation:

The rise in environmental awareness and public concern, new environmental regulations, and the unsustainable use of petroleum products have all prompted consideration of the usage of environmentally friendly materials. Natural fibers are a good substitute for synthetic fibers as they have good mechanical properties, low density, low cost, non-abrasiveness, high specific strength, biodegradability, eco-friendly and renewability whereas synthetic fibers such as glass fiber have higher density, and its production consumes 5-10 times more non-renewable energy than natural fibers. Table 1.1 represents common natural fibers commercially available and their worldwide production.

The use of natural fibers as a substitute for aramid, glass, and carbon fiber for reinforcement in polymer material has significantly grown in the past few years because of their superior advantages such as low weight, less damage to processing equipment, good tensile and flexural modulus, and minimal health hazard. Polymers either thermoplastics or thermosets reinforced with natural fiber can produce composites with high strength and specific stiffness. These composites are widely used in aerospace, construction, leisure, packing, sports, and automotive industries. Figure 1.1 represents a total of US$ 742 million in revenue generated in 2016 by the use of natural fiber composite in different applications. The major consumer of natural fiber composites is the automotive industry. To make vehicles lightweight, natural fiber composites are used as a replacement for heavy alloys and metals in non-structural parts of vehicles such as interior panels and parcel shelves. Mostly, polypropylene reinforced with 50% weight fraction natural fibers such as hemp, flax, and kenaf composites are used for front and rear door liners, door panels, seat backs, rear parcel shelves, spare tire covers, headliners, and other interior parts. It was reported that the use of natural fiber-reinforced polymer composite parts in the Tesla S P100D race car reduced its weight by 500kg. Porsche and McLerran are also replacing carbon fiber parts with natural fiber composites as they offer similar strength at reduced weight and 30% less cost. Moreover, natural fiber composites offer 5 times better impact resistance and vibration absorbance, and show ductile

behavior with no sharp shattering when crashed (Elseify et al., 2021). Figure 1.2 represents different car parts made with natural fiber-reinforced polymer composites.

Table 1.1 Common commercially available natural fibers and their world production adapted from (Mohammed et al., 2015).

Fiber Source	**World Production (10^3 ton)**
Sugar cane bagasse	75,000
Bamboo	30,000
Jute	2300
Grass	700
Flax	830
Sisal	375
Kenaf	970
Hemp	214
Abaca	70
Coir	100
Ramie	100

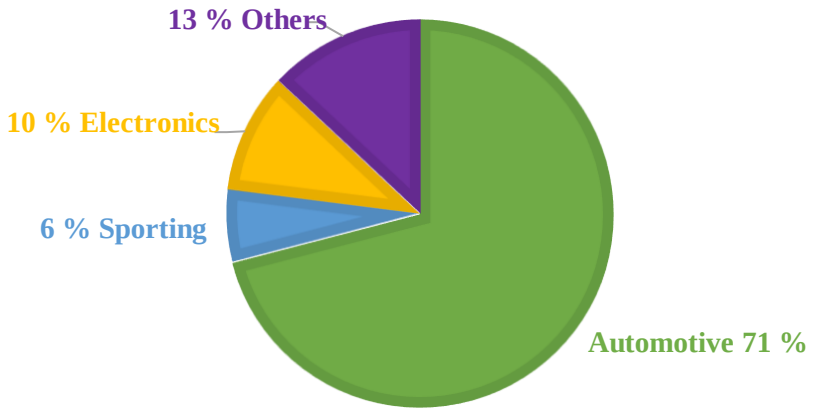


Figure 1.1 US$ 742 million revenue generated in 2016 by the use of natural fiber composites in different applications (Elseify et al., 2021).



Figure 1.2 Different car parts made with natural fiber reinforced polymer composites, a) Tesla S P100D race car representing a body made from natural fiber, b) McLaren F1 seat reinforced with natural fiber (Bcomp powerRibs), c) Porsche Motorsport 718 Cayman GT4 CS MR equipped with natural fiber body kit, adapted from (Elseify et al., 2021).

Natural fibers also have some disadvantages such as their poor compatibility with polymer matrix, limited processing temperature, and high moisture absorbance. The presence of the waxy substance and the hydrophilic nature of fiber causes them to absorb moisture and swell which hinders their bonding with polymer matrix. As a result of poor bonding, the stress cannot be effectively transferred between the polymer matrix and fibers. To counter this problem, specific treatments of natural fibers are performed to enhance their compatibility with polymers. Another challenge with using natural fibers is their low bulk density which creates challenges in

transporting, storage, and handling. It is also difficult to feed natural fiber materials with low bulk density inside polymer processing equipment like extruders for compounding with polypropylene pellets. Densification also known as the pelletization of natural fibers by applying mechanical pressure can solve this problem. Pelletization increases the bulk density of natural fibers and lowers their moisture absorbance characteristics. This makes them easy for storage, and transportation, and makes their feeding with polypropylene pellets in an extruder easy and uniform.

1.2 Research Objectives:

The primary objective of this thesis was to fabricate hemp fiber-reinforced polypropylene composites, with the express intent of exploring their use within the automobile industry. To facilitate storage, handling, and easy, and homogenous processing of hemp fibers with polypropylene in the extruder, hemp fibers were initially put through a pelletization process. This step was important for easy feeding and ensuring uniform dispersion of hemp fibers in the composite.

Moreover, to comprehend the effect of various factors such as hemp fiber particle size, different compositions of hemp hurd and bast fiber, use of additives to improve dispersion, use of a coupling agent and alkali treatment of hemp fiber to improve interfacial bonding on the mechanical properties of both hemp pellets and the resultant composite materials, a comprehensive investigation was done. These investigations intended to clarify how these variables affected the mechanical properties and functionality of the composite materials. This study aimed to improve the performance of hemp fiber-reinforced polypropylene composites for future automotive applications by analyzing the effects of these variables.

1.3 Project Outline:

This thesis is composed of 6 chapters as discussed below.

Chapter 1 provides a short introduction to the research thesis, the motivation of the author, the research objectives, and the research plan. Chapter 2 provides a literature review of materials, processing techniques, and characterization methods. Chapter 3 describes materials preparation, experimental procedures, and characterization methods. Chapter 4 and 5 presents experimental results and provides an adequate discussion about them. Chapter 4 presents and discusses hemp

pelletization results and Chapter 5 presents and discusses hemp fiber-reinforced polypropylene composites results. Finally, chapter 6 presents conclusions and recommendations for future work. Figure 1.3 represents the layout of this project.

1. Introduction
(Motivation, objective, and research plan)

2. Literature Review
(Composites (Natural + Man-made), Polypropylene, Polypropylene processing techniques, GFRPC, NFRPC, Hemp fiber, Particle size enlargement)

3. Material and Methods
(Materials, Experimental procedures, characterization methods)

4. Hemp Pelletization

Materials	Processing	Characterization
Hemp Fibers (Bast & Hurd) Additive Wax Water	Milling Mixing Pelletization Drying	Bulk Density Durability Compressive Strength Particle Size Analysis

5. Composites

Materials	Processing	Characterization
Hemp Pellets Glass Fiber Polypropylene MAPP	Extruder Injection Molding	Tensile Tests Flexural Tests Impact Tests Specific Density Melt Flow Index SEM

6. Conclusion and Recommendations.

Figure 1.3 Project outline.

CHAPTER 2: LITERATURE REVIEW

2.1 Composites:

Composites are the materials that are formed when two or more constituent materials known as a matrix and dispersed phase are combined. Matrix is a continuous phase in which the dispersed phase having different chemical, physical, and mechanical properties are dispersed to obtain a final product that has characteristics properties of both matrix and disperse phase. The purpose of making composites is to obtain improved properties than individual materials properties. The dispersed phase can increase desirable properties, like reinforcement, lightweight, electrical, or thermal conductivity for example. Composite properties can be engineered according to the desired application by altering the volume fraction of constituent materials, distribution, and geometry of the dispersed phase (size, shape, and orientation) (Egbo, 2021). The configuration of composites with different sizes, shapes, orientations, and distribution of dispersed phases are illustrated in Figure 2.1.

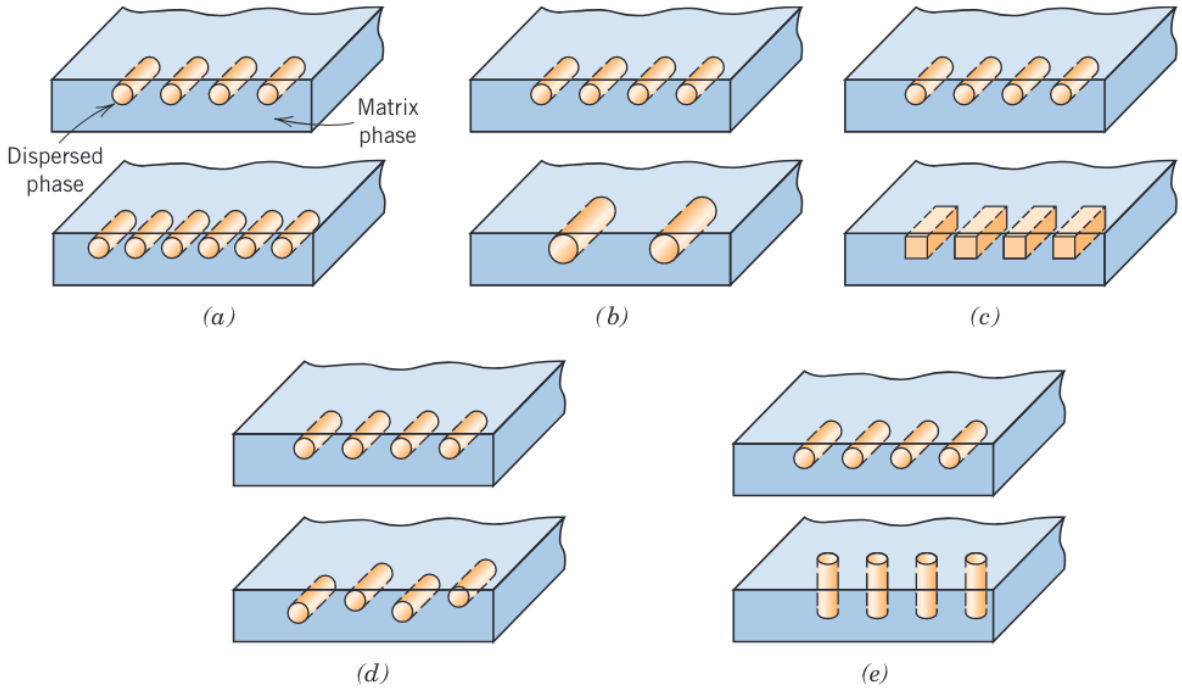


Figure 2.2 Different geometrical and spatial aspects of particles in the dispersed phase that may affect the properties of composites are illustrated schematically: (a) concentration, (b) size, (c) shape, (d) distribution, and (e) orientation, adapted from (Callister, 2007) under John Wiley And Sons License.

With technological advancement, there is a need for new materials that exhibit an uncommon set of properties that conventional materials such as polymers, ceramics, and metal alloys alone cannot demonstrate. For example, the aerospace and automotive industry is constantly researching materials that are strong, stiff, impact, and abrasion-resistant, not easily subjected to corrosion, and have low densities. These unusual properties are obtained from composite materials.

2.1.1 Composites in nature:

Bone is a magnificent example of composite. Bone structure is composed of inorganic material, organic material, and water in the following range of weight fraction 65-70%, 18-25%, and 10-12%, and in terms of volume fraction the constituents have ranges of 33-43%, 32-44% and 15-25% respectively. The inorganic material is hydroxyapatite crystals which give rigidness and compressive strength, and organic phases consist of protein molecules and collagen fibers which give flexibility and tensile strength to bone. This combination allows the bone to be both flexible and strong. The organic matrix consists of collagen fibers which is a combination of several parallel aligned tropocollagen. Tropocollagen is a rigid linear molecule that is composed of three polypeptide chains with reoccurring amino acid sequences, glycine-proline-hydroxyproline, wounding together into a tightly packed repeating triple helix structure which has a length of 300nm and diameter of 1.5nm. Moving up the hierarchal order, the fibrils are formed when tropocollagen molecules aggregate by covalently crosslinking each other at the ends and axial staggering, creating overlapping zones and gap-like region which exhibits a specific periodicity known as D-Period which has a value of 67nm. The hydroxyapatite mineral forms as stacks of thin sheets of polycrystalline, which encircle and lie between the gaps in the collagen fibrils (Murr, 2015; Rosa et al., 2022) as shown in Figure 2.2.

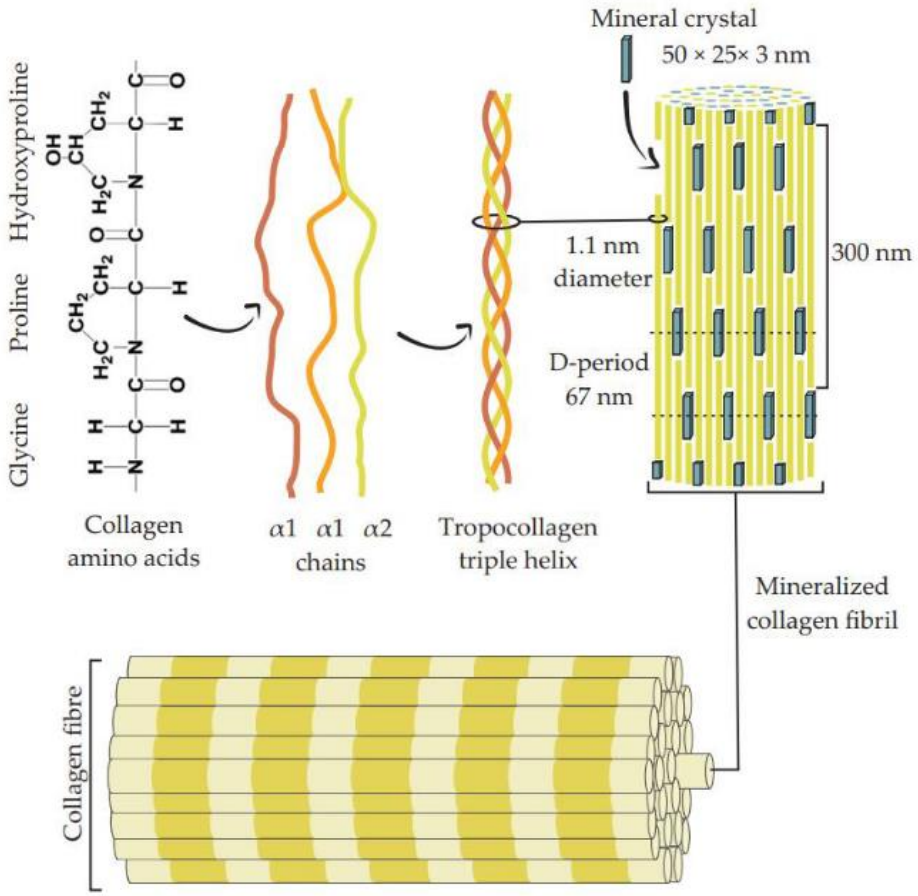


Figure 3.2 Illustration of assembling of three polypeptide chains containing α chains in a triple-helix structure forming a tropocollagen. Cross-linking of tropocollagen to form collagen fibrils with gaps called D-period. Formation of hydroxyapatite mineral in between gaps and around collagen fibrils and formation of collagen fibers by stacking together hydroxyapatite mineralized collagen fibrils, adapted from (Rosa et al., 2022) under the terms of the Creative Commons Attribution 3.0 License.

The mechanical strength of hydroxyapatite mineralized collagen fibrils such as strength, fracture energy, and elastic modulus are remarkably impacted by a uniform distribution of hydroxyapatite mineral across the collagen fibril and the contact between both constituents and less impacted by an increase in minerals volume fraction (Wang and Ural, 2019).

2.1.2 Man-Made Composites:

To achieve a unique combination of improved mechanical properties such as resistance to high temperature and corrosion, high toughness, and stiffness, as well as lightweight, scientists and engineers have innovatively combined several ceramics, polymers, natural fibers, minerals, and metals. In composites, to achieve significant improvement in mechanical properties, it is advantageous that the dispersed phase should be more rigid and stronger than the matrix and there is a strong interaction between them so load can be transferred from one phase to another. Furthermore, the dispersed phase must have chemically contrasted characteristics and a noticeable interface with the matrix. Based on the dispersed phase, composites classification is shown in Figure 2.3 (Callister, 2007; Paul and Dai, 2018).

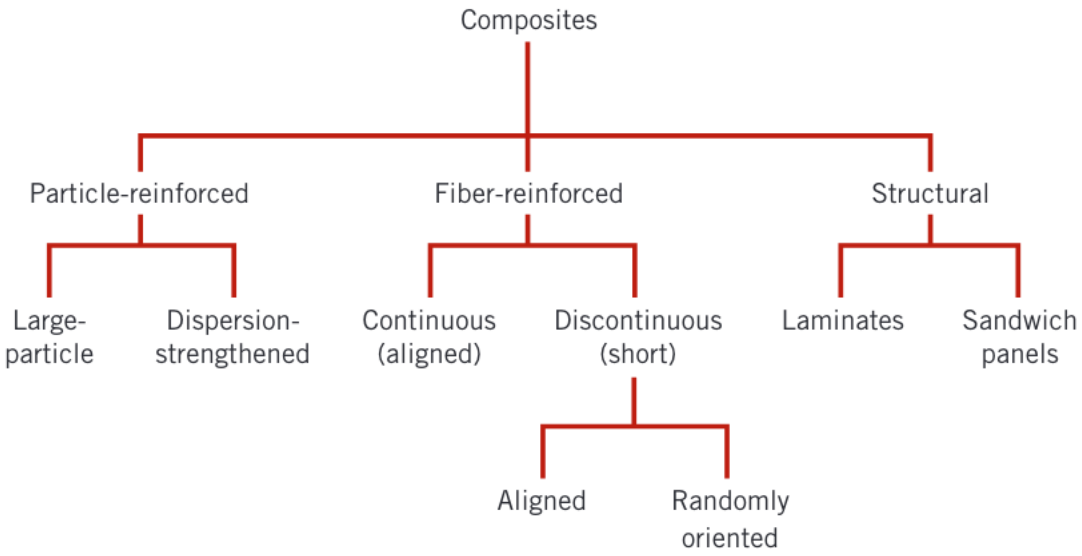


Figure 2.3 Classification of composites, adapted from (Callister, 2007) under John Wiley And Sons License.

In particle-reinforced composites, large millimeter-scale particles and small nanoscale particles having uniform axes are used as reinforcement, and in fiber-reinforced composites, fiber-like reinforcements are used which have high length-to-width ratios and structural composites are amalgamations of homogenous and composite material. The major difference between the first two classifications is the geometry of the dispersed phase.

Particle-Reinforced composites:

Based on particle size, particle-reinforced composites are further divided into large particle composites and dispersion-strengthened composites. In large particle composites, large millimeter-sized equiaxed particles are used as reinforcement. The reinforcement-matrix interaction in this case is determined using the concept of continuum mechanics. In these composites, reinforcement is responsible for major load absorbance and prevents the matrix from deformation. In dispersion-strength composites, small 10 to 100nm equiaxed particles are used. The reinforcement-matrix interaction takes place at the atomic level. In these composites, the matrix is responsible for major load absorbance and particles are responsible for restraining the advancement of dislocation along the matrix and preventing the material from undergoing plastic deformation. This improves the mechanical properties of the composites.

The mechanical performance of the composite increases by utilizing small particles, achieving uniform dispersion across the matrix, and increasing particle volume fraction. Mechanical properties of composites such as the dependence of the elastic modulus on the volume fraction, can be predicted by using the rule of mixture which states that the final properties of a two-phase composite should lie between the upper and lower bounds of individual constituent material mechanical properties and their respective volume fraction. Upper and lower bound equations are represented below,

$$E_{upper\ bound} = E_m V_m + E_r V_r$$

$$E_{lower\ bound} = \frac{E_m E_r}{E_r V_m + E_m V_r}$$

In the above expression, E denotes elastic modulus, V denotes volume fraction and subscripts m, and r denotes matrix and reinforcement. Since mechanical properties are influenced by particle size, shape, interfacial adhesion between matrix and particles, and particle distribution, the deviation of composite final properties from values predicted by the rule of mixture is considerable.

Fiber-Reinforced Composites:

An important and most widely used type of composite is fiber-reinforced composites. In this type, the reinforcement is in the form of fibers that have a high length-to-diameter ratio also known as aspect ratio. Particles with a high aspect ratio can be classified as whiskers, fiber, and wire on a diameter basis. Whiskers are crystals with very small diameters and very high aspect ratios. Whiskers provide excellent strength to the material but due to high cost, these are not extensively used as a reinforcement. Fibers have small diameters and are polycrystalline or amorphous and wires have large diameters relative to whiskers and fibers. The aspect ratio of reinforcement is an important factor in these composites. Fibers-reinforced composites are further classified on the basis of fiber orientation and aspect ratio into continuous and aligned, discontinuous and aligned, and discontinuous and randomly oriented as shown in Figure 2.4.

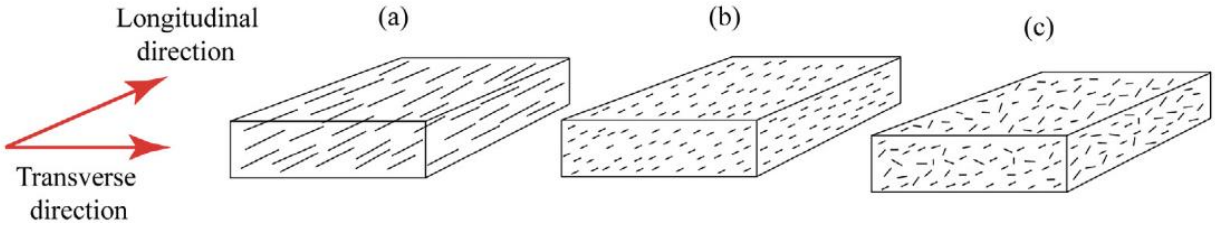


Figure 2.4 Illustration of fiber-reinforced composites (a) continuous and aligned (b) discontinuous and aligned (c) discontinuous and randomly oriented, adapted from (Egbo, 2021) under the terms of the Creative Commons Attribution 4.0 License

One of the important goals of designing a fiber-reinforced composite is to achieve high stiffness and strength on a low-weight basis. These attributes are characterized as specific modulus and specific strength which is the ratio of the elastic modulus to specific gravity and the ratio of the tensile strength to specific gravity. The fibers are stiffer and brittle, and the matrix is ductile. The final properties of composites not only depend on the properties of fibers and matrix but also on the aspect ratio of fibers and interfacial bonding between matrix and fibers. A minimum length of fibers known as critical length is required to achieve effective stiffness and strength of composite. Critical length l_c depends on diameter of fiber d, strength of interfacial bond between matrix and fiber τ_c, and fiber tensile strength σ_f^*.

$$l_c = \frac{\sigma_f^* \mathrm{d}}{2\tau \mathrm{c}}$$

To achieve significant improvement in composite mechanical properties, it is important that fiber length must be greater than critical length $l > l_c$. If the fiber length is smaller than the critical length stress is not effectively transferred from the matrix to the fibers and the system acts as a particle-reinforced composite (Callister, 2007; Egbo, 2021).

It was found experimentally that the flexural strength and tensile strength of bamboo fiber reinforced green composites (BFGC) increased with the increase in bamboo fiber length up to 15mm, with further increase in length mechanical properties were decreased. It was also observed from the micrographs of a fractured surface of tensile specimen that composites with 8mm fibers had fibers pulled out without any fiber breakage meaning fiber length was smaller than critical length and due to which load was not transferred from matrix to fibers. Whereas in composites with 15mm fibers, fiber breakage was observed meaning load was transferred effectively. The critical length was estimated to be 12mm with an aspect ratio of 60 (Takagi and Ichihara, 2004). The same was observed in the case of isophthalic polyester reinforced with 2% alkali-treated jute fibers, mechanical properties of composites increased with an increase in fiber length up to 20mm but elongation at break decreased. Above 20mm the mechanical properties were decreased this was found to be because of poor wetting of fibers (Sajin et al., 2022). Anand et al. (2022) also observed similar behavior in mechanical properties in silane-treated pineapple fiber-reinforced polyester composites. Mechanical properties of composites increased with an increase in fiber length from 5mm to 20mm. Above 20mm fiber length, mechanical properties decreased because of insufficient matrix available for complete wetting of fibers. It was reported that at lower fiber lengths, uniform dispersion of fibers in the matrix was not achieved due to which stress transfer between matrix and fibers was not efficient. Sankar et al. (2014) reported that the mechanical properties of polyester reinforced with sansevieria trifasciata fiber increased with an increase in fiber length from 2mm to 10mm. The optimum results for tensile strength were obtained from 10mm fiber length.

Under tensile load, composites with aligned and randomly oriented fibers behave differently. In the case of aligned fiber composites mechanical properties are anisotropic. Stress-

strain curve for matrix, fibers, and continuous and aligned fiber composites in which load is applied in the longitudinal direction, in the direction of aligned fibers as shown in figure 2.4(a), is represented in figure 2.5.

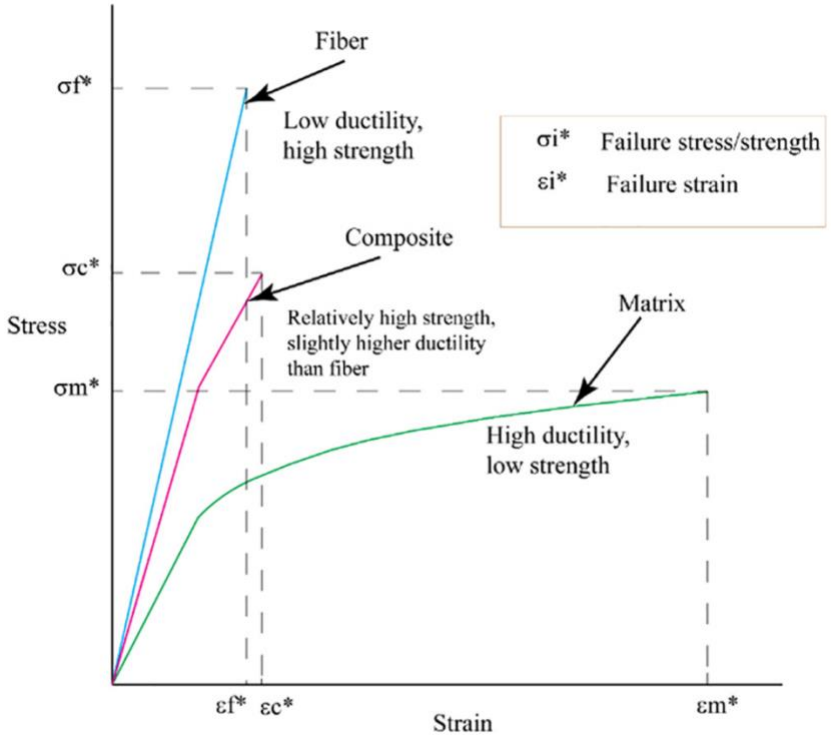


Figure 2.5 Stress-strain curve of fiber, continuous aligned fiber-reinforced composite, and matrix, adapted from (Egbo, 2021) under the terms of the Creative Commons Attribution 4.0 License.

As illustrated in Figure 2.5, fibers have higher failure strength than matrix. Fibers are brittle whereas matrix is ductile. Initially when the load is applied fibers and matrix undergo elastic deformation which is represented by the linear region of the curves and after this plastic deformation takes place. As fibers are stiffer than matrix, in composite when load is applied, matrix undergo plastic deformation first, but fibers continue to deform elastically. When more load is applied the fibers start to fracture. Because of this combination of stiff fibers and ductile matrix, fiber-reinforced composites have failure strength and strain in between of fiber and matrix.

Composites are also classified based on matrix material. There are four matrix materials commonly used. Composite classification based on matrix material is shown in Figure 2.6.

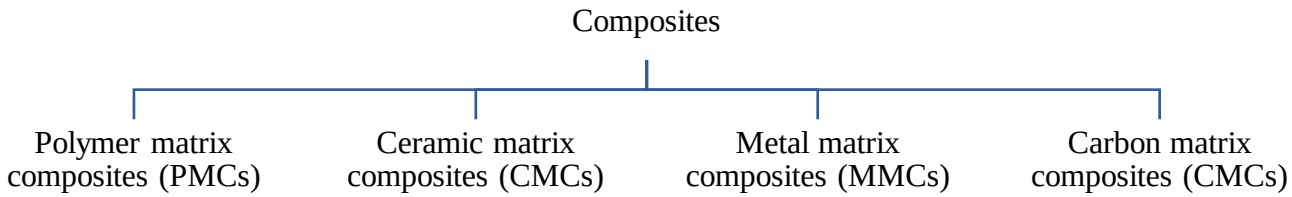


Figure 2.6 Classification of composites based on matrix materials, image by author.

Polymers are widely used as matrix materials for diverse composite applications. These are lightweight, low-cost, easily manufactured, and can be easily tailored according to the required application. Polymer matrix composites are favored over conventional metals because of these properties. Unreinforced polymers have low stiffness and are weak by addition of reinforcement these composites become strong and stiff (Zweben, 2015). Thermosets and thermoplastics are two types of polymers that are mostly widely used as matrix materials (Kumar Sharma et al., 2022; Park and Seo, 2011; Zweben, 2015).

Thermoplastics are polymers which have linear chains or lightly branched chains. These chains are chemically separated but are physically entangled with each other. These are the types of polymers that when heated, the chains slide over one another letting the polymer to flow and making it easy to re-shape it according to the desired application. Thermosets, on the other hand, have a network of cross-linked chains. These chains are chemically attached to each other. Once thermosets undergo curing, the chains are locked in their positions and cannot change their position under the influence of heat. When heat is applied to thermosets, they become hard and are degraded into char if further heated. Thermosets as compared to thermoplastics have high resistance towards corrosives and solvents as well as high strength and modulus. Thermoplastics because of their softening upon heating nature, can be easily processed using different techniques such as extrusion, injection molding, blow molding and so on (Karim et al., 2021; Peacock and Calhoun, 2006; Zweben, 2015).

This chapter will focus on the application of natural fiber-reinforced thermoplastic composites relevant to automotive applications. The objective of this project is to replace synthetic fiber-reinforced polypropylene composites with natural hemp fiber-reinforced polypropylene composites in automotive applications. Results of polypropylene composites reinforced with different compositions and types of hemp fibers and fibers supplied by different suppliers are investigated and compared.

2.2 Polypropylene:

Polypropylene was first synthesized in 1954 by Professor Natta. It is a semi-crystalline thermoplastic olefin polymer. It has a low melting point of 170°C and its density of 0.90g/cm^3 is the lowest among other thermoplastics. It is a hydrocarbon polymer composed of 14.3% hydrogen and 85.7% carbon (Purohit and Orzel, 1988). Polypropylene is obtained by the polymerization of propylene gas in the presence of an appropriate catalyst (Pavlík et al., 2019). The propylene molecule contains a methyl group attached to one of the carbon atoms. The structure of polypropylene is shown in Figure 2.7.

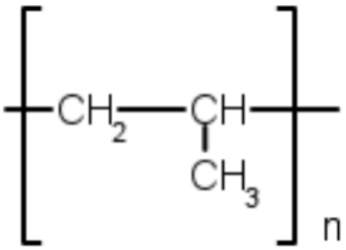


Figure 2.7 Structure of Polypropylene.

The methyl group has a mass that inhibits space and causes steric hindrance. The attached methyl group arrangement in the propylene molecule depicts a head and tail structure. The head is CH(-CH_3) end and the tail is CH_2 end. The addition of propylene molecules during dimerization can give three chain structures head-to-head, head-to-tail, and tail-to-tail. But due to methyl group steric hindrance effect, head-to-tail structure takes place. As each propylene monomer adds up, the position of methyl group of the newly attached monomer in the chain could be left-handed or right-handed. This makes polypropylene stereoregular polymer which can have three different conformations. Guilio Natta proposed rules of this stereoregularity with regards to tacticity as

isotactic, syndiotactic, and atactic (Crangle, 2017). These have different chemical and physical properties based on the position of the methyl group in the chain.

Isotactic conformation is formed when all the methyl groups are organized on one side of the chain due to the stereoregular addition of propylene monomer. Because of the steric hindrance of the methyl group, the isotactic chain takes a spiral configuration to keep repelling methyl groups away from each other (Crangle, 2017). If there is no stereoregularity and the arrangement of the methyl group is totally random then it forms an atactic form of polypropylene. This stereoregularity is controlled by the use of catalysts such as metallocene (Menyhárd et al., 2020). Isotactic polypropylene is most widely used for commercial applications constituting up to 90% of polypropylene products.

2.3 Processing Techniques of Polypropylene:

Processing of polypropylene into finished products is done by melt processes such as extrusion, injection molding, blow molding, and thermoforming. These processes depend on the flow characteristics of molten material at high temperatures. Plastics in their molten form exhibits non-Newtonian behavior as their viscosity at a constant temperature change with a change in shear rate. The measure of the flow of molten material through an orifice or channel is called the shear rate. It is very important to understand how a material will flow in its molten form through melt processing equipment. Due to this non-Newtonian behavior of plastics in their molten state, no single value of viscosity can be assigned to them that's why their viscosity values are always related to the shear rate and temperature at which they were measured and are known as apparent viscosity (Maier and Calafut, 1998). The most widely used measures of plastic viscosities are melt flow index (MFI) and melt flow rate (MFR).

2.3.1 Extrusion:

Extrusion is one of the most widely used processing methods of polypropylene (Maier and Calafut, 1998). Extrusion is a process in which plastic material is melted, mixed, and pumped through an orifice or die of a preferred cross-section at a constant rate and then cooled. The extrusion is a continuous process that produces semi-finished products that need to be further processed to form the final product. An extruder consists of single or twin screws which are fitted in the barrel of the extruder and are rotated by means of a motor. The screws are the main indicator

of extruder performance. The screws are responsible for conveying the plastic material through the barrel, melting it, compressing, homogenizing it, and pumping it out of the die. Twin-screw extruders in particular are used when additives or fillers are to be added to the thermoplastics material to make composites in which good mixing and homogenization of the molten material is crucial for the final product. The output rate of the extruder is determined by screw geometry, screw speed, and melt viscosity (Maier and Calafut, 1998). The molten material is then cooled in a water bath after it is pumped out through the orifice. The material in the form of pellets or powder is fed into an extruder via a feed throat provided at the inlet of the barrel. There are four ways to feed material to an extruder flood feed, starve feed, crammer, and melt flow. In twin screw, extruder material is fed using starve feeding technique in which feed is fed throw feeder directly onto screws. The screw's speed set is higher than the feeder deposit speed so that material can be conveyed into the barrel at a higher speed than it is deposited to avoid the pressure build-up in the extruder barrel (Giles et al., 2005). The material is then melted and mixed homogeneously under the action of compression, friction, and shear forces. The pressure in the barrel is typically between 1000 to 5000 psi. After mixing, the melt is pushed through the orifice or die and then it is pelletized after being cooled for further processing into the final product. Schematics of a typical twin-screw extruder are shown in Figure 2.8.

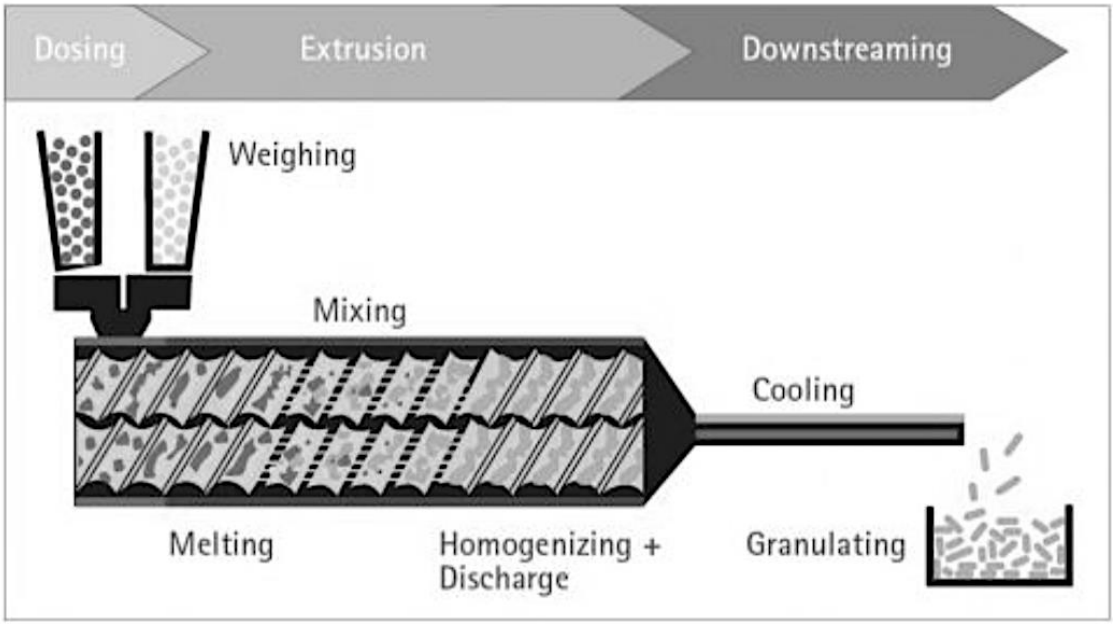


Figure 2.8 Schematics of twin screw extruder adapted from (P Chinna et al., 2011), under the terms of the Creative Commons Attribution 3.0 License.

2.3.2 Injection Molding:

Injection molding is one of the most widely used manufacturing methods for the production of polypropylene products. Almost a third of polypropylene products are processed via injection molding (Maier and Calafut, 1998). The operation of injection molding is simple. Injection molding machines can be divided into two parts, injection unit and clamping unit. In the injection unit, raw material is fed, melted, and mixed while the clamp unit function is to keep the mold halves closed during injection and open them when injected material is cooled down and ready to be ejected. Polymer resins in the form of powder or pellets are fed into the barrel of the injection molding machine through a hopper where they are conveyed by a rotating screw and heated at a temperature higher than the melting point of polymer. Once polymer is melted in a required volume it is then injected into an empty mold under pressure that exhibits the shape of the desired final product. The viscous melt is pushed into the mold by a ram and once the mold is filled the ram is kept in the forward position to maintain holding pressure. As the polymer solidifies it shrinks and to compensate for this shrinkage more molten material is injected by the ram. The temperature of the mold is typically set at 65°C. After the material in the mold solidifies, the pressure is removed, and the mold is cooled before it is opened to extract the final product. The injection molding technique involves mechanisms of pressure flow and heat transfer (Maier and Calafut, 1998). Injection molding can produce highly complex finished products in a single, automatic, and rapid operation. However, achieving uniform apparency and uniform thickness of the finished product are two main challenges in injection molding. Polymer melt temperature, polymer processibility, ram pressure, and molding cycle are the main parameters that are considered in injection molding. Polypropylene resin is an attractive choice for making injection molded parts for everyday life. Polypropylene parts are widely used in kitchen equipment, household appliances, toys, the shell of chairs, in automobile parts such as in wheel well liners, fenders, and trims, and is also a desired material to make disposable syringes to be used in the healthcare sector. Polypropylene is a preferred choice because of its good durability and stiffness, lightweight, low cost, and ease of molding. Figure 2.9 represents a schematic diagram of an injection molding machine.

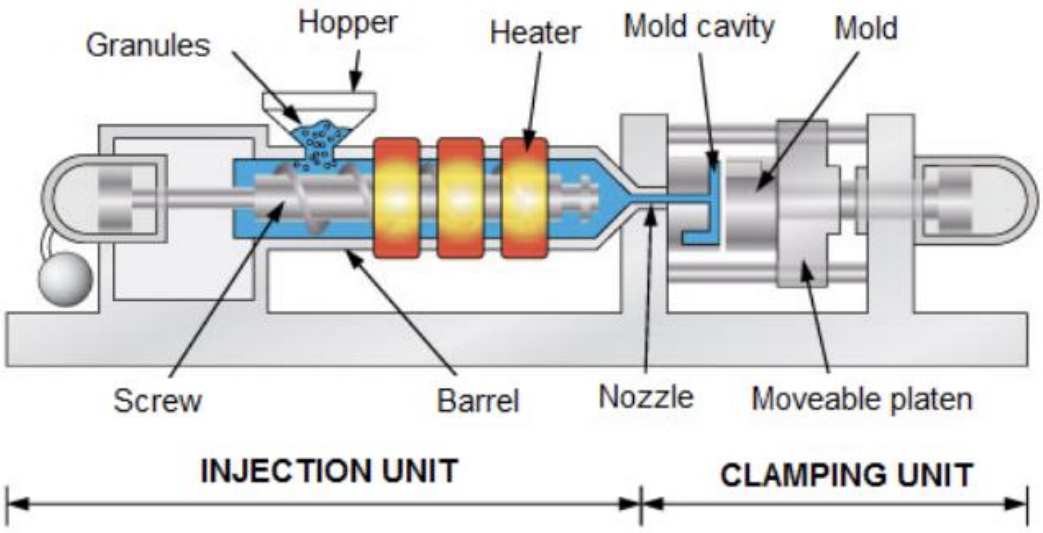


Figure 2.9 Schematic diagram of injection molding machine adapted from (Svečko et al., 2013), under the terms of the Creative Commons Attribution 3.0 License.

2.4 Thermoplastics in automotive application:

Plastics are an important part of the automotive industry. The use of plastics in automobiles is constantly increasing. The ease of processing plastics in complex shapes, their mechanical properties, low cost, and lightweight favors them over other materials. According to an estimation, a 10% reduction in vehicle weight reduces fuel consumption by 5% to 7% (Patil et al., 2017). Although using plastic parts reduces vehicle weight in addition to that it also provides some other advantages such as recyclability of parts, minimal corrosion, flexibility in integrating components, freedom of designing, and enhanced comfort and safety. Different plastics used for various applications are represented in Table 2.1.

Table 2.1 Thermoplastics and their applications in automotive, data from (Patil et al., 2017).

Thermoplastics	Automotive Application
Polyamide (PA)	Bearings, bushes, weatherproof coatings, and gears.
Polyvinyl chloride (PVC)	Pipes, electrical cables sheathing, instruments panels, door panels.
Polycarbonate (PC)	Headlamp lenses, bullet-proof glass substitute, bumpers.
Polypropylene (PP)	Cable insulations, automotive indoor and outdoor carpets, dashboard, bumpers, door panels, battery casing, fenders, mud flaps, radiator grills, Fascia panels, accelerator pads.
Acrylonitrile/Butadiene/Styrene (ABS)	Dashboards, vehicle body parts, door handles, door covers, wheel covers, ventilation system.
Polyethylene (PE)	Door panels, consoles, body side protective moldings, hand grips, boot interior, sound deadening, boot mats.
Polyoxymethylene (POM)	Fuel systems, speaker grills, aerosol valves, interior and exterior trims.
Polyethylene Terephthalate (PET)	Wiper arm, engine cover, headlamp retainer, engine cover.
Polybutylene terephthalate (PBT)	Door handles, carburettor components, locking system housings, fog lamp housing and bezels, sunroof front parts.

The use of plastic parts has now become inevitable in automotive industry. Polymers are superior to metals in terms of their easy processing, light weight, low cost, resistance to chemicals, noise reduction, wear resistance, vibration dampening, high temperature performance, high heat resistance and high flowability. An average vehicle weighs about 1200 kg and contains around 10

to 15% of plastic and plastic composite components. Although one car model may include up to 13 distinct polymers. About 66% of all plastic parts used in cars are made up of only three different types: polypropylene (32%), polyurethane (17%), and PVC (16%) (Patil et al., 2017).

This chapter will focus on polypropylene-based composite applications in automobiles. Although polypropylene is a versatile material, pure material cannot meet the requirements of advanced applications where lightweight and high mechanical properties are required. Therefore, polypropylene composites are the solution. The mechanical properties of polypropylene can be improved significantly by reinforcing it with natural (plant fibers) or synthetic fibers (glass fibers).

Currently, some automotive companies such as Ford, Audi, Volvo, BMW, Mitsubishi, Peugeot, Saab, Opel, Renault, Fiat, Daimler Chrysler, and Volkswagen are using natural fiber composites for different car parts such as underbody trim, headliner panels, spare tire cover, boot linings, side doors panels, consoles, dashboards, bumper, and seat back panels. For the dashboard, it is recommended that the material should be of high quality that can absorb vibrations and be highly resistant to wear. In addition to high-quality material, it should also be lightweight to improve the fuel efficiency of the vehicle. The recommended polymers for dashboards with highly resistant properties are polypropylene and polycarbonate. It was also found that recycled fiber composite's mechanical properties were higher than pure material. Research was also conducted on the use of natural fiber composites for bumpers. It was found that the energy absorption of a natural fiber composite bumper was similar to an aluminum bumper beam, but it was 56% lighter than an aluminum bumper and 78% lighter than a steel bumper (Fitri et al., 2021).

2.5 Glass Fiber Reinforced Thermoplastic Composites:

Glass fibers are the most common reinforcement material used in the polymer matrix. Glass fibers are a popular choice for reinforcing polymer matrix because of their low cost, high chemical resistance, high tensile strength, and good insulating properties. Glass fiber reinforced polypropylene composites are widely used in industries like aerospace, automotive, construction and in sports equipment. Two types of glass fibers that are commonly used are E-glass and S-glass. E-glass is the cheapest type of glass fiber and is widely used in different industries as a reinforcing material. S-glass is a special grade of glass fiber. It has the highest tensile strength and is used for developing missile casings and aircraft components. S-glass because of high manufacturing cost

and compositional differences is more expensive than E-glass (Etcheverry and Barbosa, 2012). Glass fibers have good dimensional stability and do not creep, and these qualities are transferred to composites that use glass fibers as reinforcement. Glass is a generally inert substance thus fibers are protected from chemical and solvent attacks as well as biological assaults.

The mechanical properties of glass fiber reinforced composites (GFRPC) depend on the properties of glass fiber, polymer matrix, fiber-matrix interface, and geometry, orientation, and distribution of reinforcement (Zhai et al., 2016). Usually, glass fibers are added in the 30-50 wt.% loadings (Yoo et al., 2011).

Investigation of tensile properties of polypropylene composites reinforced with short glass fiber (SGF/PP) and short carbon fiber (SCF/PP) was done by (Fu et al., 2000). It was observed that the addition of glass fiber significantly improved tensile properties as compared to neat PP. However, a slight increase in tensile properties was observed as fiber volume fraction increased from 8% to 25%. This behavior was reported due to a decrease in the mean fiber length of fibers as the volume fraction of fibers increased. This reduction in mean fiber length with an increase in fiber volume fraction affected the tensile properties of composites negatively. A similar was true for SCF/PP composites. Rahman et al. (2013) studied the effect of glass fiber volume fraction on the impact strength of GF/PP composite and found as volume fraction increased from 15 wt.% to 45 wt.% the impact strength of composite increased. However, fiber degradation was also observed during processing as fiber volume fraction increased.

Apart from fiber length and volume fraction, the effectiveness of glass fiber as a reinforcement also depends on the adhesion between polymer matrix and glass fibers. The mechanical strength of the adhesive bond between fiber and matrix is greatly affected by interfacial zone structure which is determined by the amount of molecular or local segmental polymer diffusion over the interface. Low diffusion will result in an interface with poor adherence. High adhesive strength can be anticipated only when there are significant polar contacts or chemical bonds present across the interface (Etcheverry and Barbosa, 2012).

To improve interfacial adhesion, several researchers have tried different fiber surface treatments and matrix modification. Luo et al. (2017) treated commercial glass fiber with a film former that contained a specific ratio of β-nucleating agent TMB-5 and maleic anhydride grafted

polypropylene (MPP) compatibilizer. Furthermore, the modification of the PP matrix was also done by adding MPP in different concentrations. It was observed that both the tensile and impact strength of polypropylene composite reinforced with 20 wt.% film former glass fiber and with 2wt.% MPP coupling agent (PP/2MPP/GFf) was enhanced by 100% and 178% as compared to polypropylene composite reinforced with 20 wt.% commercial glass fiber (PP/GFc). This remarkable improvement in mechanical properties was attributed to improved interfacial adhesion by MPP and the formation of β-transcrystallinity at the interface. This improved interfacial adhesion between PP and GF was also verified by SEM analysis of fractured surfaces. Debonding between fiber and matrix was observed in the PP/GFc composite whereas in the PP/GFf composite bonding was improved and a thin layer of PP was observed on the fiber surface. In PP/2MPP/GFf composite bonding was further improved and a thick layer of PP covering glass fiber was observed.

2.6 Natural Fiber-Reinforced Thermoplastic Composites:

Natural fiber composites have become a viable substitute for glass fiber-reinforced composites in numerous applications since the 1990s. Natural fibers such as flax have low density (1.5 g/cm^3) and low cost ($0.22 to $1.1/kg) as compared to glass fiber which has higher density (2.6 g/cm^3) and higher cost ($1.30 to $2.00/kg). Moreover, glass fiber production has a more severe impact on the environment. Non-renewable energy required for the production of glass fiber is 5-10% times more than energy required for natural fiber production. As a result, glass fiber production also produces significantly higher pollutant emissions than natural fibers. Another advantage of using natural fibers to reinforce composites is to achieve similar mechanical properties as from GFRP composites, higher volume fraction of natural fiber is required in composites. The volume and weight of the base synthetic polymer matrix employed in the composite are decreased because of the greater fiber volume fraction. The use of natural fiber composites in automobiles also improves fuel efficiency and reduces emissions due to their lightweight. NFRP composite (hemp/PP, hemp/epoxy, China reed/PP) car parts are reported to be 20-30% lighter than ABS and GFRP composite parts (Joshi et al., 2004).

Renewability, biodegradability, high specific strength, low-cost, and low-density characteristics of natural fibers makes them a superior choice for reinforcing thermoplastics. However, thermoplastics such as polypropylene are non-polar and hydrophobic in nature and natural fibers on the other hand are polar and hydrophilic in nature. Due to the presence of hydroxyl

groups and C-O-C connections on the surface of the natural fibers, there is a significant disparity in the surface energy of the two materials, which contributes to the poor bonding between the polymer matrix and fiber. This poor bonding results in poor mechanical properties of the composite material as stress cannot effectively transfer from matrix to fibers. Fiber reinforcing efficiency is determined by fiber-matrix contact and the capability to transfer stress from the matrix to the fiber (Jarukumjorn and Suppakarn, 2009).

The performance of composites is greatly influenced by interfacial bonding between natural fibers and polymer matrix. To enhance the interfacial bonding between hydrophilic natural fibers and hydrophobic polymers many researchers have used coupling agents and performed surface treatment of fibers by chemicals.

2.6.1 Chemical Treatments:

Plant fibers are composed of lignin, hemicellulose, and cellulose. Lignin enhances reactivity, thus allowing it to react to chemical alterations like acetylation more effectively. However, the main component of plant fibers that is considered essential for composite manufacturing is cellulose. Higher cellulose content means higher stiffness of fibers. Cellulose contains three hydroxyl groups in its structure, which form hydrogen bonds in macromolecular cellulose structure. While one of the hydroxyl groups forms intramolecular hydrogen bonds, the other two form intermolecular connections. The presence of hydroxyl groups on the fiber surface can form hydrogen bonds with interacting polymer matrix. However, fiber surfaces are covered with impurities such as waxy substances and pectin. These impurities hinder the interaction of fibers with the polymer matrix. Chemical treatments can remove these impurities and can make the fiber surface rougher. Higher surface roughness provides higher anchorage points available for mechanical interlocking with polymer matrix which then results in improved interfacial bonding (Mwaikambo and Ansell, 2002). Some of these chemical treatments and their effects are summarized in Table 2.2.

Table 2.2 List of different chemical treatments employed to process natural fibers adapted from (Sun, 2018), under the terms of the Creative Commons Attribution 3.0 License.

Treatment method	Treatment effect
Alkaline treatment	Extractable materials, such as lignin, waxes and oil covering materials are removed, the fiber surface becomes cleaner and more uniform
Silane treatment	Forms a chemical link between the fiber surface and the matrix and improves the fiber matrix adhesion
Acetylation treatment	Provides rough surface topography with less number of void contents
Benzoylation treatment	Enhances the thermal stability and moisture resistance of the fiber
Peroxide treatment	Reduces the moisture absorption tendency by the fiber and improves thermal stability
Maleated coupling agents	Improves the wettability of the fiber and enhances the interfacial adhesion
Sodium chlorite treatment	Removes moisture and enhances the hydrophobic nature of the fiber
Acrylation and acrylonitrile grafting	Reduces the hydrophilic hydroxyl groups from the fiber structure and improves the moisture-resistance property
Isocyanate treatment	Enhances thermal stability and the moisture-resistance property of the fiber
Stearic acid treatment	Improves dispersion and water-resistance properties
Permanganate treatment	Reduces the hydrophilic nature of the fiber and enhances the thermal stability
Triazine treatment	Increases the moisture-resistance properties
Fatty acid derivate treatment	Improves the wetting and adhesion of the fiber surface into the matrix
Fungal treatment	Produces a rough interface for better interlocking with the matrix

Alkaline treatment also known as mercerization of natural fibers is one of the most common chemical treatments. Alkaline treatment improves surface roughness by removing impurities from fiber surface and disrupting hydrogen bonding in network system. Alkali treatment also cause depolymerization of cellulose and reveal short cellulose, this improves mechanical properties of fibers. Moreover, hydroxyl groups present on natural fiber are also ionized to alkoxide by aqueous NaOH. Following equation represents reaction of NaOH with fibers (Li et al., 2007; Mwaikambo and Ansell, 2002; Sun, 2018).

$$Fiber - OH + NaOH \longrightarrow Fiber - O - Na + H_2O$$

Cai et al. (2016) investigated the effect of 5, 10, and 15 wt.% NaOH treatment for 2 hours on abaca fibers reinforced epoxy composites. The authors observed from SEM analysis of abaca fibers that after alkali treatment hollow lumen present in untreated fiber had disappeared as shown in figure 2.10. It was postulated that inclusion of sodium ion in cellulose structure broke the bonds between cellulose sheets and caused swelling of fiber which collapsed lumen. Moreover, as NaOH concentration increased, fiber experienced more shrinkage and weight loss. They found that 5 wt.% NaOH treated abaca fiber composites tensile strength and young modulus increased by 8 and 36% as compared to untreated fibers. However, 10 and 15 wt.% treated fiber composites had slightly lower tensile strength, but their Young's modulus were decreased by 34 and 49%. It was concluded that lower concentration of NaOH treatment produced fibers with minimum fibrillation and high cellulose crystallinity. Whereas high concentration of NaOH treatment reduced cellulose crystallinity and increased fibrillation and this surface change caused poor adhesion of fibers with epoxy resin which resulted in poor mechanical properties.

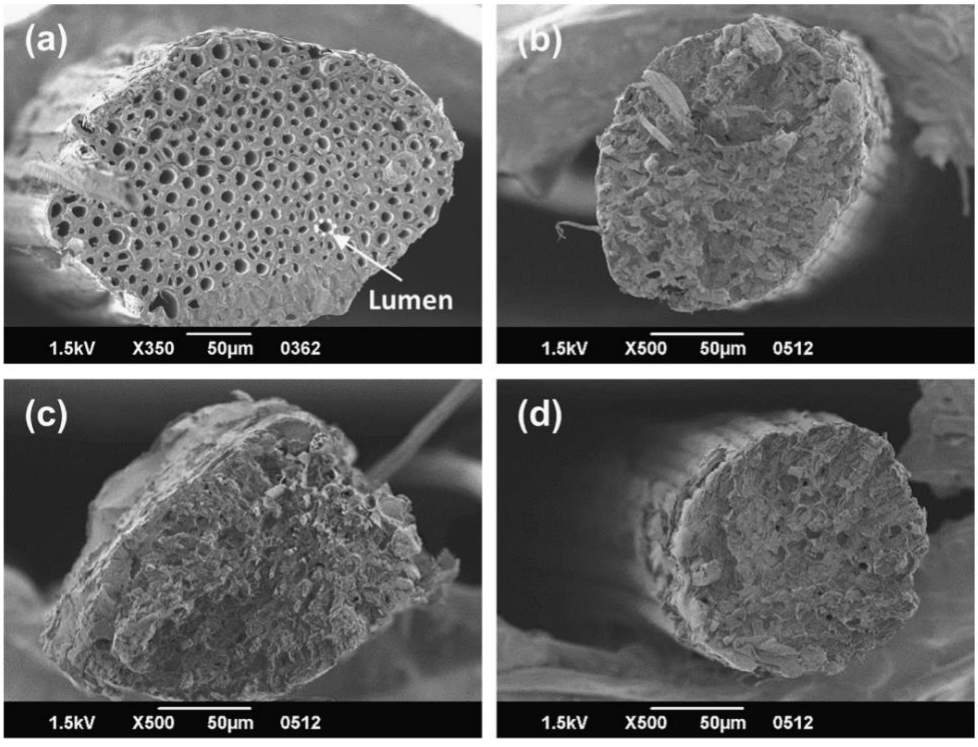


Figure 2.10 SEM analysis of abaca fiber, a) untreated fibers, b-d) fiber treated with 5, 10 and 15 wt.% NaOH, adapted from (Cai et al., 2016), under Elsevier license

Nam et al. (2011) investigated the effect of 3, 5, and 7 wt.% NaOH treatment on surface morphology and mechanical properties of coir fiber and coir fiber reinforced poly(butylene succinate) composites. The effect of different fiber mass content (10-30%) on the mechanical properties of composites was also investigated. It was found that at 5% NaOH concentration, globular particles present on the fiber surface were removed in great proportion making the surface rougher, and tensile properties were also increased. The tensile modulus and strength of fibers increased by 113% and 71% when treated with 5% NaOH solution for 72 hours. They observed that further increases in NaOH concentration and soaking time made the fiber surface smoother by removing all the globular particles and decreasing their mechanical properties. They concluded that 5% NaOH treatment for 72 hours was optimum. They then prepared composites with a different mass content of untreated and 5% alkali-treated fibers and found that composites with 25% fibers exhibited the highest tensile and flexural properties due to adequate wetting of fibers. The mechanical properties of alkali-treated fiber composites were significantly higher than untreated fiber composites.

2.6.2 Coupling Agent:

Apart from the chemical treatment of fibers, another effective method of increasing bonding between natural fibers and the polymer is to add a coupling agent such as maleic anhydride to the polypropylene matrix. The responsibility of the coupling agent is to increase compatibility between fiber and polypropylene. Polypropylene chains bond with MA to create maleic anhydride grafted polypropylene (MAPP). MAPP then serves as a connection between nonpolar matrix and polar natural fibers. MAPP interacts with unreactive polypropylene matrix by forming chain entanglements and the natural fiber surface reacts strongly with the MA functional group to form hydrogen and covalent bonds. The mechanical properties of the material up to and above the glass transition temperature are significantly influenced by the polymer chain entanglement. Extensive research has been done on the effect of MAPP in natural fiber-reinforced polymer composite. It has been reported by many researchers that the addition of MAPP increased mechanical properties and reduced water absorption of composites.

Sullins et al, (2017) investigated the effect of 5% NaOH treated hemp fiber and addition of 5 wt.% MAPP on mechanical properties of 15 and 30 wt.% hemp fiber reinforced polypropylene composites. They found that both NaOH treated fiber composites and MAPP coupling agent

composites had higher mechanical properties then composites with untreated fiber and no MAPP. The composites with 30 wt.% fiber had significantly higher tensile and flexural properties because of adequate dispersion and wetting. Their main finding was that in composites effect of the MAPP coupling agent was higher than NaOH treatment of fibers. The composites with 5 wt.% MAPP and untreated fibers regardless of their fiber volume fraction exhibited better interfacial bonding and mechanical properties as compared to other material variances such as NaOH-treated fiber composites.

In another study, the effect of different concentrations of MAPP (2, 3, 5, and 7 wt.%) was investigated on the properties of 30 wt.% cellulose reinforced (PP-cellulose) and oil palm empty fruit bunch fiber reinforced polypropylene (PP-EFBF) biocomposites. It was observed that the addition of MAPP up to 2 wt.% significantly increased the tensile and impact strength of PP-EFBF composites, further increase in MAPP concentration exhibited a decrease in mechanical properties. However, the flexural modulus of both PP-cellulose and PP-EFBF decreased by the addition of MAPP. It was postulated that composite stiffness is reduced because of the plasticizing effect of low molecular weight MAPP. Moreover, the mechanical properties of PP-cellulose composites were higher than PP-EFBF composites and no significant effect of MAPP was observed on PP-cellulose composite properties which indicates that MAPP is more efficient with lignocellulosic fibers (Khalid et al., 2006).

2.7 Industrial Hemp:

Industrial hemp is one of the oldest cultivated crops in the world. It is typically planted for its fiber and seeds. Industrial hemp is a kind of cannabis but with a low THC content of <0.3%. Hemp fibers have been in use for many centuries for different applications such as in textiles, paper, biocomposites, energy, medical use, and the food industry. The paper used in the first copies of the Bible was made from hemp fiber (Manaia et al., 2019).

Hemp crop in a whole contains stalk, leaves, and flowers. The hemp stalk on the outside is covered with epidermis also known as bark and inside it is divided into two parts, the outer bast fiber layer and inner woody core also known as hurd. Hemp stalk contains around 35% bast fiber and 65% hurd fiber. Hemp plant is mainly cultivated to obtain bast fiber. Bast fiber because of their higher mechanical properties and high cellulose content have been interest of various

industries. Hurd fiber on the other hand was treated as a waste material but now extensive research is being done to utilize them. Bast fiber consists of 57-77% cellulose, 9-14 % hemicellulose, and 5-9% lignin whereas hurd fiber consists of 40-48% cellulose, 18-24% hemicellulose, and 21-24% lignin (Bokhari et al., 2021). Figure 2.11 represents the structure of the hemp stem and fiber. Hurd fibers are present in the woody core of xylem tissue and bast fibers are present in the primary and secondary layers of phloem. Figure 2.11 c) represents a typical structure of bast fiber. It has a multi-layered cell wall structure which consists of a primary cell wall and a secondary cell wall. The secondary cell wall is made of three layers S1, S2, and S3. The S2 layer is thickest and has high strength because of the presence of high cellulose content at about 50% (Manaia et al., 2019).

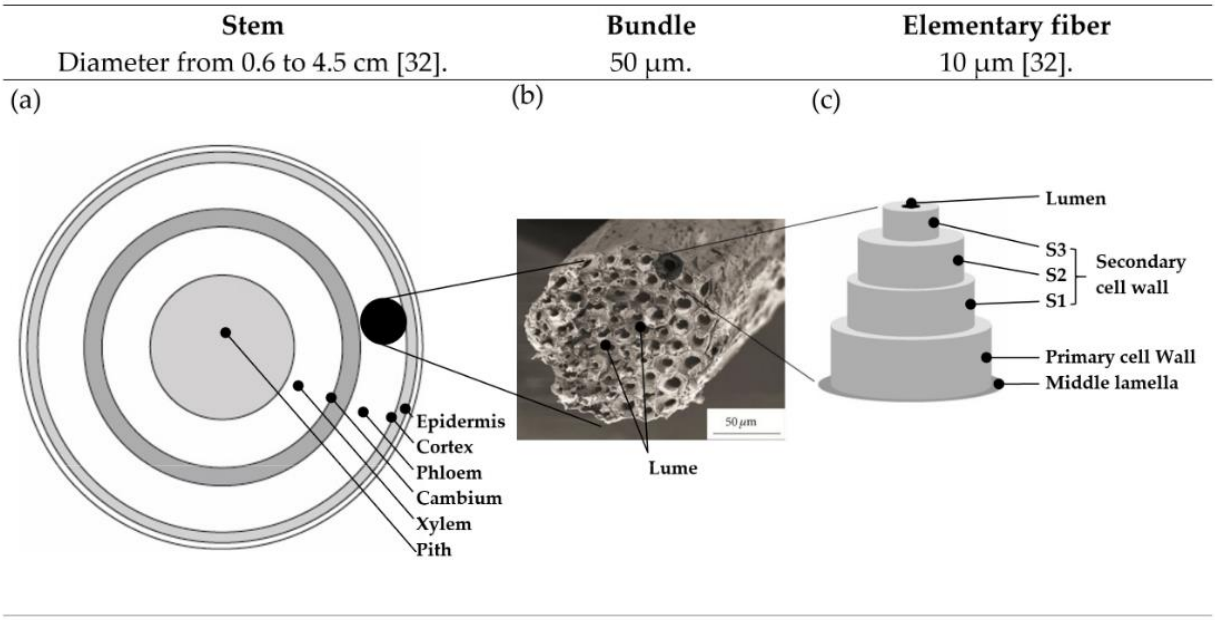


Figure 2.11 Structure of hemp stem and fiber, a) longitudinal hemp stem section, b) hemp fiber bundle morphology, c) depiction of hemp bast fiber, adapted from (Manaia et al., 2019) under the terms of the Creative Commons Attribution 3.0 License.

Hurd fibers are short and have low mechanical properties and cellulose content as compared to bast fiber. However, their low density of 0.24-0.26g/cm^3 makes them useful for lightweight and insulation applications. Hemp hurd has higher cellulose content and lower lignin content than wood which can replace wood in wood/polymer composites and can produce low-weight composites with enhanced mechanical properties than wood/polymer composites (Li et al., 2017a).

Because of the hollow structure of hurd fiber, it can be also used as a sound-absorbing material. Su et al. (2022) prepared hemp stalk/polycaprolactone sound-absorbing composites. They investigated the effect of different fiber sizes (1, 6, and 11 mm), different fiber mass fractions (30, 40, 50, and 60%), and different thicknesses (1, 1.5, 2, and 2.5 cm) of material on sound absorbing properties of composites. Their results depicted that when sound energy strikes the hemp stalk, the force between the chain segments, the distinctive hollow structure, and the large specific surface of the hemp stalk all work together to attenuate the sound energy and transform it into heat and mechanical energy during the propagation process, producing a good sound absorption effect. They concluded that hemp stalk reinforced polycaprolactone sound-absorbing composites with 6 mm fiber size, 50% fiber loading, 1.5 cm thickness, and 0.3 g/cm^3 density exhibited the highest sound-absorbing properties with an average sound absorption coefficient of 0.44, noise reduction coefficient value of 0.42 and highest sound absorption coefficient value of 1.00. They also concluded that the sound-absorbing properties of hemp stalk at low frequencies are not very good. With their results, they confirmed that waste hemp stalks have good sound-absorbing properties due to their structure.

Hemp bast fibers are long fibers, that have high cellulose content, low lignin content, long cell length, low microfibrillar angle, and high mechanical properties. These properties of hemp bast fiber make them highly useful for a wide range of high-performance applications. Among natural fibers, hemp bast fibers have high strength and stiffness. They have specific stiffness comparable to glass fiber. Hemp bast fibers have higher mechanical properties than other natural fibers except flax and ramie fiber. Flax fibers have relatively higher properties than hemp fiber, but hemp fibers are cheaper, easier to grow, require minimum water, require no pesticides, and produce a higher quantity of fibers as compared to flax fiber. Table 2.3 represents the chemical composition and mechanical properties of plant and glass fibers. Table 2.4 represents the advantages and disadvantages of hemp fiber over other natural fibers.

Table 2.3 Chemical composition of different plant fibers and mechanical properties of plant fibers and glass fibers. Data from (Manaia et al., 2019)

Fiber	Lignin (%)	Hemicellulose (%)	Cellulose (%)	Density (g/cm^3)	Length (mm)	Young's Modulus (%)	Tensile Strength (MPa)	Specific Stiffness (E/ρ) (GPa)
Hemp	3.5-5.7	15-20	70-74	1.4	5–55	30–70	550–1110	21–50
Flax	2-2.2	18-20	64-72	1.5	5–900	27–80	345–1830	18–53
Jute	12-13	18-22	61-72	1.3–1.5	2–120	10–55	393–800	6–34
Sisal	8	10	78	1.3–1.5	900	9.4–28	507–855	6–18
Ramie	0.4-0.9	5-15	69-91	1.5	900–1200	44–128	400–938	29–85
E-glass				2.5	Continuous	70	2000–3000	28

Table 2.4 Advantages and disadvantages of hemp over other natural fibers, data from (Sen and Reddy, 2011).

Advantages	Disadvantages
1. Hemp produces strong fibers with tensile strength ranging between 550 – 1110 MPa. 2. Hemp plants grow faster than other natural fibers. Hemp plants are ready to harvest after 3 months. 3. Hemp produces more fibers per acre than trees. 4. Hemp does not require any pesticides and require very little use of fertilizer. 5. Hemp yarn is robust and has the highest water resistance of any natural fiber. 6. Compared to kenaf, hemp requires less moisture to grow. 7. Hemp generates more fiber than most other fiber crops in regions typically north of the 40th latitude, typically outpacing flax by 10%. 8. Hemp has modest net nutritional requirements and requires little cultivation when the leaves are removed properly.	1. Separation of bast fibers is a labour-intensive process. 2. Growing restriction of hemp in different parts of world. 3. Low bast fiber content than flax and kenaf.

Bast fibers of hemp are separated mechanically or manually, this process is known as decortication. Before decortication, the hemp stem is subjected to a microbial process known as retting to loosen bonds between fibers and separate the fiber bundle from the central stem. There are several different retting processes among them the most common is dew retting. In this process after harvesting, the plants are spread out evenly in the field to let microorganisms attack and separate fibers from the xylem and cortex. To ensure uniform retting, plants are turned over regularly. Also, to prevent microorganisms from breaking down cellulose, the process is monitored carefully and is stopped at the appropriate time. The optimum time of the whole process depends on weather conditions, usually, it takes 3-6 weeks. If plants are subjected to retting more than the required time then microorganisms will degrade cellulose and reduce the mechanical performance of fibers, this phenomenon is called over-retting. Although the dew retting process is favored by farmers because of low labor cost, it requires appropriate temperature ranges and moisture due to which this process cannot be utilized worldwide (Ramesh, 2018).

2.8 Particle Size Enlargement:

Natural fibers have low bulk density. This creates challenges for transportation, storage, and handling. It is difficult to feed natural fiber materials with low bulk density inside polymer processing equipment like extruders for compounding with polypropylene. This section will review the processes and mechanism of particle size enlargement to provide background knowledge for increasing the bulk density of natural fibers using pelletization.

2.8.1 Overview:

Size enlargement is a process in which through compaction or agglomeration, fine particles are formed into large permanent masses in which original particles can still be observed. Size enlargement enhances the effectiveness of fine materials either in downstream processing step or as a finished product agglomerate. Usually, the initial material is in the form of fine powder which is then agglomerated into large agglomerates in which original small particles can still be identified but this is not true in some cases such as in manufacturing of amorphous agglomerates by cooling molten material. Size enlargement processes have been utilized for hundreds of years for different applications such as manufacturing of clay bricks from fine clay particles for construction application, manufacturing different items from metal powder, and making solid tablets of

medicinal agents. Today, size enlargement processes are widely utilized in many industries. The objectives of size enlargement are as follows, (Capes, 2013; Green and Southard, 2019)

1. Elimination of risks or losses associated with dust handling, as in the briquetting of waste particles.
2. Product renewal or improved product appearance.
3. Providing a predetermined quantity to make dispensing and measuring easier, as in the case of medicinal tablets or granules of agricultural chemicals.
4. Production of structurally usable forms, such as the pressing of complex shapes in powder metallurgy.
5. Reducing lump formation and caking, as in fertilizers granulation.
6. Increased bulk density for tableting feeds, easy storage, and easy transportation.
7. Enhanced flow properties, as in granulation of ceramics for pressing or pharmaceuticals for tableting.
8. Reduced handling risks, especially when working with unpleasant powders like caustic flaking.
9. Control of solubility such as in instant food products.
10. Control of surface-to-volume ratio such as with catalyst supports.
11. Improvement in the heat-transfer properties of materials like ores or glass for furnace feed.
12. Formation of non-segregating mixtures of powder ingredients containing uniformly distributed main ingredients such as in pharmaceutical granules or agricultural chemicals.
13. Removal of particulates from liquids such as in the flocculation of clay particles with the use of polymeric additives.

There are many ways to induce agglomeration. It is possible to atomize a slurry or solvent onto the bed of particles to coat either the particle or granule surfaces. On the other hand, the spray drops might create tiny nuclei that eventually clump together. A binder in solid form might also be in powder feed as one of the components or it might be dissolved in slurry or solvent. In the case of soluble particles, the solvent alternatively may cause dissolution and recrystallization. Heat can also cause agglomeration by either causing controlled sintering of the particle bed or by partially melting a feed component that serves as a binder. Agglomeration can also be achieved by applying excess pressure to create compacts like briquettes (Green and Southard, 2019).

2.8.2 Mechanisms of Size Enlargement:

2.8.2.1 Binding Mechanisms:

In densified products, the physical forces binding the particles together determine the durability and strength of agglomerates. The binding forces present between individual particles of agglomerates are as follows (Green and Southard, 2019):

Solid Bridges: Solid bridges between particles can be formed by solidification of bonding agents such as resin and glue, by crystallization of substances dissolved in feed during drying, or by sintering of ores. The common examples of this are briquetting of plastics and metals, cement binders used for flue dust pellets, iron ore pellets induration, and salts crystallization in fertilizer granulation.

Liquid Bridges: Liquid bridges induce cohesion through capillary suction and interfacial forces. The saturation level affects how strong the liquid bridges are in a granule. In granules, the state of saturation determines the strength of liquid bridges. Figure 2.12 represents several different states that can be identified when a liquid is used to hold an assembly of particles together. When a very low amount of liquid is used the saturation state is called the pendular state in which liquid remains trapped at the particle's point of contact as discrete lens-shaped rings. As liquid quantity increases it assumes a funicular state in which liquid rings merge and form a continuous network of liquid with air gaps between them. When all air gaps are eliminated from the agglomerate capillary state is achieved. The strongest particle strength is often observed in the capillary condition. The strength of liquid bonds is greatly influenced by liquid viscosity. With further increase in liquid content beyond capillary state the granule will be converted into a liquid droplet with powder suspended in it and will exhibit weak strength similar to that of liquid droplet. Lastly, poorly wetting solids may generate pseudo-droplets with air entrapped inside of them.

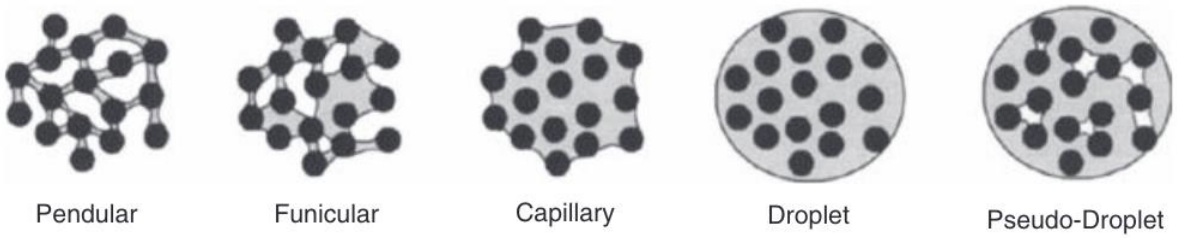


Figure 2.12 Different saturation states of liquid-bound granules, adapted from (Green and Southard, 2019)

Intermolecular and electrostatic forces: Very fine particles with diameters less than 1 μm can be bonded together into agglomerates under agitation by intermolecular and electrostatic forces without forming any material bridges. However, with large particles, these forces are insufficient to form agglomerates because of particle weight. High compaction pressures flatten interparticle interactions plastically and significantly increase short-range forces. The adhesion of fine particles during flow, handling, and storage is a common example of this mechanism.

Mechanical Interlocking: This mechanism refers to shape-related bonding which is the entanglement of fibrous particles during compression or agitation. The effect of mechanical interlocking on the strength of agglomerates is very little.

2.8.2.2 Compaction Mechanism:

In this size enlargement method, particles are compacted and densified by forcing them together in a confined space using external forces. Initially, when external forces are applied at low stress levels, it first reorganizes particles eliminating any macrovoids between them. After that, as external stress is increased, the microvoids between particles are eliminated as particles undergo elastic deformation to accommodate additional densification and strain. To this point, the increased density can be reversed by removing applied stress and stirring the powder. If further stress is applied, particles undergo plastic deformation or fragmentation. In the case of plastic deformation, the contact area between particles increases which increases the compact's bulk cohesion. The fragmentation of particles broadens their size distribution, allowing fine particles to fill the microvoids and increase contact area between particles and contact density for cohesion. If applied stress is further increased beyond this point, the density of compact will get closer to true density of material.

In industrial unit operation, the key steps involved in densification are as following, (Green and Southard, 2019).

Powder Filling: Compact weight variability and powder filling are greatly influenced by powder flowability, bulk density, powder-tool wall friction and any contributing feed segregation tendencies. If flowability of powder is poor, then weight of final product will be inconsistent. For example, in briquetting or roll pressing, the density of final product might be inconsistent if feed material exhibits poor flowability.

Stress application and removal: Increase in stress results in increase in density. Some equations representing powder compaction in cylindrical die cavities are shown in table 2.5. However, no one acceptable equation is present to represent all situation. In high-capacity rotary equipment, the impact of variables like equipment size and the design of the compacting surfaces further complicates the situation.

Table 2.5 Equations used to represent powders compression, adapted from (Capes, 2013).

Equation	Materials Used
$\log p = mV_R + b$	Particles of sodium chloride, sulfur and T.N.T. Range of non-metallic powders.
$\frac{V_0 - V}{V_0 - V_s} = a_1 \exp(-k_1/p) + a_2 \exp(-k_2/p)$	Four ceramic powders.
$\log \frac{1}{1-\rho_R} = mp + b$	Polystyrene Particles and variety of metallic powders.
$\log p = m \log \rho_a + b$	Industrial metal powders

Nomenclature:
p = pressure applied to the compact
V = compact volume at p
V_0 = compact volume at zero pressure
V_S = volume of solid material (void-free)
$V_R = V/V_S$
ρ_s = true density of solid material
ρ_a= bulk or apparent density of compact

$\rho_R = \rho_a / \rho_s$
m, b, k_1, k_2, a_1, a_2 are constants.

Ejection: When stress is removed, the compact undergoes expansion because of the remaining plastic recovery of powder. This recovery is influenced by the elastic modulus of the compacted materials as well as any entrapped air that may still expand. This expansion can cause flaw development and loss of bonding between particles. Compact ejection is the final step of stress removal in which any leftover elastic stresses are eliminated. If elastic recovery is significant than fracture and delamination of strain will be caused by strain gradient.

2.8.3 Extrusion Presses:

In this size enlargement method, the material is formed and compacted by pressing through an orifice or die. The feed suitable for this process is that responds to mechanical heat and pressure to develop into a cohesive, sticky mass during extrusion. Optimal agglomeration and cohesion by pelleting depends on the following factors (Capes, 2013),

1. Particle size distribution
2. Moisture content
3. Operating temperature
4. Use of lubricants or binders

2.8.3.1 Roll-type extrusion presses (Pellet mill):

The biomass compaction into pellets and briquettes is an old process known for more than 130 years (Stelte et al., 2012). Pellets mills are widely used to compact large quantities of material at low cost, but the final product is less uniform as compared to tableting and molding presses. These machines compact material caught in the nip between rollers by forcing material in a plastic state through a die or orifice. Friction is produced between biomass and the steel surface of the die due to which heat is generated which facilitates biomass compression. Once plasticized material is forced through the holes, adjustable knives are used to cut rod-like extrudate into pellets of the required length. The optimum pressure required for compaction is determined by calculating the resistance of material through the holes which is a function of the length of the hole divided by the diameter of the hole raised to a power of three. The pellet mill consists of two main elements: a

die with holes that serve as the mold and the rollers that press the raw materials through the die holes. To meet specific product requirements different roll die thicknesses, special tapers, and entrance characteristics are in use.

The two most popular pellet mills are flat die and ring-type die pellet mills. Flat die pellet mill has a flat horizontal surface with holes in it and rollers are running on top of it pushing the material through the die. This type of mill is used for small to medium-scale operations. Ring-type die pellet mill has a round die with holes in it and two or three rollers mounted in a vertical plane. When operated, the die rotates around fixed rollers which force the material through the die holes. This type of pellet mill is used for medium to large-scale operations. Figure 2.13 represents schematics of flat die and ring-type die pellet mills.

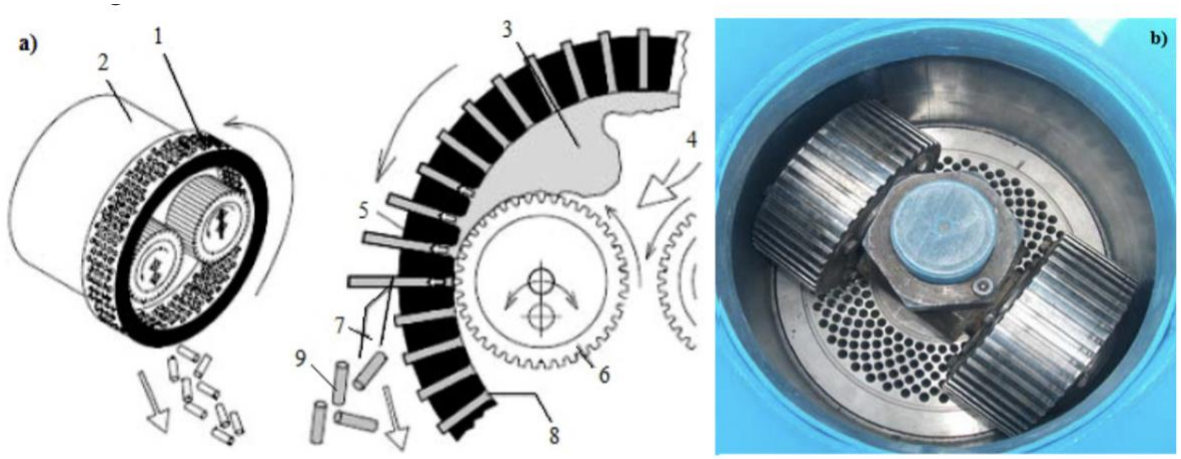


Figure 2.13 Schematic of Pellet Mills, a) Ring-type die pellet mill b) flat die pellet mill, 1. ring type die; 2. gear; 3. crushed material; 4. material input; 5. die; 6. rollers; 7. knife/cutter; 8. die hole for compressing pellet; 9. pellets, adapted from (Zabava et al., 2018)

Moreover, the uniform feeding of material over the die surface is crucial for optimal pellet mill functioning. Impellers in the feed chute may be used to disperse the material equally and accelerate the material entering the die speed. Plows are also employed to provide uniform distribution, these are placed next to the die surface and are integrated with the roller assembly (Capes, 2013; Green and Southard, 2019).

2.8.4 Characterization of Pellets:

To determine the efficiency of inter-particle bonds formed during compaction of biomass material, the pellets are subjected to some mechanical tests that are discussed below.

2.8.4.1 Compressive Resistance:

A common measure used for evaluating the quality of agglomerates is compressive resistance. This test is used to stimulate the compressive stress applied on the pellets due to the weight of top pellets during storage in silos and when crushed in a screw conveyor or chewed by the animals. The compressive resistance (or hardness or crushing resistance) is the highest crushing load a briquette/pellet can withstand before breaking or cracking. This test provides a fast assessment of the pellet quality as soon as they leave the pellet mill, and it also helps in modifying the pelleting process to enhance the quality of the pellets. A diametrical compression test is used to measure compressive resistance in which individual pellets are placed in between flat parallel plates that have surface areas greater than the briquette/pellet. A load is applied at a constant increasing rate until the pellet breaks or cracks. That load at which a pellet fractures is the compressive strength of the pellet and is reported as stress or force.

Different test apparatuses have been used to measure the compressive strength of pellets such as Stokes tester, Kahl tester, tablet hardness tester, Schleuniger tester, Kramer shear strength tester, and universal testing machine. It is important to note that this test only determines the compressive strength of pellets, it does not reveal the dusting potential of briquettes/pellets during storage, handling, and transportation (Kaliyan and Vance Morey, 2009).

2.8.4.2 Durability:

Durability test also known as abrasive resistance test simulates handling of pellets via either pneumatic or mechanical means. It can be characterized as the pellet's capability to withstand shock and vibrations. In the feed industry, pellet durability indicates the quality of the pellet. High durability means high-quality pellets. Different equipment such as Holman tester, Ligno tester, and tumbling can have been used to measure the durability of pellets.

In the tumbling can method the pellet durability index (PDI) is determined. This test replicates the mechanical handling of pellets and predicts any potential fines that may result from

that handling. In this method, 500 g of pellets after sieving are fed into the test chamber of the tumbling can and then it is rotated for 10 minutes at 50 rpm. The pellets abrade and create fines due to the shearing and impact of pellets with each other and with the walls of the test chamber of the tumbling can. After 10 minutes, the pellets are carefully collected and sieved with a sieve size that is roughly 0.8 times the diameter of the pellets and weighed again. The pellet durability index is than calculated using the following formula,

$$Pellet\ Durability\ Index = \frac{weight\ after\ tumbling}{weight\ before\ tumbling} \times 100$$

The tumbling can is the most used method for determining durability in feed manufacturing industries in U.S (Kaliyan and Vance Morey, 2009). The tumbling can process has been modified by certain feed mill operators who include steel nuts, bolts, or ball bearings in the tumbling can before the pellets are tumbled. Using the modified procedure, very hard pellets, such as those used in dairy feed, have been tested. The durability of pellets is considered low if it is below 70 %, medium if it is in between 70 - 80 % and high if it is above 80 % (Younis et al., 2018).

Apart from compressive resistance and durability of pellets some other tests of pellets are also caried out. Bulk density of pellets is another important property of pellets. It refers to biomass pellets mass per unit volume. It is measured using following equation,

$$Bulk\ Density\ (\rho_{bulk}) = \frac{mass\ of\ pellets\ (kg)}{volume\ of\ beaker\ (m^3)}$$

Bulk density also reflects quality of pellet. Higher the bulk density lower the transportation and storage cost and higher energy output and combustion efficiency (Zabava et al., 2018).

Impact resistance is another pellet quality test. This test replicates stresses experienced by briquettes/pellets when they are dropped from a certain height onto a flat surface such as emptying

of pellets from trucks onto ground. In this test, test specimen is dropped from a certain height several times and then impact resistance index (IRI) is calculated using following equation,

$$IRI = \frac{(N \times 100)}{n}$$

Where,

N = number of drops

n = number of pieces after N drops

All above-mentioned pellet characteristics are influenced by several factors during processing. These factors and their influence on pellet quality are explained in detail in next section.

2.8.5 Factors Affecting Pellet Quality:

2.8.5.1 Effect of Moisture Content of Feed on Strength of Pellets:

Water serves as a lubricant and a binding agent. Water increases the contact area between particles and enhances van der Waals' forces between them. When feed contains water-soluble ingredients such as sodium phosphate, potassium salt, calcium chloride, starch, sugar, and soda ash, water helps briquetting. It has been shown by several studies that the durability and strength of pellets increase with increasing moisture content until it reaches an optimum level. Water is incompressible, a high moisture content above optimum level might prevent particles from undergoing complete flattening and releasing natural binders. The optimum level of moisture content is different for different biomass materials. Feeds with high fiber content are not able to absorb high moisture so the water remains on the particle's surface providing extra lubrication between particles during pelletization. This causes the pellets to extrude faster at the center than the exterior and forms a "Christmas tree" shape of pellets which reduces their durability.

The effect of moisture content on the mechanical properties of both oak sawdust and pine sawdust logs prepared at 138 MPa pressure was studied (Li and Liu, 2000). It was found that when the initial moisture content was less than 4%, the prepared logs could not maintain their quality and started to expand by absorbing moisture from air due to which they became fragile after a few days. The logs prepared with initial moisture content above 13% exhibited low density and were

easily disintegrated when small handling forces were applied. Logs made with an initial moisture content of 8% exhibited both long-term performance and high density.

Frodeson et al. (2019) prepared pellets from four different polysaccharides and three different kinds of wood such as beech xylan, hemicellulose–locus bean gum mannan, cellulose-Avicel, apple pectin, pine, beech, and spruce. They investigated the effect of different moisture content from 0 - 15% on the hardness and density of pellets along with the compression force and frictional force required to prepare them. They found that with an increase in moisture content up to 9-10% the energy requirement of compressing xylan increased and above 10% moisture content it decreased. Also, for xylan, compression time increased with an increase in moisture content whereas for locus bean gum, spruce, and beech the compression time reduced with an increase in moisture content. The effect of moisture content on the density and hardness of pellets varied more for polysaccharides than for wood pellets. The maximum density and hardness among polysaccharides were exhibited by Avicel at the moisture content of 8%. For all wood pellets, the optimal moisture content to achieve the highest density was in the range of 5-8% however for hardness optimal moisture content was different for different woods. For pine, it was 5-9%, beech 8-11%, and spruce 6-10%.

2.8.5.2 Effect of Particle Size of Feed:

Feed particle greatly influences the durability of pellets. Generally smaller the particle size higher the durability. Fine particles because of their high surface area tend to absorb more moisture than large particles and, therefore, can undergo a greater degree of conditioning. The presence of large particles in pellets is disadvantageous because large particles act as fissure points, causing pellets to crack and fracture. Many researchers have suggested different particle sizes of different feed materials for achieving higher durability. It has been suggested that particle size to produce durable pellets should be 0.5-0.7 mm and particle size above 1 mm can act as the pellet's predetermined breaking point (Kaliyan and Vance Morey, 2009; Williams et al., 2018; Younis et al., 2018). Although fine particles can produce durable pellets but due to the increased cost of the process fine particles are undesirable. A wide particle size distribution can also produce high-quality pellet because the particle mixture will produce interparticle bonding with almost no interparticle gaps.

In one of the studies, Harun and Afzal (2016) prepared pellets with wood biomass, pine and spruce, and different agricultural biomasses such as timothy hay, reed canary grass, and switchgrass. They investigated the effect of three different particle size ranges (150 - 300 μm, 300 - 425 μm, and 425 - 600 μm) on the density and yield stress of pellets. They found that pellets with a particle size range of 150 – 300 μm exhibited the highest density and yield stress. They concluded that the pellet's mechanical properties were dependent on particle size and pellets produced with smaller particle sizes are stronger than pellets with larger particle sizes.

In another study, Zafari and Kianmehr (2014) investigated the effect of different particle sizes (0.3, 0.9, and 1.5 mm), moisture content (35%, 40%, and 45%), die length (8, 10, and 12 mm) and piston compaction speed (2, 6 and 10 mm/s) on durability and compressive strength of municipal solid waste pellets. They found that pellets with smaller particle sizes exhibited greater compressive strength and durability than pellets with large particles. Pellets prepared with small particle size (0.3 mm) and with initial moisture content between 40-43% displayed the highest durability and compressive strength than other pellets. They concluded that raw material moisture content and particle size had a significant effect on pellet properties, however, die length and piston speed effect was negligible.

2.8.5.3 Effect of Additives or Binders:

Additives and binders in the range of 0.5-5% are used to enhance the mechanical properties of pellets when pellets quality is poor and is not able to meet required quality standards. A binder either in solid or liquid form has the ability to form bridges or cause chemical reactions to enhance bonding between particles and improve pellet quality. Preheating or steam conditioning of feed is important to provide moisture and heat to activate the embedded or additional binders. Binders are also added to produce high-quality pellets and reduce process energy consumption. According to European specifications, a maximum of 2 wt.% of binders are allowed to be used in the production of biomass pellets (Younis et al., 2018). In the animal feed industry, the most used binders are lignosulfonates, molasses, proteins, starches bentonite, and modified cellulose binders. Environmental friendliness and cost of the binders are the primary factors in the selection of binders.

Ahn et al. (2014) investigated the effect of different organic binders such as rapeseed flour (RF), bark (BK), coffee meal (CM), lignin (LP), and pinecones (PC) powder on the durability of tulip tree (TUT) and larch pellets (LAR). They observed high durability for TUT and LAR pellets with RF, LP, and CM binders. It was postulated that high durability with the use of these binders was due to the plasticizing of proteins present in LP and RF by the heat generated during the pelletizing process and this acted as a binder between wood particles enhancing pellets durability. On the other hand, TUT and LAR pellets with PC and BK binders had significantly lower durability. This was assumed because of the low chemical reactivity of tannin present in BK and PC and it requires high temperatures to act as a binding agent. It was also found that by increasing binder concentration from 0 to 10%, the durability of TUT pellets increased however LAR pellet's durability was not affected significantly by the increase in binder concentration.

Hu et al. (2015) studied the effect of four kinds of binders namely starch, lignin, sodium hydroxide (NaOH), and calcium hydroxide ($Ca(OH)_2$) on mechanical properties, combustion characteristics, compressive process, and basic fuel properties of rice husk char pellets. For mechanical properties, it was observed that for pellets with lignin and $Ca(OH)_2$ binder, the compressive strength increased with an increase in binder content up to 10%. Above 10% binder content, it decreased. As compared to the 0.65 MPa compressive strength of no-binder pellets, pellets with 10% lignin and $Ca(OH)_2$ binders exhibited higher compressive strength of 3.82 and 5.55 MPa, and their volume density also increased. The highest compressive strength and volume density were observed for pellets with NaOH binder. The compressive strength increased with an increase in NaOH concentration up to 15% and for volume density up to 20%. The compressive strength of pellets with NaOH binder was above 20 MPa at 15% concentration and volume density ranged from 1163 to 1298 kg/m^3 with varied binder concentration. The increase observed in pellets with NaOH binder was due to NaOH ability to capture moisture and retain it within the pellet increasing its hardness. Moreover, since 98% silica is present in rice husk, mixing and compressing it with NaOH can form sodium silicate which is a cementing agent which increases its mechanical properties. Starch pellets exhibited poor mechanical properties even lower than pellets with no binder. However, for moisture uptake rate, starch pellets absorbed less moisture than lignin. NaOH pellet's moisture absorption was observed to be very high as it is an alkali that has high water-absorbing properties

2.8.5.4: Effect of Temperature:

Another important factor affecting the pelletization of biomass is temperature. High temperature affects moisture contained in the feed by evaporating it during pelletization. During pelletization, feed temperature is increased either directly (steam conditioning or friction) or indirectly (conduction-based heating system) to release and activate added or inherent binders and promote protein denaturation and starch gelatinization. High temperature also facilitates in plastic deformation of thermoplastic particles. Plastic deformation is essential to establish permanent bonds between particles (Kaliyan and Vance Morey, 2009). A decrease in pressure and friction with an increase in temperature has also been observed in some cases. This decrease in pressure could be a result of lignin and hemicellulose undergoing glass transition at elevated temperatures. The glass transition temperature of lignin and hemicellulose ranges from 77 to 128°C and 54 to 142°C. The pelletization of these softened polymers can reduce pressure and friction (Fang et al., 2019).

Jiang et al. (2014) investigated the effect of die temperature on Chinese fir/sewage slug (CFSP), camphor/sewage slug (CSP), and rice straw/sewage slug (RSSP) pellets along with other process parameters such as pressure, biomass particle size, sludge ratio, and moisture content on mechanical properties of pellets. A comparison of the quality of the pellet prepared with 55 MPa pressure, 15% moisture content, and 50% sludge content at different temperatures (10-170°C) was made. It was observed that relaxed pellet densities and Meyer hardness increased significantly with an increase in temperature from 30 to 110°C, but a further increase in temperature reduced these properties. At low temperatures, pellet quality was poor because the proteins and lignin present in feed did not act as a binder and the main bonding forces in pellets were short-range forces such as van der Waals forces, hydrogen bridges, mechanical interlocking, and free chemical bonds. As the temperature rose, the proteins denatured, and lignin softened and formed bonds between particles. When pellets cooled down lignin and protein formed solid bridges between particles which increased the pellet's strength. Also, because of lignin softening at high temperatures, the biomass particles became more flexible, and under compression, particles were able to pack tightly reducing empty spaces in the pellet which increased the density of pellets.

CHAPTER 3: MATERIALS AND METHODS

3.1 MATERIALS:

3.1.1 Hemp Fibers:

Whole hemp fiber, hemp bast fiber and hemp hurd fiber were used in this project provided by different suppliers. Table 3.1 represents sample name, fiber type and supplier names. All fibers used in this project were dew-retted for 2 to 4 weeks.

Table 3.1 Different Hemp fiber description.

Sample Name	Fiber Type	Supplier
TwH	Whole hemp	Tangho Paraguay
T.H	Hemp hurd	Tangho Paraguay
VB.B	Hemp bast	Valley-Bio Canada
VB.H	Hemp hurd	Valley-Bio Canada
I.B	Hemp bast	IND-Hemp USA
I.H	Hemp hurd	IND-Hemp USA
AG.wH	Whole hemp	A.G USA
AG.B	Hemp bast	A.G USA
AG.H	Hemp hurd	A.G USA

3.1.2 Surfactant:

Arquad 2HT-75 provided by Sigma Aldrich Canada was used as a wax in hemp pellets for easy processing of pellets and enhancing fiber dispersion in composites. According to the supplier Arquad 2HT-75 contains 75% di(hydrogenated tallow) dimethylammonium chloride, approximately 14% of 2-propanol and around 11% of impurities such as water. Hydrogenated tallow is produced from animal fatty deposits, especially from suet which is hard fat around kidneys of sheep and cattle, and it contains palmitic acid (16 carbon chains), stearic acids (18 carbon chains) and glyceryl esters of oleic. Due to presence of homologs and impurities, average molecular weight of Arquad 2HT-75 cannot be calculated accurately (Sarkar et al., 2011). This

surfactant has a wax-like appearance. Later, in this thesis, this surfactant will be referred to as wax. The melting point of this wax was reported by the supplier as 40 ºC. This wax was heated to 60 ºC in the presence of a small amount of water before adding it to the fibers for homogenous mixing.

3.1.3 Polypropylene:

Isotactic homopolymer polypropylene with a melt flow index of 23 g/10min was used.

3.1.4 Compatibilizer:

G-3015 grade of maleic anhydride grafted polypropylene provided by Eastman was used as a coupling agent in polypropylene composites. This grade is recommended for polypropylene composites and has a molecular weight of 47000 g/mol, its viscosity at 190 ºC is 18000 cP and it has an acid number of 15 mg KOH/g.

3.1.5 Chemical Treatment:

Alkaline treatment of TwH fibers milled in 1.5 mm size was performed with Sodium Hydroxide (NaOH) provided by Sigma Aldrich. TwH fibers were soaked in 5 wt.% NaOH solution for 4 hours at room temperature. After that fibers were washed with water until a neutral pH of 7 was achieved.

3.2 METHODS

3.2.1 Processing Methods:

3.2.1.1 Size Reduction Equipment (Knife Mill):

The equipment used to mill fiber was Thomas Wiley Mill Model 4 shown in Figure 3.1. It has six stationary blades and four rotating blades which rotates at a speed of 800 rpm. This mill was used to grind long hemp fibers into three different sizes using different sizes of sieve.



Figure 3.1 Thomas Wiley Mill model 4, image from (labwrench.com).

The different sieves that were used had opening sizes of 3mm, 1.5mm and 1mm respectively. Figure 3.2 represents different sieves used in the mill.

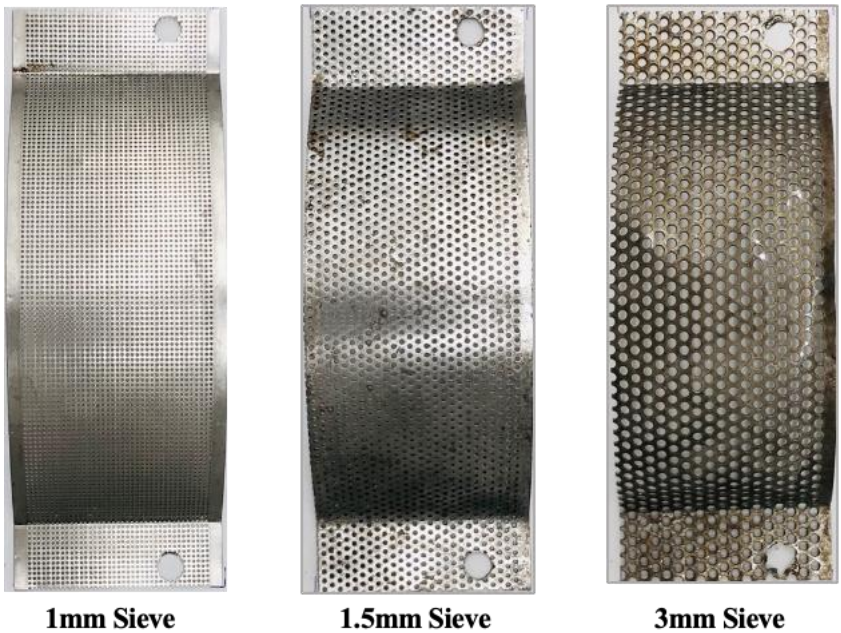


Figure 3.2 Sieves used to mill, image by author.

The sieves with the openings of 1mm, 1.5mm and 3mm openings had an available area of 3092mm^2 , 2430 mm^2 and 4500 mm^2 respectively, for the material to pass through. Picture of the fiber milled with these different sieves are shown in chapter 4.

3.2.1.2 Size Enlargement Process (Pelletization):

After milling, the fibers were mixed with water in a kitchen mixer for 4 minutes to increase the moisture content of the fibers to 33-34%. The initial moisture content of the fibers was kept constant for all samples. In some formulations, Arquad 2HT-75 wax was also added to the fibers during mixing. This material was then fed to a pellet mill for pelletizing. After pelletization, the moisture content of the fibers was between 20-24%.

The pellets were dried in an oven at 105 ºC until moisture was below 1% for storage and to be further used in the composite process. Colorado Mill Equipment's CME ECO-3 flat die pellet mill was used for pelletizing hemp fibers. This type of mill is recommended for the pelletizing of hemp fiber and biomass. According to the supplier, this mill has a 3hp motor and the capacity to produce 30-150 lb/hr of pellets depending on feed characteristics. The pellet mill is shown in Figure 3.3.

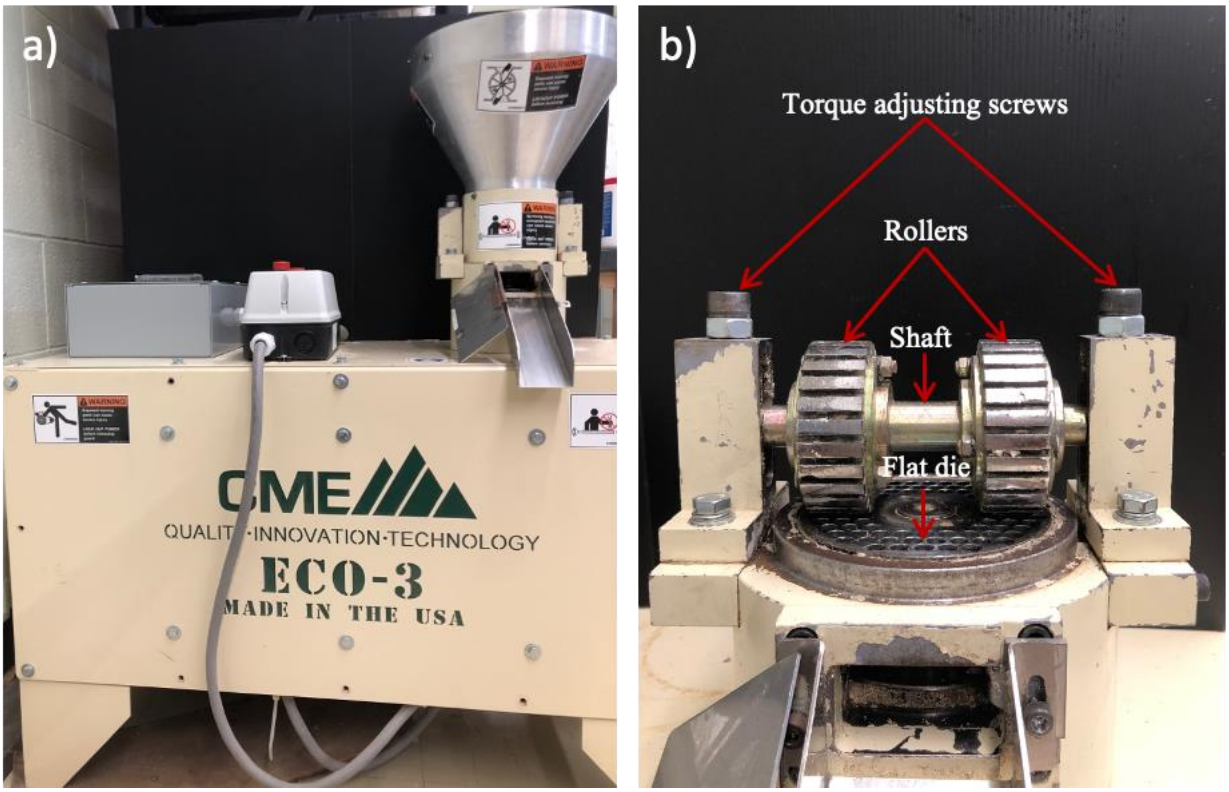


Figure 3.3 a) CMO ECO-3 flat die pellet mill, b) roller and flat die setup, image by author.

The flat die is 104 mm in diameter and 21 mm in thickness. It has 84 holes in hexagonal geometry for pellet formation. The hexagonal geometry of the die produces 2 times more pellets as compared to the radial geometry (Paredes-Rojas et al., 2020). The dimension of each hole is 4 mm in diameter and 21 mm in length. The total active area for material to compress through the die is 24,278 mm^2. The flat die is shown in Figure 3.4. The rollers seen in Figure 3.3 b), have the main role of compressing hemp fiber into the die-forming pellets. The pressure applied by the roller can be adjusted by adjusting the torque on the screws at the end of the roller shaft. In this research, a minimum torque of 0.5 Nm was applied to avoid overheating due to friction.

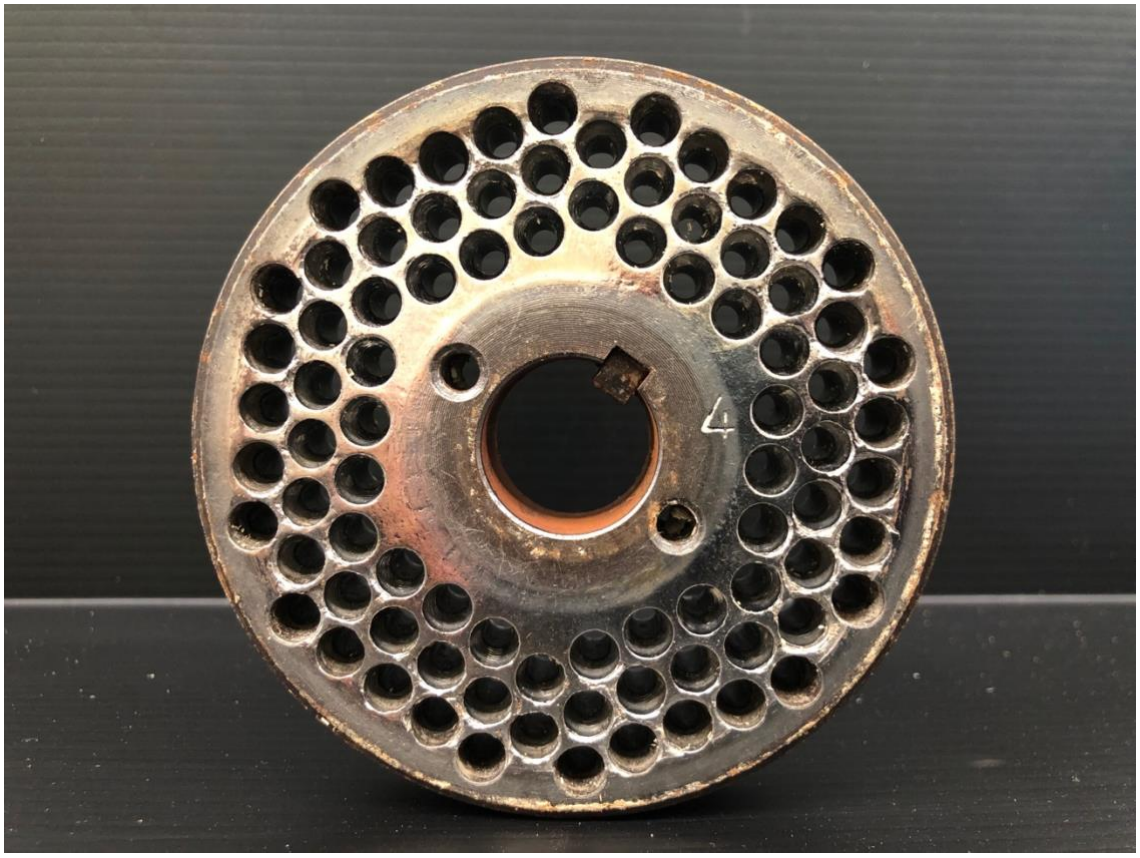


Figure 3.4 Flat die with 4 mm diameter holes in hexagonal geometry, image by author.

3.2.1.3 Melt Compounding via Twin Screw Extruder:

Hemp polymer composites were prepared by melt blending in a Thermo Scientific Haake MiniLab co-rotating twin-screw conical extruder. The composite mixture of 100 g in weight was initially hand mixed for achieving homogeneity. Different formulations of composites prepared

are given in Tables 5.1, 5.3, 5.5, 5.7 and 5.9. Prior to extrusion, the hemp pellets were dried in an oven at 105 °C until the moisture content of the pellets dropped below 1%. The operating conditions of the extruder were a temperature of 200 °C and a screw speed of 100 rpm. Inside the extruder, polypropylene pellet melts and undergoes intense mixing with hemp fibers. The shear force generated by rotating screws breaks fiber agglomerates (pellets) and ensures good dispersion by thoroughly mixing with molten PP. As the material progresses in the extruder barrel, the shearing forces and mixing increase due to the narrowing of the barrel, and then homogeneously mixed material exits through the flush orifice in the form of an extrudate which is then cooled in contact with air followed by pelletization before being fed into the injection molding machine. Figure 3.5 shows the Thermo Scientific Haake MiniLab Micro-compounder.

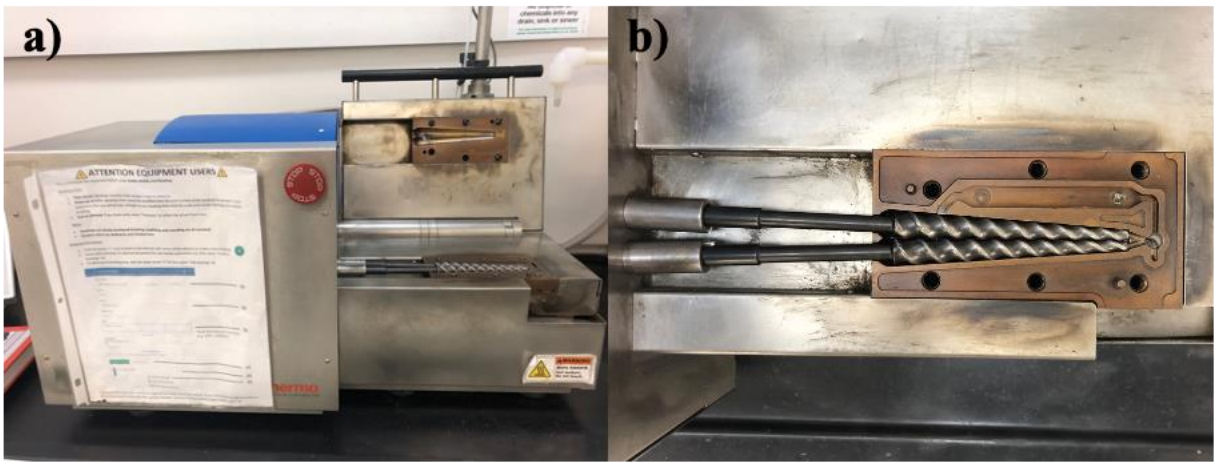


Figure 3.5 a) Haake Minilab Microcompunder, b) conical screws, image by author.

3.2.1.4 Injection Molding:

The extrudate from the extruder was cut into small pieces and then fed into a laboratory injection molding machine from Ray-Ran Test Equipment Ltd., UK., for melting into bars and dog bones according to the dimensions provided by ASTM standards for mechanical properties testing. The extrudate cut into small pieces was fed into the injection machine where the temperature of the barrel was set at 200 °C and the temperature of the mold tool at 80 °C. It was allowed to melt for 10 minutes and after that, 100 psi of pressure was applied to move the ram down into the barrel pneumatically and push the material out into the mold platen through the nozzle. The pressure was released after 15 seconds and after that, rectangular bars and dog bone-shaped bars were extracted

from the mold and inspected for any imperfections. Figure 3.6 shows the flexural, tensile, and impact test specimens of pure polypropylene, glass fiber-reinforced polypropylene (PP/GF), and hemp fiber-reinforced polypropylene (PP/HF) composites.

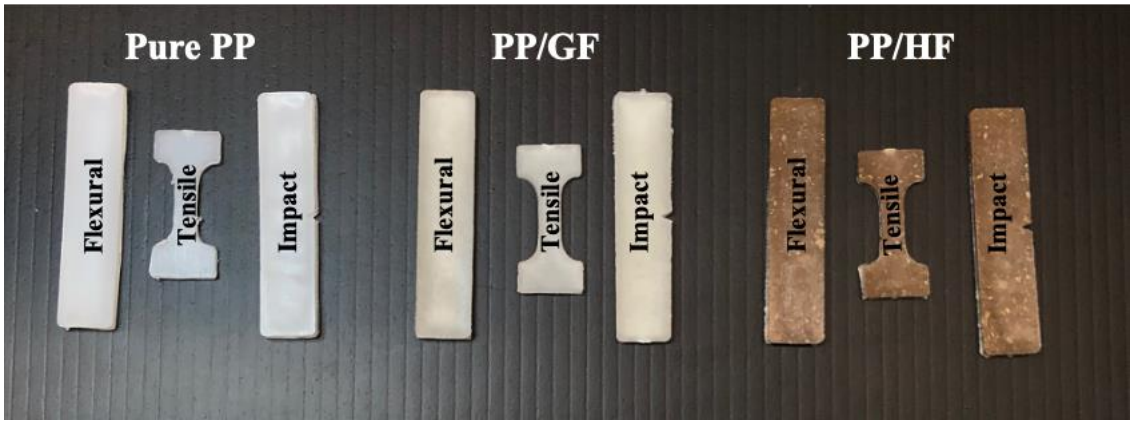


Figure 3.6 Flexural, tensile, and impact test specimen of pure PP, PP/GF, and PP/HF composites, image by author.

3.2.2 Characterization:

3.2.2.1 Size Analysis Equipment:

Particle size analysis was done using a sieve shaker and optical microscope. RO-TAP sieve shaker model RX-29 from W.S Tyler with 10 sieves with different openings was used to perform sieve shaker analysis. 100 g of sample was fed into the top sieve and sieve shaking was performed for 10 minutes. Once the test was complete, the weight of each sieve was recorded and subtracted from the weight of the empty sieve. Results were displayed in the form of a histogram. The sieve shaker and sieves used with different openings are shown in Figure 3.7.

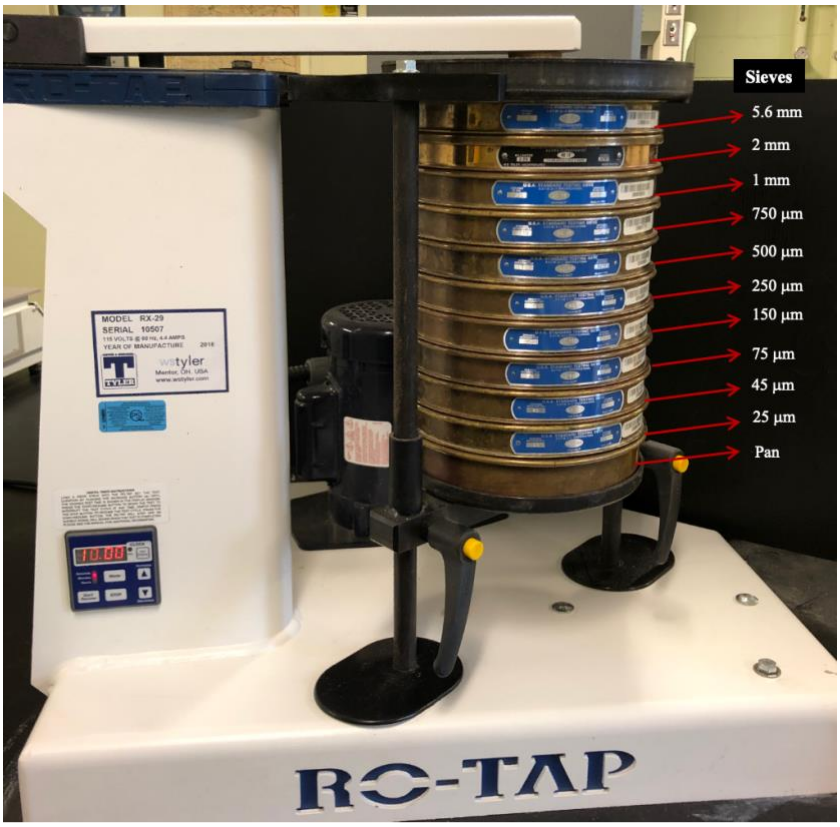


Figure 3.7 RO-TAP Sieve shaker with ten sieves, image by author.

Leica MZ6 digital microscope connected with Leica Flexacam C3 camera was used to take images of the fiber at 0.63x magnification. The hemp fibers were arranged on a glass slide without touching each other. Pictures of 100-150 particles of each sample were taken. ImageJ software was used to measure width, length, and aspect ratio of the fibers and then histogram of particle size distribution was prepared using Origin Pro and Microsoft excel software.

3.2.2.2 Scanning Electron Microscope:

The morphology of hemp fibers and hemp fiber reinforced polypropylene composites was observed using Quanta FEG ESEM at 20 kV accelerating voltage. Fractured pieces of composites after impact strength test were cut and fixed on aluminum stub using double sided adhesive carbon tape in such a way that fractured surface was facing upward in the direction of SEM electron source. All samples were sputter coated with 10 nm layer of gold to make the surface of the samples electronically conductive.

3.2.2.3 Moisture Content:

The moisture content of hemp fiber and pellets was determined using an Ohaus MB 45 moisture analyzer. Sample weight in between 0.5 – 1 gram was placed on an aluminum pan in the analyzer. The sample was heated at 105°C until all the moisture was evaporated. The moisture content results were then displayed by the analyzer in percentage.

3.2.3 Pellet Mechanical Properties:

Pellet durability index test (PDI), compression strength test, and bulk density tests of pellets were performed.

3.2.3.1 Pellet Durability Index (PDI):

The pellet durability index (PDI) test was done according to ISO 17831-1 using a tumbling machine equipped with a dust-tight wooden testing box with a stainless-steel baffle to mix the pellets as shown in Figure 3.8. The dimensions of the tumbling machine are in accordance with ISO 17831-1, which are as follows:

- Testing box inner dimensions: 300 mm width, 300 mm height, and 125 mm breadth.
- Mixing baffle dimensions: 230 mm in length and width 50 mm.

Pellets were sieved using a 3.5 mm round diameter holes sieve. Then 500 g of pellets were weighed and carefully placed in the testing box of the tumbling machine and the box was closed with dust dust-tight screen. The test was carried out at 60 rpm for 10 minutes. After that, all the material from the test box was collected and sieved again with a 3.5 mm sieve to remove dust and small broken pellets and then the pellets were weighed again and PDI was determined the using following formula.

$$\text{Pellet Durability Index (PDI)} = \frac{\text{Pellets weight retained on sieve after tumbling}}{\text{Pellets weight before tumbling}} \times 100$$

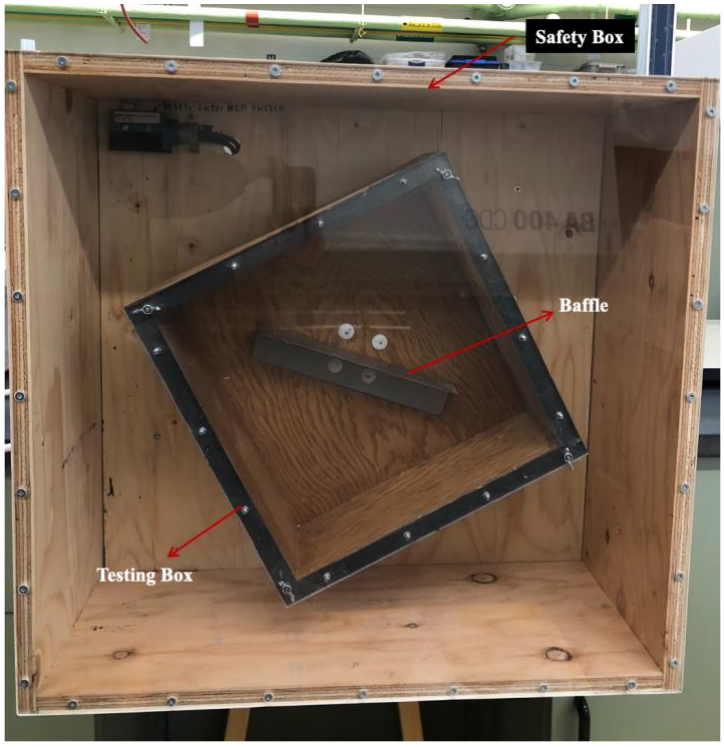


Figure 3.8 Pellet tumbling machine, image by author.

3.2.3.2 Specific Compression Strength:

Single pellet crush test was performed according to ASTM D4179 using universal testing machine Test Resource actuator 120Q1000. From each sample 10 random pellets were selected, their diameter, length and weight were measured. These pellets were one by one placed in radial orientation on a circular surface and compression load was applied at the rate of 5 mm/min. The specific compression strength (N/mm) for each pellet was calculated by using the formula bellow, and the average specific compression strength and standard deviation of 10 specimen was calculated and reported.

$$\text{Specific Compression Strength} = \frac{\text{Maximum compression force applied}}{\text{diamter of pellet}}$$

3.2.3.3 Pellets Bulk Density:

The bulk density of pellets was measured according to ASABE Standard S269.4 and the pellets were loosely filled in a 500 cm^3 cylindrical container. The container was tapped 5 times to adjust the pellets and more pellets were added until the container was full. Excess pellets from the surface were removed by a flat tool. The container was weighed on a semi-analytical scale and the weight of the pellets was determined by subtracting the weight of the empty container. Then, bulk density was calculated using the following formula,

$$\rho_p = \frac{m}{V}$$

Where 'ρ_p' is the pellets bulk density, 'm' is the weight of pellets and 'V' is the volume of the cylindrical container.

3.2.4 Composite Mechanical Properties:

The injection molded composites were preconditioned prior to mechanical tests at room temperature of 23 ± 2 °C and relative humidity of 50 ± 5 % for 40 hours according to ASTM standard D618-08.

3.2.4.1 Flexural Properties:

Flexural strength and modulus of composites was determined using three-point bending technique according to ASTM D790-10 standard using a universal testing machine Test Resource actuator 120Q1000. The rectangular bars were placed on two supports and the load was applied at the center of the bar by using a load nose at the rate of 13.9 mm/min. The load was continuously applied at the center until the outer surface of the bar was raptured or 5% strain was achieved. For each composite formulation, 10 bars were tested for flexural strength and modulus. The flexural strength and modulus of the composite was calculated using the following equations,

$$\text{Flexural Stress} = \sigma_f = \frac{3PL}{2bd^2}$$

$$\text{Flexural strain} = \varepsilon_f = \frac{6Dd}{L^2}$$

$$\text{Modulus of elasticity} = E_B = \frac{\text{flexural stress}}{\text{flexural strain}}$$

Where,

P = load at given point on curve (N),

L = Support span (mm)

b = width of the bar (mm)

d = thickness of the bar (mm)

D = maximum deflection at center (mm)

3.2.4.2 Tensile Properties:

Tensile strength and modulus of composites was determined according to ASTM D1708-10 standards using a universal testing machine Test Resource actuator 120Q1000. The dog-bone shaped bar was placed between the tight grips of the testing machine in such a way that the rectangular portion of the bar was exposed to the force of stretching and the distance between the lower and upper grip after closing was 22 $\pm$ 0.05 mm. The stretching force was applied on the sample at a rate of 5mm/min. For each composite formulation 10 dog-bone shaped bar were tested and average tensile strength and modulus were calculated. Following formulas were used to calculate tensile strength and modulus,

$$\text{Tensile strength} = \frac{\text{maximum load}}{\text{cross} - \text{secttional area}} = \frac{\text{maximum force}}{\text{unit cross} - \text{sectional area}}$$

$$\text{Yeild strength} = \text{Tensile stress at yield}$$

$$\text{Elastic modulus} = \frac{\text{stress}}{\text{strain}} = \frac{\text{force/cross-sectional area}}{\text{change in length/orignal length}}$$

3.2.4.3 Impact Strength:

The impact strength of the composite was performed using a Monitor Impact Tester from Testing Machine Inc (TMI), New Castle, DE. The test was performed according to ASTM 256-10 test method-A standard. After injection molding, a notch was made on each rectangular bar using a milled notch cutter at an angle of 45 ± 1° and 2.5 mm deep. Prior to impact testing, the specimens were conditioned at room temperature and relative humidity of 50 ± 10% for 40 hours. A notch increases the chances of a brittle failure as it creates a stress concentration point. After making the notch, the width of the specimen is measured from the notch, and the value is inserted into the machine. After that, the notched specimen is placed vertically on the mount of the impact tester and a 1 ft.lb pendulum-type hammer is released which breaks the specimen and records the energy required to break it. Impact strength is then reported in Joules/meter. Ten specimens of each composite formulation were tested, and average impact strength was reported.

3.2.4.4 Melt Flow Index (MFI):

The melt flow index of the composites was determined by using a Dynisco D4001DE MFI tester according to ASTM D1238. The die used in this test was 4mm in length and had a bore of 1.048 mm. The machine was operated at a temperature of 230 °C and 4 g of material was fed into the barrel of the machine and was given 5 minutes to melt. Once melted, a load of 2.16 kg was applied on the top to push the molten material out of the die. Nine sample cuts were made at regular intervals of 15 seconds. Two repetitions of each composite formulation were performed. Average MFI was then reported in g/10min units.

3.2.4.5 Composite Specific Density:

The density of composites was determined after injection molded rectangular bars were preconditioned for 40 hours at a room temperature of 23 ± 2° C and relative humidity of 50 ± 5 %. The density calculations were done according to ASTM D792 test method B. The weight of each rectangular specimen was measured in air and then in ethanol. As hemp fiber composites are lighter than water, ethanol was used to avoid floatation of bars during weight measurement. Weight in air and in ethanol were measured using a Mettler Toledo analytical equipped with a special gravity kit. The specific gravity and density of composites were measured using the following formula,

$$\text{Sp gr } 23/23\,°\text{C} = \frac{a}{a-b}$$

$$D^{23C}, \frac{kg}{m^3} = \text{Sp gr } 23/23\,°\text{C} \times \text{density of ethanol}$$

Where,

a = apparent mass of specimen in air

b = apparent mass of specimen immersed in ethanol

CHAPTER 4: HEMP PELLETIZATION RESULTS AND DISCUSSION

4.1 INTRODUCTION:

As hemp fibers have low density transporting them is a challenge and costly as they occupy more space. Pelletization is a great way to densify hemp fibers into pellets which occupy less space resulting in saving costs in storage and transportation. The main objective of this chapter was to prepare hemp pellets and investigate the effect of different factors such as fiber size, additive (wax), different compositions of hurd and bast fibers, and chemically treated fibers on the mechanical properties of hemp pellets. Figure 4.1 shows a comparison between the space occupied by 200 grams of hemp bast fibers and 200 grams of hemp bast pellets and Figure 4.2 represents the flow diagram of the pelletization process. The results of particle size analysis obtained from sieve shaker and optical microscope analysis are also presented and discussed.



Figure 4.4 Comparison between space occupied by 200 grams of hemp bast fibers (left) and 200 grams of hemp bast pellets (right).

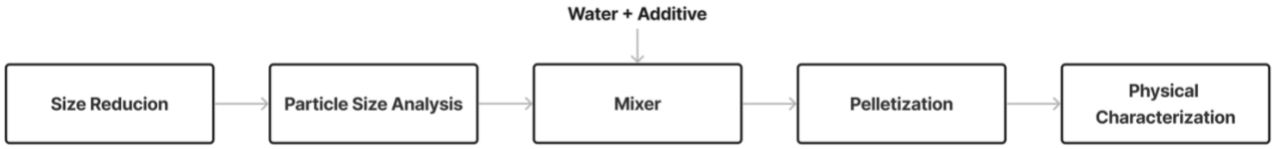


Figure 4.2 Flow diagram of hemp fiber pelletization process.

The results are divided into the following sections:

4.2: Characterization of hemp fibers.

4.3: Preparation of hemp pellets with different bast fiber size and with or without wax.

4.4: Preparation of hemp hurd pellets.

4.5: Hemp pellets with different compositions of hemp bast and hurd fibers.

4.6: Pelletizing of whole hemp fibers treated with NaOH.

4.7: Change in fiber size after pelletization.

4.2 CHARACTERIZATION OF HEMP FIBERS:

For pelletizing hemp fibers, it is important that the fiber size must be reduced to a size smaller than the die hole of the pellet mill (4 mm) so that fibers may pass through the hole forming a pellet without blocking it (Garcia-Maraver, 2015). Therefore, hemp fibers were milled in a knife mill using sieves with openings of 1 mm, 1.5 mm, and 3 mm. The fibers milled using these sieves had a broad particle size distribution.

Having a particle size distribution for pelletizing is beneficial as longer fibers can easily entangle and form an agglomerate while smaller fibers having higher surface area can fill in the gaps between longer fibers resulting in pellets with high durability and density as compared to pellets with uniform size fibers. The visual representation of hemp bast and hemp hurd fibers milled into sizes of 1 mm, 1.5 mm, and 3 mm size using a Wiley Mill is shown in Figure 4.3.

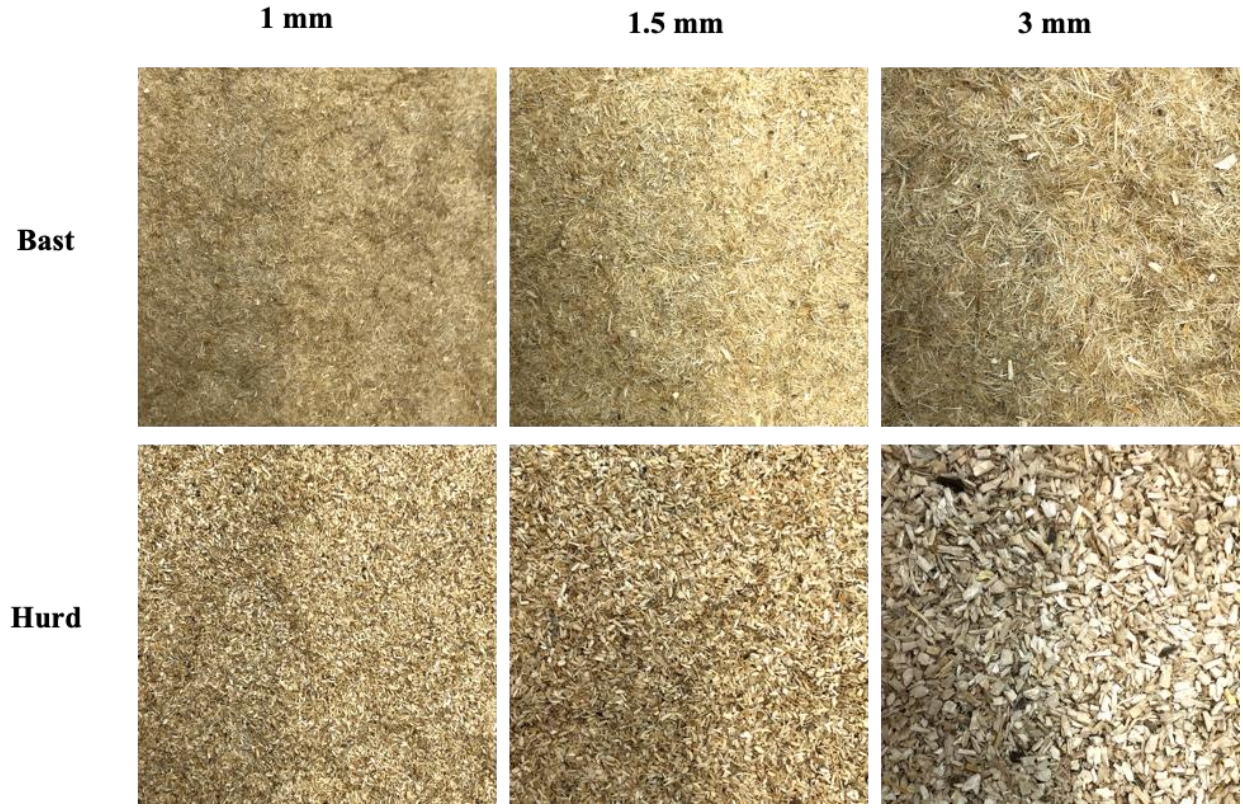


Figure 4.3 Visual representation of hemp bast and hemp hurd fiber milled in 1 mm, 1.5 mm, and 3 mm sizes.

4.2.1 Particle size analysis:

Sieve shaker analysis and optical microscope analysis of hemp bast and hemp hurd fibers milled in sizes of 1 mm, 1.5 mm, and 3 mm were performed. Table 4.1 shows the sieve size and particle size range obtained in each sieve in the sieve shaker. Figure 4.4 represents the results of the sieve shaker analysis. Bast fibers milled in 1 mm and 1.5 mm sizes are observed to have similar particle size distribution. Both have significant fibers in the size range of 250 μm – 500 μm, while 1.5 mm fiber also contains a small amount of fibers in the size range of 750 μm – 1 mm.

Sieve shaker analysis of 3 mm milled bast fiber was unsuccessful because of the flexible characteristics of bast fibers and long size, mechanical interlocking of fibers occurred and they formed a cake-like structure in the top sieve which restricted the fibers from falling through the sieves as shown in figure 4.5. Hurd fibers size range also shifts from a majority smaller 250 μm – 500 μm size range in 1 mm milled fibers to a majority longer 1 mm – 2 mm size range in 3 mm milled fibers.

Table 4.6 Sieve shaker sieves size and corresponding particle size range.

Sieve Size	Particle Size Range
25 μm	25 μm - 45 μm
45 μm	45 μm - 75 μm
75 μm	75 μm - 150 μm
150 μm	150 μm - 250 μm
250 μm	250 μm - 500 μm
500 μm	500 μm - 710 μm
710 μm	710 μm - 1 mm
1 mm	1 mm - 2 mm
2 mm	2 mm - 5.6 mm
5.6 mm	>5.6 mm

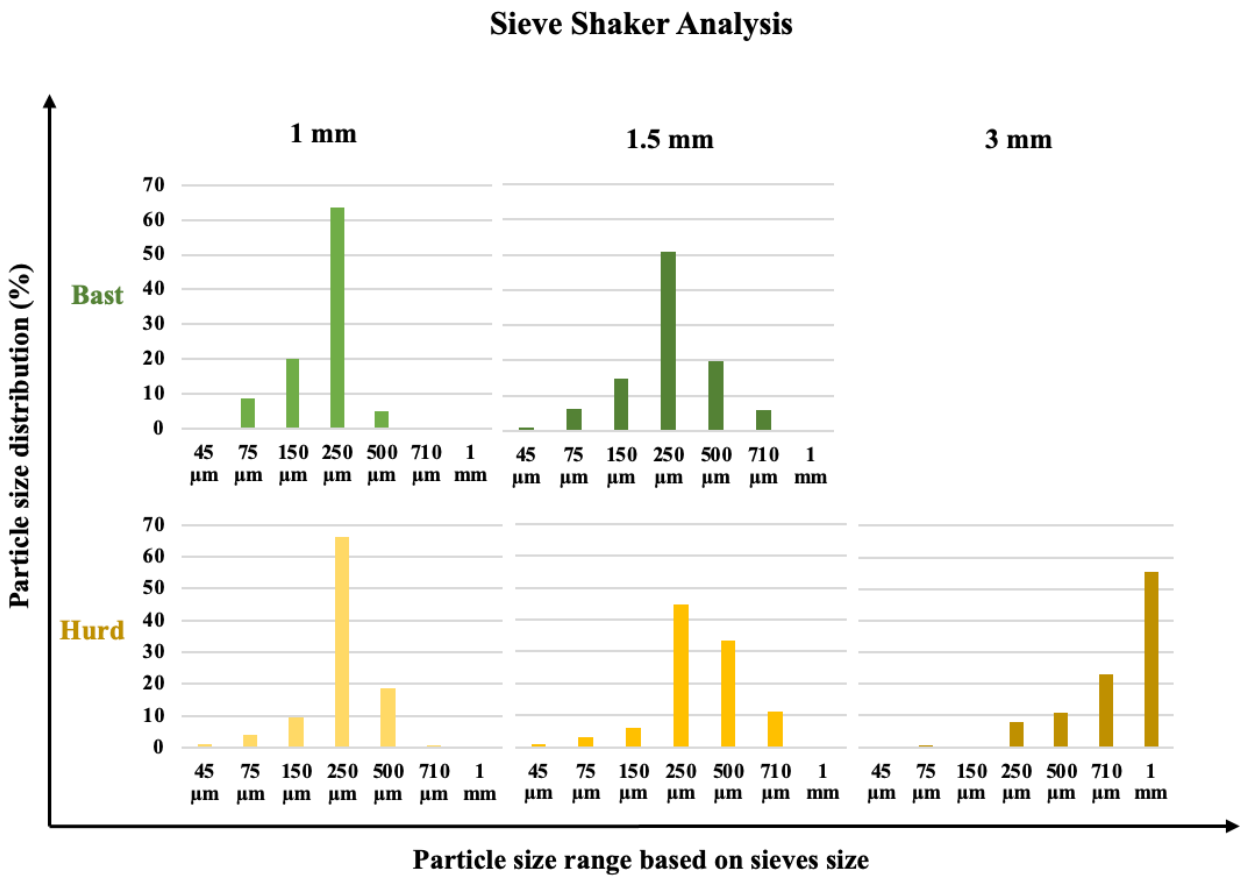


Figure 4.4 Sieve shaker analysis results of 1 mm, 1.5 mm, and 3 mm milled hemp bast and hurd fibers.



Figure 4.5 Cake-like formation of 3 mm milled bast fibers in sieve shaker.

Optical microscope analysis of milled hemp bast and hurd fibers in sizes of 1 mm, 1.5 mm, and 3 mm was also performed. The reason for performing size analysis of hemp bast and hemp hurd fiber separately is that although after milling, the length distribution of both fibers might be similar, the aspect ratio of both fibers tends to be significantly different. Hemp bast fibers are thinner than hemp hurd fibers as shown in Figure 4.6.

Fiber characteristics such as fiber length and aspect ratio are significant factors that influence the properties of pellets and composites. Figure 4.6 represents the optical microscope results in the form of three-dimensional graphs providing a comprehensive visualization of the relationship between fiber length distribution, aspect ratio distribution, and frequency of occurrence. The primary objective of three-dimensional graphs was to provide a multidimensional perspective on how fiber length and aspect ratio distribution are influenced when different sieve sizes (1, 1.5, and 3 mm) are used during milling.

It was found that bast fibers milled in 1 mm size had fibers with lengths ranging from 0.8 to 3.5 mm and aspect ratios ranging from 4 to 30 with the majority of fibers with lengths and aspect ratios ranging from 1.6 to 2.5 mm and 4 to 10. Whereas hurd fibers milled in 1 mm size had length and aspect ratio ranging between 0.8 mm to 3 mm and 1 to 6, respectively, with the majority of fibers with lengths and aspect ratio ranging between 1.1 mm to 2 mm and 2.1 to 4. Similarly, bast and hurd fiber milled in 1.5 mm size had fiber lengths ranging from 1 mm to 6 mm and 0.8 mm to 3 mm, respectively, with the majority of fibers with lengths ranging from 2 mm to 4 mm and 1.1 mm to 2 mm and aspect ratios ranging from 1 to 30 and 1 to 6, respectively, with the majority of fibers aspect ratio ranging from 11 to 20 and 2.1 to 4. Finally, bast and hurd fibers milled to a size of 3 mm had lengths ranging from 1 mm to 7.5 mm and 1 mm to 6 mm, and aspect ratios ranging from 1 to 45 and 1 to 4.5, respectively. The majority of the fibers had lengths and aspect ratios between 2.6 mm to 5 mm, 15 to 30, and 2 mm to 4 mm, 1.6 to 3 respectively. It is interesting to note a significant difference between the aspect ratios of bast and hurd fibers. This significant difference in aspect ratios is due to the huge difference between the diameters of bast and hurd fibers.

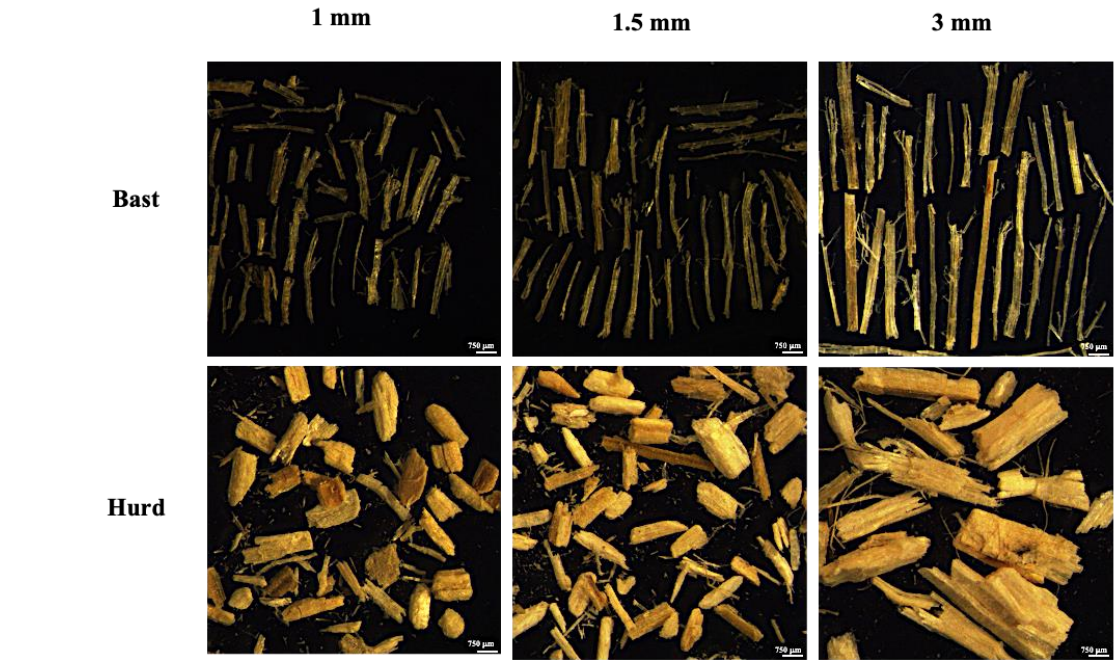


Figure 4.6 Visual appearance of bast and hurd fiber milled in 1-, 1.5- and 3-mm size under optical microscope.

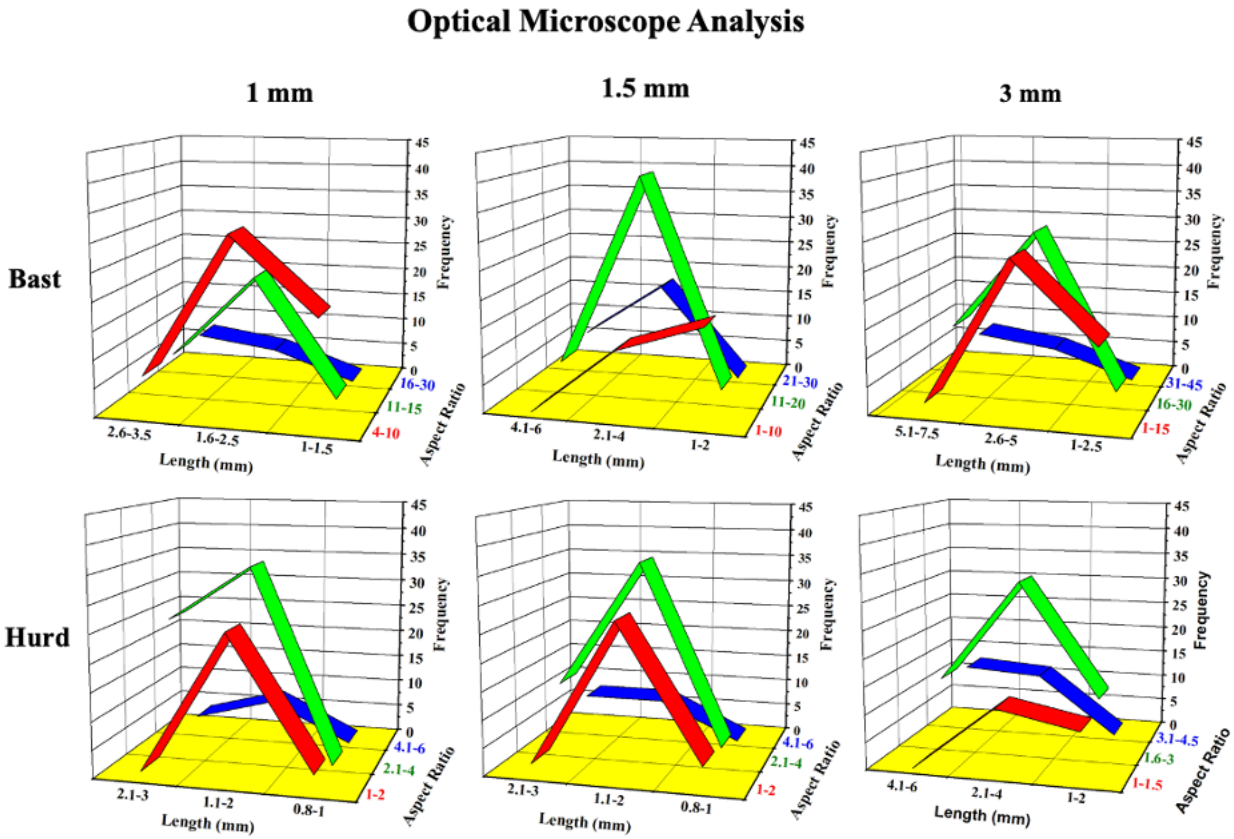


Figure 4.7 Optical microscope analysis results of hemp bast and hurd fibers milled in 1-, 1.5- and 3-mm size.

4.3 HEMP PELLETS WITH DIFFERENT FIBER SIZE AND WITH OR WITHOUT WAX.

Whole hemp pellets were prepared in 1 mm, 1.5 mm, and 3 mm sizes. The objective was to study the effect of different fiber sizes and the addition of wax on the mechanical properties of pellets. Particle size plays an important role in the mechanical properties of pellets.

According to the literature, pellet density increases with finer particle size. The finer fibers have more surface area than coarser fibers. It was reported that finer fibers produce more friction with the press channel wall of the pellet mill because of their higher surface area (Stelte et al., 2012). Due to this phenomenon, it could be speculated that by decreasing the particle size, the surface area of fibers increases which creates more friction due to fiber contact with each other and with pellet die-hole walls resulting in increased temperature. Because of this increase in temperature, the waxes on the fiber surface and lignin can undergo glass transition resulting in better wetting and contact with surrounding fibers producing a pellet with higher mechanical properties.

In literature, the optimum particle size is suggested to be less than 5 mm in diameter whereas it was reported that good pellets were obtained with particle diameters of 0.6-0.8 mm and 0.5-0.7 mm. It was also suggested that particle diameters greater than 1 mm in pellets may act as breaking points (Kaliyan and Vance Morey, 2009; Theerarattananoon et al., 2011; Younis et al., 2018; Zafari and Kianmehr, 2014).

The diameter of bast fibers milled in 1 mm, 1.5 mm, and 3 mm size was found to be in the range of 0.1-0.5 mm whereas the diameter of hemp hurd was observed to vary from 0.1-1.5 mm for fibers milled in 1 mm and 1.5 mm size. And for fibers milled in 3 mm size the diameter was calculated to be in the range of 0.3-2.7 mm.

Moreover, in addition to different fiber sizes, the effect of 5 wt.% binder (wax) on the mechanical properties of hemp pellets was also investigated. Binders in weight percentage of 0.5-5% were used to increase the mechanical properties of the pellets when the desired pellet quality was not obtained. A binder can increase inter-particle bonding by forming solid bridges or by causing a chemical reaction (Kaliyan and Vance Morey, 2009).

Zhai et al. (2018) reported that by adding 10-20 wt.% of sugar cane molasses, the mechanical properties of hydrochar pellets increased significantly. It was observed through SEM analysis that molasses formed solid bridges that connected smaller particles resulting in reduced spaces between particles and creating strong attraction forces between them. Hence, this resulted in increasing the mechanical properties of the pellets.

And lastly, in this present research, the initial moisture content of fibers was fixed between 30-34%. Water also behaves as a binding agent and helps in developing van der Waals' forces between fibers, increasing their area of contact. In literature, different moisture contents for different fibers are suggested.

Jackson et al. (2016) investigated the effect of different moisture contents on pellet formation of wheat straw, switchgrass, and miscanthus biomass milled in 3 mm size. It was reported that at 10% moisture content the formation of pellets did not take place at all. By increasing the moisture content from 10% to 15, and from 20 to 25%, pellet production increased with increasing moisture content, with most pellets produced at 25% moisture content. However, for hemp fibers, an initial moisture content of 30-34% was found to be efficient in our study. Table 4.2 represents the formulations and mechanical properties results of the pellets in question and these results are further discussed in the following sections.

Table 4.7 Formulation and mechanical properties of whole hemp pellets with different fiber size and with and without wax.

Fiber Type: Whole hemp fiber from Tangho Paraguay (TwH) **Additive wax:** Arquad-2HT (Dimethyldioctadecylammonium Chloride) **Fiber initial moisture content:** 30-34%					
Sample Name	**Fiber Milled Size (mm)**	**Wax (wt.%)**	**Specific Compressive Strength (N/mm)**	**Pellet Durability Index (%)**	**Pellet Bulk Density (g/cm^3)**
1TwH-0W	1.0	0	747.5±20^{b}	95	0.42±0.003^{d}
1.5TwH-0W	1.5	0	757.5±20^{b}	95	0.40±0.004^{d}
3TwH-0W	3.0	0	739.6±57^{a,b}	91	0.27±0.006^{a}
1TwH-5W	1.0	5	694.0±22^{a}	93	0.30±0.004^{b}
1.5TwH-5W	1.5	5	734.6±17^{a,b}	89	0.34±0.005^{c}
3TwH-5W	3.0	5	811.0±19^{c}	94	0.35±0.003^{c}

In sample names '(1/1.5/3)TwH', the first number represents fiber milled size and the first letters represent fiber type; and '-(0/5)W' represents pellets with 0 wt.% or 5 wt.% wax. All results were analyzed using the Tukey test with a significance level of 5% to determine the significant difference between the mechanical properties of these pellets. The superscripts (a,b,c,d) in Table 4.2 represent if the measured mechanical properties of the pellets in question are statistically different from each other or not. If the superscripts of different samples in each mechanical property (same column) have the same letter, then those values are statistically the same.

4.3.1 Specific compressive strength:

Specific compressive strength results of pellets are shown in Figure 4.8. It was expected that smaller fibers would produce more compact and stronger pellets with high specific compressive strength than pellets with bigger fiber sizes, as previously discussed in the literature. But from the Tukey analysis of the results presented here, no significant difference in compressive strength of pellets with different fiber sizes was observed.

Pradhan et al. (2021) investigated the effect of different milled fiber sizes on pellet quality. The study compared pellets made from milled biomass waste leaves in sizes of 25.4 mm and 6.25 mm. No significant effect on pellet quality was observed.

Kaliyan and Vance Morey, (2009) also found that finer particle size tends to produce good quality pellets as compared to coarse particle size because they act as pre-determined breaking points in pellets reducing mechanical properties of the pellets, but no significant difference was observed in compressive strength. This could also mean that the size difference between the 1 mm, 1.5 mm, and 3 mm milled fibers did not significantly affect the compressive strength.

Moreover, during pelletization, the temperature of the pellet mill die and rollers increased up to 60°C due to friction. It is speculated that such temperature could cause the natural fiber waxes to undergo glass transition causing them to flow and then hardening again resulting in increased hardness of pellets. A higher temperature would be required to cause the lignin to undergo a glass temperature transition and help as a binding agent. The lignin glass transition temperature (T_g) varies among natural fibers. The T_g of lignin generally ranges from 100 to 180°C (Poletto, 2017).

For pine and eucalypt samples, the T_g of lignin was reported to be in the range of 60 to 90°C (Irvine, 1985)

The effect of wax Arquad-2HT additive was observed on the compressive strength of pellets prepared here. From the literature, it was suggested that dairy feed pellets hardness was increased by 27% from 131.4 N to 166 N by the addition of 2.5% lignosulfonate (Kaliyan and Vance Morey, 2009). Samples without wax additives prepared with different fiber sizes have approximately the same compressive strength. But adding 5 wt.% wax changed to the compressive strength of samples with different sizes. The highest compressive strength of 811.0 N/mm was observed for pellets prepared with wax additive and 3 mm fibers.

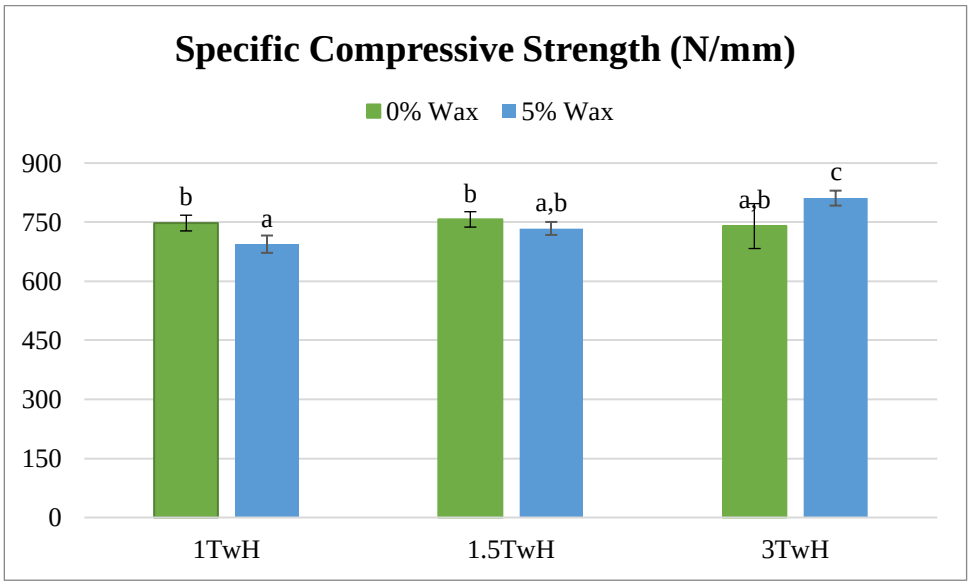


Figure 4.8 Specific compressive strength of whole hemp pellets with different fiber sizes and with and without wax.

4.3.2 Pellet Bulk Density:

Figure 4.9 depicts the bulk density results of the pellets. As expected, bulk density of pellets increased by decreasing fiber size. The bulk density of 1 mm and 1.5 mm milled fiber pellets was similar while 3 mm milled fiber pellets density was significantly lower. This is because small fibers can fill the empty spaces between the entangled larger fibers, resulting in increased density.

Another reason discussed in the literature is that smaller fibers have higher surface area, which facilitates better dispersion of moisture in the pre-pelletizing stage, this results in better

binding of fibers during pelletization hence increasing the bulk density property of the pellets (Mostafa et al., 2019). However, some authors did not observe a significant effect of particle size on the apparent density of the pellets (Pradhan et al., 2021).

It was expected that pellets with the addition of 5 wt.% additive (wax) would exhibit better bulk density than pellets without wax, but the results obtained were not in accordance with this expectation. Bulk density was reduced by 29% for pellets containing 1 mm fibers and by 15.6% for pellets containing 1.5 mm fibers. However, the bulk density of 3 mm fiber pellets was increased by 30%. An assumption could be made that Arquad-2HT is a dihydrogenated tallow dimethylammonium chloride which improves the flowability of fibers by reducing the friction between fibers and pellet die holes wall in the pellet mill during pelletization.

Improved flowability of smaller fibers reduces the increase in temperature during pelletization. Low temperature does not activate the natural binding mechanism of fibers (i.e. softening of waxes and lignin). Mostafa et al. (2019) also reported that at low temperatures, the bond between neighboring particles was observed to be weak. On the other hand, for 3 mm fiber pellets, it could also be speculated that the addition of 5 wt.% wax reduced their resistance to flow due to their size, which resulted in better packing of the pellet, hence increasing the bulk density.

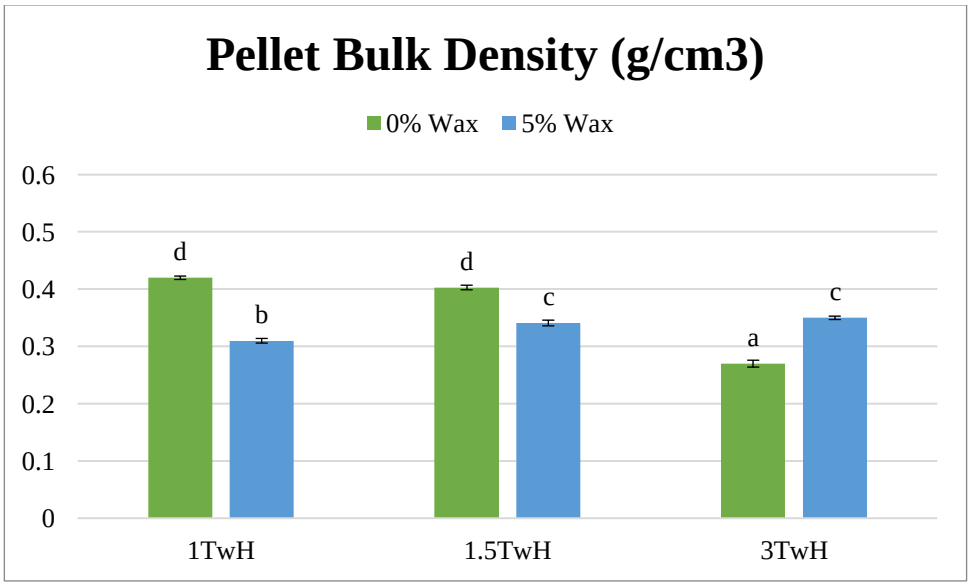


Figure 4.9 Bulk density of whole hemp pellets with different fiber sizes and with and without wax.

4.3.3 Pellet Durability Index (PDI):

According to Tabil et al., (1997), pellet durability is considered low if PDI is less than 70%, medium if PDI is in between 70-80%, and high if PDI is above 80%. The results of PDI are shown in Figure 4.10. The durability of all pellets prepared here was observed to be high. No significant effect of fiber size and use of additive (wax) was observed on the durability of pellets. These results are in accordance with other authors (Pradhan et al., 2021) as they also did not observe any effect of fiber milled size on pellet durability. PDI of all pellets in this section is significantly above 80%, it is concluded that whole hemp pellets exhibit excellent durability regardless of the size of fibers and use of additives.

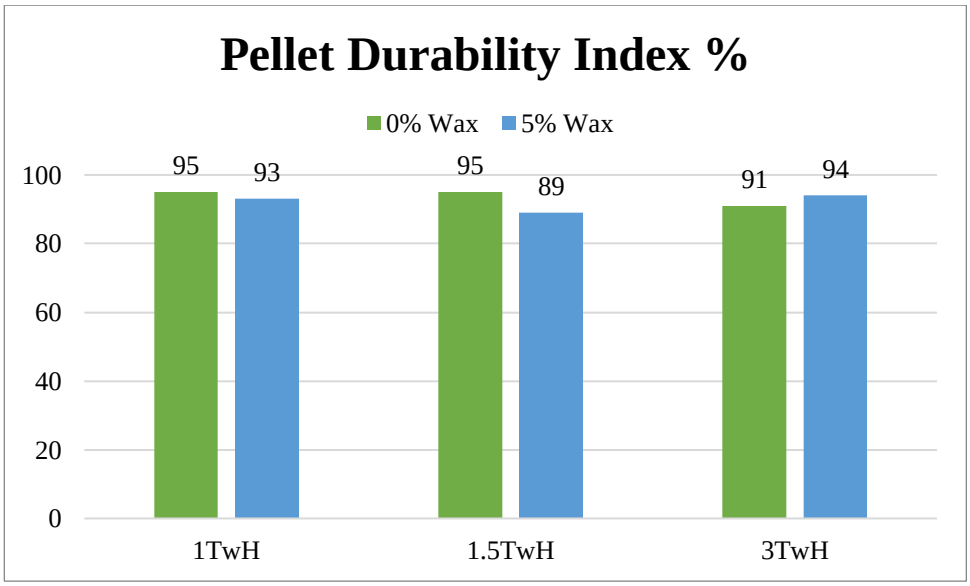


Figure 4.10 PDI of whole hemp pellets with different fiber size and with and without wax.

From the above analysis of the properties of the pellets, it can be concluded that the effect of different sizes of milled fiber of 1 mm, 1.5 mm and 3 mm and the use of additive (wax) on the specific compressive strength and durability of the pellets was not significant. However, it was observed that the bulk density of 3 mm milled fiber pellets was significantly lower than that of 1 mm and 1.5 mm milled fiber pellets. Regarding the use of wax, it negatively affected the bulk density of 1 mm and 1.5 mm fiber pellets and positively affected the bulk density of 3 mm fiber pellets.

4.4 HEMP HURD PELLETS:

The objective of this section is to explore the production of the hemp pellets using hurd (as opposed to bast fiber explored in the previous section). Hemp stem contains 60-80% woody core also called hurd fibers and 20-40% bast fibers.

Bast fibers are deemed to be more valuable as they are stronger than hurd fibers and have higher cellulose content. Bast fibers are mainly used for applications such as fabrics, non-woven fabrics, paper production, producing nano-cellulose and in different industries such as automotive, construction and geotextiles.

Hurd fibers are treated as a waste material generated during the production of bast fiber. Around 95% of hurd fibers are used for animal litter and only 5% is used in construction (Balčiūnas et al., 2013). Hemp hurd is similar to wood but has higher cellulose content and lower lignin content than wood. Hurd fibers are composed of 17-19% lignin, 34-48% cellulose, 21-25% hemicellulose, 1-2% ash, and 4% extractives (Stulpinaite et al., 2023). Although hurd fibers are weaker than bast fibers, their low density can make them useful for replacing wood in wood fiber-reinforced plastic composites. For this purpose, an attempt was made here to explore making hurd fiber pellets.

However, pelletization of hurd fibers is a challenge. Morselli et al., (2021) mixed hurd fibers with 50 wt.% fir sawdust in order to form pellets. Pelletization of hemp hurd is difficult due to its composition and structure. When pelletizing whole hemp or bast fiber, the high aspect ratio and flexible characteristics of bast fibers facilitate in mechanical interlocking of fibers, holding them in the form of a pellet which results in a compact pellet. Hurd fibers, on the other hand, have a lower aspect ratio and fragile structure, due to which there is no mechanical interlocking of fibers.

In this section of the present research, several attempts were made to make hurd pellets. Initially, an attempt was made to produce pellets with hurd fibers with an initial moisture content of 30-34%. However, this attempt was unsuccessful as the material passed through the pellet mill die without forming any pellets. Moisture is an important constituent of pellet formation. Water increases fiber's contact area and promotes bonding via intermolecular forces such as Van der Waal’s forces. Water significantly affects the binding between fibers in pellets. However, it is important to determine the optimum moisture level of biomass feed.

Different biomass feeds have different optimum moisture levels. If the moisture content is high, the pellet quality will be degraded as the pellet will expand more when ejected from the pellet mill as water is incompressible and will break bonds between fibers. And, if the moisture content is low, significant binding required to keep fibers together will not occur due to the absence of capillary forces responsible for maintaining the structure of the pellet (Fang et al., 2019; Younis et al., 2018; Zafari and Kianmehr, 2014).

So, to investigate the moisture content of the hurd fibers required for the formation of pellets at pellet die temperatures below 45°C, the moisture content was increased. Another attempt was made to produce hurd pellets with an initial moisture content of 45-50%., but this attempt was also unsuccessful. The moisture content was further increased to 60-65%, and in this attempt, pellets were formed although the pellet quality was not good. Furthermore, a small amount of bast fibers and wax was also added to improve pellet quality. Pellet formulations and mechanical properties are represented in Table 4.3. Pellet mechanical properties are further discussed in the following sections.

Table 4.8 Hurd pellets formulations and mechanical properties.

Fiber Type: Tangho Paraguay Hurd (T.H), IND-Hemp U.S.A Bast (I.B) **Additive wax:** Arquad-2HT (Dimethyldioctadecylammonium Chloride) **Initial moisture content:** 60-65%							
Sample Name	**Hurd %**	**Bast %**	**Fiber Milled Size (mm)**	**Wax %**	**Specific Compressive Strength (N/mm)**	**Pellet Durability Index %**	**Pellet Bulk Density (g/cm^3)**
H1	100	0	1.5	5	11 ± 2.6^{a}	48	0.143 ± 0.002^{c}
H2	90	10	1.5	5	171 ± 34^{b}	62	0.114 ± 0.004^{a}
H3	85	15	1.5	5	315 ± 32^{c}	65	0.143 ± 0.005^{c}
H4	90	10	50% 1.5, 50% 1.0	10	436 ± 39^{d}	55	0.133 ± 0.002^{b}

Figure 4.11 represents the visual aspect of hurd pellets with an initial moisture content of 60-65%. All results were analysed using Tukey test with significance level of 5% to determine significance difference between mechanical properties of these pellets. The superscripts (a,b,c,d) represents if the measured mechanical properties of pellets in question are statistically different

from each other or not. If superscripts of different samples in each mechanical property (same column) have same letter than those values are statistically same.

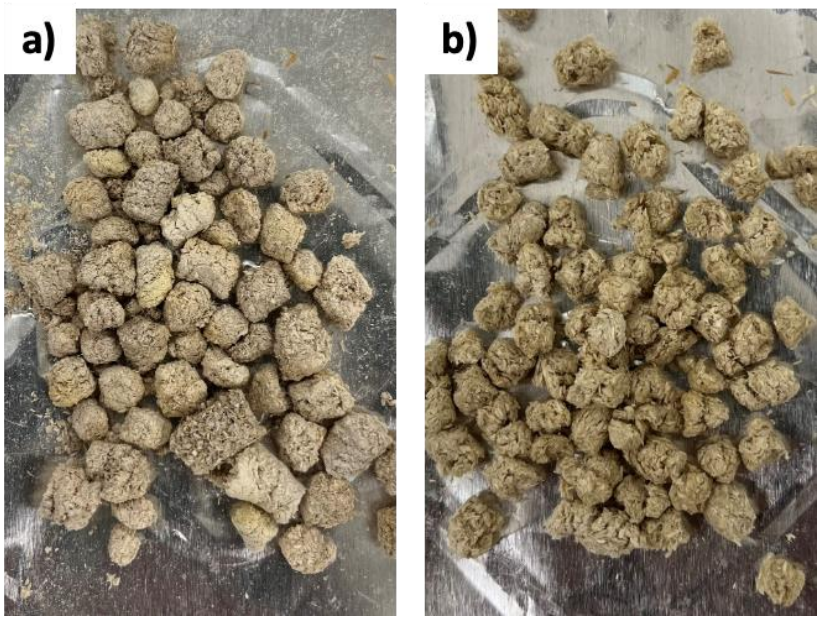


Figure 4.11 Hurd Pellets, a) 100% Hurd fiber pellets (H1), b) 85/15% Hurd and bast fiber pellets (H3).

4.4.1 Specific Compressive Strength:

Figure 4.12 represents the specific compressive strength of hurd pellets. As observed from the results, the compressive strength of hurd pellets is very low. The hurd pellets formed were very weak, and it was difficult to measure the length and width measurements of the pellets without breaking them during the compressive strength test.

Li and Liu, (2000) also observed very low abrasion resistance, impact resistance index, and density of oak chips pellets. Oak chips are similar to hurd fibers. Oak chips were broken into pieces during impact and tumbling tests, and they were not able to produce long logs of oak chips for compressive strength tests.

With the aim to create better pellets, 10% and 15% bast fibers were added in samples H2 and H3. In sample H4, in addition to 10% bast fibers, 10% additive (wax) and two milled fiber sizes (1 and 1.5 mm) were used. As seen in the results, the specific compressive strength increased with increasing bast fiber concentration and the highest value observed was for sample H4. By adding bast fibers, the compaction of the pellets improved somewhat due to the mechanical

interlocking of bast fibers. Even though the strength of the pellets increased with the addition of bast fibers, it was still significantly lower than the strength of the whole hemp fiber pellets shown in Figure 4.8. This is due to high initial moisture content, as excess moisture after pellet drying left empty spaces in the pellet resulting in poor strength of pellets.

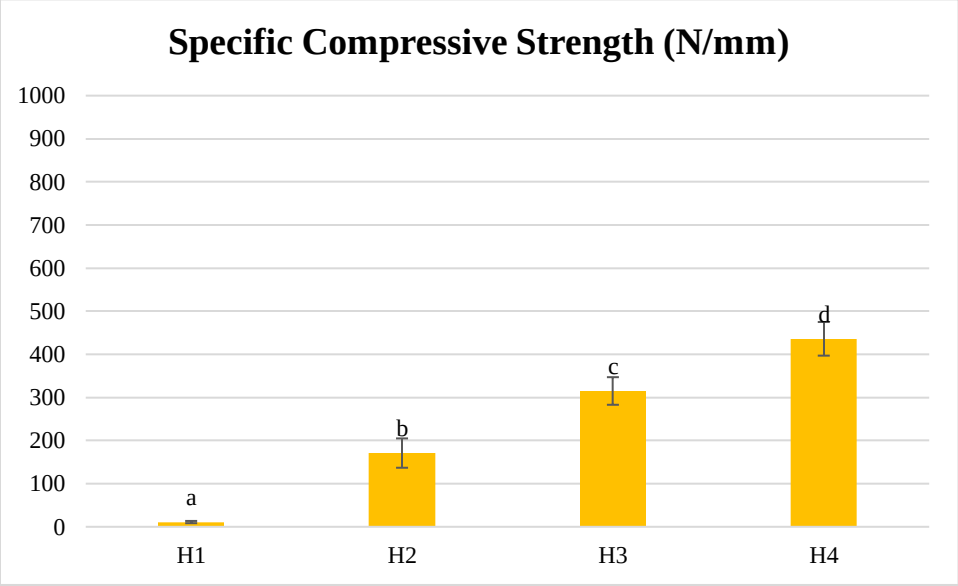


Figure 4.12 Specific compressive strength of hurd pellets.

4.4.2 Pellet Bulk Density:

Figure 4.13 depicts the bulk density results of hurd pellets. The bulk density of the pellets was observed to be significantly lower as compared to the whole hemp pellets in the previous section. As mentioned earlier, due to the very high moisture content, the extra water occupies space between the fibers as it cannot be absorbed by the fibers and when the pellets are dried, this excess water evaporates leaving empty spaces in the pellet structure. The presence of empty spaces in pellets lowers their density and other mechanical properties. The addition of bast fiber and increase in additive concentration did not show any effect on bulk density, so it could be concluded that the effect of the high moisture content is dominant over the effect of the pellet fiber composition and the use of the additive.

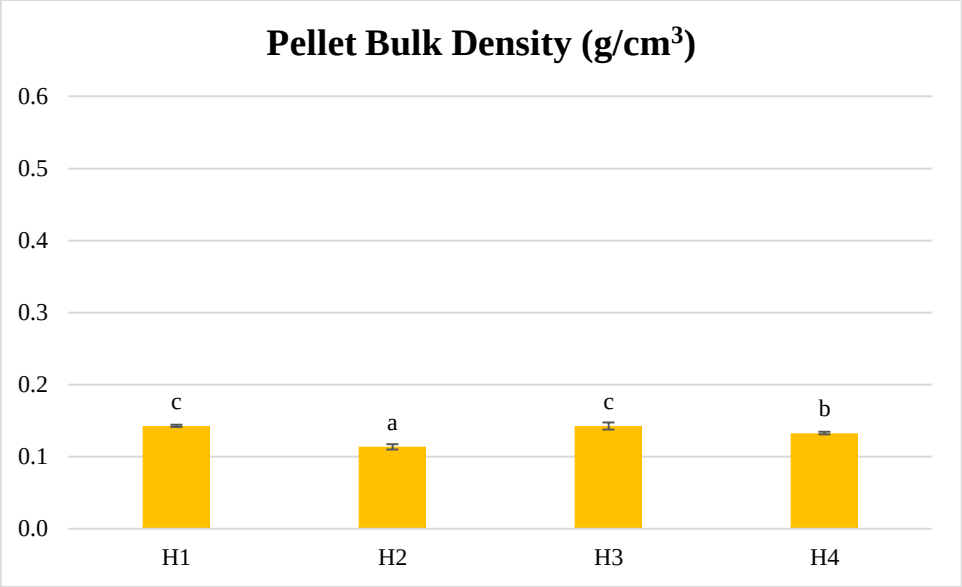


Figure 4.13 Bulk density of hurd pellets.

4.4.3 Pellet Durability Index (PDI):

PDI results of hurd pellets are represented in Figure 4.14. The durability of all pellets was observed to be very low. According to Tabil et al. (1997) , pellet durability is considered low below 70%. The durability of pellets is greatly influenced by moisture content. An increase in moisture content increases the durability of the pellet until optimum moisture level is achieved. Further increase in moisture content will cause the pellet to swell which causes the binding forces bringing the fibers together dominated by forces pulling the fibers apart causing the pellet to disintegrate (Fang et al., 2019). Another assumption for low mechanical properties is that at high moisture content fibers swell and expand. After pelletization when pellets are dried, the moisture evaporates and fibers in pellets shrink creating empty spaces and cracks in the pellets reducing their mechanical properties.

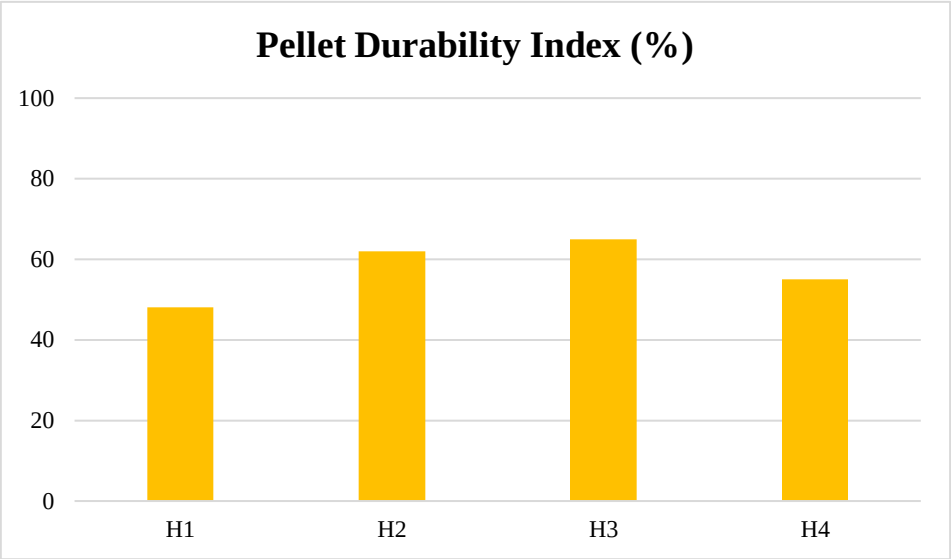


Figure 4.14 PDI of Hurd pellets.

From these attempts at making hurd pellets, it was observed that temperature had a dominant effect over moisture content on the formation and the mechanical properties of the hurd pellets. It was observed that hurd pellets although weak only started to form when the temperature of the pellet die increased above 40°C, and the strength of the hurd pellets increased with further increase in temperature. Due to the high moisture content, the temperature of the pellet die did not increase above 45°C, so all the pellets formed were very weak.

The temperature probably influences the chemical components of biomass fibers such as proteins, lignin, and starch. When temperature is increased, lignin may soften and act as a binder enhancing adhesion between fibers and making pellets stronger and denser according to other authors (Carone et al., 2011). Stelte et al. (2011) investigated the effect of temperature on the bonding and strength of pellets. For pellets prepared at 20 ºC and 100 ºC, it was observed that pellets prepared at 20°C had low strength and poor bonding whereas pellets prepared at 100°C exhibited good bonding and high strength. At low temperature, waxes and lignin in fibers hinders adhesion and act as a boundary layer, and at high temperature, these waxes and lignin softens and interdiffusion forming solid bridges between particles and improving bonding and strength of pellets.

Figure 4.15 represents the effect of temperature on the visual appearance of hurd pellets with initial biomass moisture content between 30-34%. As the temperature increased, the pellets became more compact, and their surfaces became smoother exhibiting a glossier appearance.



Figure 4.15 Visual appearance of hurd pellets at different temperature ranges.

4.5 HEMP PELLETS WITH DIFFERENT COMPOSITIONS OF HEMP BAST AND HURD FIBERS:

From the previous section, it was observed that hurd pellets had weak strength and durability as compared to whole hemp pellets from section 4.3. However, the mechanical properties of hurd pellets improved by adding bast fibers in small concentrations. The objective of this section is to explore pellets made with different compositions of hemp bast and hurd fibers to investigate the optimum composition of bast and hurd fiber. The goal is to create conditions that are easy to flow through the die in the pellet mill resulting in pellets with good mechanical properties.

Pellets were also compared with pellets made from fibers provided by different suppliers to determine which supplier offers better fibers for this project. Harun and Afzal, (2016) found that when woody and agricultural biomass were mixed, the mechanical properties of the pellets were improved.

Both 100% bast and 100% hurd fibers are difficult to flow through the pellet machine, as bast fibers due to their high mechanical interlocking and high cohesion characteristics form agglomerates that get stuck between the pellet mill die and roller blocking the roller from moving. On the other hand, hurd fibers have poor mechanical interlocking, poor cohesion, and brittle characteristics, which leads to difficult pellet formation. It was also observed that temperature had a dominant effect on the mechanical properties instead of moisture. So, in this section, all pellets were made with initial biomass moisture content between 30-34%, and the temperature of the pellet mill die was maintained between 50-60°C. As there was no temperature regulator on the pellet mill, the temperature was increased by operating the pellet mill initially without adding any fibers to it. Once the temperature was higher than 50°C, fibers were added. The temperature on the surface of the die and pellets was measured with a handheld infrared thermometer device. Water was also sprayed to prevent the temperature rising above 60°C when needed. Table 4.4 represents the formulations and mechanical properties of pellets prepared from fibers provided by different suppliers and in different compositions of hemp bast and hurd fibers. Pellet mechanical properties are further discussed in the following sections.

Table 9.4 Formulation and mechanical properties of hemp pellets with different compositions of bast and hurd fibers.

Fiber Milled Size: 1.5 mm. **Initial moisture content:** 30-34%						
Sample Name	**Fiber Type**	**Hurd %**	**Bast %**	**Specific Compressive Strength (N/mm)**	**Pellet Durability Index %**	**Pellet Bulk Density (g/cm3)**
100H	**V.B.B, T.H**	100	0	$720\pm31^{c,d}$	86	0.15 ± 0.002^{a}
80H, 20B		80	20	671 ± 28^{b}	77	0.21 ± 0.002^{b}
60H, 40B		60	40	$666\pm19^{a,b}$	86	0.23 ± 0.002^{b}
40H, 60B		40	60	626 ± 19^{a}	86	0.17 ± 0.005^{a}
20H, 80B		20	80	$742\pm27^{d,e}$	97	0.41 ± 0.002^{f}
100B		0	100	760 ± 23^{e}	97	0.30 ± 0.007^{d}
100H	**I.B, I.H**	100	0	$741\pm29^{d,e}$	86	0.32 ± 0.006^{e}
80H, 20B		80	20	$696\pm19^{b,c}$	90	0.27 ± 0.004^{c}
60H, 40B		60	40	$706\pm25^{b,c,d}$	91	$0.30\pm0.008^{d,e}$
40H, 60B		40	60	$734\pm22^{c,d,e}$	95	$0.28\pm0.006^{c,d}$
20H, 80B		20	80	860 ± 16^{f}	98	0.43 ± 0.001^{f}
100B		0	100	921 ± 17^{g}	99	0.52 ± 0.02^{g}

All results were analysed using Tukey test with significance level of 5% to determine significant difference between the mechanical properties of these pellets. The superscripts (a,b,c,d,e,f,g) represent if the measured mechanical properties of pellets in question are statistically different from each other or not. If superscripts of different samples in each mechanical property have same letter then those values are statistically the same.

4.5.1 Specific Compressive Strength:

The specific compressive strength of different compositions of bast and hurd pellets is represented in Figure 4.16. The overall specific compressive strength of pellets increases with an increase in bast fiber concentration. It is important to compare the 100H pellets mechanical properties with the mechanical properties of hurd pellets in section 4.3.2. The mechanical properties of hurd pellets have significantly increased by using less moisture content (30-34%) and high temperatures (50-60°C). It is then concluded that in the pelletizing of hurd pellets, temperature has a dominant effect over moisture content on the mechanical properties of pellets.

Moreover, it is also observed from Figure 4.16 that hurd fiber pellets prepared from fibers provided by different companies (ValleyBio and IND-Hemp) have similar specific compressive strength, however for bast fiber pellets IND-Hemp bast fiber pellets strength is significantly higher than ValleyBio bast fiber pellets.

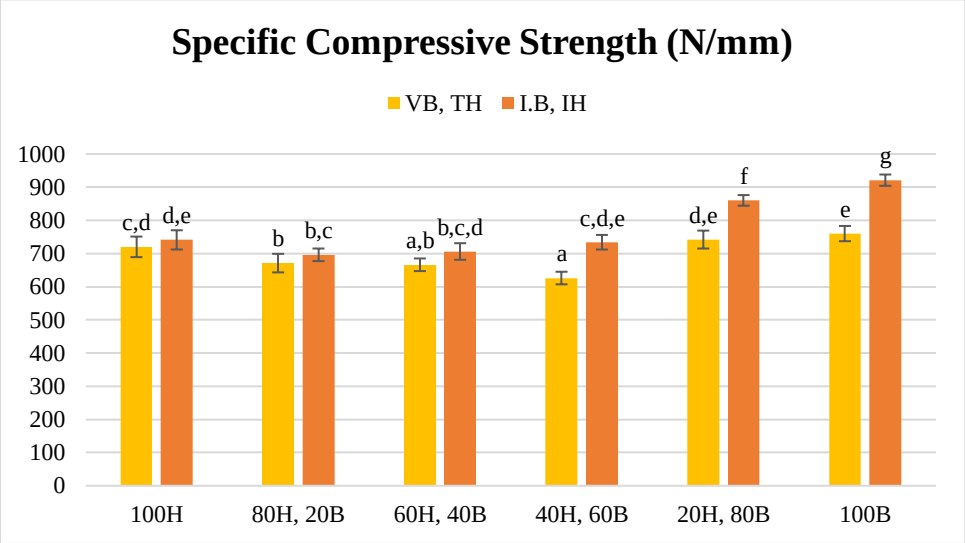


Figure 4.16 Specific compressive strength of pellets with different compositions of hemp bast and hurd fibers.

4.5.2 Pellet Bulk Density:

Figure 4.17 depicts pellet bulk density results. It was observed that the bulk density of pellets prepared from IND-Hemp bast (I.B) and hurd (I.H) fibers was significantly higher than pellets with Valley Bio Bast (VB.B) and Tangho hurd (T.H) fibers. It was also observed that for IND-Hemp fiber pellets the bulk density was slightly reduced by the addition of 20% and 60% bast fibers but increased significantly for pellets with 80% and 100% bast fiber pellets. The higher concentration of bast fibers undergoes good mechanical interlocking due to higher entanglements making the pellets more compact and stronger. In addition to this increased mechanical interlocking, temperature also facilitates the formation of bonds by softening the waxes and lignin. Due to these dominant bonding mechanisms, bast pellets are stronger and denser than other formulations of hurd and bast pellets. Figure 4.18 represents the visual appearance of whole hemp, bast, and hurd pellets along with the pellet average diameter. The Bast pellet diameter was smaller

than the pellet die hole (4 mm) whereas both whole hemp and hurd pellets had diameters higher than the pellet die hole, meaning that the bast pellets did not undergo expansion after leaving the pellet mill die.

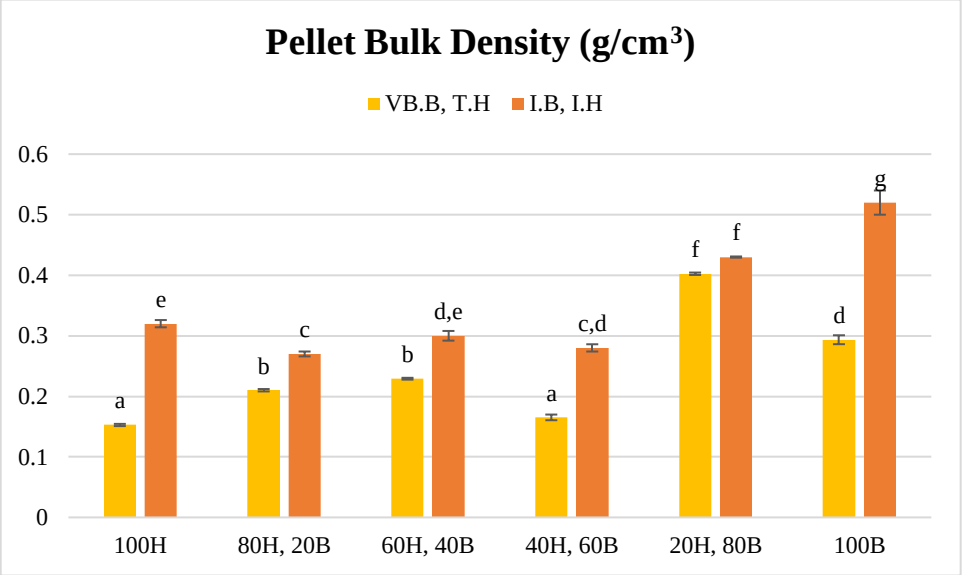


Figure 4.17 Bulk density of pellets with different compositions of hemp bast and hurd fibers.

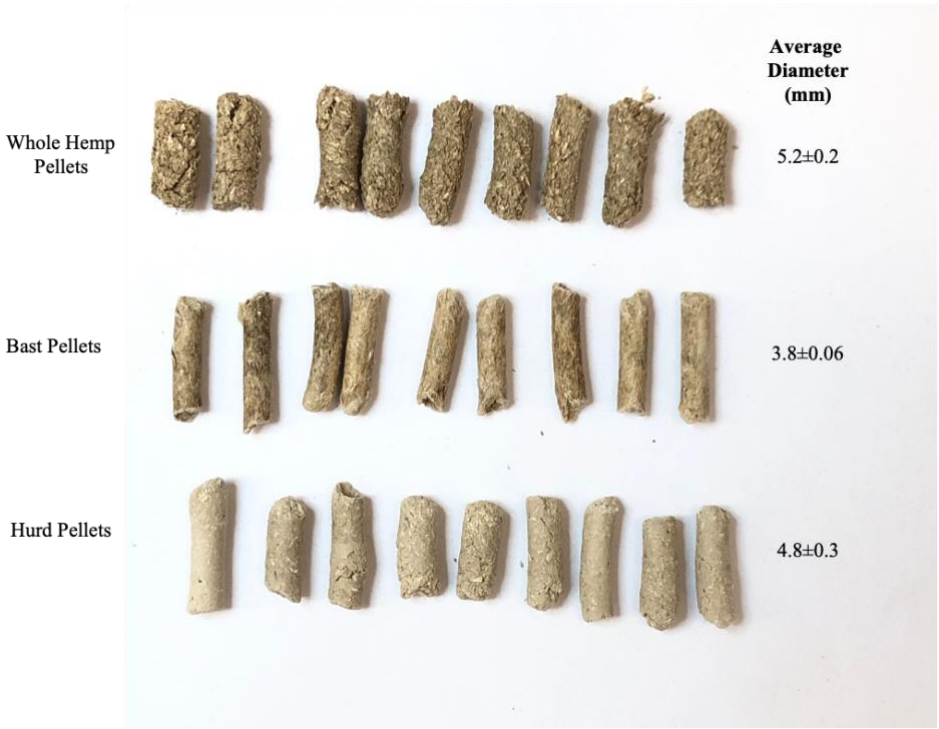


Figure 4.18 Visual appearance of whole hemp, bast, and hurd pellets.

4.5.3 Pellet Durability Index:

PDI results of pellets are shown in Figure 4.19. The durability of all pellets was observed to be high. As alluded to previously, the durability is considered high above 80%, and moderate if PDI is in between 70-80%. In this case, the durability of almost all pellets was above 80%. The durability of pellets increased by increasing the concentration of bast fibers. The highest PDI of 99% was observed for I.B pellets.

According to other authors, pellets with high durability are considered good quality pellets (Kaliyan and Vance Morey, 2009). So, it could be concluded that hemp fibers produce good quality pellets that can withstand destructive forces and maintain their structure without reducing fines during transportation and handling. These results are in accordance with Theerarattananoon et al. (2011) in which they prepared pellets with sorghum stalk, big bluestem, corn stover, and wheat straw milled in sizes of 3.2 mm and 6.5 mm. The durability of their pellets was above 80% and no significant effect of particle size was observed on pellet durability.

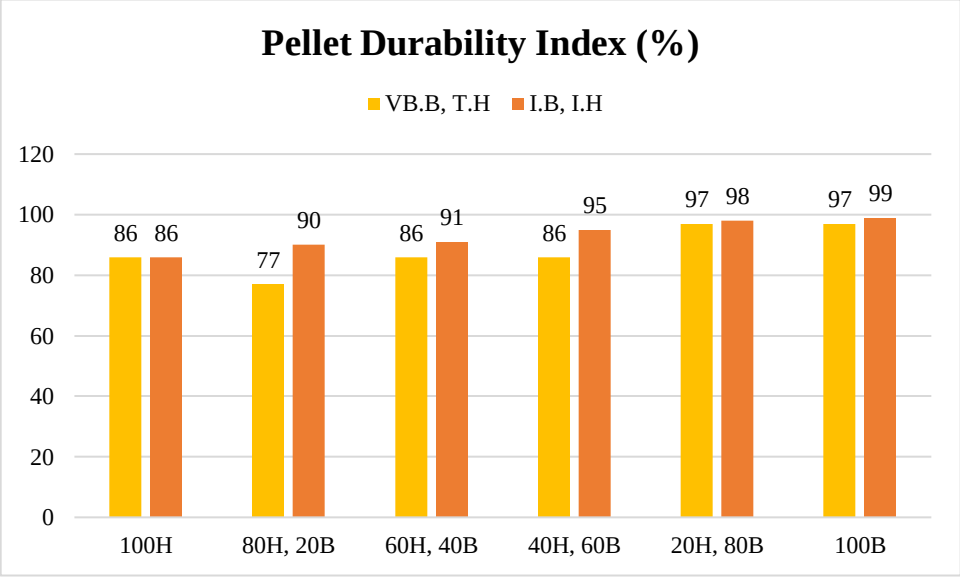


Figure 4.19 PDI of pellets with different compositions of hemp bast and hurd fibers.

From these results presented here, it is concluded that fibers from the IND-Hemp USA supplier produced stronger pellets than fibers from Valley-Bio Canada and Tangho Paraguay. The

mechanical properties of pellets increased with increasing bast fiber concentration and were observed highest for 100% bast pellets.

However, processing of both 100% bast and 100% hurd fiber is a challenge. As mentioned earlier, bast fibers due to high mechanical interlocking agglomerates in between pellet mill rollers die and get stuck. On the other hand, hurd fiber pelleting requires special conditions such as high temperature which can increase power consumption and the cost of the overall process.

Figure 4.20 represents a 1 mm bast and hurd pellet under an optical microscope. It can be observed that bast fibers are entangled whereas no entanglement is observed in hurd pellets and cracks are also observed in hurd pellets.

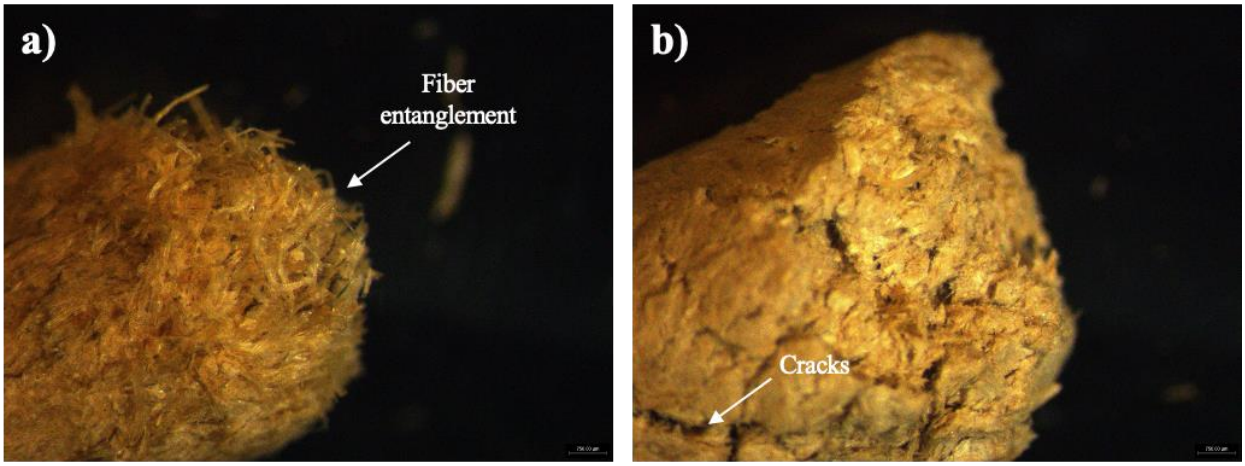


Figure 4.20 a) 1 mm bast fiber pellet, b) 1 mm hurd fiber pellet.

An attempt was also made to produce pellets with 100% bast fibers milled in 3 mm size but this attempt was unsuccessful as long bast fibers blocked the rollers from moving as shown in Figure 4.21. The (60H,40B) pellets were the easiest to flow through the pellet mill and a large quantity of pellets was produced in a short period of time. Moreover, the mechanical properties of these pellets were also observed to be good, but slightly lower than 100% bast pellets. So, in this section, it is concluded that in terms of processibility and moderately high mechanical strength, the composition of 60% hurd fiber and 40% bast fiber composition is optimum.



Figure 4.21: 3 mm bast fiber stuck between roller and hopper preventing the roller from moving.

4.6 PELLETIZING OF WHOLE HEMP FIBERS TREATED WITH NAOH

The objective of this section is to explore the role of chemical treatment on the surface of hemp toward improving the formation of pellets. An attempt was made to prepare pellets from whole hemp fibers that were treated with 5wt.% NaOH in water.

Alkaline treatment of fibers which is also called mercerization is an effective way to remove impurities making fibers more compatible with polymer by exposing reactive OH groups on the fiber surface. NaOH treatment selectively removes certain amounts of lignin and waxes from the fiber surface making the surface rougher which enhances bonding with the polymer. Maichin et al. (2020) investigated the effect of different concentrations (1, 3, 5, 8, 10, and 12%) of NaOH treatment on fiber surfaces. The authors observed that as NaOH concentration increased the contact angle decreased which was then concluded that an increase in NaOH concentration removed more impurities. The alkaline treatment increases surface roughness by distributing hydrogen bonding in fiber network structure yielding extra sites for mechanical interlocking. This way along with removing lignin and other impurities it depolymerizes cellulose and exposes crystallites. It was also reported by the researchers that NaOH treatment increased amorphous cellulose content while decreasing crystalline cellulose (Li et al., 2007).

In the present research, whole hemp fibers from Tangho Paraguay (TwH) were soaked in 5 wt.% NaOH solution for 4 hours and later they were washed with water until a neutral pH of 7 was achieved. The SEM analysis of treated and untreated fibers is shown in Figure 4.22. It can be observed that the waxy layer on the untreated fiber surface is removed after NaOH treatment and the fiber surface has become cleaner and rougher.

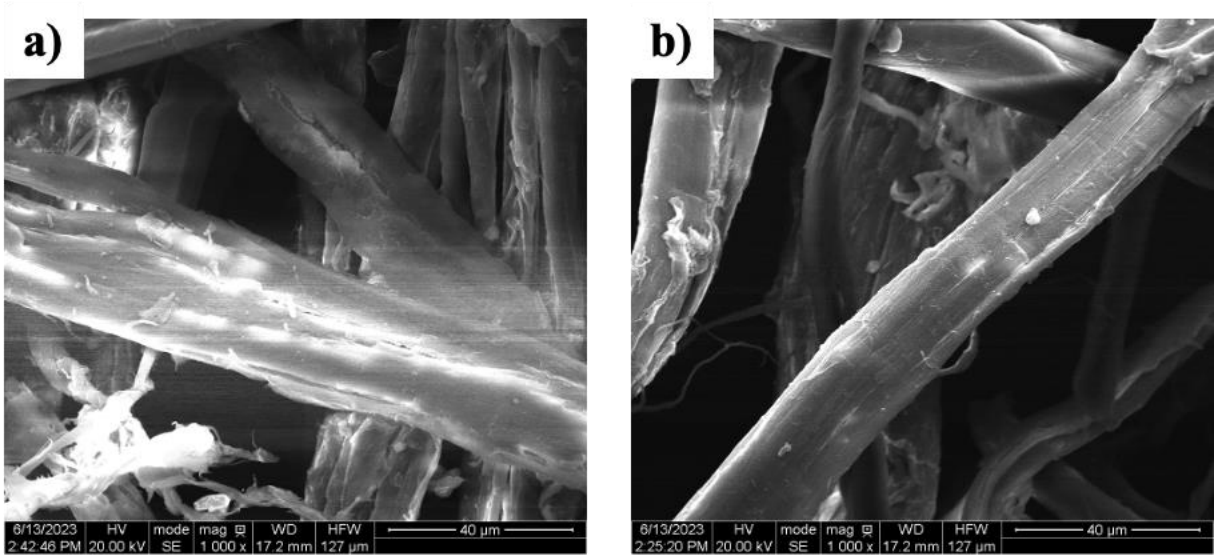


Figure 4.22 SEM analysis of hemp fibers at 1000X magnification a) untreated TwH fiber, b) 5 wt.% NaOH treated TwH fiber.

Figure 4.23 represents the FTIR analysis of untreated and treated hemp fibers. The figure represents an increase in peak in between 3200-3500 cm^{-1}. This increase in peak is caused by an increase in hydroxyl group stretching vibrations due to the removal of impurities from the fiber surface exposing more hydroxyl groups. The decrease in carbonyl group C=O peak intensity at 1600 cm^{-1} represents a decrease in hemicellulose content. The increase in peak at 1100 cm^{-1} represents an increase in C-O-C stretching vibrations of cellulose content on the fiber surface which is exposed after removal of impurities. Also, a decrease in peak at 1250 cm^{-1} represents a decrease in lignin acetyl groups C-O stretching indicating a decrease in lignin concentration.

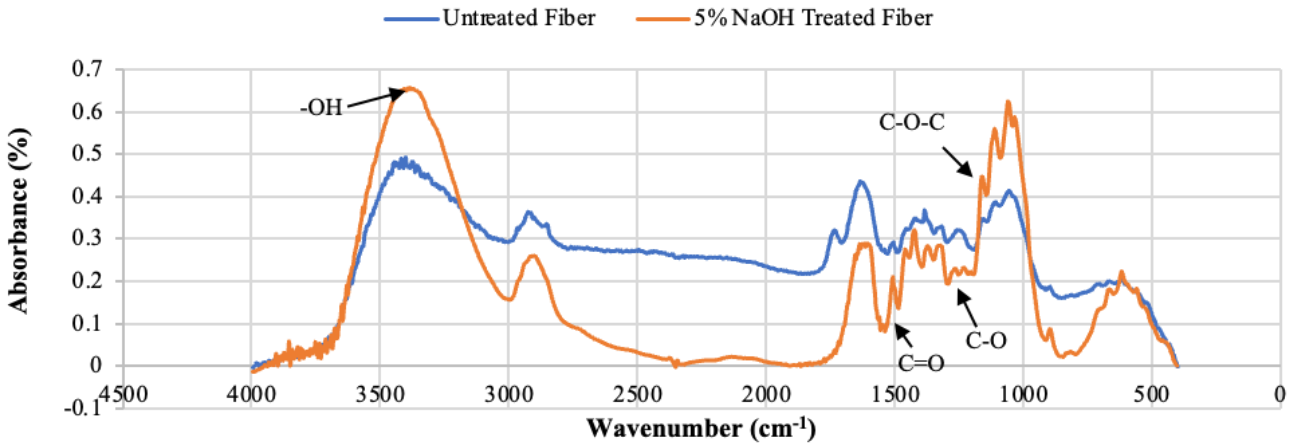


Figure 4.23 FTIR spectrum of untreated TwH and 5 wt.% NaOH TwH fibers.

Moreover, a change in the color of hemp fiber was also observed after NaOH treatment. Figure 4.24 represents a change in the color of hemp fibers before and after NaOH treatment. After NaOH treatment, fibers were lighter in color than untreated fibers.

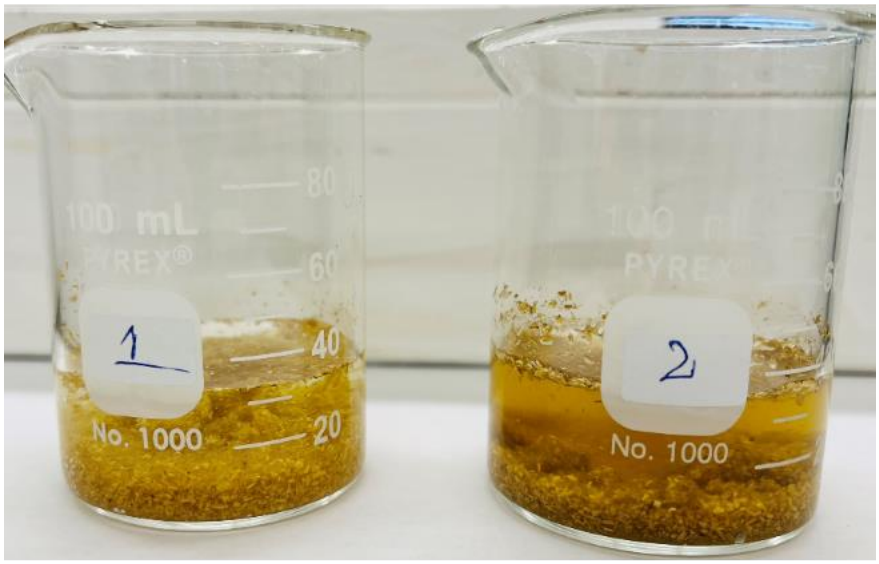


Figure 4.24 Change in color in NaOH treated (1) and untreated (2) hemp fibers.

A water absorption test of fibers was also carried out according to ASTM standard D570-98. First, the fibers were dried at 103°C for 24 hours in the oven and then their initial weight (W_0) was measured. Then fibers were soaked in water for 24 hours as shown in Figure 4.24. After that,

a very fine mesh strainer was used to remove excess water and carefully collect fibers without losing them. Fibers were weighed again to measure their wet weight (W_t) and then their water absorption capacity was measured according to the following equation. This test was carried out two times for each sample.

$$W_a\ (\%) = \frac{W_t - W_0}{W_0} \times 100$$

It was observed that NaOH treated fibers water absorption or uptake was reduced by 12 ± 8 % as compared to untreated fibers.

Alkalization depolymerizes native cellulose I structure to cellulose II producing short length crystallites. Mwaikambo and Ansell, (2002) observed effect of different concentration (0, 0.8, 2, 4, 6, 8, 30 and 400 %) of NaOH treatment on hemp, sisal, jute, and kapok fibers. It was observed through wide-angle x-ray diffraction (WAXRD) that crystallinity index of fibers increased initially at low concentrations (0, 0.8, 2, 4, 6 and 8%) and then decreased at high concentration of NaOH. The crystallinity index was referred to as packing order of crystallites not the crystallinity. The order of crystallites was improved due to thickening of cell wall during alkali treatment. This improvement in crystallites packing order could prevent water penetration. Moreover, the removal of impurities from fiber surface results in reducing the capillary effect responsible of drawing water into fiber. And lastly, hydrophilic hemicellulose is also removed which results in less water absorption capacity of fiber.

The attempt of pelletizing NaOH-treated hemp fibers was not successful. The NaOH treatment removes impurities from fiber surface and increases the cohesive characteristics of fibers by making the surface rougher and providing additional anchoring points for mechanical interlocking. Due to increased cohesion, fibers agglomerated in a cake-like structure in between the pellet mill die and roller and were not able to pass through die holes. The agglomerates are shown in Figure 4.25.



Figure 4.25 Cake-like agglomerates of NaOH-treated TwH fibers formed in between pellet mill die and rollers.

4.7 CHANGE IN FIBER SIZE AFTER PELLETIZATION:

The objective of this section is to evaluate possible changes in particle sizes before and after the pelletization step. Particle size analysis of 1-, 1.5-, and 3-mm milled fibers was done after pelletization to observe change in particle size. It is important to investigate the change in particle size after pelletization as it can affect the mechanical properties of composites prepared with such pellets.

Figure 4.26 represents the appearance of 1 mm milled bast and hurd fibers before and after pelletization. It can be observed that bast fibers were able to withstand shear stresses applied during pelletization and were able to maintain their shape whereas hurd fibers were disintegrated during the pelletization process. Only 20% of hurd fibers were able to be measured with an optical microscope after pelletization. Figure 4.27 represents bast fiber lengths before and after pelletization and Figure 4.28 represents their aspect ratios.

As previously mentioned, the 3 mm milled bast fibers were not able to be pelletized, their particle size analysis could not be done. No significant change in bast fiber length was observed after pelletization so it can be concluded that bast fibers are able to withstand shear stresses applied during pelletization and maintain their length. However, their aspect ratio distribution was slightly increased after pelletization.

Hurd fiber lengths and aspect ratios before and after pelletization are shown in Figures 4.29 and 4.30. It can be observed that hurd fiber lengths were reduced after pelletization whereas their aspect ratio distribution increased. This is because hurd fibers were disintegrated into thinner fibers during pelletization and their aspect ratio distribution increased. From these results, it could be concluded that hurd fiber undergoes size change during pelletization whereas bast fibers maintain their size.

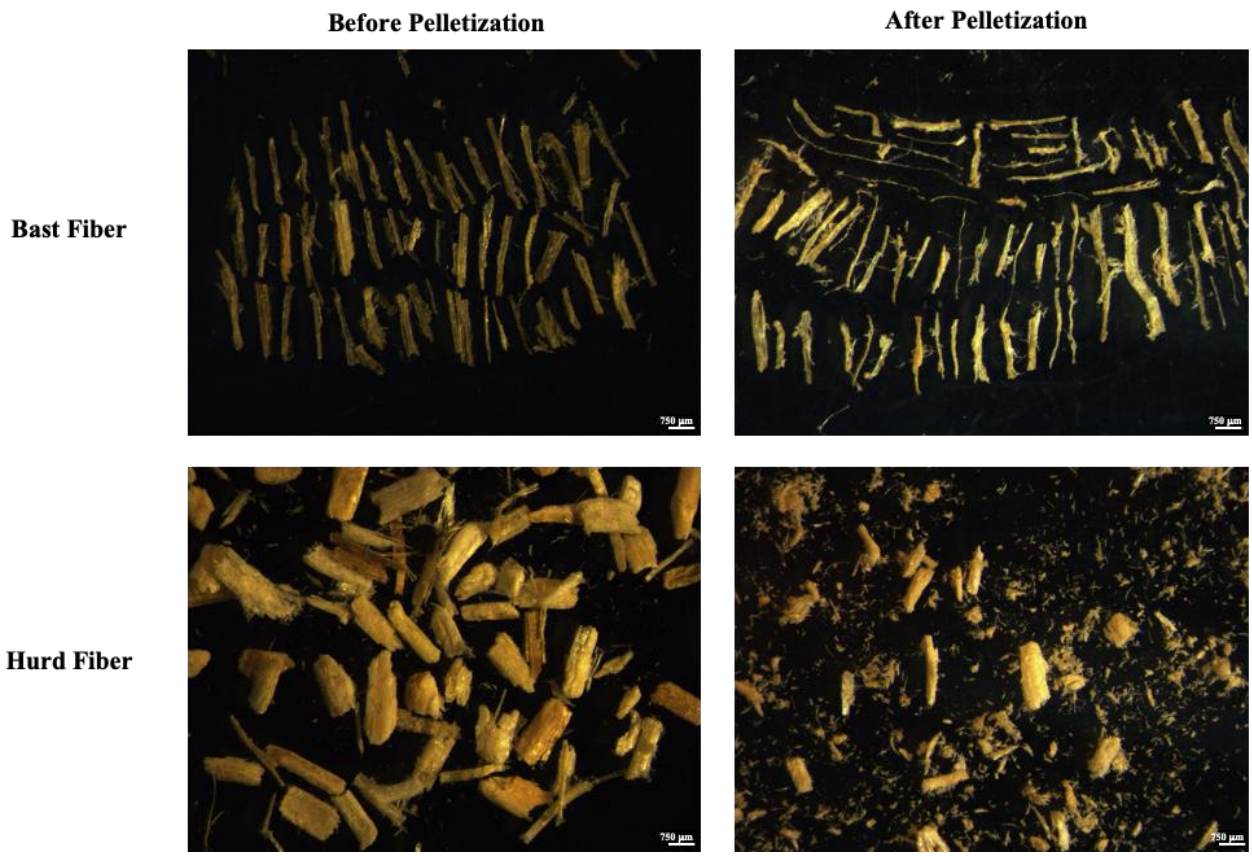


Figure 4.26 Appearance of 1 mm milled bast and hurd fiber before and after pelletization.

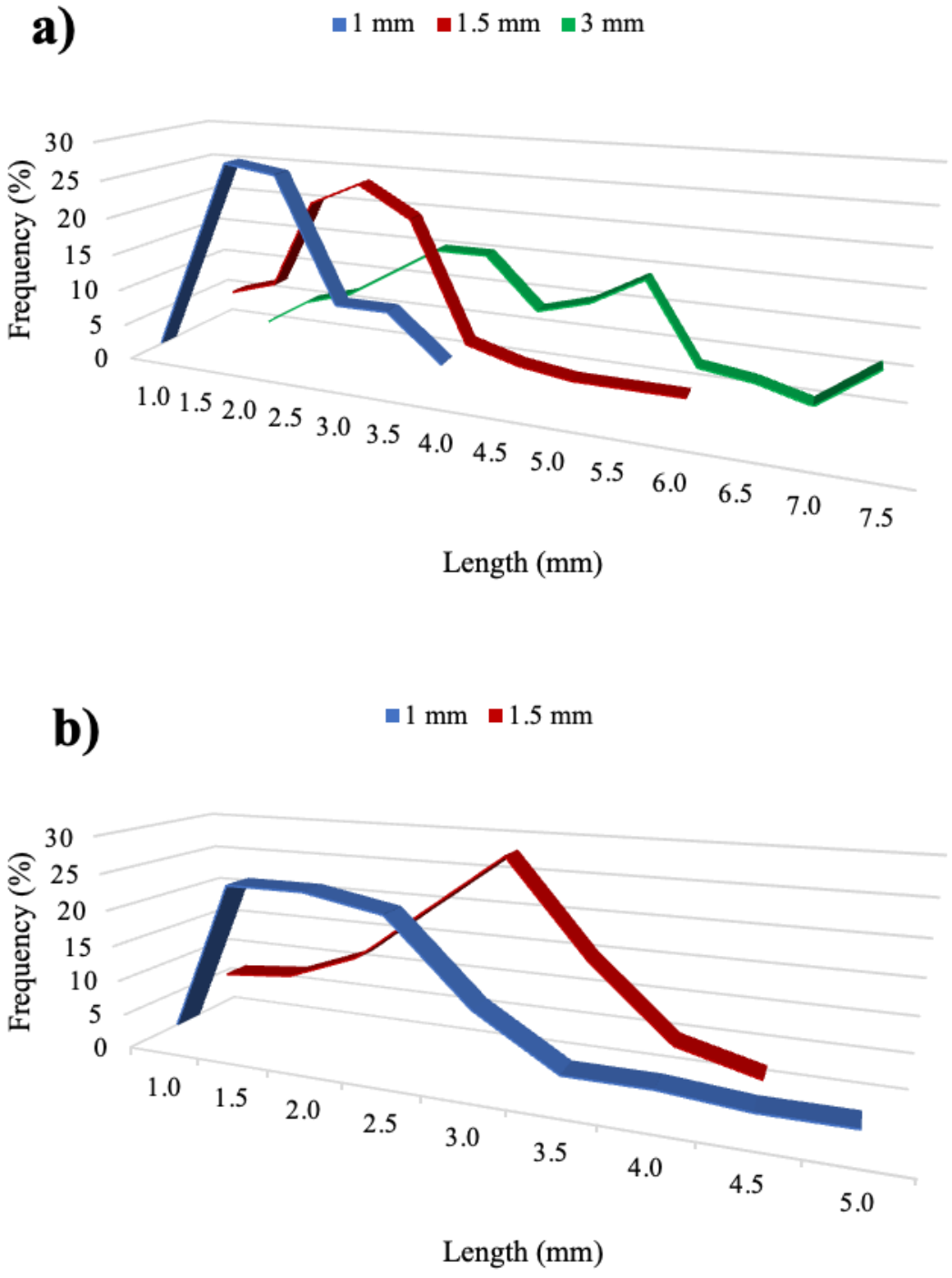


Figure 4.27 Bast fiber lengths a) before pelletization, b) after pelletization.

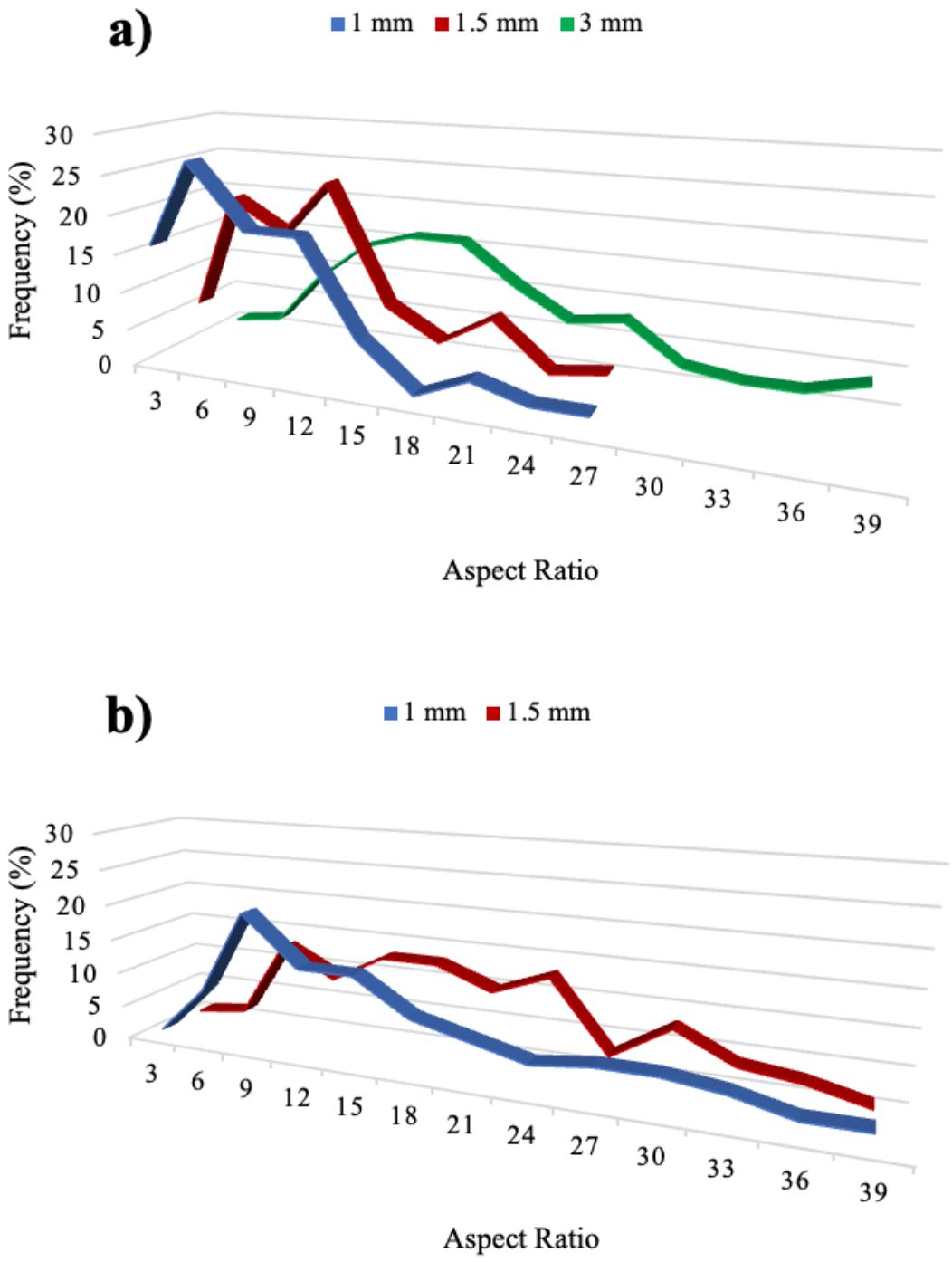


Figure 4.28 Bast fiber aspect ratio a) before pelletization, b) after pelletization.

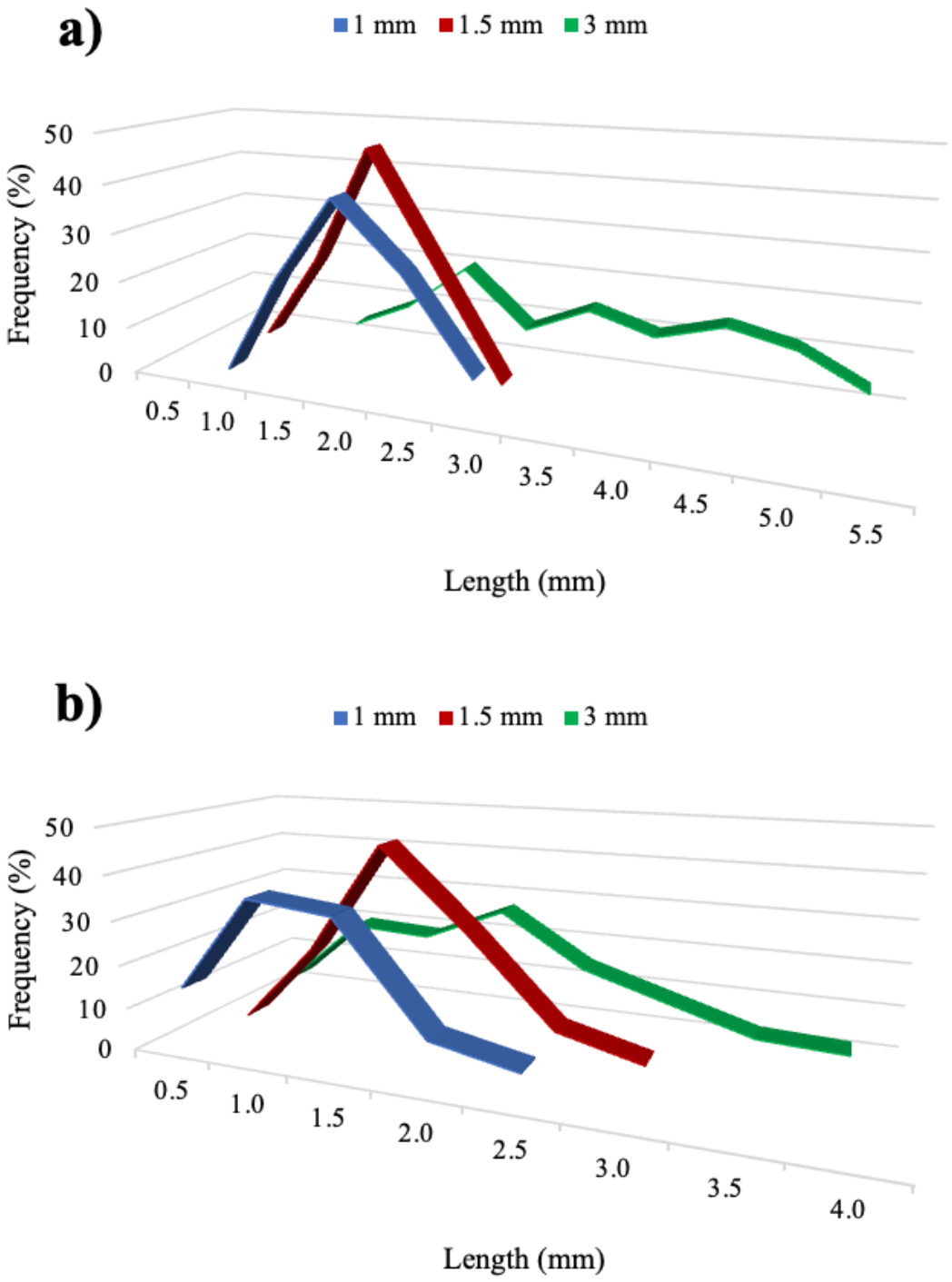


Figure 4.29 Hurd fiber lengths a) before pelletization, b) after pelletization.

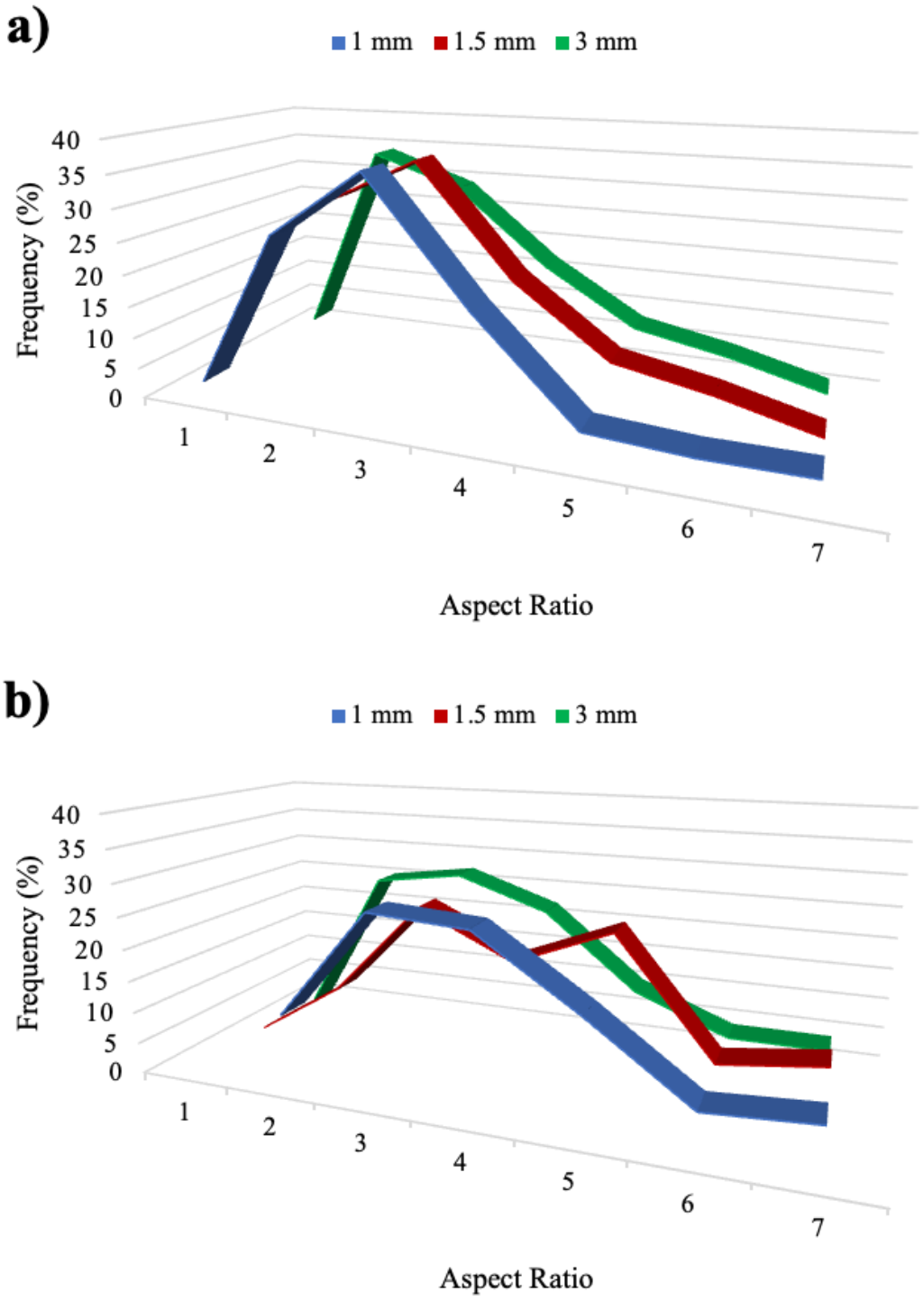


Figure 4.30 Hurd fiber aspect ratio a) before pelletization, b) after pelletization.

CHAPTER 5: COMPOSITES

RESULTS AND DISCUSSION

5.1 INTRODUCTION:

In this chapter polypropylene composites reinforced with different hemp fibers and pellets were prepared and their results were analyzed. Flexural modulus and strength, tensile modulus and strength, impact strength, melt flow index (MFI), and specific flexural modulus (SFM) properties of composites were analyzed. Figure 5 represents the flow chart of the composite-making process.

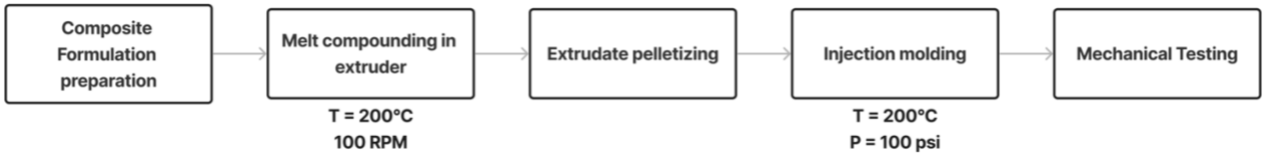


Figure 5 Flow chart of the composite-making process.

The results are divided into the following six sections:

5.2 Effect of chemically treated fiber and coupling agent on mechanical properties of composites.

5.3 Effect of fiber length and use of wax on the mechanical properties of composites.

5.4 Effect of hemp bast and hurd fibers of different sizes on the mechanical properties of composites.

5.5 Composites containing hemp pellets with different compositions of hurd and bast fiber from different suppliers.

5.6 Effect of hemp fiber from different countries on the mechanical properties of composites.

5.7 Comparison Between Composite with Fiber and Pellet.

5.2: EFFECT OF CHEMICALLY TREATED FIBER AND COUPLING AGENT ON MECHANICAL PROPERTIES OF COMPOSITES.

The composites were prepared with untreated hemp fiber, 5 wt% NaOH treated hemp fiber, 0.5 wt% MAPP coupling agent, and 5 wt% NaOH treated hemp fiber and 0.5 wt% MAPP, according to the composition presented in table 5.1, to investigate the effect of bonding between the polypropylene matrix and the hemp fibers. These composites were prepared using whole hemp fibers, not pellets as discussed in Chapter 4, because the pelletization of NaOH-treated fibers was not successful due to increased agglomeration. Table 5.1 represents the formulation of composites and table 5.2 represents their mechanical properties results which are further discussed in the following section.

Table 5.1 Formulation of composites with NaOH-treated fibers and MAPP.

Fiber Type: Retted whole hemp fiber from Tangho Paraguay (TwH) **Milled Fiber size:** 1.5 mm **Fiber moisture content:** 0-1 wt.%				
Sample Name	**PP wt.%**	**Hemp Fiber wt.%**	**Fiber NaOH treatment wt.%**	**MAPP wt.%**
PP	100	0	0	0
20TwH	80	20	0	0
20TwH-5Na	80	20	5	0
20TwH+ 0.5 MA	79.5	20	0	0.5
20TwH-5Na+ 0.5MA	79.5	20	5	0.5

Table 5.2 Mechanical properties of composites with NaOH-treated fibers and MAPP.

Sample Name	**Flexural Modulus (MPa)**	**Flexural Strength (MPa)**	**Tensile Modulus (MPa)**	**Tensile Strength (MPa)**	**Impact Strength (J/m)**	**Melt Flow Index (g/10min)**	**Density (kg/m^3)**	**Specific Flexural Modulus (MPa.m^3/kg)**
PP	813±17^{a}	31.5±0.4^{a}	118±7^{a}	15.0±1.6^{a}	27.9±1.4^{c}	23±0.1^{b}	925±0.9	0.88±0.02^{a}
20TwH	1243±25^{b}	33.6±0.3^{b}	131±6^{a}	19.3±1.7^{a,b}	10.7±0.6^{a}	10.2±0.3^{a}	961±3.0	1.29±0.03^{b}
20TwH-5Na	1315±21^{c}	35.8±0.6^{c}	118±8^{a}	16.0±1.4^{a,b}	11.8±0.9^{a,b}	9.0±1.8^{a}	963±3.4	1.37±0.02^{c}
20TwH+ 0.5 MA	1354±34^{c,d}	40.5±0.8^{d}	181±11^{b}	23.4±1.8^{b}	12.4±0.9^{b}	10.5±0.3^{a}	964±3.4	1.40±0.04^{c,d}
20TwH-5Na+ 0.5MA	1384±23^{d}	40.4±0.6^{d}	129±9^{a}	19.0±2.8^{a,b}	13.1±0.5^{b}	9.6±0.8^{a}	962±2.0	1.44±0.02^{d}

The data were statistically evaluated using the Tukey test to compare the means of the mechanical properties of the composites at a 95% confidence level. Different letters, in the same column, represent significant differences ($p<0.05$) between the means obtained through the Tukey Test.

5.2.1 Flexural Properties:

The flexural modulus and flexural strength of neat PP and composites are shown in Figures 5.1 and 5.2. It was observed that by adding 20wt% hemp fibers (20TwH), the flexural modulus increased by 53% as compared to neat polypropylene. For the other compositions where hemp fiber was treated with 5 wt% NaOH (20TwH-5Na), with the addition of 0.5 wt% MAPP coupling agent in the composite (20TwH+ 0.5 MA), and in the composite containing both 5 wt% NaOH treated hemp fiber and 0.5 wt% MAPP (20TwH-5Na+ 0.5MA) the improvement in the flexural modulus of the composite was even better, representing an increase of 60%, 67% and 70%, respectively, when compared to pure polypropylene.

The flexural strength increased significantly with the addition of 20% hemp fiber to the composite, reaching 29% in the 20TwH+ 0.5 MA sample when compared to pure polypropylene.

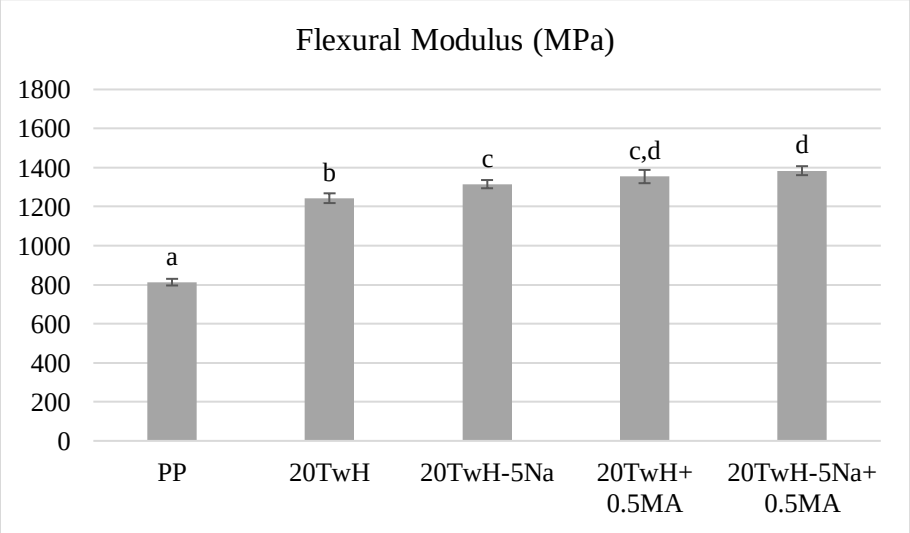


Figure 5.1 Flexural modulus of composites with NaOH-treated fibers and MAPP.

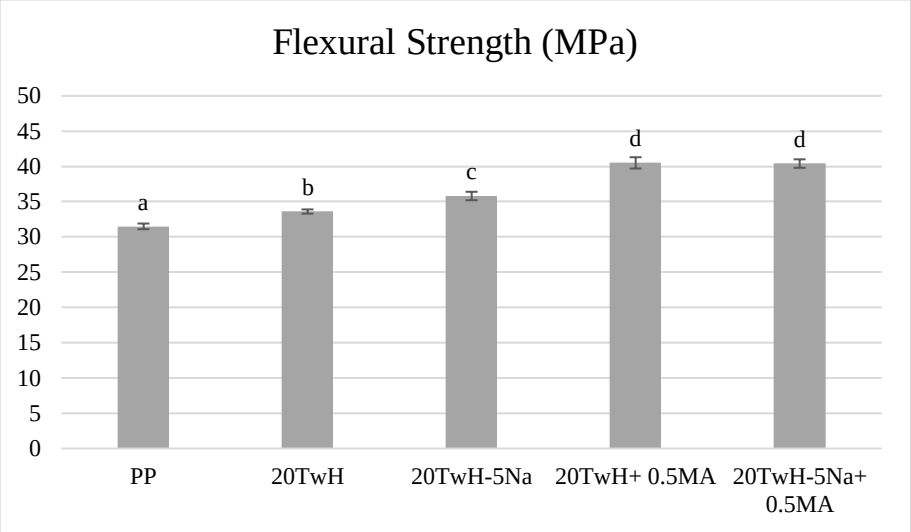


Figure 5.2 Flexural Strength of composites with NaOH treated fibers and MAPP.

5.2.2 Tensile Properties:

The tensile modulus and tensile strength of the composites are shown in Figures 5.3 and 5.4. It was observed that there was no significant improvement in the tensile modules of the composite by the addition of 20wt% fibers (20TwH) and NaOH-treated fibers also did not have any improvement in the tensile modulus even with the addition of MAPP. Composites with untreated fibers and 0.5% MAPP (20TwH+0.5MA) displayed a 35% increase in tensile modulus as compared to neat PP.

The addition of hemp fibers slightly improved the tensile strength of the composites. Similar tensile strengths were shown by the 20TwH, 20TwH-5Na, and 20TwH-5Na+ 0.5MA, while the 20TwH+0.5MA showed the highest tensile strength.

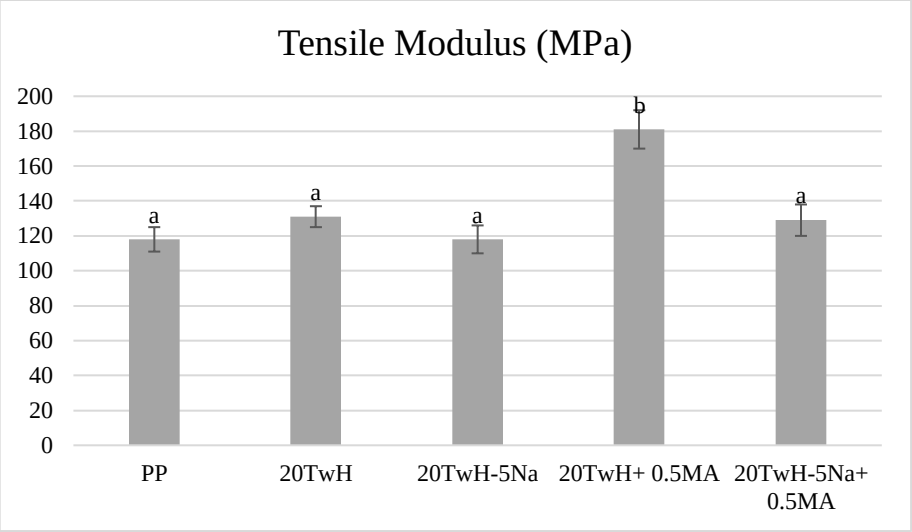


Figure 5.3 Tensile modulus of composites with NaOH-treated fibers and MAPP.

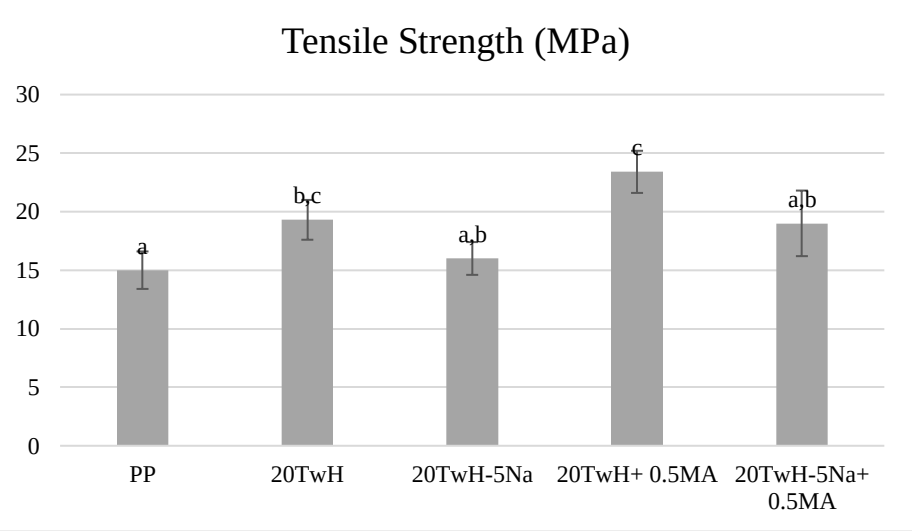


Figure 5.4 Tensile strength of composites with NaOH-treated fibers and MAPP.

It was observed that the 20TwH-5Na composite displayed the most improvement in mechanical properties. NaOH-treated fiber composites also had a positive effect on mechanical properties, but MAPP was found to be more efficient.

Owen et al. (2015), investigated the effect of sisal fibers treated for 24 hours with different concentrations of NaOH (2%, 5%, 10%, and 20%) on sisal fiber-reinforced epoxy composite's mechanical properties. It was found that NaOH-treated fiber composites had higher tensile and

flexural properties than untreated fibers and 2% NaOH-treated fiber provided the optimum tensile and flexural properties. The NaOH treatment removed impurities and lignin from the fiber surface making the fibers thinner and lighter and making the surface more rougher promoting mechanical anchoring between polymer and fibers.

5.2.3 Impact Strength:

The impact strength of composites is shown in Figure 5.5. The addition of fibers decreased the impact strength of composites by approximately 62%. The NaOH-treated fiber composites and composites with MAPP showed a slight improvement in impact strength, but the values were still significantly lower when compared to pure PP.

The addition of fibers to the polymer matrix tends to reduce impact strength due to two mechanisms: the addition of fibers restricts the motion of polymer molecules which reduces the ductility of the polymer matrix making them stiffer and more brittle which it is not able to absorb impact energy; and fibers in polymer creates stress concentration points at the end of the fibers where there is abrupt change in load transfer and stiffness, or areas where interfacial adhesion is poor due to this less energy is required for crack propagation (Marcovich and Villar, 2003; Nourbakhsh et al., 2008).

Owen et al. (2015), also reported a decrease in impact strength with the addition of sisal fibers in a polyester matrix. The impact strength was improved by treating fibers with NaOH. Fibers treated with 5% NaOH showed greater impact strength than other concentrations (2%,10%,20%) of NaOH-treated fibers, however, it was still lower than the impact strength of neat polyester.

Nourbakhsh et al. (2008), investigated the effect of 3% MAPP and 5% polybutadiene isocyanate (PBNCO) coupling agents on mechanical properties of wood-fiber reinforced polypropylene composites. It was found that impact strength was reduced by the addition of fibers, and composites with 3% MAPP improved the impact strength, but it was still lower than neat PP. Wood fiber polypropylene composites with both 3% MAPP and 5% PBNCO coupling agents showed impact strength equivalent to neat PP which indicates chemical compatibility between fibers and polymer increased by these coupling agents.

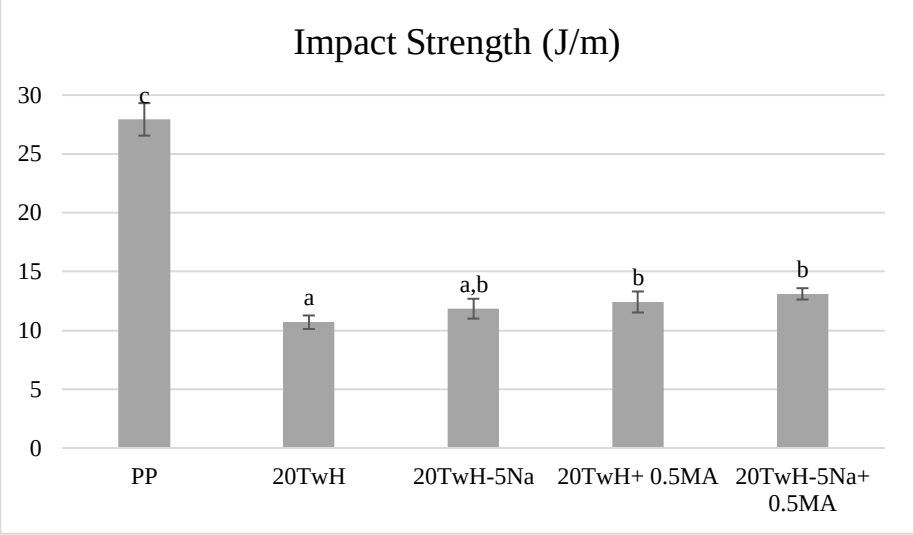


Figure 5.5 Tensile strength of composites with NaOH-treated fibers and MAPP.

5.2.4 Melt Flow Index:

Melt flow index (MFI) results are shown in Figure 5.6. As expected, MFI decreased with the addition of fibers. When 20% fibers were added to the polymer matrix, MFI was reduced by 55% as compared to neat PP. It was reported in the literature that by increasing the fiber content in the composites, the MFI decreased. It was also reported that the addition of 5% MAPP had a negative effect on MFI and the use of alkaline treated and mild-bleached fibers had better MFI than composites with untreated fibers due to better dispersion of the fibers in the polymer matrix (Soleimani et al., 2008). However, in our study, the composites with 0.5%MAPP and with treated and untreated fibers showed statistically similar results.

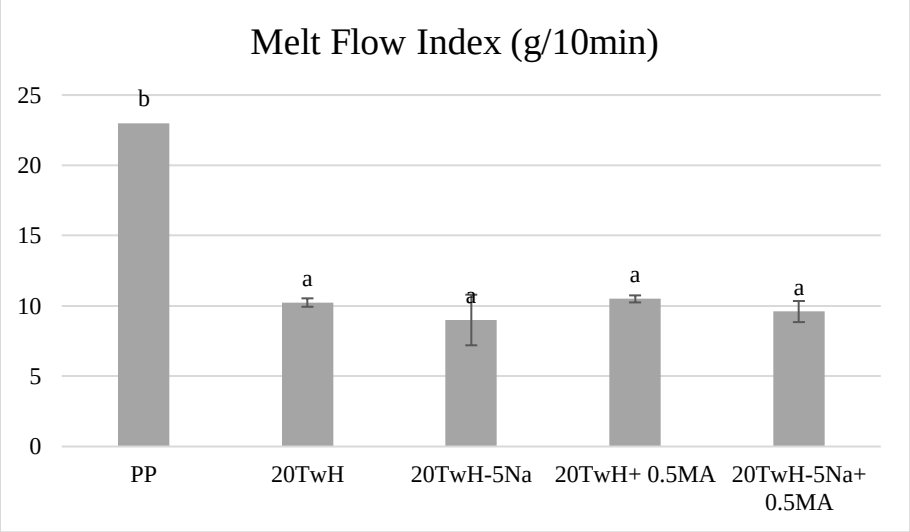


Figure 5.6 Melt flow index (MFI) of composites with NaOH-treated fibers and MAPP.

5.2.5 Specific Flexural Modulus (SFM):

Specific flexural modulus refers to the flexural modulus normalized by composite density. It measures the stiffness of composites relative to their mass. The Following equation can be used to calculate the specific flexural modulus of composites.

$$Specific\ Flexural\ Modulus\ (SFM) = \frac{Flexural\ Modulus}{Composite\ density}$$

The densities of the composites and neat PP are given in Table 5.2. As expected, densities of composites were increased with the addition of 20wt% fibers. The specific flexural modulus results are shown in Figure 5.7. As expected, the specific flexural modulus increased significantly with the addition of fibers as compared to neat PP. High specific flexural modulus indicates that the material is stiffer compared to its mass which is useful in applications where materials with high stiffness and light weight are required. The SFM was improved by NaOH-treated fibers and the use of MAPP. The 20TwH+0.5MA and 20TwH-5Na+0.5MA composites presented the highest SFM which indicates that composites containing 0.5% MAPP had better interfacial adhesion between the matrix and the fibers, and the load was more efficiently transferred as compared to composites without MAPP.

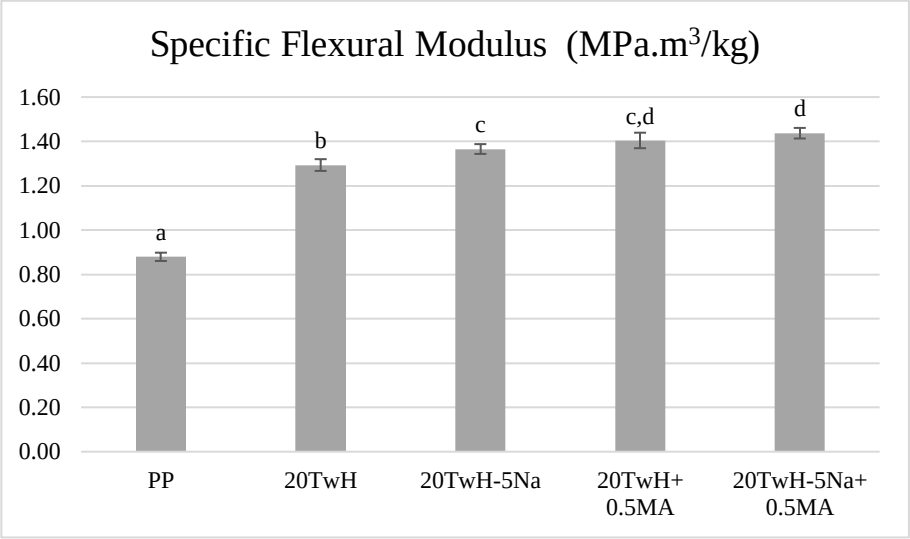


Figure 5.7 Specific Flexural Modulus (SFM) of composites with NaOH-treated fibers and MAPP.

5.2.6 Scanning Electron Microscopy (SEM):

As discussed in the literature review, an efficient interaction between matrix and fibers is quite important for effective load transfer and achieving high mechanical properties. To investigate whether fibers treated with NaOH, or the addition of MAPP coupling agent provide better interaction between fibers and polymer, SEM analysis of fracture surfaces of these composites was performed.

Figure 5.8 shows SEM analysis of composite with 20wt% untreated hemp fiber (20TwH) without MAPP. It is noticeable that there is a limited interaction between the fiber and matrix. The gap suggests insufficient bonding between the fiber and PP matrix and fiber seems to be de-bonding from the matrix.

Figure 5.9 shows SEM analysis of 20wt% NaOH-treated hemp fibers without MAPP (20TwH-5Na). It can be observed that by using NaOH-treated fibers the bonding between fibers and matrix has improved but still, there are very narrow gaps at some points. Figure 5.10 represents SEM analysis of the fractured surface of composites with 20wt% untreated fibers with 0.5wt% MAPP (20TwH+0.5MA). Efficient wetting of fibers with polymer can be clearly observed. There are no gaps between the fiber and the PP matrix. Figure 5.11 also represents great interaction and no gaps between fiber and polymer in composites with 20wt% NaOH treated fibers and 0.5wt% MAPP (20TwH-5Na+0.5MA). These SEM analysis results also support the mechanical results of

composites discussed earlier. The 20TwH+0.5MA and 20TwH-5Na+0.5MA have better mechanical properties because of good interaction between polymer and fibers which promotes efficient load transfer between them.

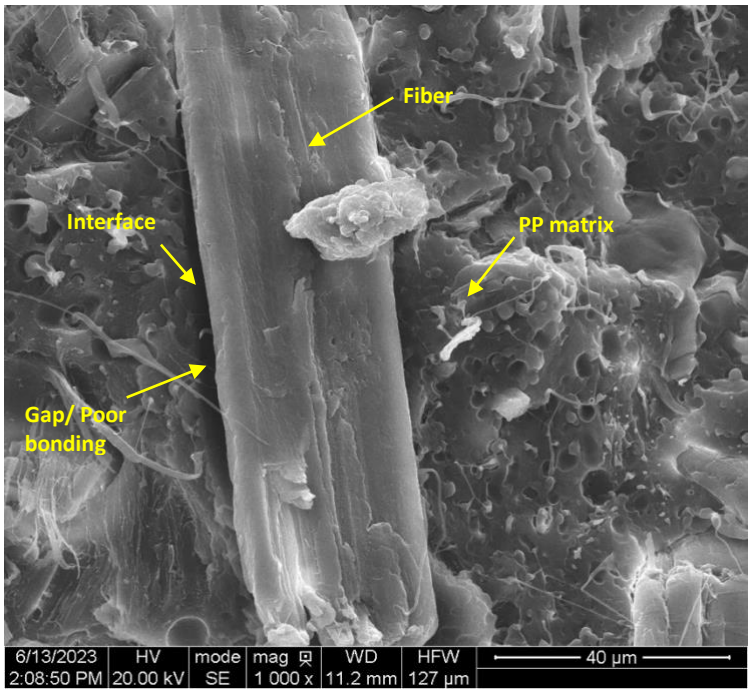


Figure 5.8 SEM of 20TwH composite (1000X).

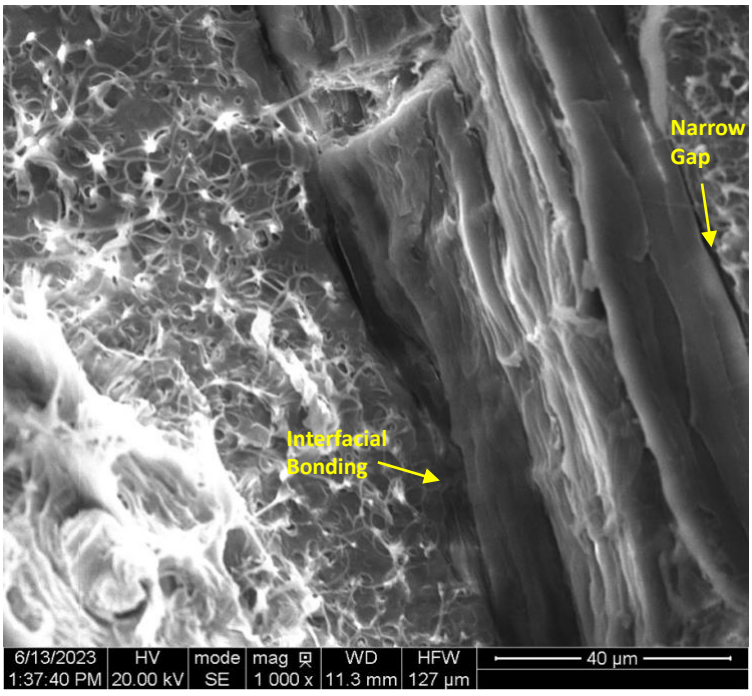


Figure 5.9 SEM of 20TwH-5Na composite (1000X).

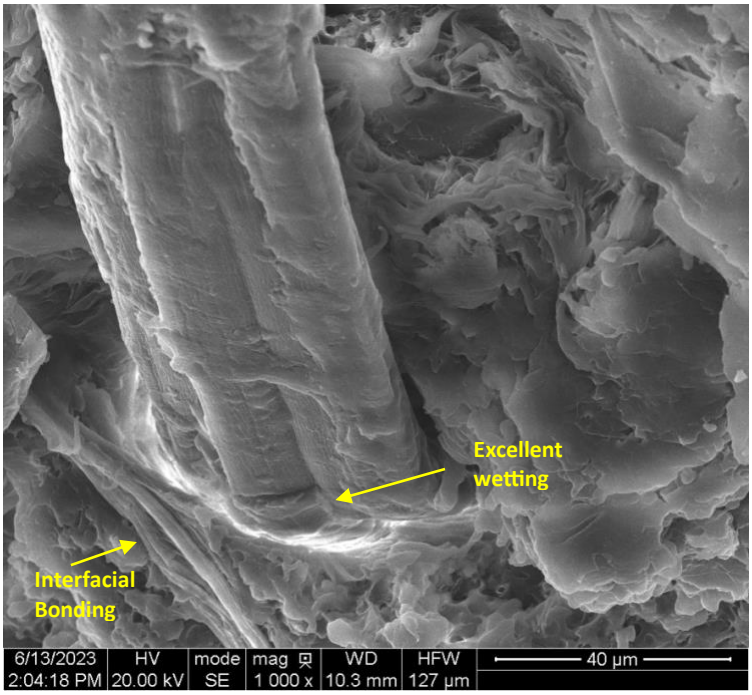


Figure 5.10 SEM of 20TwH+0.5MA composite (1000X).

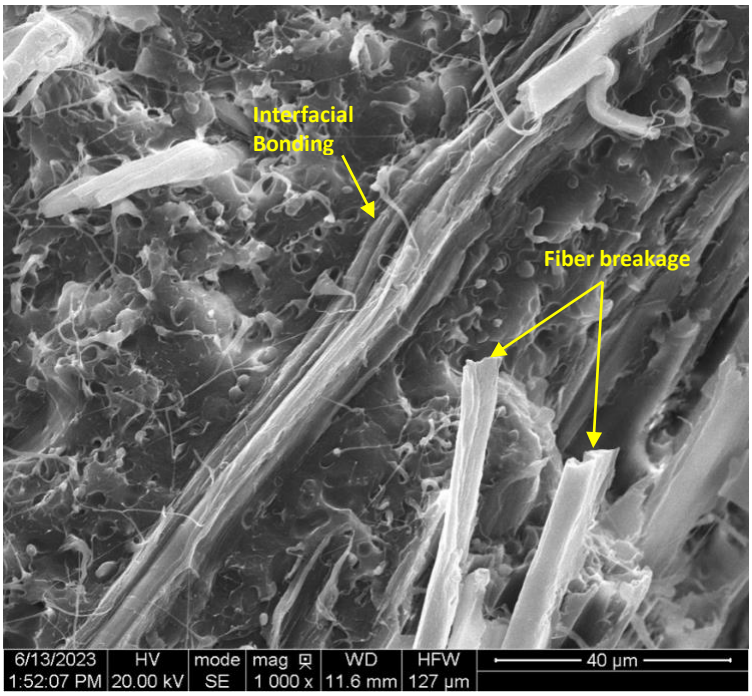


Figure 5.11 SEM of 20TwH-5Na+0.5MA composite (1000X).

The bonding between fiber and PP matrix was improved by NaOH treatment of fibers, however, excellent interfacial bonding and mechanical properties were achieved by the addition of 0.5% MAPP.

The addition of the MAPP coupling agent provided better interfacial adhesion even with untreated fibers. The mechanical properties of composites with MAPP and treated and untreated fibers were similar, except that composites made with untreated fibers and MAPP have better tensile properties. Therefore, it is concluded that good mechanical properties can be achieved with the addition of 0.5% MAPP coupling agent without performing NaOH treatment of fibers.

These results are in accordance with literature studies which state that mechanical properties increased with fibers NaOH treatment and use of MAPP coupling agent and better results were obtained from composites with MAPP. MAPP facilitates polar acid-base intractability and can form covalent bonds with hydroxyl groups present on natural fiber surface (Hassan et al., 2010; Sullins et al., 2017b).

Moving on with this research, a 0.5% MAPP coupling agent will be used in all Polypropylene-hemp fiber/pellets composites. From previous work in our laboratory, it was determined that 0.5wt% MAPP is the optimal amount for 20wt% natural fiber composites.

5.3: EFFECT OF FIBER LENGTH AND USE OF WAX ON MECHANICAL PROPERTIES OF COMPOSITES.

In this section, composites were prepared with pellets of different fiber sizes and with or without wax. The objective was to study the effect of fiber size and wax on the mechanical properties of composites.

It was expected that the addition of wax in pellets would help in easy deagglomeration of fibers during melt compounding and good dispersion would be achieved which would incur higher mechanical properties than composites without wax. It is important to note that no additional wax was added in composite manufacturing, 5wt% wax with respect to fiber weight was added during the pelletization process. In all composites, 0.5wt% of the MAPP coupling agent was also used.

Hemp pellets with different fiber sizes (1, 1.5, and 3 mm) were also used to investigate the effect of fiber length on the mechanical properties of composites.

Zhang et al., (2017) investigated the effect of five different lengths (4, 8, 12, 16, and 20 mm) of glass fiber in long glass fiber reinforced poly (butylene terephthalate) LGF/PBT composites. It was observed that mechanical properties increased with an increase in glass fiber length up to 12 mm, above those mechanical properties decreased. The homogenous dispersion of the glass fiber in the PBT matrix was found to be achievable in lengths of 4, 8, and 12 mm without any phenomenon of the fibers aggregating in the matrix, which improved the mechanical properties. However, in composites with glass fiber lengths of 16- and 20-mm inhomogeneous dispersion was observed with the phenomenon of reunion of fibers in the matrix, which resulted in a decrease in mechanical properties.

To achieve good mechanical properties from short fiber-reinforced polymer composites, it is essential to achieve good fiber dispersion in the polymer matrix. Fibers must be separated from each other and there must be no agglomeration. Homogenous dispersion is essential in composite properties otherwise some regions of the composites will be weaker (matrix-rich) and some regions will be stronger (fiber-rich). Two factors influence fiber dispersion that are inter-fiber interaction and entanglement due to fiber length (Dufresne, 2013). The addition of wax to the fibers during the pelletization process assists in better flowability of the material through the pellet mill and the

wax also reduces the inter-fiber interaction which helps in better dispersion during melt compounding in the extruder in composites manufacturing.

Cheng et al. (2020) developed a thin layer of wax around the cellulose that reduced agglomeration due to fiber interaction and was easily melted during composite processing without restricting the bond between cellulose and polymer. The authors used paraffin wax and a mixture of surfactants to coat cellulose surfaces to restrict inter-fiber interaction. The results of wax-coated microcrystalline-cellulose and a mixture of wax and surfactants coated microcrystalline-cellulose were compared and found that the mixture of wax and surfactants formed a very thin layer around the cellulose surface encapsulating them with a very minor change in particle length and width.

The formulation of the pellets studied in this section is given in Table 4.2. Table 5.3 represents the formulation of the composites and table 5.4 represents their mechanical properties results which are further discussed in the following sections.

Table 5.3 Formulation of composites with Hemp pellets of different fiber sizes and with and without wax.

Fiber Type: Whole hemp fiber from Tangho Paraguay (TwH) **Pellet moisture content:** 0-1 wt.%			
Sample Name	**PP wt.%**	**Hemp Pellet wt.%**	**MAPP wt.%**
PP	100	0	0
20P-1TwH-NW	79.5	20	0.5
20P-1TwH-W	79.5	20	0.5
20P-1.5TwH-NW	79.5	20	0.5
20P-1.5TwH-W	79.5	20	0.5
20P-3TwH-NW	79.5	20	0.5
20P-3TwH-W	79.5	20	0.5

In sample names, ‘20P’ represents 20wt% of pellets used, ‘(1/1.5/3)TwH’ represents fiber milled size and fiber type, and ‘NW/W’ represents pellets with no wax and with wax.

Table 5.4 Mechanical properties of composites with Hemp pellets of different fiber sizes and with and without wax.

Sample Name	Flexural Modulus (MPa)	Flexural Strength (MPa)	Tensile Modulus (MPa)	Tensile Strength (MPa)	Impact Strength (J/m)	Melt Flow Index (g/10min)	Density (kg/m^3)	Specific Flexural Modulus (MPa.m^3/kg)
PP	813±17^{a}	31.5±0.4^{a}	118±7^{a}	15.0±1.6^{a}	27.93±1.4^{c}	23±0.1^{c}	925±0.9	0.88±0.02^{a}
20P-1TwH-NW	1044±18^{b}	36.6±0.5^{b}	129±9^{a}	19.1±1.7^{b,c}	11.87±0.9^{b}	13±0.8^{b}	966±1.4	1.08±0.02^{b}
20P-1TwH-W	1094±19^{c}	36.6±0.6^{b}	153±16^{b}	20.2±1.8^{c}	9.98±0.8^{a}	10.6±0.6^{a,b}	968±4	1.13±0.02^{c}
20P-1.5TwH-NW	1227±17^{d}	39.4±0.6^{c}	155±15^{b}	19.9±1.2^{c}	11.63±1^{b}	11.05±1.34^{a,b}	958±3.2	1.28±0.02^{d}
20P-1.5TwH-W	1283±39^{e}	39.9±1.6^{c}	127±10^{a}	19.3±2.8^{c}	10.02±0.83^{a}	9.5±0.61^{a}	971±2.5	1.32±0.04^{d,e}
20P-3TwH-NW	1326±33^{e}	40.8±1.2^{c}	119±7^{a}	21.7±1.7^{c}	10.67±0.76^{a,b}	11.1±0.2^{a,b}	965±7.3	1.38±0.03^{f}
20P-3TwH-W	1311±23^{e}	40.4±0.7^{c}	119±14^{a}	16.0±1.5^{a,b}	10.01±0.8^{a}	9.2±0.03^{a}	973±3.6	1.35±0.02^{e,f}

The data were statistically evaluated using the Tukey test to compare the means of the mechanical properties of the composites at a 95% confidence level. If the measured mechanical properties of the composites in question are statistically different from one another, it is indicated by the superscripts (a,b,c,d,e,f). When the superscripts of various samples for each mechanical attribute have the same letter, the values are considered to be statistically equivalent.

5.3.1 Flexural Properties:

Figures 5.12 and 5.13 depicts flexural modulus and flexural strength of the composites in question. The flexural modulus increased significantly by the addition of hemp pellets as compared to neat PP. The flexural modulus increased with an increase in fiber size. The highest flexural modulus was recorded for composites with 1.5mm fiber pellets with wax (20P-1.5TwH-W), and for 3mm fiber pellets with and without wax (20P-3TwH-NW/W). It was also observed that by the addition of wax, the flexural modulus was slightly improved for the composites. This confirms the assumption that wax helped in better dispersion of the fibers in the polypropylene matrix.

It was expected that by addition of pellets with higher aspect ratio fibers would increase the flexural modulus of the composites and this assumption was also confirmed by these results. Compared to smaller fibers, large fibers have less surface area which when added to the polymer matrix results in better coverage by the polymer (Atta-Obeng et al., 2012).

Similar results were observed for flexural strength. The flexural strength increased with an increase in fiber size from 1mm to 1.5mm. It was observed that the flexural strength for composites with 1.5 mm and 3 mm fibers was the same with and without wax, which may be due to the fiber attrition during pelletization, melt compounding in the twin-screw extruder, and injection molding. Similar results were also observed in the literature, the flexural modulus and strength of silane-treated pineapple leaf polyester composites increased with an increase in fiber size up to 20 mm (Anand et al., 2022).

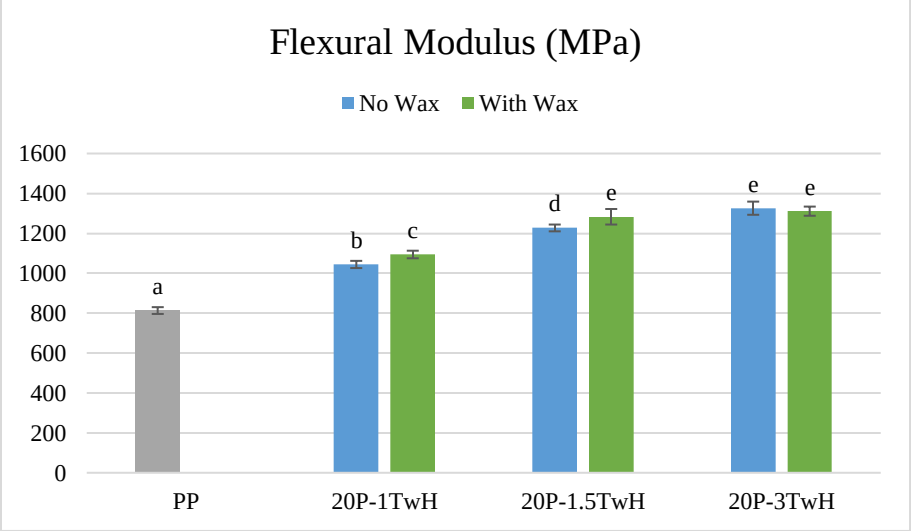


Figure 5.12 Flexural modulus of composites with hemp pellets of different fiber sizes and with and without wax.

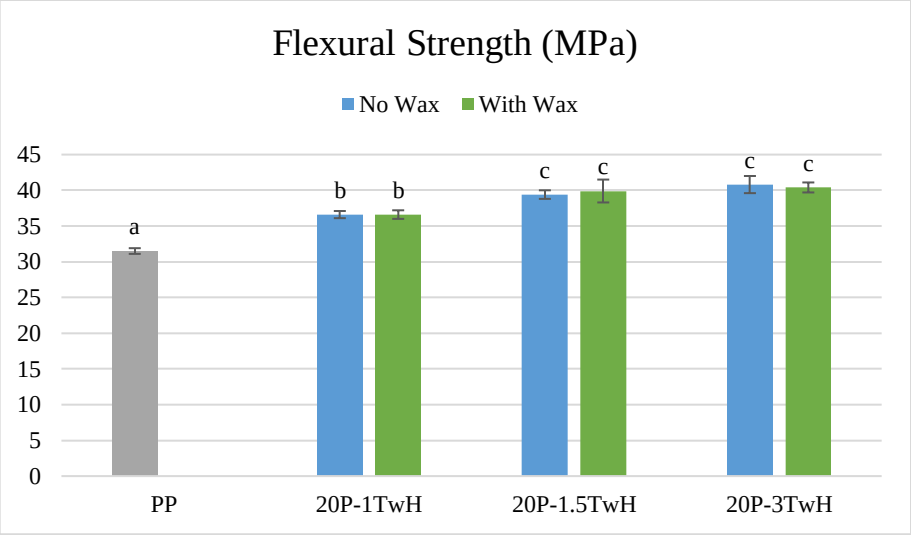


Figure 5.13 Flexural strength of composites with hemp pellets of different fiber sizes and with and without wax.

5.3.2 Tensile Properties:

Tensile modulus and strength results are shown in Figures 5.14 and 5.15. In Figure 5.14, it was observed that the tensile modulus of composites without wax increased with an increase in fiber size from 1mm to 1.5mm by 16.7%. No significant change was observed in the composites with 1mm and 3mm fibers when compared to neat PP. It was found that in composites with wax, the tensile modulus of composites with 1mm fibers increased by 15.6% when compared to 1mm composites without wax, whereas the tensile modulus of composites with 1.5mm fibers reduced by 18% when compared to the composite without wax.

The addition of wax had a positive effect on the tensile modulus of 1mm fiber composites and a negative effect on 1.5mm fiber composites. No effect of fiber length and wax was observed on the tensile modulus of 3mm fiber composites, which is similar to the tensile modulus of neat PP.

Tensile strength was increased by 25% with the addition of fibers as compared to neat PP. No significant effect of fiber length on tensile strength was observed. The effect of wax was also not significant, it had a negative effect on 3mm hemp fiber composites.

Sankar et al. (2014) observed that tensile properties increased with increasing fiber size, where polyester composites reinforced with 20wt% NaOH treated sansevieria trifasciata fibers

(STF) of different fiber lengths (2-10mm) were prepared and tensile properties increased with increase in fiber length.

Another study investigated the effect of different fiber volumes (10, 20, and 30%) and different fiber sizes (125, 250, and 50µm) on the mechanical properties of mengkuang-reinforced HDPE composite. Optimum tensile modulus and tensile strength were observed at 20% fiber loading of 250 µm fiber sizes and our results corroborate with this research (Wan Mohamed et al., 2018).

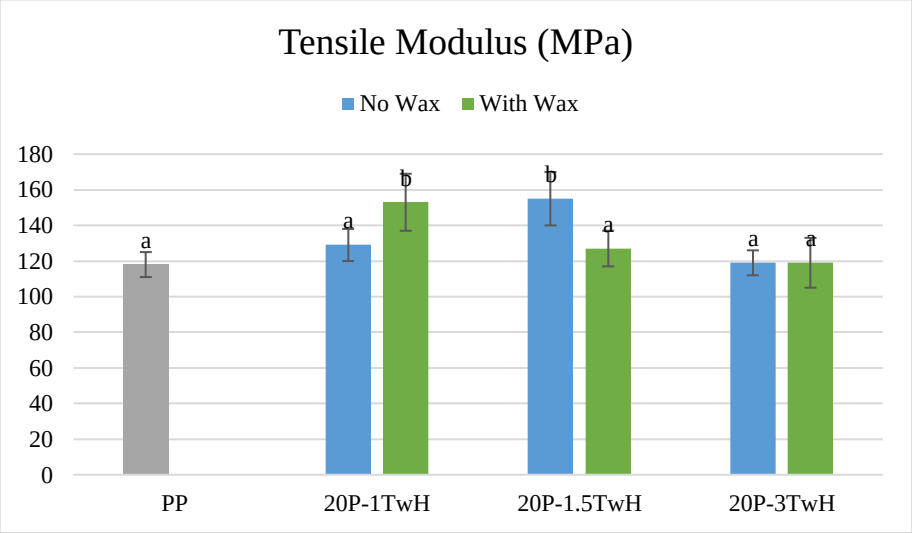


Figure 5.14 Tensile modulus of composites with hemp pellets of different fiber size and with and without wax.

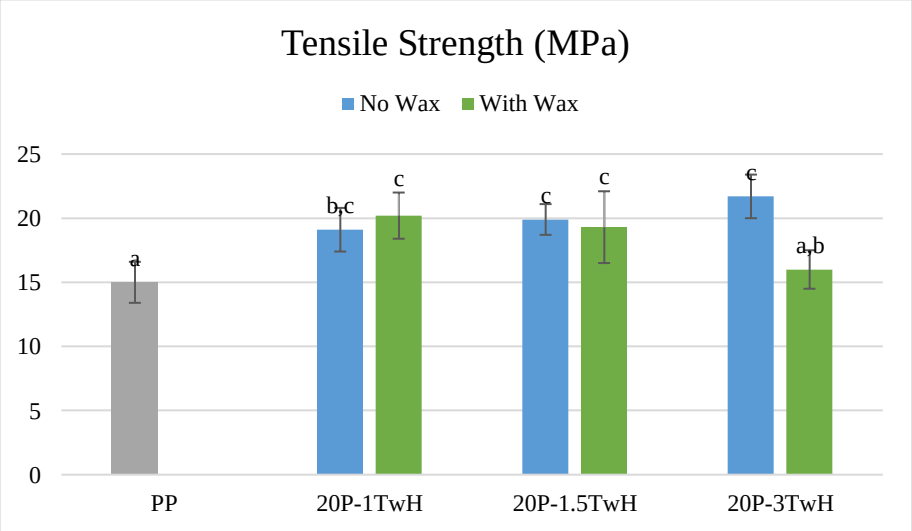


Figure 5.15 Tensile strength of composites with hemp pellets of different fiber sizes and with and without wax.

5.3.3 Impact strength:

Figure 5.16 depicts the impact strength of composites with hemp pellets of different fiber sizes, with and without wax. The impact strength of composites was reduced significantly as compared to neat PP. This is because fibers interrupt the local motion of polymer chains when stress is applied as explained in section 5.2.3. The impact strength of composites remained the same with an increase in fiber length. Other authors also found that impact strength decreased with an increase in fiber length because stress transfer efficiency was reduced due to the weak adhesion of large fibers (Hassan et al., 2010; Wan Mohamed et al., 2018), in the following results no significant change was observed in impact strength due to change in length. Composites with wax had a slight negative effect on impact strength as compared to composites without wax.

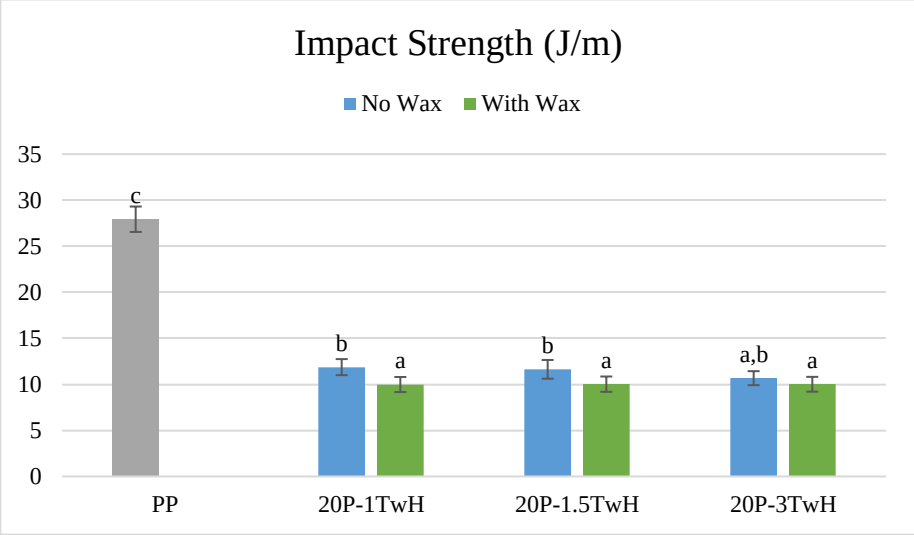


Figure 5.16 Impact strength of composites with hemp pellets of different fiber sizes and with and without wax.

5.3.4 Melt Flow Index:

Melt flow index results of composites with hemp pellets of different fiber sizes and with and without wax are shown in Figure 5.17. The melt flow index decreased significantly with the addition of fibers. It was expected that an increase in fiber size would decrease the melt flow index as large fibers tend to hinder the flow of polymer increasing its viscosity (Leão et al., 2008). This was confirmed by the results, the melt flow index of 1mm hemp fiber composites was higher than

1.5mm and 3mm hemp composites. Moreover, the incorporation of wax into the pellets had a negative effect as the melt flow index of composites with wax had lower MFI than the composites without wax.

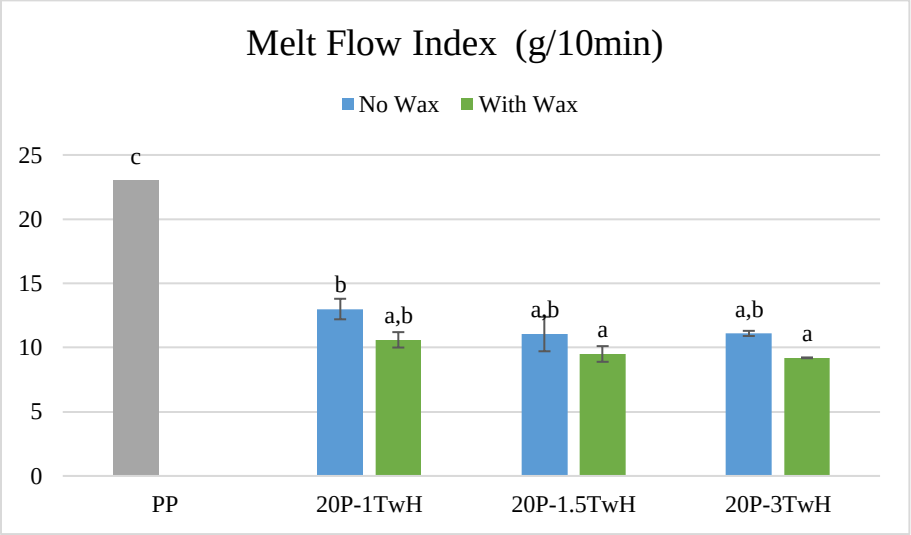


Figure 5.17 Melt flow index of composites with hemp pellets of different fiber sizes and with and without wax.

5.3.5: Specific Flexural Modulus:

The specific flexural modulus (SFM) of the composites in question is shown in Figure 5.18. SFM increased with an increase in fiber length. An increase of 18.5%, 31%, and 36% was observed in the composites without wax containing fiber sizes of 1, 1.5, and 3mm, respectively, when compared to pure PP. The addition of wax in hemp pellets slightly improved the SFM of the composites compared to composites without wax.

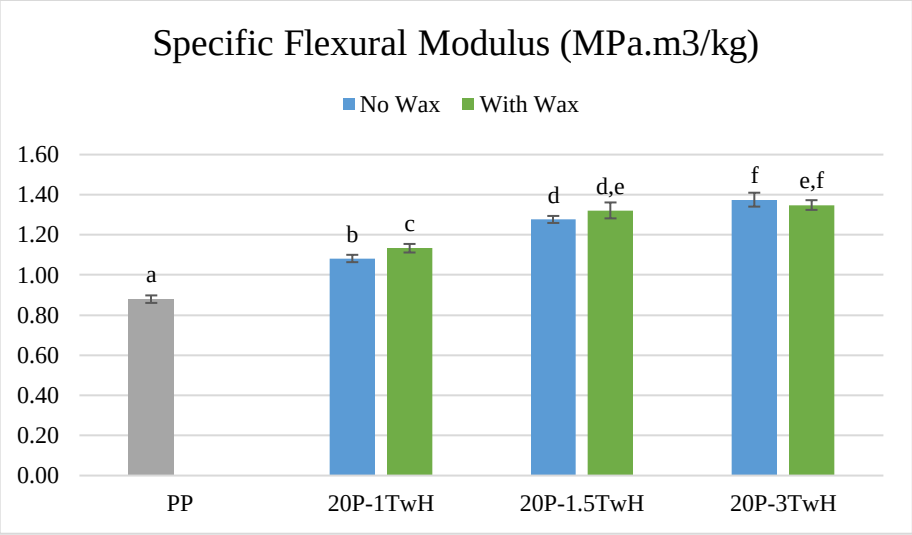


Figure 5.18 SFM of composites with hemp pellets of different fiber sizes and with and without wax.

Overall, the mechanical properties of the composites were affected by changes in fiber size, although the effect was not too significant. The addition of wax slightly improved the flexural properties, but other mechanical properties were reduced. In all the results 20P-1.5TwH-NW composite results were consistent and higher than other composites. Moving forward in research, 1.5mm fiber pellets will be used for composite manufacturing.

5.4 EFFECT OF HEMP BAST AND HURD FIBERS OF DIFFERENT SIZES ON THE MECHANICAL PROPERTIES OF COMPOSITES.

As discussed in the literature review, whole hemp contains 35% bast fibers and 65% woody core (hurd) fibers. Hemp bast fibers are longer, stronger, and stiffer, and have high cellulose content of 57-77% and low lignin content of 5-9%. These attributes of bast fiber make them highly valuable for industrial applications. Hurd fibers, on the other hand, are treated as a waste material.

About 95% of hurd fibers are used for animal litter and only 5% is used in construction applications (Balčiūnas et al., 2013). Hurd fibers are weaker than bast fibers but have low density. Hurd fibers have cellulose content of 40-48% which is higher than wood and have comparable lignin content of 21-24% which makes them superior to wood (Gümüşkaya et al., 2007; Li et al., 2017b; Momeni et al., 2021; Stevulova et al., 2014, 2013; Xiao et al., 2019).

Because of the above-mentioned differences between both fibers, in this section, polypropylene composites were prepared with bast and hurd fibers milled in 1mm and 3mm sizes. The objective was to investigate the effect of individual fibers and their lengths on the mechanical properties of composites. The fiber bonding with the PP matrix was also analyzed with SEM.

Moreover, the results were also compared with polypropylene-glass fiber composites. The length and aspect ratio distribution of bast and hurd fibers milled in 1mm and 3mm sizes is presented in Chapter 4.

Table 5.5 represents the formulation of the composites and table 5.6 represents their mechanical properties results which are further discussed in the following sections.

Table 5.5 Formulation of composites with hemp bast, hurd, and glass fiber.

Fiber Type: UP Bast from USA (U.B), Valley-Bio Hurd (VB.H), Glass Fiber (GF) **Fiber moisture content:** 0-1%					
Sample Name	**PP wt.%**	**Bast fiber wt.%**	**Hurd Fiber wt.%**	**Glass Fiber wt.%**	**MAPP wt.%**
PP	100	0	0	0	0
10GF	90	0	0	10	0
20F-1U.B	79.5	20	0	0	0.5
20F-3U.B	79.5	20	0	0	0.5
20F-1VB.H	79.5	0	20	0	0.5
20F-3VB.H	79.5	0	20	0	0.5
20GF	80	0	0	20	0

In sample names, '20F' represents 20wt% of fibers used, '(1/3) (U.B/VB.H)' represents fiber milled size and fiber type.

Table 5.6 Mechanical properties of composites with hemp bast, hurd, and glass fiber.

Sample Name	**Flexural Modulus (MPa)**	**Flexural Strength (MPa)**	**Tensile Modulus (MPa)**	**Tensile Strength (MPa)**	**Impact Strength (J/m)**	**Melt Flow Index (g/10min)**	**Density (kg/m^3)**	**Specific Flexural Modulus (MPa.m^3/kg)**
PP	813±17^{a}	31.5±0.4^{a}	118±7^{a}	15±1.6^{a}	27.90±1.40^{d}	23±0.1^{b}	925±0.9	0.88±0.02^{a}
10GF	1513±53^{b}	58.1±0.9^{d}	146±8^{b}	26±2.0^{d}	21.80±1.04^{b}	25.4±2.4^{b}	947±0.9	1.60±0.06^{b}
20F-1U.B	1683±19^{c}	46.4±0.5^{c}	162±17^{b,c}	25±2.3^{c,d}	12.87±0.65^{a}	8.8±0.5^{a}	970±0.2	1.74±0.02^{d}
20F-3U.B	1639±53^{c}	46.5±0.6^{c}	171±10^{c}	26±0.6^{c,d}	13.41±0.53^{a}	9.0±2.2^{a}	966±0.3	1.70±0.05^{c,d}
20F-1VB.H	1537±34^{b}	43.0±0.3^{b}	161±25^{b,c}	23±3.1^{c}	12.72±0.33^{a}	9.4±0.2^{a}	960±1.0	1.60±0.03^{b,c}
20F-3VB.H	1449±26^{b}	41.0±1.0^{b}	116±5^{a}	19±1.4^{b}	13.25±0.40^{a}	9.4±1.9^{a}	954±0.9	1.52±0.03^{b}
20GF	3311±104^{d}	98.4±3.9^{e}	147±8^{b}	32±1.1^{e}	24.60±0.85^{c}	36.1±0.9^{c}	1014±5.4	3.27±0.10^{e}

All results were statistically analyzed using one-way analysis of variance (ANOVA) followed by the Tukey test at the significance level of 5% to determine significant difference between the mechanical properties of these composites. Different letters, in the same column, represent significant differences ($p<0.05$) between the means obtained through the Tukey Test.

5.4.1 Flexural Properties:

Figures 5.19 and 5.20 show the flexural modulus and strength results of the composites. It was observed that by the addition of 10% GF the flexural modulus increased by 46%. The addition of 20% bast and hurd fiber increased the flexural modulus by approximately 50% and 47% respectively, compared to neat PP.

It was expected that composites with bast fibers would have higher flexural modulus, which was confirmed by the results. It was also observed that the flexural properties were similar for both fiber sizes. Composites with hurd fibers presented slightly lower flexural modulus than bast fiber composites. The results also showed that 20% bast fiber composites had 10% higher flexural modulus than 10% glass fiber composites while hurd fiber composites had similar flexural modulus as 10% glass fiber composite.

The flexural strength increased by 32% and 27% with the addition of 20% bast and hurd fibers, respectively, when compared to neat PP. Hurd fiber had slightly lower flexural strength than bast fiber composites. The flexural strength of the 10% glass fiber composite was 20% higher than the bast and hurd fiber composites.

The flexural properties of 20% bast and hurd composites were comparable to 10% glass fiber composites, however, 20% glass fiber composite flexural properties were significantly higher than other composites. To obtain similar flexural properties as 20% glass fiber composites, it is suggested to increase the hemp fiber loading to 30 or 40%. No effect of bast and hurd fiber size was observed on the flexural properties. Both 1mm and 3mm sizes had similar flexural properties.

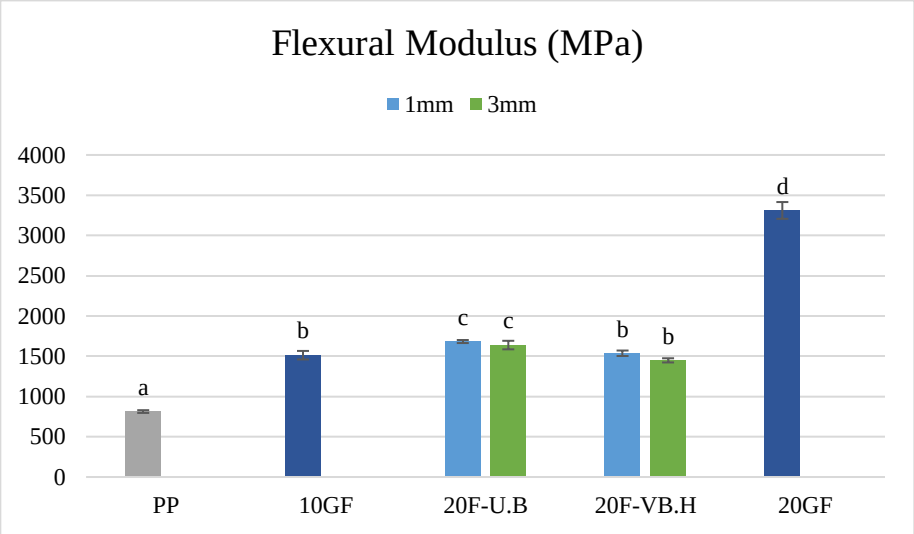


Figure 5.19 Flexural modulus of composites with hemp bast, hurd and glass fiber.

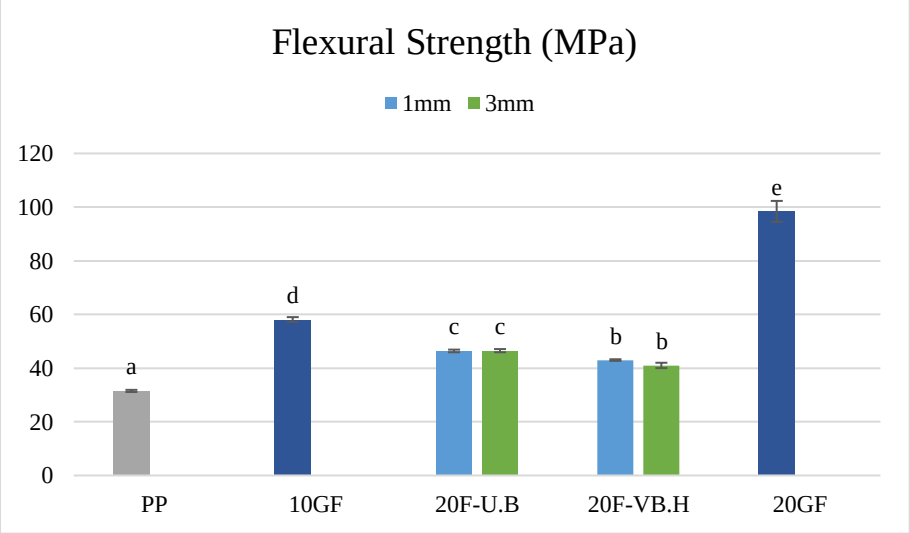


Figure 5.20 Flexural strength of composites with hemp bast, hurd and glass fiber.

5.4.2 Tensile Properties:

Tensile modulus and tensile strength results are shown in Figures 5.21 and 5.22. It was observed that by the addition of 10 and 20% glass fiber the tensile modulus increased by 19% as compared to neat PP, and the addition of 20% bast and hurd fiber significantly increased the tensile modulus.

The highest tensile modulus was observed for 3mm bast fiber composites (20F-3U.B), which was 31% higher than neat PP and 14% higher than 10 and 20% glass fiber composites.

The tensile modulus for 3mm bast fiber composites was slightly higher than 1mm bast fiber composites because large fibers have fewer fiber ends which tends to create less stress concentration points as compared to small fibers where cracks can initiate when load is applied (Panthapulakkal and Sain, 2007). No increase was observed in the tensile modulus of the 3mm hurd fiber composite. These results depict that 20% bast and hurd composites had a favorable tensile modulus as 10 and 20% glass fiber composites.

The tensile strength of 10% glass fiber composites and 20% bast fiber composites for both fiber sizes (1 and 3mm) increased by 42% as compared to neat PP. The tensile strength of 1mm hurd fiber also increased by 35% whereas 3mm hurd fiber showed a very slight improvement in tensile strength as compared to neat PP. The highest tensile strength was observed for 20% glass fiber, which was 53% higher than neat PP and 20% higher than bast fiber composites.

Panthapulakkal and Sain, (2007) prepared glass fiber and hemp hybrid composites with polypropylene. The flexural and tensile strength results of composites containing 15%GF, 25% hemp fiber, 5% compatibilizer, and 55% polypropylene were compared with 40% glass fiber reinforced polypropylene composites. It was found that the tensile and flexural strength of 40% glass fiber composites were significantly higher than the hybrid composite. However, the flexural modulus of the hybrid composite was similar to the 40% hemp/glass fiber hybrid composite.

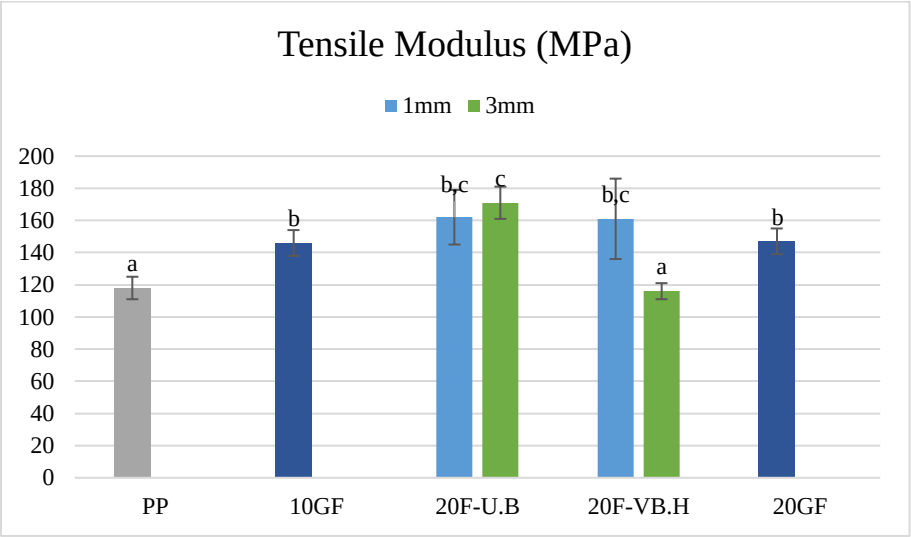


Figure 5.21 Tensile modulus of composites with hemp bast, hurd and glass fiber.

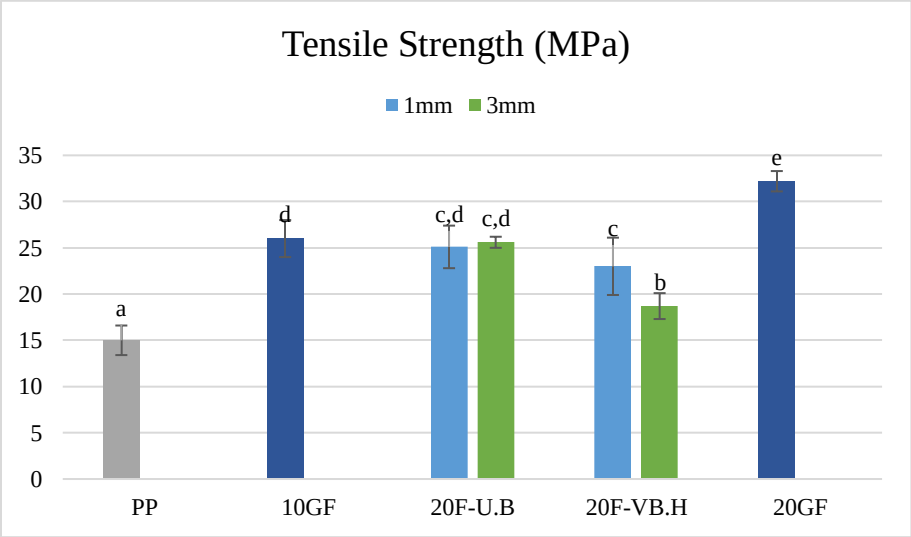


Figure 5.22 Tensile strength of composites with hemp bast, hurd and glass fiber.

5.4.3 Impact Strength:

Figure 5.23 shows the impact strength of composites with hemp bast, hurd, and glass fiber. Impact strength decreased by adding fibers in the polypropylene matrix. The impact strength of 10 and 20% glass fiber composites was slightly lower than neat PP. The impact strength of 20% bast and hurd fiber was approximately 53% lower as compared to neat PP and approximately 40% lower than glass fiber composites. The impact strength of bast and hurd fiber composites with 1 and 3mm fiber sizes was statistically observed to be the same. The higher impact strength of glass fiber composites than bast and hurd fiber composites could be attributed to the fact that glass fiber is stiffer and stronger than natural fibers and the brittle nature of glass fiber allows it to absorb more energy by fracturing or through crack propagation.

The reason for the lower impact strength of glass fiber composites as compared to the neat PP, is due to the addition of fibers creates stress concentration points at the fiber end and restricting the polymer chains movement when subjected to load. It was also observed in the literature, that when 15% glass fiber was added to polypropylene, fracture energy (W) of the composite was reduced by 60% as compared to neat PP, and no significant effect of 30% and 45% glass fiber loading was observed on fracture energy when tested at 25°C temperature (Rahman et al., 2013b).

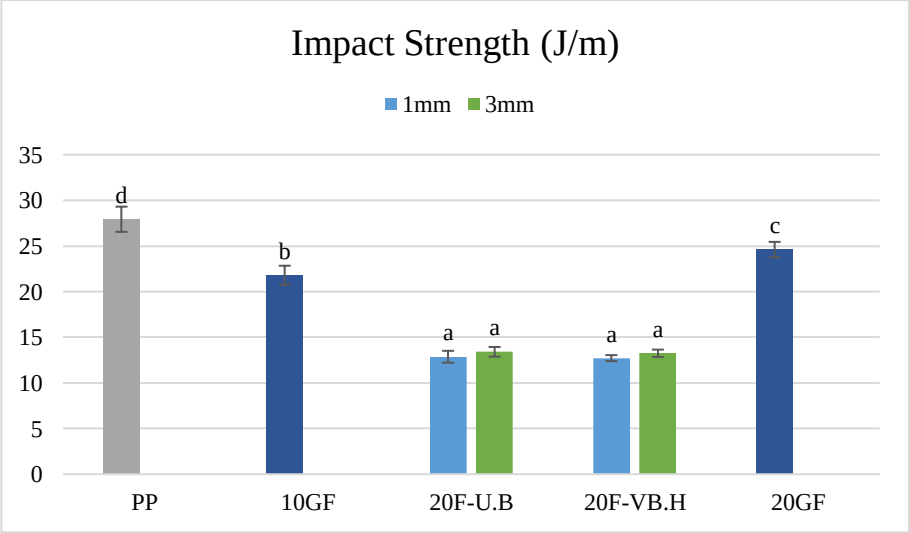


Figure 5.23 Impact strength of composites with hemp bast, hurd, and glass fiber.

5.4.4 Melt Flow Index:

It was observed from the melt flow index results shown in Figure 5.24 that MFI increased with an increase in glass fiber volume fraction. The MFI of composite with 20% glass fiber increased by 56.5% as compared to neat PP. However, MFI composites with hemp fibers were reduced by 60% as compared to neat PP. The increase in MFI of glass fiber composites could be because glass fiber is a good heat conductor, during melting it can conduct and dissipate heat more effectively, hence reducing composite viscosity.

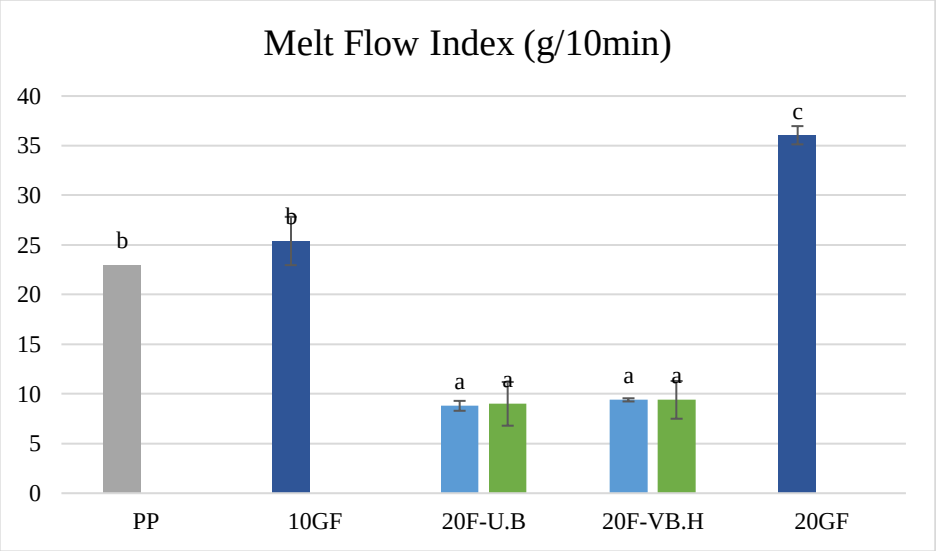


Figure 5.24 Melt flow index of composites with hemp bast, hurd, and glass fiber.

5.4.5 Specific Flexural Modulus:

Specific flexural modulus (SFM) results are shown in Figure 5.25. The results showed that bast fiber composites had slightly higher SFM as 10% GF composites and hurd fiber composites had similar SFM as 10% GF. The highest SFM was observed for 20% GF composites which was 46% higher then 20% bast fiber composites.

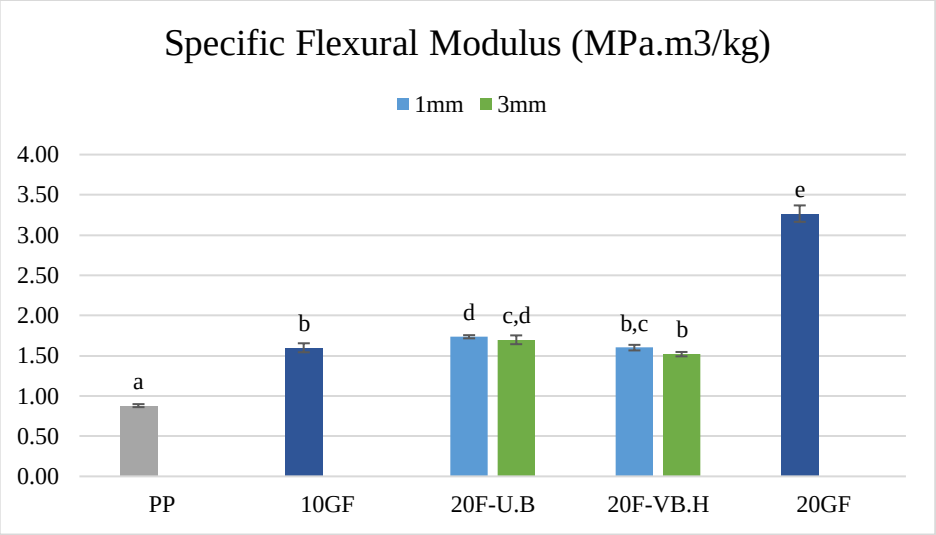


Figure 5.25 Specific flexural modulus of composites with hemp bast, hurd, and glass fiber.

5.4.6 Scanning Electron Microscope (SEM):

To observe the interaction between different fibers and polypropylene matrix, SEM analysis of fractured surfaces of composites was performed. Figure 5.26 represents SEM analysis of bast fiber composites. Good interaction between bast fiber and PP matrix was observed. Figure 5.27 also showed good interaction between hurd fibers and the PP matrix. The 0.5wt.% of the MAPP coupling agent improved adhesion between both fibers (bast and hurd) and the PP matrix. However, in the glass fiber composites in Figure 5.28, fiber pullouts were observed instead of fractured fibers.

Glass fiber pull-out could be due to a reduction in fiber length below the critical fiber length required during the extrusion and injection molding process. Fu et al. (2000) estimated that the critical fiber length required for 25wt% short glass fiber reinforced polypropylene composites was 887.92 µm. From Figure 5.28 it can be observed that the fiber length is smaller than 887.92 µm. Moreover, it was also observed from the literature that glass fiber length decreased by an increase in fiber content because of increased interaction between brittle fiber causes breakage (Panthapulakkal and Sain, 2007).

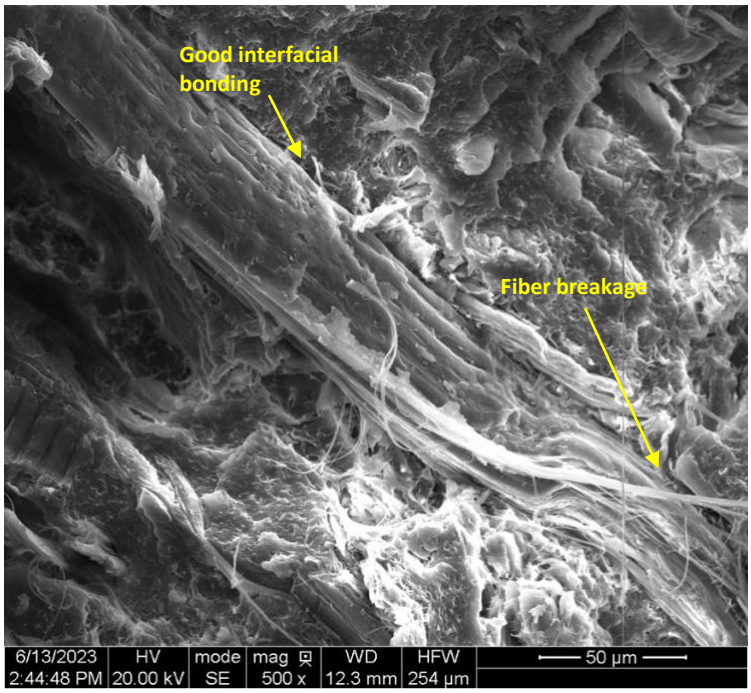


Figure 5.26 SEM of 20F-U.B composite (500X).

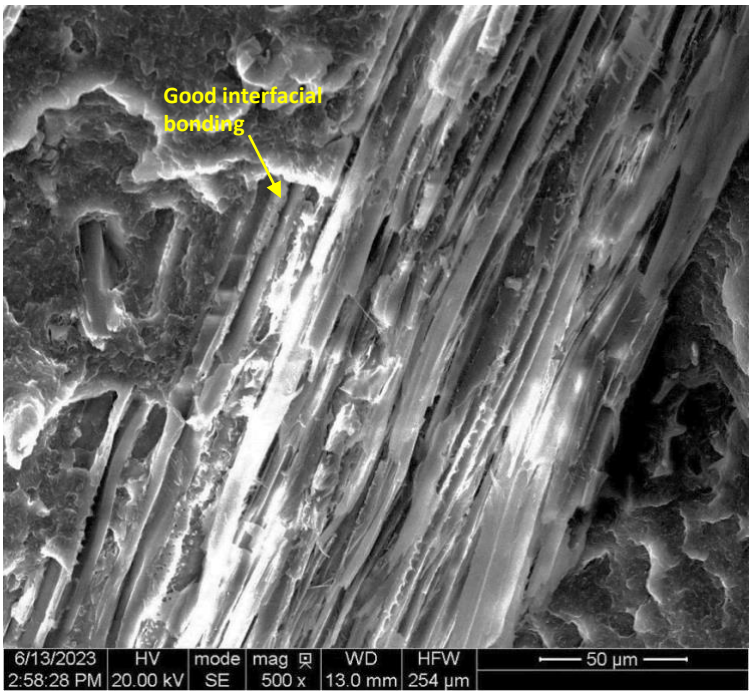


Figure 5.27 SEM of 20F-VB.H composite (500X).

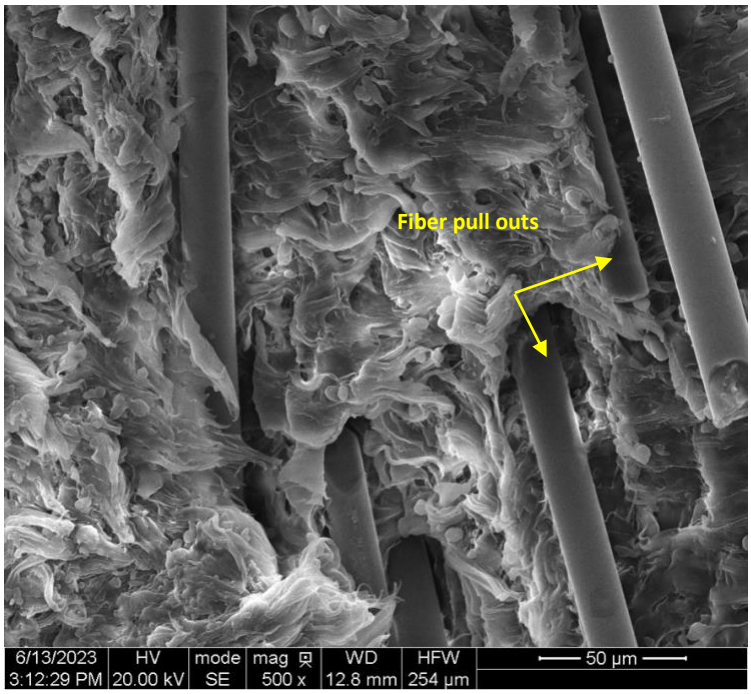


Figure 5.28 SEM of 10GF composite (500X).

5.5 COMPOSITES CONTAINING HEMP PELLETS WITH DIFFERENT COMPOSITIONS OF HURD AND BAST FIBER FROM DIFFERENT SUPPLIERS.

As discussed earlier, whole hemp contains 35% bast fiber and 65% hurd fibers. In this section composites were prepared from hemp pellets with different concentration of bast and hurd fibers provided by different suppliers and compared with each other. The goal was to determine which composition of bast and hurd gives the best results for the composites and to evaluate the effect of fibers from different parts of the world (Canada, U.S.A, and Paraguay).

Table 5.7 represents the formulation of the composites and table 5.8 represents their mechanical properties results which are further discussed in the following sections.

Table 5.7 Formulation of composites with hemp pellets of different composition of bast and hurd fiber from different suppliers.

	Pellet Fiber Type: Valley-Bio Canada Bast (VB.B), Tangho Paraguay Hurd (T.H), IND-Hemp U.S.A Bast (I.B), IND-Hemp U.S.A Hurd (I.H), Glass Fiber (GF) **Milled pellet fiber size:** 1.5mm **Pellet moisture content:** 0-1%						
				Hemp Pellet Composition			
	Sample Name	**PP wt.%**	**Hemp Pellet wt.%**	**Hurd fiber wt.%**	**Bast Fiber wt.%**	**Glass Fiber wt.%**	**MAPP wt.%**
	PP	100	0	0	0	0	0
	10GF	90	0	0	0	10	0
	20GF	80	0	0	0	20	0
Composites with VB.B, T.H pellets	20P-100H	79.5	20	100	0	0	0.5
	20P-80H, 20B	79.5	20	80	20	0	0.5
	20P-60H, 40B	79.5	20	60	40	0	0.5
	20P-40H, 60B	79.5	20	40	60	0	0.5
	20P-20H, 80B	79.5	20	20	80	0	0.5
	20P-100B	79.5	20	0	100	0	0.5
Composites with I.B, I.H pellets	20P-100H	79.5	20	100	0	0	0.5
	20P-80H, 20B	79.5	20	80	20	0	0.5
	20P-60H, 40B	79.5	20	60	40	0	0.5
	20P-40H, 60B	79.5	20	40	60	0	0.5
	20P-20H, 80B	79.5	20	20	80	0	0.5
	20P-100B	79.5	20	0	100	0	0.5

In sample names, '20P' represents 20wt% of hemp pellets used, '(80H,20B)' represents hurd and bast content of pellet used.

Table 5.8 Mechanical properties of composites with hemp pellets of different composition of bast and hurd fiber from different suppliers.

	Sample Name	Flexural Modulus (MPa)	Flexural Strength (MPa)	Tensile Modulus (MPa)	Tensile Strength (MPa)	Impact Strength (J/m)	Melt Flow Index (g/10min)	Density (kg/m^3)	Specific Flexural Modulus (MPa.m^3/kg)
	PP	813±17^{a}	31.5±0.4^{a}	118±7^{a,b}	15±1.6^{a}	27.90±1.40^{f}	23.0±0.1^{c}	925±0.9	0.88±0.02^{a}
	10GF	1513±53^{f,g}	58.1±0.9^{g}	146±8^{c,d,e}	26±2.0^{e}	21.80±1.04^{d}	25.4±2.4^{c}	947±0.8	1.60±0.06^{g,h}
	20GF	3311±104^{h}	98.4±3.9^{h}	147±8^{c,d,e}	32±1.1^{f}	24.60±0.85^{e}	36.1±0.9^{d}	1014±5.4	3.27±0.10^{i}
Composites with V.B.B, T.H pellets	20P-100H	1500±49^{f,g}	45.6±0.6^{e,f}	167±8^{e}	26±0.9^{e}	10.54±0.70^{a}	6.7±0.1^{a}	962±3.0	1.56±0.05^{f,g,h}
	20P-80H, 20B	1334±36^{b,c}	42.8±0.7^{c,d}	155±26^{d,e}	22±4.1^{c,d}	11.17±0.82^{a}	8.0±0.5^{a,b}	965±1.4	1.38±0.04^{b,c}
	20P-60H, 40B	1334±27^{b,c}	43.0±0.7^{c,d}	151±17^{d,e}	23±1.2^{d,e}	12.19±0.81^{a,b,c}	8.8±0.4^{a,b}	964±4.0	1.38±0.03^{b,c}
	20P-40H, 60B	1383±24^{c,d}	43.0±0.9^{c,d}	156±16^{d,e}	23±1.4^{c,d,e}	11.60±0.46^{a,b}	8.8±1.1^{a,b}	963±3.4	1.44±0.03^{c,d}
	20P-20H, 80B	1250±53^{b}	39.9±0.8^{b}	157±27^{d,e}	21±2.9^{c,d}	13.30±0.62^{c}	8.2±0.5^{a,b}	965±2.75	1.30±0.06^{b}
	20P-100B	1286±17^{b}	40.7±1.1^{b,c}	163±13^{d,e}	24±1.6^{d,e}	13.10±1.60^{b,c}	8.0±0.3^{a,b}	963±0.75	1.34±0.02^{b}
Composites with I.B, I.H pellets	20P-100H	1587±36^{g}	48.0±1.1^{f}	118±4^{a,b}	18±1.9^{a,b}	10.60±0.35^{a}	10.2±0.7^{b}	963±6.5	1.65±0.04^{h}
	20P-80H, 20B	1487±53^{e,f}	45.0±1.3^{d,e}	111±9^{a}	17±1.5^{a,b}	10.90±0.60^{a}	9.0±0.4^{a,b}	966±2.2	1.54±0.05^{e,f,g}
	20P-60H, 40B	1323±49^{b,c}	43.0±0.8^{c,d}	119±5^{a,b}	19±1.2^{b,c}	10.83±1.00^{a}	9.3±0.5^{a,b}	964±5.0	1.37±0.05^{b,c}
	20P-40H, 60B	1396±53^{c,d,e}	43.0±1.5^{c,d,e}	123±5^{a,b,c}	20±1.8^{b,c,d}	11.40±0.85^{a,b}	9.1±0.3^{a,b}	962±6.3	1.45±0.06^{c,d,e}
	20P-20H, 80B	1466±38^{d,e,f}	43.0±0.8^{c,d}	118±6^{a,b}	20±1.5^{b,c,d}	11.60±0.90^{a,b}	8.0±0.1^{a,b}	964±6.5	1.52±0.04^{d,e,f,g}
	20P-100B	1417±54^{c,d,e,f}	43.0±1.0^{c,d,e}	141±5^{b,c,d}	21±0.7^{c,d,e}	10.80±0.70^{a}	7.8±0.3^{a,b}	963±10.0	1.47±0.06^{c,d,e,f}

All results were analysed using Tukey test with significance level of 5% to determine significant difference between mechanical properties of these composites. The superscripts (a,b,c,d,e,f,g,h,i) represents if the measured mechanical properties of composites in question are statistically different from each other or not. If superscripts of different samples in each mechanical property have same letter then those values are statistically same.

5.5.1 Flexural Properties:

Figures 5.29 and 5.30 show the flexural modulus and strength of composites. Analyzing Figure 5.29, it can be observed that the flexural modulus of composites with 100% hurd fiber pellets is slightly higher than composites with 100% bast fiber pellets, although the difference is not too significant. Other composites with different compositions of bast and hurd fiber pellets have resulted in between the results of 100% hurd and bast fiber pellet composites, although the results are relatively similar. As observed in the previous section, 10% GF composites have a similar flexural modulus as 20% hemp fiber pellet composites.

From Figure 5.30, it can be observed that all composites prepared with hemp pellets of different compositions of hurd and bast fibers have similar results. The flexural strength of 10% GF is slightly higher than that of 20% hemp fiber pellet composites.

In both properties analyzed, flexural modulus and strength, no significant variation was observed between hemp fibers from different suppliers.

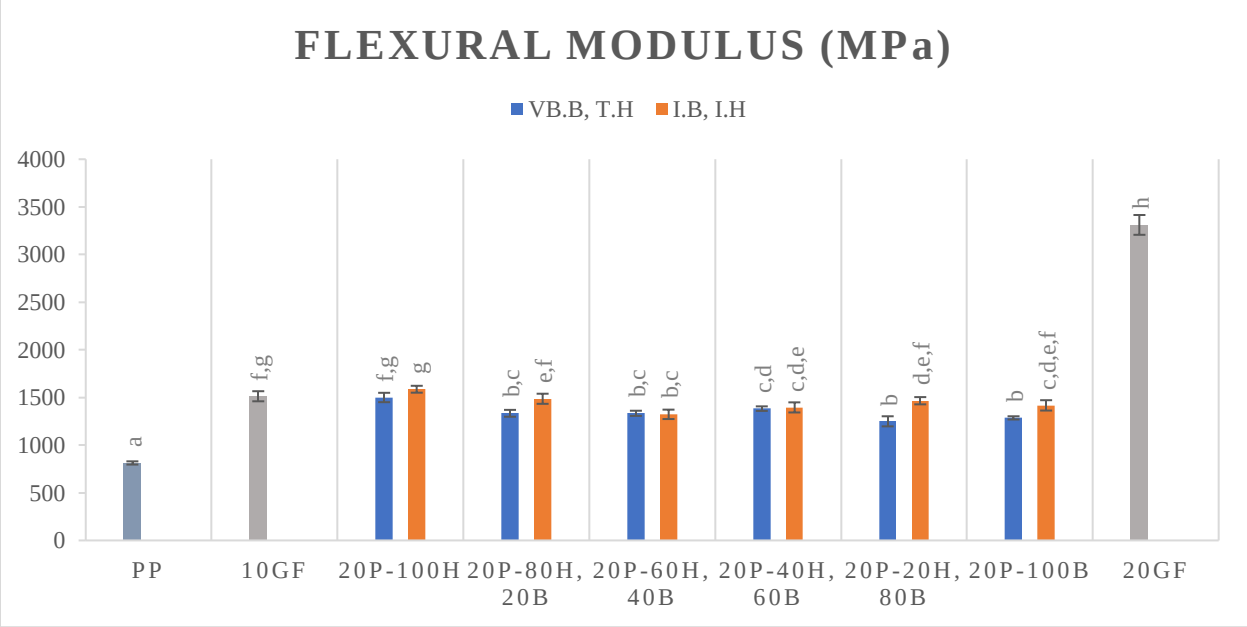


Figure 5.29 Flexural modulus of composites with hemp pellets of different compositions of bast and hurd fiber from different suppliers.

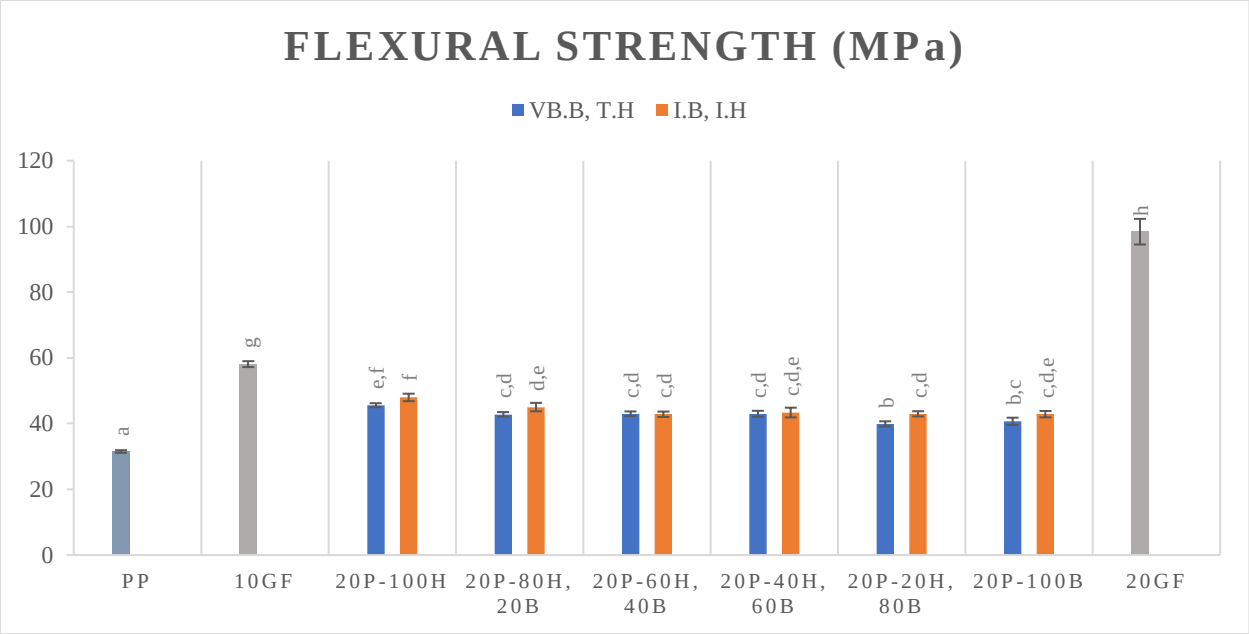


Figure 5.30 Flexural strength of composites with hemp pellets of different compositions of bast and hurd fiber from different suppliers.

5.5.2 Tensile Properties:

Figures 5.31 and 5.32 represent the tensile modulus and strength of the composites in question. From Figure 5.31, it is observed that composites prepared with pellets of different compositions of bast and hurd fiber have similar tensile modulus which indicates that different compositions of bast and hurd do not have any significant effect on tensile modulus of composites. On the other hand, it is interesting to notice the difference in the tensile modulus between composites prepared with hemp fiber supplied from different suppliers. Composites prepared with hemp fibers from the U.S.A, IND-Hemp bast (I.B), and IND-Hemp hurd (I.H) presented significantly lower tensile modulus than composites with hemp fiber from Canadian company Valley-Bio bast (VB.B) and Tangho Paraguay hurd (T.H). Composites with IND-Hemp fibers had similar tensile modulus as neat PP for all different hurd and bast compositions. Composites with VB.B and T.H fiber had higher tensile modulus than neat PP, 10 and 20% GF composites.

Figure 5.32 represents the tensile strength of the composites. The tensile strength results also depicted a similar trend as tensile modulus. The tensile strength of composites with pellets prepared with fibers supplied by Valley-Bio and Tangho Paraguay was higher than composites

with pellets prepared with fibers supplied by IND-Hemp U.S.A. Composites with 20% glass fiber (20GF) presented slightly higher tensile modulus than 20% hemp fiber composites.

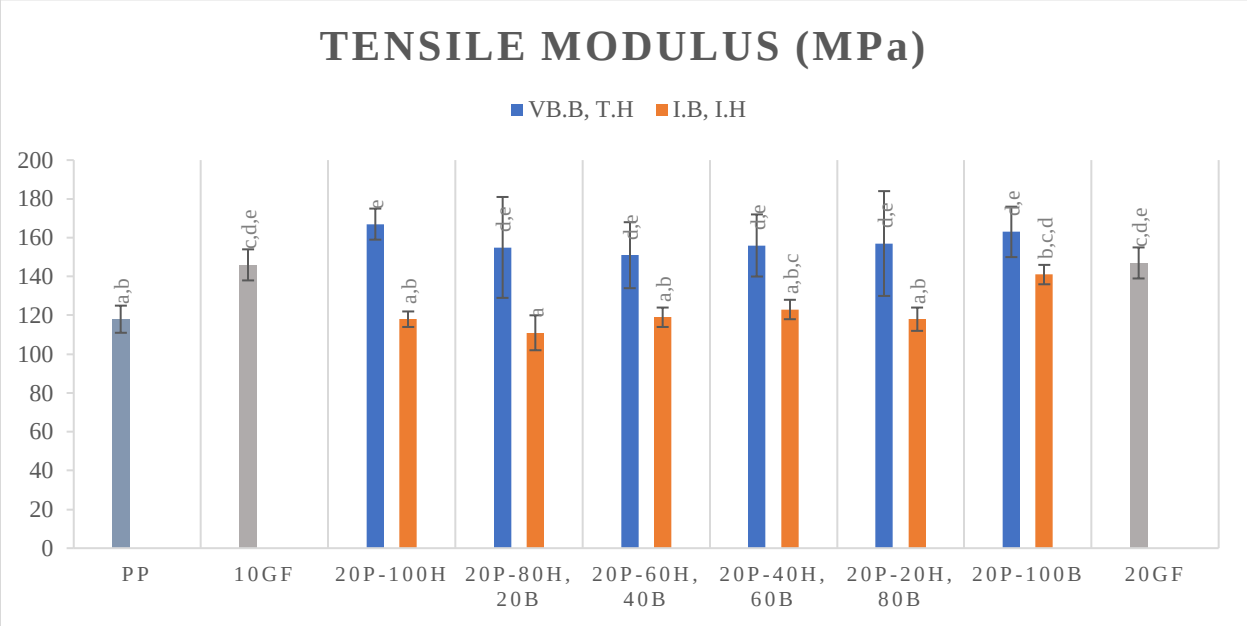


Figure 5.31 Tensile modulus of composites with hemp pellets of different composition of bast and hurd fiber from different suppliers.

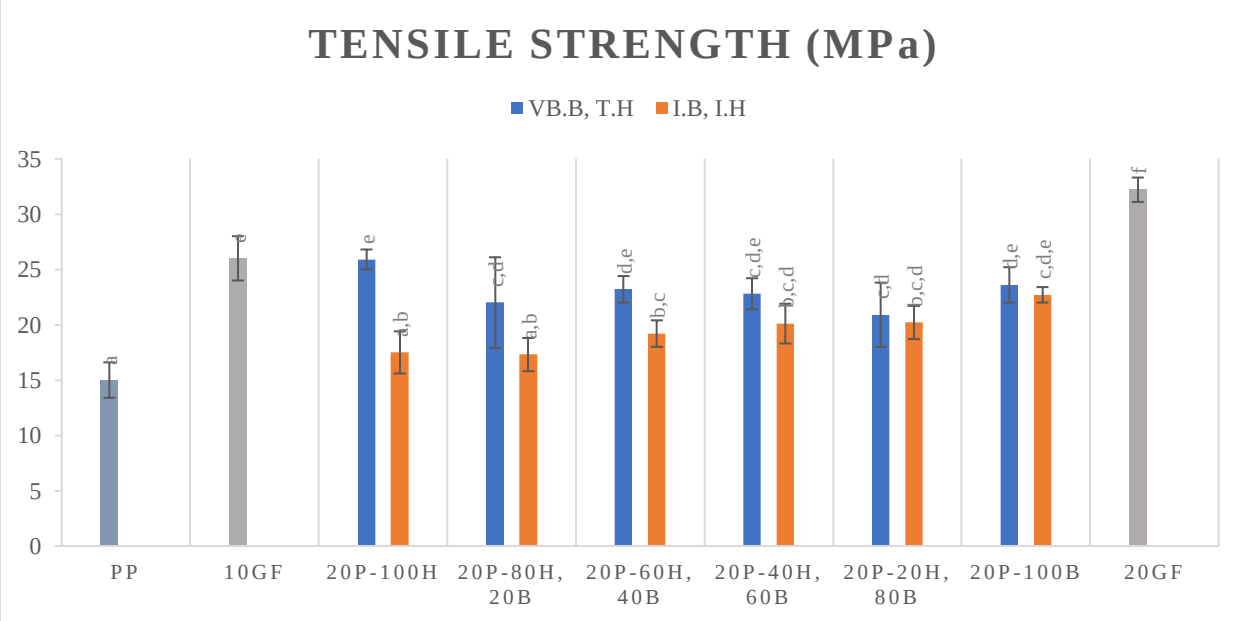


Figure 5.32 Tensile strength of composites with hemp pellets of different composition of bast and hurd fiber from different suppliers.

5.5.3 Impact Strength:

Figure 5.33 shows the impact strength of composites with hemp pellets of different compositions of bast and hurd fibers from different suppliers. The impact strength of all composites with different bast and hurd composition pellets and fibers from different suppliers exhibited similar results. The highest impact strength was observed for neat PP, and 20 GF composites showed slightly lower impact strength than neat PP.

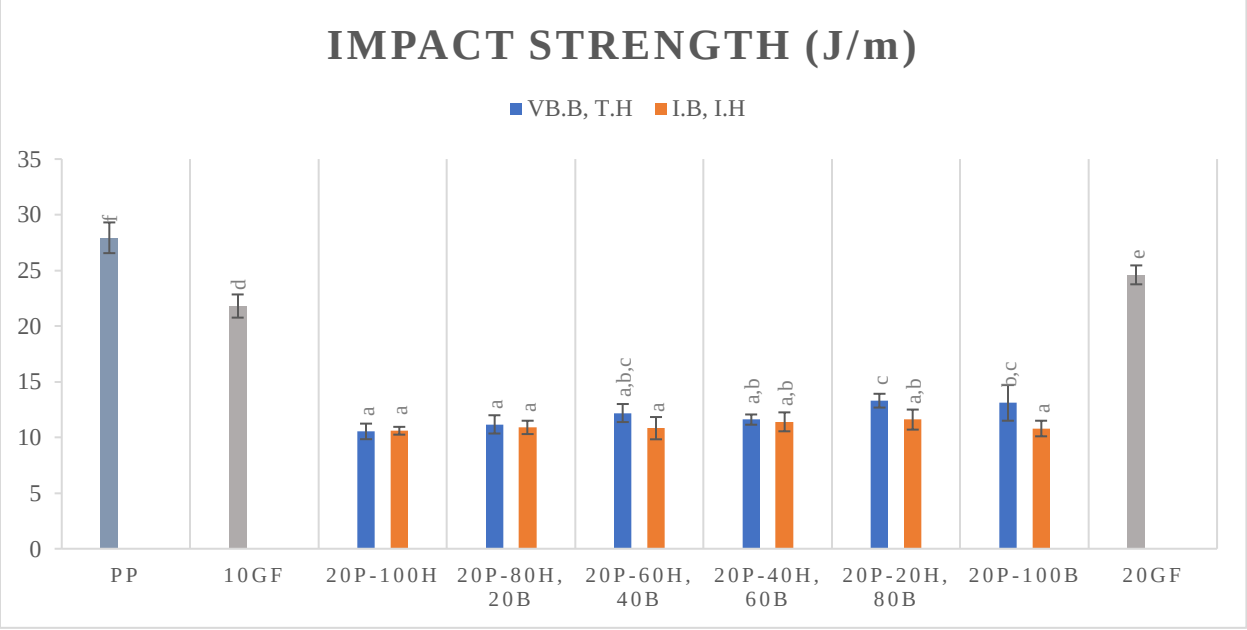


Figure 5.33 Impact strength of composites with hemp pellets of different compositions of bast and hurd fiber from different suppliers.

5.5.5 Melt Flow Index:

The MFI results are presented in Figure 5.34. All the composites with different compositions of hemp bast and hurd exhibited similar MFI.

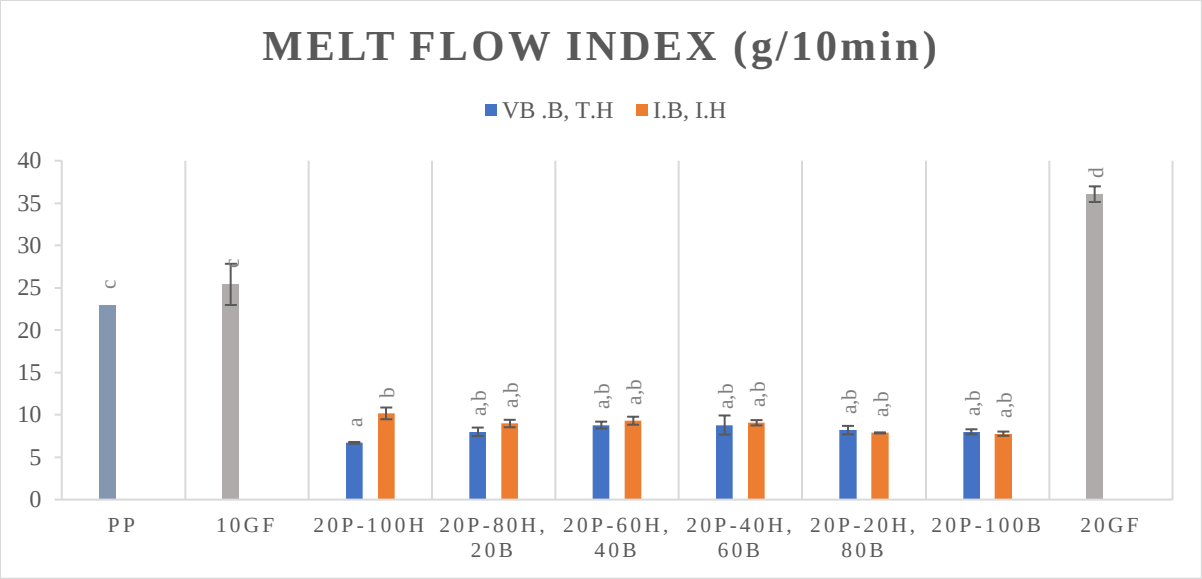


Figure 5.34 Melt flow index of composites with hemp pellets of different compositions of bast and hurd fiber from different suppliers.

5.5.5 Specific Flexural Modulus:

The results of the composites' specific flexural modulus are shown in Figure 5.35. It is observed that different compositions of hurd and bast fibers in pellets have no significant effect on the specific flexural modulus of the composites. The specific flexural modulus of composites with hemp pellets prepared from fibers supplied by IND-Hemp was slightly higher than other composites.

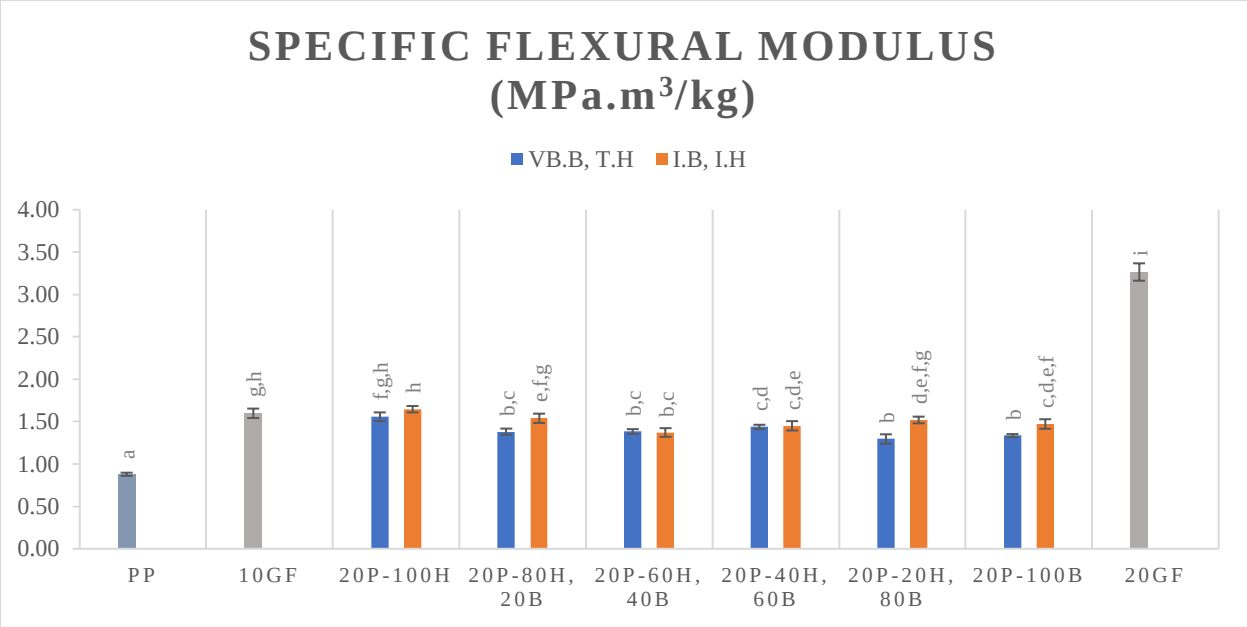


Figure 5.35 Specific flexural modulus of composites with hemp pellets of different compositions of bast and hurd fiber from different suppliers.

From all the above-mentioned results in this section, it was determined that different composition of hurd and bast fiber in composites does not have any significant effect on the mechanical properties of the composites. However, it was observed from tensile properties and specific flexural modulus that fibers from different places/suppliers have some effect on the mechanical properties of the composites. This will be further investigated in the next section. It was also determined that 20% hemp fiber composites can replace 10 %GF composites.

5.6 EFFECT OF HEMP FIBER FROM DIFFERENT COUNTRIES ON THE MECHANICAL PROPERTIES OF THE COMPOSITES.

In this section, composites with hemp pellets prepared from fibers provided by different suppliers/countries were analyzed to determine their effect on the mechanical properties of the composites.

From the previous section, it was observed that tensile properties and specific flexural modulus were different for composites with pellets prepared with fibers from different suppliers (Valley-Bio Canada, IND-Hemp USA, and Tangho Paraguay). The fiber quality varies from place to place because of different locations, altitudes, soil characteristics (nutrients), climate conditions of that area, harvest time, and different storage conditions and time (Karimah et al., 2021).

Composites with pellets of whole hemp fiber, 100% hurd fiber, and 100% bast fiber from different suppliers and countries were prepared and their results are compared in the following sections. Table 5.9 represents the formulation of the composites and Table 5.10 represents their mechanical properties results which are further discussed in the following sections.

Table 5.9 Formulation of composites with pellets of whole hemp fiber, bast fiber, and hurd fiber provided by different suppliers.

Pellet Fiber type: Tangho Paraguay whole hemp (TwH), Tangho Paraguay hurd (T.H), A.G USA whole hemp (AG.wH), A.G USA bast (AG.B), A.G USA hurd (AG.H), Valley-Bio Canada bast (VB.B), IND-Hemp USA bast (I.B), IND-Hemp USA hurd (I.H). **Milled pellet fiber size:** 1.5mm **Pellet moisture content:** 0-1% **MAPP wt.%:** 0.5%				
Sample Name	**PP wt.%**	**Whole Hemp Pellet wt.%**	**Bast Pellet wt.%**	**Hurd Pellet wt.%**
PP	100	0	0	0
20P-TwH	79.5	20	0	0
20P-AG.wH	79.5	20	0	0
20P-VB.B	79.5	0	20	0
20P-I.B	79.5	0	20	0
20P-AG.B	79.5	0	20	0
20P-T.H	79.5	0	0	20
20P-I.H	79.5	0	0	20
20P-AG.H	79.5	0	0	20

In sample names, '20P' represents 20wt% of pellets used, ' (TwH, AG.wH/VB.B, I.B, AG.B/T.H, I.H, AG.H)' represents supplier of fiber and fiber type as given in table 5.9.

Table 5.10 Mechanical properties of composites with pellets of whole hemp fiber, bast fiber, and hurd fiber provided by different suppliers.

Sample Name	Flexural Modulus (MPa)	Flexural Strength (MPa)	Tensile Modulus (MPa)	Tensile Strength (MPa)	Impact Strength (J/m)	Melt Flow Index (g/10min)	Density (kg/m^3)	Specific Flexural Modulus (MPa.m^3/kg)
PP	813±17^{a}	31.5±0.4^{a}	118±7^{a}	15±1.6^{a}	27.9±1.4^{b}	23.0±0.10^{b,c}	925±0.9	0.88±0.02^{a}
20P-TwH	1227±17^{b}	39.4±0.4^{b}	155±15^{b}	19.9±1.2^{b}	11.6±1.0^{a}	11.0±1.34^{a}	969±2.0	1.20±0.02^{b}
20P-AG.wH	1207±37^{b}	40.0±0.9^{b}	108±9^{a}	19.5±2.5^{b}	11.2±0.5^{a}	9.7±0.28^{a}	969±4.7	1.25±0.04^{b}
20P-VB.B	1286±17^{b}	40.7±1.1^{b}	163±13^{c}	23.6±1.6^{c}	13.1±1.6^{b}	8.0±0.30^{a}	963±0.8	1.34±0.02^{b}
20P-I.B	1417±54^{c}	43.0±1^{c}	141±5^{b}	22.7±0.7^{c}	10.8±0.7^{a}	7.8±0.25^{a}	963±10.0	1.47±0.06^{c}
20P-AG.B	1418±91^{c}	44.1±2^{c}	123±5^{a}	20.5±0.5^{b}	11.2±1.0^{a}	9.1±1.01^{a}	971±4.8	1.46±0.09^{c}
20P-T.H	1500±49^{c}	45.6±0.6^{c}	167±8^{b}	25.9±0.9^{c}	10.5±0.7^{a}	6.7±0.10^{a}	963±4.0	1.56±0.05^{c}
20P-I.H	1587±36^{d}	48.0±1.1^{d}	118±4^{a}	17.5±1.9^{a}	10.6±0.4^{a}	10.2±0.69^{b}	963±6.5	1.65±0.09^{d}
20P-AG.H	1295±83^{b}	40.4±1.6^{b}	135±25^{a}	21.9±2.7^{b}	9.7±0.6^{a}	11.3±0.03^{b}	948±13.0	1.37±0.09^{b}

All results were analysed using Tukey test with significance level of 5% to determine significance difference between mechanical properties of these composites. The superscripts (a,b,c,d) represents if the measured mechanical properties of composites in question are statistically different from each other or not. If superscripts of different samples in each mechanical property have the same letter then those values are statistically the same.

5.6.1: Flexural Properties:

Figures 5.36 and 5.37 represent the flexural modulus and strength, respectively, of composites with different whole hemp fiber pellets, bast fiber pellets, and hurd fiber pellets. In Figure 5.36 a), Flexural modulus results of composites with pellets prepared from whole hemp fiber supplied by Tangho Paraguay (20P-TwH) and AG USA (20P-AG.wH) are shown. The results depict a 33% increase in flexural modulus by the addition of 20wt.% hemp fiber pellets as compared to neat PP. The flexural modulus of composites with different whole hemp sources is observed to be similar.

Figure 5.36 b) shows flexural modulus results of composites with pellets of different bast fiber suppliers. The composites with IND-Hemp bast (20P-I.B) and A.G bast (20P-AG.B) fiber pellets had 9% higher flexural modulus than Valley-Bio bast composites and 42% higher than neat PP. The flexural modulus results of hurd fiber composites from Figure 5.36 c) suggest that IND-Hemp hurd composites (20P-I.H) have higher flexural modulus than Tangho hurd composites (20P-T.H) and A.G hurd composites (20P-AG.H). IND-Hemp Hurd composite (20P-I.H) had 18% higher flexural modulus than A.G hurd composite (20P-AG.H), and 49% higher than neat PP.

Flexural strength results of composites with whole hemp fibers are shown in Figure 5.37 a). The flexural strength for both composites from different suppliers of hemp fibers was observed to be the same. A slight difference was observed in the flexural strength of the composites with bast fibers from different suppliers in Figure 5.37 b). It was observed that IND-Hemp bast (20P-I.B) and AG bast (20P-AG.B) had slightly higher flexural strength than Valley-Bio bast (20P-VB.B). From Figure 5.37 c), it is observed that the flexural strength of the 20P-I.H composite was higher than 20P-T.H and 20P-AG.H composites.

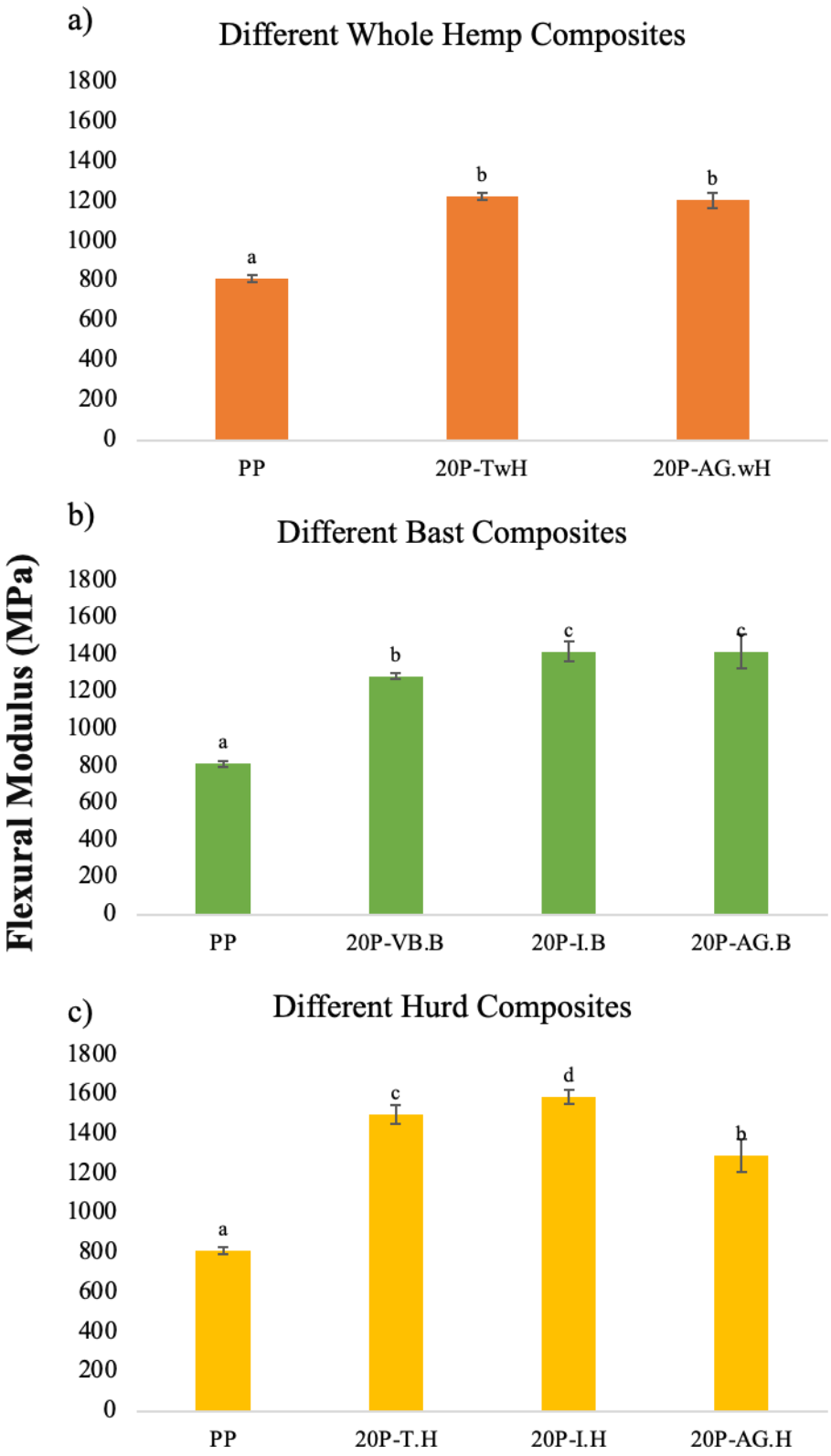


Figure 5.36 Flexural Modulus of composites with a) different whole hemp fiber pellets, b) different bast fiber pellets, and c) different hurd fiber pellets.

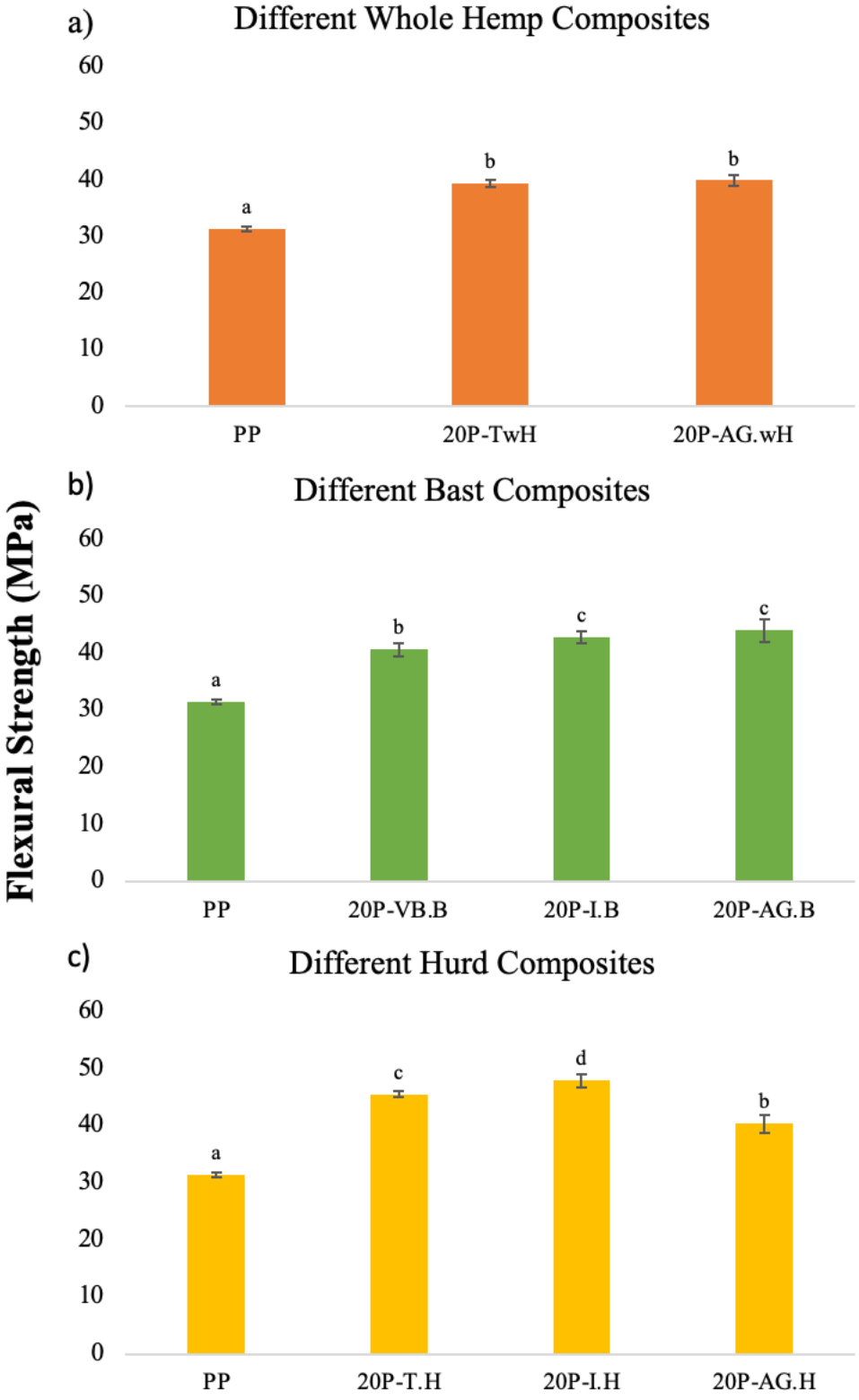


Figure 5.37 Flexural Strength of composites with a) different whole hemp fiber pellets, b) different bast fiber pellets, and c) different hurd fiber pellets.

5.6.2: Tensile Properties:

The tensile modulus and strength of composites prepared from different whole hemp fiber pellets, bast fiber pellets, and hurd fiber pellets are shown in Figures 5.38 and 5.39, respectively. From Figure 5.38 a), it is observed that Tangho whole hemp composites (TwH) had 30% higher tensile modulus than A.G whole hemp composite (AG.wH). The results of tensile modulus of composites with bast fiber from different supplier shown in Figure 5.38 b), outlines that 20P-VB.B composites had higher tensile modulus than other bast fiber composites. The tensile modulus of 20P-AG.B composites was observed to be similar to neat PP. From Figure 5.38 c), the highest tensile modulus was observed for 20P-T.H composites, and 20P-I.H and 20P-AG.H had similar tensile modulus as neat PP.

For composites with whole hemp fibers in Figure 5.39 a), it is observed that the tensile strength of both 20P-TwH and 20P-AG.wH composite are similar to each other and 25% higher than neat PP. For composites with bast fibers, it was observed from Figure 5.39 b), that 20P-VB.B and 20P-I.B composites have similar tensile strength which is slightly higher than 20P-AG.B composite tensile strength. Lastly, analyzing Figure 5.39 c), it can be seen that the 20P-T.H composites have the highest tensile strength, which is 29% higher than neat PP and 20P-I.H composite, and 19% higher than 20P-AG.H composites.

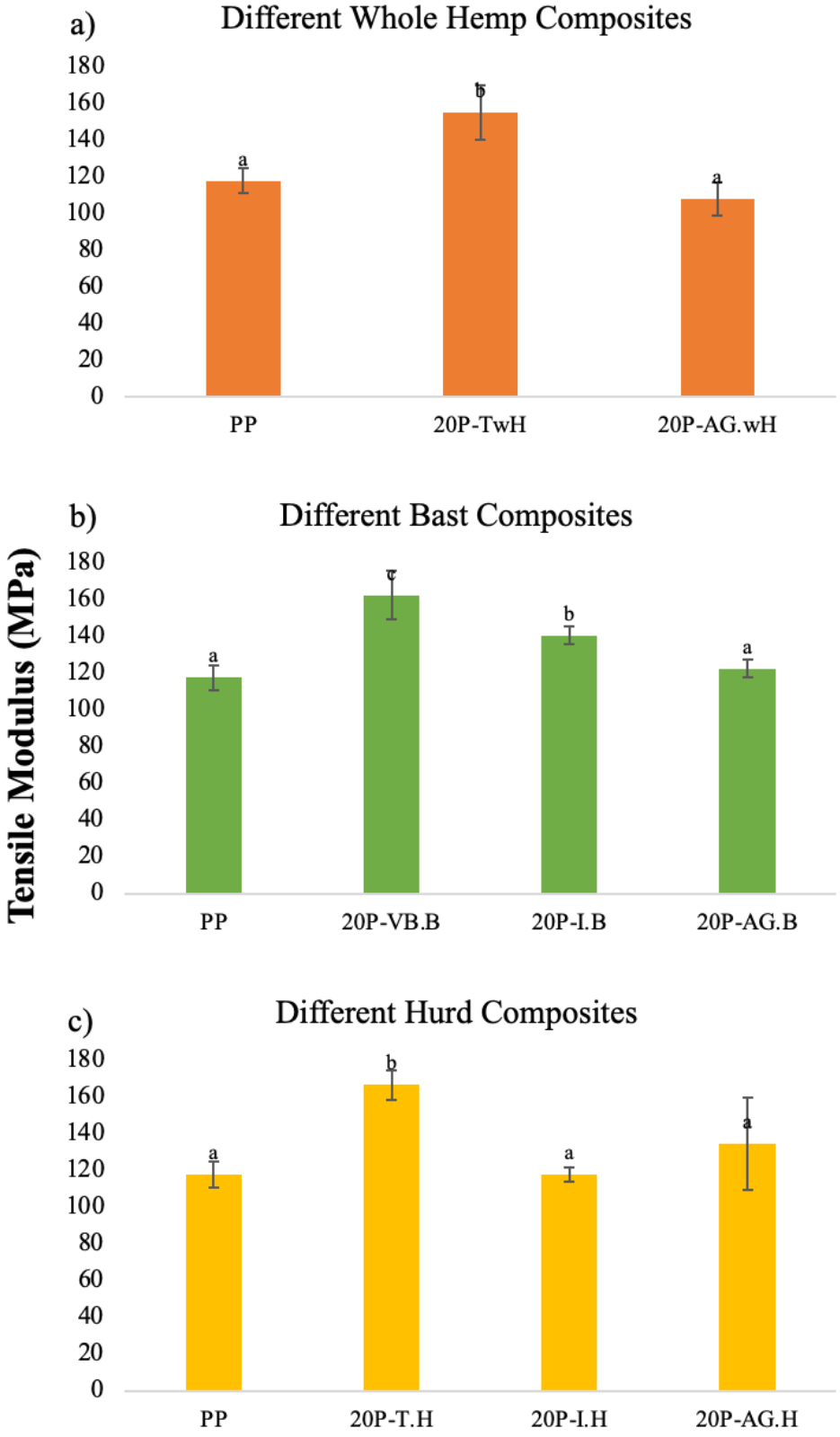


Figure 5.38 Tensile Modulus of composites with a) different whole hemp fiber pellets, b) different bast fiber pellets, and c) different hurd fiber pellets.

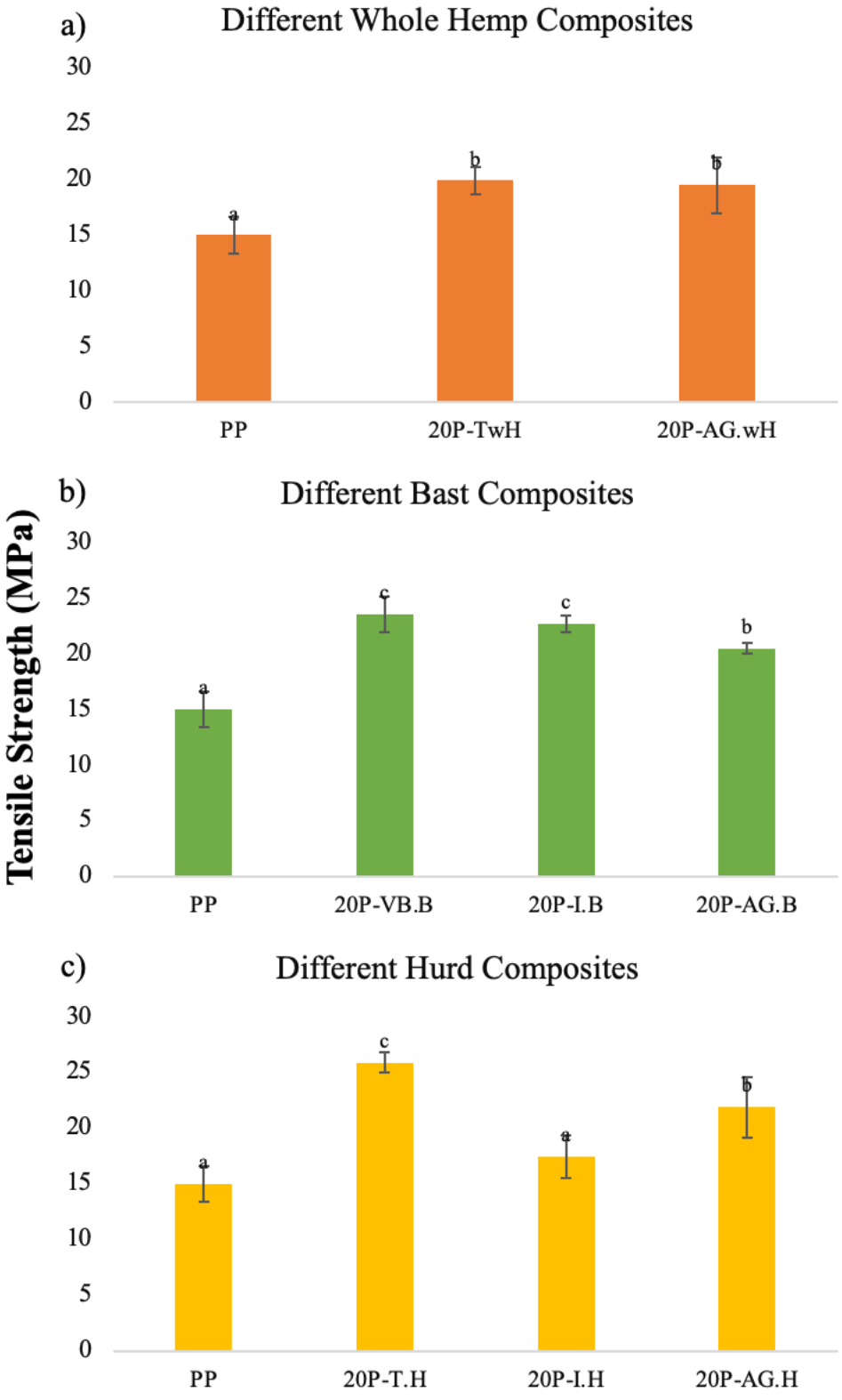


Figure 5.39 Tensile modulus of composites with a) different whole hemp fiber pellets, b) different bast fiber pellets, and c) different hurd fiber pellets.

5.6.3 Impact strength:

The impact strength of composites prepared with fibers from different suppliers is shown in Figure 5.40. It is observed from Figure 5.40 a), that the impact strength of the composite is reduced by the addition of fibers. The impact strength of composites with whole hemp fibers was reduced by 58% as compared to neat PP. The impact strength of 20P-TwH and 20P-AG.wH composites was found to be similar to each other. Figure 5.40 b) shows that the impact strength of 20P-VB.B composites was slightly higher than 20P-I.B and 20P-AG.B composites and 53% lower than neat PP. Figure 5.40 c) shows the impact strength results of composites with hurd fibers from different suppliers. All composites presented similar impact strengths, which are 62% lower than those of pure PP.

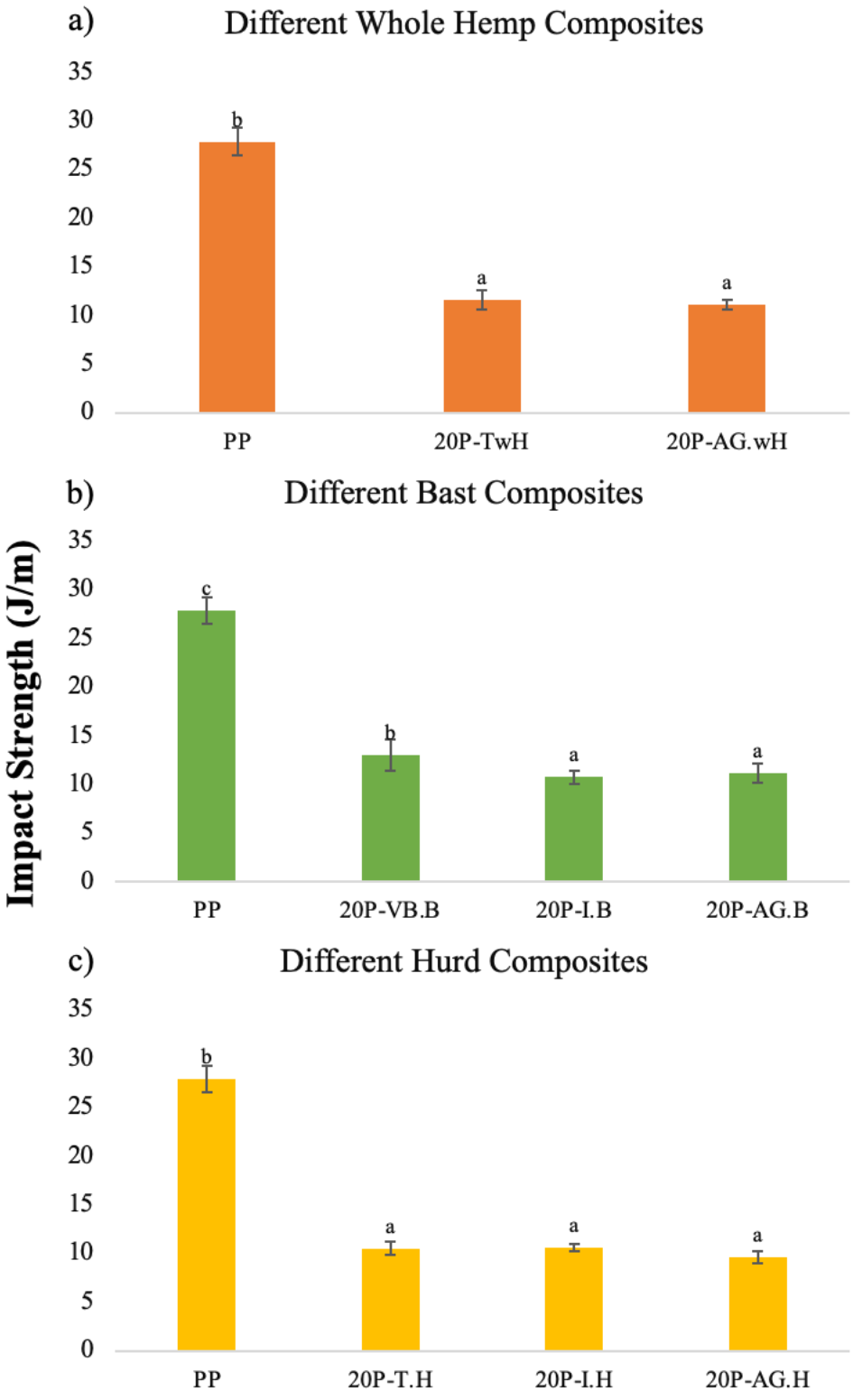


Figure 5.40 Impact strength of composites with a) different whole hemp fiber pellets, b) different bast fiber pellets, and c) different hurd fiber pellets.

5.6.4 Melt Flow Index:

Figure 5.41 depicts melt flow index results. It is observed that the effect of whole hemp, bast, and hurd fibers from different suppliers on the MFI of the composites is negligible. All the composites were observed to display similar MFI.

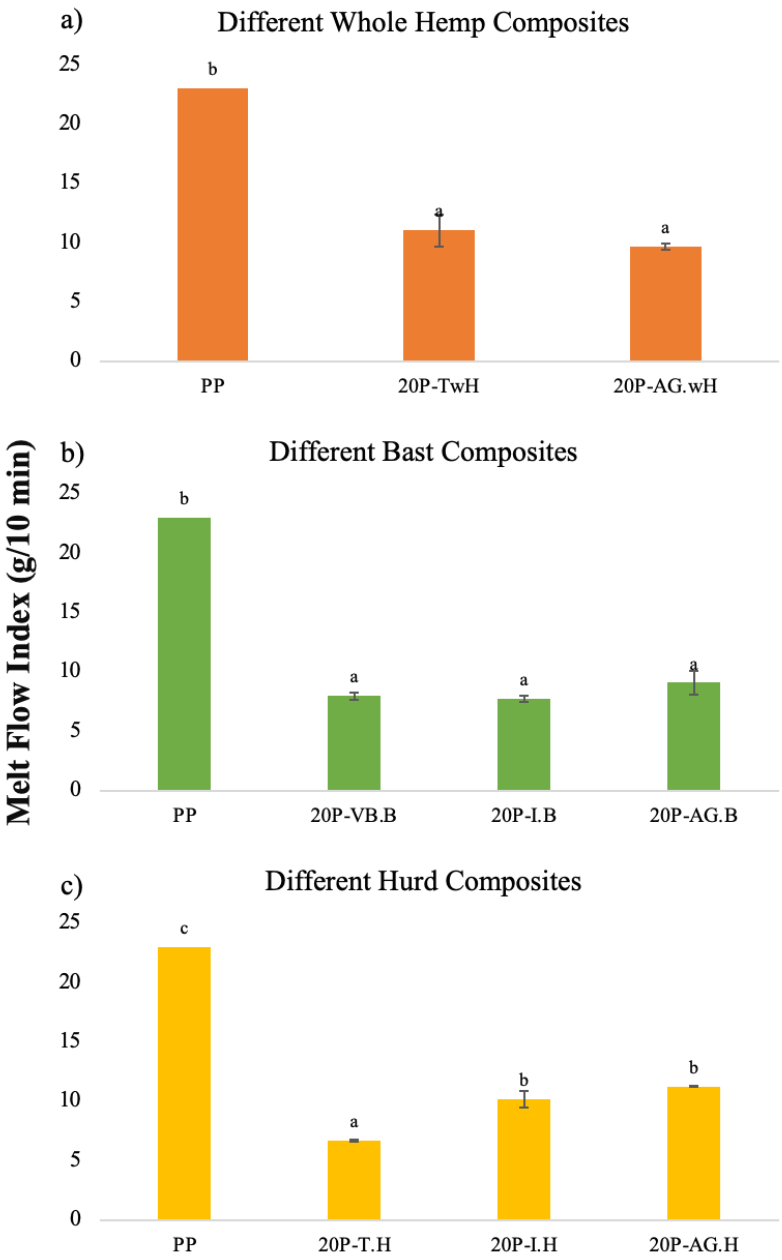


Figure 5.41 Melt flow index of composites with a) different whole hemp fiber pellets, b) different bast fiber pellets, and c) different hurd fiber pellets.

5.6.5: Specific Flexural Modulus:

Specific flexural modulus results of composites are shown in Figure 5.42. Figure 5.42 a) represents that the specific flexural modulus of composites with whole hemp fibers from different suppliers are similar to each other and 31% higher than neat PP. For composites with bast fibers in Figure 5.42 b), 20P-I.B and 20P-AG.B composites have slightly higher SFM than 20P-VB.B and 40% higher than neat PP. SFM of hurd fiber composites shown in Figure 5.42 c) depicts that 20P-I.H composites have slightly higher SFM than 20P-T.H, 17% higher than 20P-AG.H composites and 47% higher than neat PP.

Based on the findings shown above, it was found that fibers from different suppliers and different countries have a slight effect on the mechanical properties of the composites. From the analysis of the whole hemp fiber composites, it was observed that all their mechanical properties are similar except for tensile modulus, the 20P-TwH tensile modulus was 30% higher than 20P-AG.wH composites. For bast fiber composites, 20P-VB.B had slightly lower flexural modulus and strength than 20P-I.B and 20P-AG.B composites but showed higher tensile modulus and impact strength. Lastly, for hurd fiber composites, 20P-T.H composites presented similar flexural properties as 20P-I.H composites but had significantly higher tensile properties, the other mechanical properties were similar.

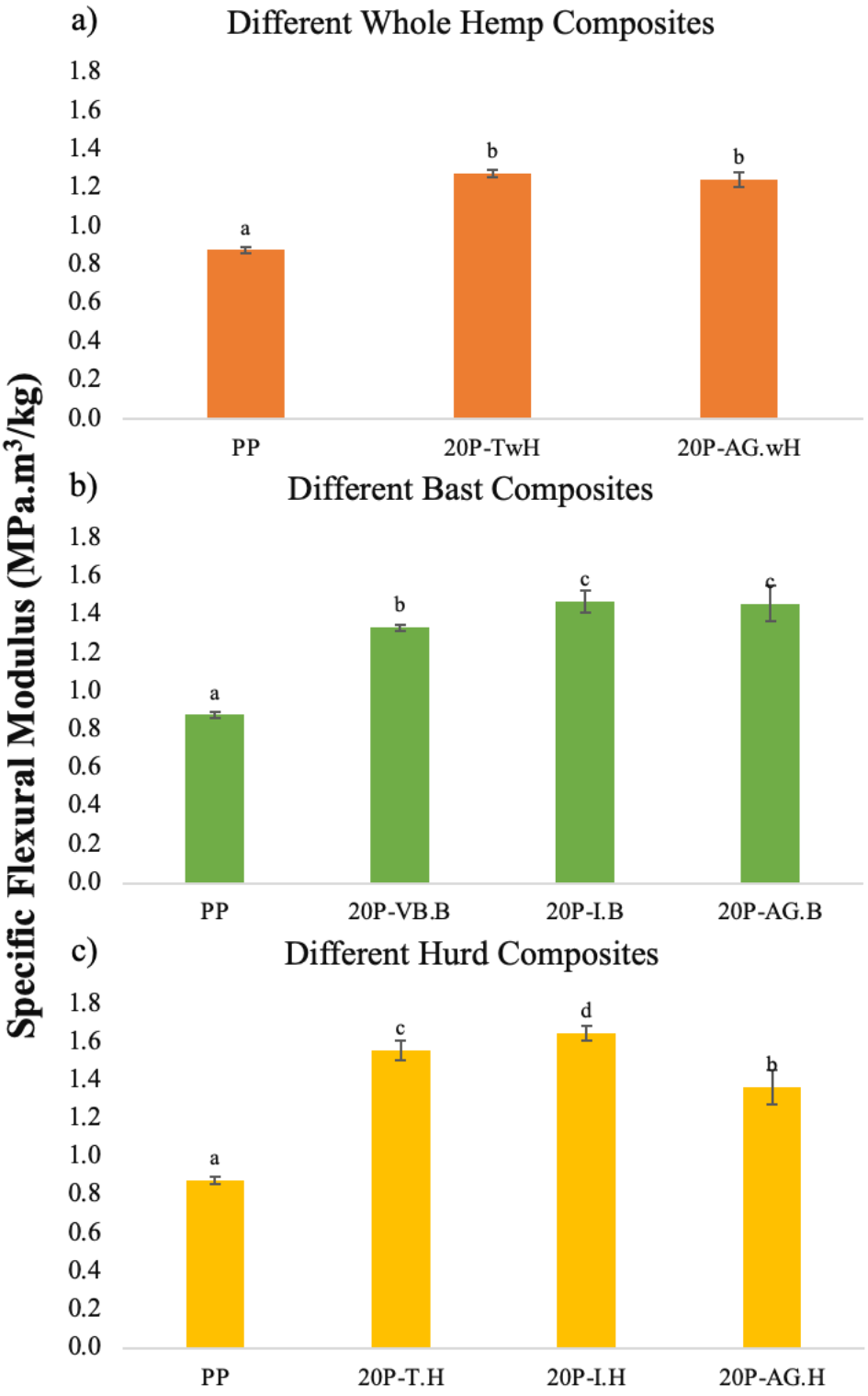


Figure 5.42 Specific flexural modulus of composites with a) different whole hemp fiber pellets, b) different bast fiber pellets, and c) different hurd fiber pellets.

5.7 COMPARISON BETWEEN COMPOSITE WITH FIBER AND PELLET:

This section presents a comparative investigation of the mechanical properties of polypropylene composites reinforced with hemp fiber and hemp pellets. The objective of this study was to evaluate the individual effects of two different reinforcement feeding types on the structural and performance properties of the composites. It is important to note that because of the low density of hemp fibers, they tend to reside on top of polypropylene pellets while being fed into the extruder. This non-uniform feeding of hemp fiber poses a significant challenge in attaining a uniform and consistent extrudate. So, to achieve a homogenous mixing of hemp fibers with polypropylene, first polypropylene pellets were milled in Wiley Mill (knife mill) and then mixed with hemp fibers before feeding into the extruder as shown in figure 5.43 (a). On the contrary, the use of hemp pellets offers the advantage of easy mixing with polypropylene pellets and facilitates homogeneous feeding into the extruder as shown in Figure 5.43 (b).

The composite formulation and mechanical properties are presented in Table 5.11 and Figure 5.44. Tukey analysis with a significance level of 5% was also done to determine significant differences between the mechanical properties of these composites.

Tuckey analysis showed that composites with pellets had lower flexural and tensile properties as compared to composites with fiber. The observed difference could be ascribed to the improper deagglomeration of hemp pellets during the extrusion process, resulting in the non-uniform distribution of the fibers inside the polypropylene matrix. However, the dispersion of fibers from hemp pellets can be improved by the use of additives.

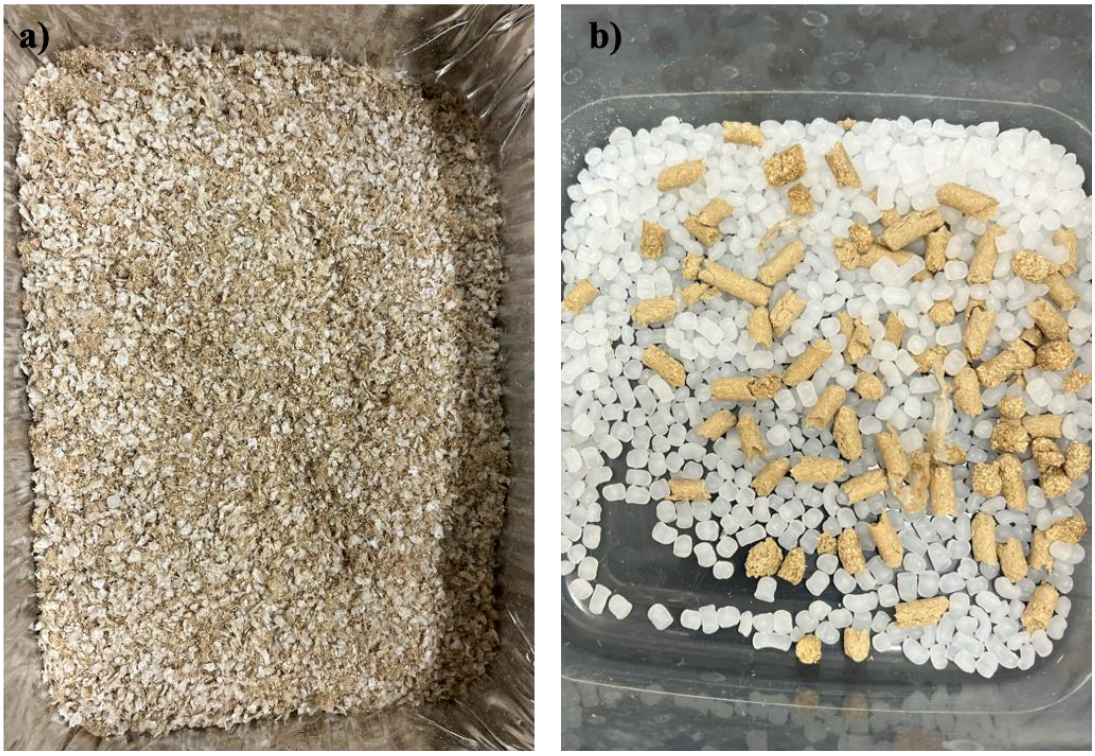


Figure 5.43 Pre extrusion mix a) hemp fiber and PP milled, b) hemp and PP pellets.

Table 5.11 Formulation and mechanical properties of composites with hemp fiber and pellets.

Composite Formulation: 79.5% PP + 0.5% MAPP + 20% Hemp fiber/pellet **Fiber type:** Tangho Paraguay whole hemp fiber (TwH) **Milled fiber size:** 1.5mm **Hemp fiber/pellet moisture content:** 0-1%								
Sample Name	**Flexural Modulus (MPa)**	**Flexural Strength (MPa)**	**Tensile Modulus (MPa)**	**Tensile Strength (MPa)**	**Impact Strength (J/m)**	**Melt Flow Index (g/10min)**	**Density kg/m^3**	**Specific Flexural Modulus (Mpa.m^3/kg)**
20F-TwH	1354±34^b	40.5±0.8^b	181±11^b	23.4±1.8^b	12.4±0.9^a	10.5±0.25^a	964±3.4	1.4±0.04^b
20P-TwH	1227±17^a	39.4±0.4^a	155±15^a	19.9±1.2^a	11.63±1.0^a	11.05±1.34^a	969±2	1.2±0.02^a

In sample names, '20F/P' represents 20wt% of fibers/pellets used, and TwH represents supplier of fiber and fiber type.

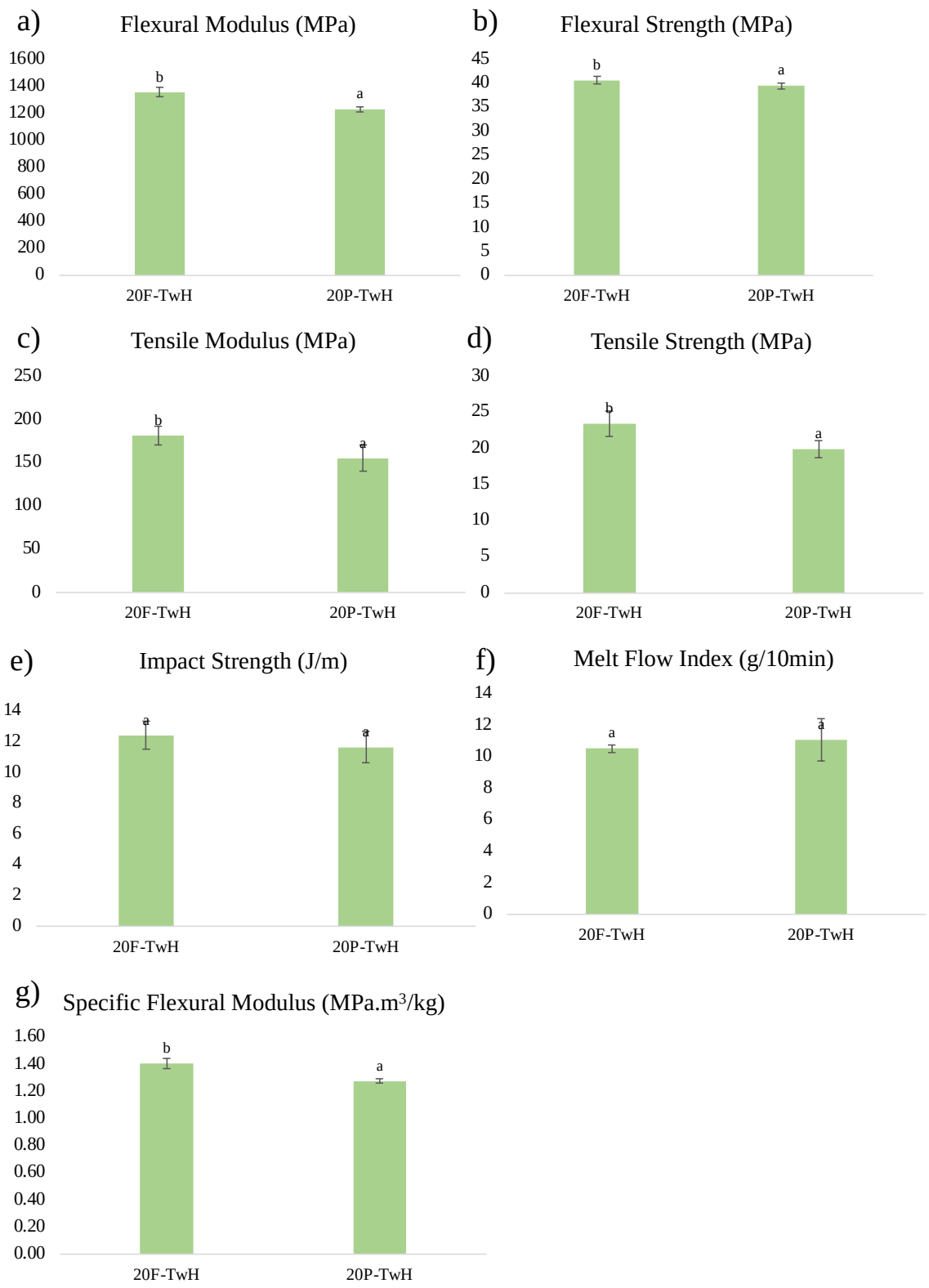


Figure 5.44 Mechanical properties of composites with hemp fiber and pellets, a) Flexural Modulus, b) Flexural Strength, c) Tensile Modulus, d) Tensile Strength, e) Impact strength, f) Melt flow index, g) Specific flexural modulus.

CHAPTER 6: CONCLUSION AND RECOMMENDATIONS

The primary objective of this thesis was to contribute to the progress of hemp fiber-reinforced polypropylene composites. Nevertheless, a noteworthy difficulty arose due to the hemp fibers' low bulk density, presenting a considerable challenge to their effective integration into the composite matrix through the extrusion process. The current research undertook a comprehensive method to tackle this restriction by employing hemp fiber pelletization. This approach was utilized with the aim of improving the overall handling, transportation, and storage of hemp fibers, while concurrently facilitating their smooth feeding with polypropylene pellets during the extrusion process. This research explored the development of composite materials and introduced a novel method to make natural fibers suitable for composite manufacturing. This research significantly contributes to the progress of sustainable materials in the field of composite technology.

The effect of several variables was investigated on the mechanical properties of both hemp pellets and composites. These variables were particle size, use of additives, different compositions of hemp bast and hurd fiber, use of coupling agent, and alkali treatment of fibers. Based on a detailed analysis of the effect of these variables on hemp pelletization and the mechanical properties of composites, the main conclusions are presented as follows.

1. The effect of different fiber sizes (1, 1.5, and 3 mm) and the addition of an additive (wax) was investigated on the mechanical properties of both hemp pellets and composites. For pellets, it was found that the effect of different particle sizes and the use of wax on the specific compressive strength and durability was not significant. However, for pellets with 3 mm fibers, bulk density was observed to be significantly lower than pellets with 1- and 1.5-mm fibers. The use of wax considerably lowered the bulk density of pellets with 1- and 1.5-mm fibers and significantly improved the bulk density of pellets with 3 mm fibers. For composites, no significant effect of particle size was observed on mechanical properties. The use of wax slightly improved the flexural modulus but reduced other mechanical properties.
2. An attempt was made to prepare 100% hurd pellets. It was found that to form hurd pellets at pellet die temperature below 45°C, the feed moisture content needed to be around 60-65%. However, the pellets formed were very weak and did not meet the

standards for durability, bulk density, and compressive strength. Later it was observed that temperature had a significant effect on the formation and mechanical properties of hurd pellets. It was found that the hurd pellets, although weak, began to form at the pellet matrix temperature of around 45°C, and as the temperature increased, the strength of the hurd pellets also increased.

3. The effect of different compositions of bast and hurd fiber and different fiber origins was also investigated on the mechanical properties of pellets and composites. For pellets, the pellets with IND Hemp USA fibers were found to have better mechanical properties than pellets with Valley Bio Canada hemp fibers. The mechanical properties of pellets increased with an increase in bast fiber concentration. For composites, the tensile properties of composites with Valley Bio Canada fiber pellets were significantly higher than composites with IND Hemp USA fiber pellets. Other mechanical properties were observed to be similar.
4. 5 wt.% NaOH treatment of hemp fibers removed impurities from the fiber surface and reduced water absorption of fibers by 12 ± 8 %. However, pelletization of NaOH-treated fibers was not successful because of increased agglomeration due to an increase in cohesion between fibers by the removal of impurities and exposure of hydroxyl groups on the fiber surface. For composites, the interfacial adhesion and mechanical properties were improved by NaOH treatment of fibers, however, the use of 0.5 wt.% MAPP coupling agent displayed better interfacial adhesion and mechanical properties.
5. Pelletization of whole hemp fiber, bast fiber, and hurd fiber from different suppliers was performed and composites were prepared to study the effect of fibers from different suppliers on the composite's mechanical properties. However, slight effects of different fiber origins were observed.
6. The densification of the hemp fibers utilizing the pelletization process demonstrated here also has a significant contribution in decreasing the cost and carbon emissions associated with the transportation of the hemp fibers from its source to the destination for manufacturing composites.
7. Lastly, the change in particle size of hemp bast and hurd fibers after pelletization was also investigated. It was found that bast fibers were able to maintain their size during pelletization while hurd fibers underwent significant size change.

This study provides some recommendations for future work which are,

1. Additional investigation is required to enhance and optimize the natural fiber pelletization process. This entails conducting an examination of various pelletization techniques and equipment to improve the quality and uniformity of the pellets. The development of cost-effective and energy-efficient pelletization systems will play a significant role in facilitating industrial-scale production.
2. Investigate the effect of the use of nanocellulose as a binding agent for hemp pellets on the mechanical properties of composites.
3. Create mathematical models to better comprehend and correlate each composite property and fit those models with pertinent literature data.
4. Perform long-term durability investigations to evaluate the effectiveness of hemp-reinforced polypropylene composites in practical situations. This encompasses the influence of environmental elements such as UV radiation, moisture absorbance, temperature fluctuations, and mechanical strain.
5. Use of alternative additives to enhance fiber dispersion and improve mechanical properties of composites.
6. Conduct research to investigate recyclability of hemp fiber reinforced polypropylene composites.

LETTER OF COPYRIGHT PERMISSION

JOHN WILEY AND SONS LICENSE
TERMS AND CONDITIONS

Oct 15, 2023

This Agreement between Mr. Gulzeb Khan Khakwani ("You") and John Wiley and Sons ("John Wiley and Sons") consists of your license details and the terms and conditions provided by John Wiley and Sons and Copyright Clearance Center.

License Number	5650090084570
License date	Oct 15, 2023
Licensed Content Publisher	John Wiley and Sons
Licensed Content Publication	Polymer International
Licensed Content Title	Materials science and engineering. An introduction 2nd Edition W. D. Callister, Jr John Wiley & Sons, New York, 1991. pp. xxi 791, price E53.00. ISBN 0-471-50488-2
Licensed Content Author	W. W. Wright
Licensed Content Date	Feb 26, 2007
Licensed Content Volume	30
Licensed Content Issue	2
Licensed Content Pages	2

Print This Page

ELSEVIER LICENSE
TERMS AND CONDITIONS

Oct 15, 2023

This Agreement between Mr. Gulzeb Khan Khakwani ("You") and Elsevier ("Elsevier") consists of your license details and the terms and conditions provided by Elsevier and Copyright Clearance Center.

License Number	5650100078216
License date	Oct 15, 2023
Licensed Content Publisher	Elsevier
Licensed Content Publication	Elsevier Books
Licensed Content Title	Advanced Composite Materials for Aerospace Engineering
Licensed Content Author	S. Rana,R. Fangueiro
Licensed Content Date	Jan 1, 2016
Licensed Content Pages	15
Start Page	1
End Page	15
Type of Use	reuse in a thesis/dissertation
Portion	figures/tables/illustrations

Print This Page

ELSEVIER LICENSE
TERMS AND CONDITIONS

Oct 15, 2023

This Agreement between Mr. Gulzeb Khan Khakwani ("You") and Elsevier ("Elsevier") consists of your license details and the terms and conditions provided by Elsevier and Copyright Clearance Center.

License Number	5650101455283
License date	Oct 15, 2023
Licensed Content Publisher	Elsevier
Licensed Content Publication	Elsevier Books
Licensed Content Title	Polyolefin Fibres
Licensed Content Author	A CRANGLE
Licensed Content Date	Jan 1, 2009
Licensed Content Pages	32
Start Page	3
End Page	34
Type of Use	reuse in a thesis/dissertation
Portion	figures/tables/illustrations
Number of figures/tables/illustrations	1

Print This Page

ELSEVIER LICENSE
TERMS AND CONDITIONS

Oct 05, 2023

This Agreement between Mr. Gulzeb Khan Khakwani ("You") and Elsevier ("Elsevier") consists of your license details and the terms and conditions provided by Elsevier and Copyright Clearance Center.

License Number	5642371267906
License date	Oct 05, 2023
Licensed Content Publisher	Elsevier
Licensed Content Publication	Composites Part A: Applied Science and Manufacturing
Licensed Content Title	Effect of alkali treatment on interfacial bonding in abaca fiber-reinforced composites
Licensed Content Author	Ming Cai,Hitoshi Takagi,Antonio N. Nakagaito,Yan Li,Geoffrey I.N. Waterhouse
Licensed Content Date	Nov 1, 2016
Licensed Content Volume	90
Licensed Content Issue	n/a
Licensed Content Pages	9
Start Page	589
End Page	597

Type of Use	reuse in a thesis/dissertation
Portion	figures/tables/illustrations
Number of figures/tables/illustrations	1
Format	both print and electronic
Are you the author of this Elsevier article?	No
Will you be translating?	No
Title	Hemp fiber pelletization and hemp reinforced polypropylene composites
Institution name	university of waterloo
Expected presentation date	Nov 2023
Portions	Fig 2
Requestor Location	Mr. Gulzeb Khan Khakwani 209 Buttercup Court Waterloo, ON N2V 2W8 Canada Attn: Mr. Gulzeb Khan Khakwani
Publisher Tax ID	GB 494 6272 12
Total	0.00 CAD
Terms and Conditions	

REFERENCES

Ahn, B.J., Chang, H., Lee, S.M., Choi, D.H., Cho, S.T., Han, G., Yang, I., 2014. Effect of binders on the durability of wood pellets fabricated from Larix kaemferi C. and Liriodendron tulipifera L. sawdust. Renewable Energy 62, 18–23. https://doi.org/10.1016/j.renene.2013.06.038

Anand, P.B., Lakshmikanthan, A., Chandrashekarappa, M.P.G., Selvan, C.P., Pimenov, D.Y., Giasin, K., 2022. Experimental Investigation of Effect of Fiber Length on Mechanical, Wear, and Morphological Behavior of Silane-Treated Pineapple Leaf Fiber ReinforcedPolymer Composites.

Atta-Obeng, E., Via, B.K., Fasina, O., 2012. EFFECT OF MICROCRYSTALLINE CELLULOSE, SPECIES, AND PARTICLE SIZE ON MECHANICAL AND PHYSICAL PROPERTIES OF PARTICLEBOARD. WOOD AND FIBER SCIENCE 44.

Balčiūnas, G., Vėjelis, S., Vaitkus, S., Kairytė, A., 2013. Physical Properties and Structure of Composite Made by Using Hemp Hurds and Different Binding Materials. Procedia Engineering 57, 159–166. https://doi.org/10.1016/j.proeng.2013.04.023

Bokhari, S.M.Q., Chi, K., Catchmark, J.M., 2021. Structural and physico-chemical characterization of industrial hemp hurd: Impacts of chemical pretreatments and mechanical refining. Industrial Crops and Products 171, 113818. https://doi.org/10.1016/j.indcrop.2021.113818

Cai, M., Takagi, H., Nakagaito, A.N., Li, Y., Waterhouse, G.I.N., 2016. Effect of alkali treatment on interfacial bonding in abaca fiber-reinforced composites. Composites Part A: Applied Science and Manufacturing 90, 589–597. https://doi.org/10.1016/j.compositesa.2016.08.025

Callister, W.D., 2007. Materials science and engineering: an introduction, 7th ed. ed. John Wiley & Sons, New York.

Capes, C.E., 2013. Particle Size Enlargement. Elsevier.

Carone, M.T., Pantaleo, A., Pellerano, A., 2011. Influence of process parameters and biomass characteristics on the durability of pellets from the pruning residues of Olea europaea L. Biomass and Bioenergy 35, 402–410. https://doi.org/10.1016/j.biombioe.2010.08.052

Cheng, Q., Zhou, C., Pan, Y., Via, B., 2020. Morphological Characterization of Wax and Surfactant–Encapsulated Microcrystalline Cellulose for Better Dispersion. Forest Products Journal 70, 226–231. https://doi.org/10.13073/FPJ-D-19-00070

Crangle, A., 2017. Types of polyolefin fibres, in: Polyolefin Fibres. Elsevier, pp. 3–32. https://doi.org/10.1016/B978-0-08-101132-4.00001-1

Dufresne, A., 2013. Cellulose-Based Composites and Nanocomposites, in: Handbook of Biopolymers and Biodegradable Plastics. Elsevier, pp. 153–169. https://doi.org/10.1016/B978-1-4557-2834-3.00008-2

Egbo, M.K., 2021. A fundamental review on composite materials and some of their applications in biomedical engineering. Journal of King Saud University - Engineering Sciences 33, 557–568. https://doi.org/10.1016/j.jksues.2020.07.007

Elseify, L., Midani, M., El-Badawy, A., Jawaid, M., 2021. Manufacturing Automotive Components from Sustainable Natural Fiber Composites. https://doi.org/10.1007/978-3-030-83025-0

Etcheverry, M., Barbosa, S.E., 2012. Glass Fiber Reinforced Polypropylene Mechanical Properties Enhancement by Adhesion Improvement. Materials 5, 1084–1113. https://doi.org/10.3390/ma5061084

Fang, Z., Smith, Jr, R.L., Tian, X.-F. (Eds.), 2019. Production of Materials from Sustainable Biomass Resources, Biofuels and Biorefineries. Springer Singapore, Singapore. https://doi.org/10.1007/978-981-13-3768-0

Fitri, M., Mahzan, S., Anggara, F., 2021. The Mechanical Properties Requirement for Polymer Composite Automotive Parts - A Review. International Journal of Advanced Technology in Mechanical, Mechatronics and Materials 1, 125–133. https://doi.org/10.37869/ijatec.v1i3.38

Frodeson, S., Henriksson, G., Berghel, J., 2019. Effects of moisture content during densification of biomass pellets, focusing on polysaccharide substances. Biomass and Bioenergy 122, 322–330. https://doi.org/10.1016/j.biombioe.2019.01.048

Fu, S.-Y., Lauke, B., Mäder, E., Yue, C.-Y., Hu, X., 2000. Tensile properties of short-glass-fiber- and short-carbon-fiber-reinforced polypropylene composites. Composites Part A: Applied Science and Manufacturing 31, 1117–1125. https://doi.org/10.1016/S1359-835X(00)00068-3

Garcia-Maraver, A., 2015. Biomass Pelletization Process, in: Garcia-Maraver, A., Perez-Jimenez, J.A. (Eds.), WIT Transactions on State of the Art in Science and Engineering. WIT Press, pp. 53–66. https://doi.org/10.2495/978-1-84566-062-8/004

Giles, H.F., Wagner, J.R., Mount, E.M., 2005. Extrusion: the definitive processing guide and handbook, PDL handbook series. William Andrew Pub, Norwich, NY.

Green, D.W., Southard, M.Z. (Eds.), 2019. Perry's chemical engineers' handbook, Ninth edition, 85th anniversary edition. ed. McGraw Hill Education, New York.

Gümüşkaya, E., Usta, M., Balaban, M., 2007. Carbohydrate components and crystalline structure of organosolv hemp (Cannabis sativa L.) bast fibers pulp. Bioresource Technology 98, 491–497. https://doi.org/10.1016/j.biortech.2006.02.031

Harun, N.Y., Afzal, M.T., 2016. Effect of Particle Size on Mechanical Properties of Pellets Made from Biomass Blends. Procedia Engineering, Proceeding of 4th International Conference on Process Engineering and Advanced Materials (ICPEAM 2016) 148, 93–99. https://doi.org/10.1016/j.proeng.2016.06.445

Hassan, A., Salema, A.A., Ani, F.N., Bakar, A.A., 2010. A review on oil palm empty fruit bunch fiber-reinforced polymer composite materials. Polym Compos 31, 2079–2101. https://doi.org/10.1002/pc.21006

Hu, Q., Shao, J., Yang, H., Yao, D., Wang, X., Chen, H., 2015. Effects of binders on the properties of bio-char pellets. Applied Energy 157, 508–516. https://doi.org/10.1016/j.apenergy.2015.05.019

Irvine, G.M., 1985. The significance of the glass transition of lignin in thermomechanical pulping. Wood Sci. Technol. 19, 139–149. https://doi.org/10.1007/BF00353074

Jackson, J., Turner, A., Mark, T., Montross, M., 2016. Densification of biomass using a pilot scale flat ring roller pellet mill. Fuel Processing Technology 148, 43–49. https://doi.org/10.1016/j.fuproc.2016.02.024

Jarukumjorn, K., Suppakarn, N., 2009. Effect of glass fiber hybridization on properties of sisal fiber–polypropylene composites. Composites Part B: Engineering 40, 623–627. https://doi.org/10.1016/j.compositesb.2009.04.007

Jiang, L., Liang, J., Yuan, X., Li, H., Li, C., Xiao, Z., Huang, H., Wang, H., Zeng, G., 2014. Co-pelletization of sewage sludge and biomass: The density and hardness of pellet. Bioresource Technology 166, 435–443. https://doi.org/10.1016/j.biortech.2014.05.077

Joshi, S.V., Drzal, L.T., Mohanty, A.K., Arora, S., 2004. Are natural fiber composites environmentally superior to glass fiber reinforced composites? Composites Part A: Applied Science and Manufacturing 35, 371–376. https://doi.org/10.1016/j.compositesa.2003.09.016

Kaliyan, N., Vance Morey, R., 2009. Factors affecting strength and durability of densified biomass products. Biomass and Bioenergy 33, 337–359. https://doi.org/10.1016/j.biombioe.2008.08.005

Karim, M.R.A., Tahir, D., Haq, E.U., Hussain, A., Malik, M.S., 2021. Natural fibres as promising environmental-friendly reinforcements for polymer composites. Polymers and Polymer Composites 29, 277–300. https://doi.org/10.1177/0967391120913723

Karimah, A., Ridho, M.R., Munawar, S.S., Adi, D.S., Ismadi, Damayanti, R., Subiyanto, B., Fatriasari, W., Fudholi, A., 2021. A review on natural fibers for development of eco-friendly bio-composite: characteristics, and utilizations. Journal of Materials Research and Technology 13, 2442–2458. https://doi.org/10.1016/j.jmrt.2021.06.014

Khalid, M., Ali, S., Abdullah, L.C., Ratnam, C.T., Choong, S.Y.T., 2006. EFFECT OF MAPP AS COUPLING AGENT ON THE MECHANICAL PROPERTIES OF PALM FIBER EMPTY FRUIT BUNCH AND CELLULOSE POLYPROPYLENE BIOCOMPOSITES. International Journal of Engineering and Technology 3.

Kumar Sharma, A., Bhandari, R., Sharma, C., Krishna Dhakad, S., Pinca-Bretotean, C., 2022. Polymer matrix composites: A state of art review. Materials Today: Proceedings 57, 2330–2333. https://doi.org/10.1016/j.matpr.2021.12.592

Leão, A.L., Fernandes Teixeira, R.M., Ferrão, P.C., 2008. Production of Reinforced Composites with Natural Fibers for Industrial Applications – Extrusion and Injection WPC. Molecular Crystals and Liquid Crystals 484, 157/[523]-166/[532]. https://doi.org/10.1080/15421400801904393

Li, X., Tabil, L.G., Panigrahi, S., 2007. Chemical Treatments of Natural Fiber for Use in Natural Fiber-Reinforced Composites: A Review. J Polym Environ 15, 25–33. https://doi.org/10.1007/s10924-006-0042-3

Li, X., Xiao, R., Morrell, J.J., Zhou, X., Du, G., 2017a. Improving the performance of hemp hurd/polypropylene composites using pectinase pre-treatments. Industrial Crops and Products 97, 465–468. https://doi.org/10.1016/j.indcrop.2016.12.061

Li, X., Xiao, R., Morrell, J.J., Zhou, X., Du, G., 2017b. Improving the performance of hemp hurd/polypropylene composites using pectinase pre-treatments. Industrial Crops and Products 97, 465–468. https://doi.org/10.1016/j.indcrop.2016.12.061

Li, Y., Liu, H., 2000. High-pressure densiÿcation of wood residues to form an upgraded fuel. Biomass and Bioenergy.

Luo, G., Li, W., Liang, W., Liu, G., Ma, Y., Niu, Y., Li, G., 2017. Coupling effects of glass fiber treatment and matrix modification on the interfacial microstructures and the enhanced mechanical properties of glass fiber/polypropylene composites. Composites Part B: Engineering 111, 190–199. https://doi.org/10.1016/j.compositesb.2016.12.016

Maichin, P., Suwan, T., Jitsangiam, P., Chindaprasirt, P., 2020. Hemp Fiber Reinforced Geopolymer Composites: Effects of NaOH Concentration on Fiber Pre-Treatment Process. KEM 841, 166–170. https://doi.org/10.4028/www.scientific.net/KEM.841.166

Maier, C., Calafut, T., 1998. Polypropylene: the definitive user's guide and databook, PDL handbook series. Plastics Design Library, Norwich, NY.

Manaia, J.P., Manaia, A.T., Rodriges, L., 2019. Industrial Hemp Fibers: An Overview. Fibers 7, 106. https://doi.org/10.3390/fib7120106

Marcovich, N.E., Villar, M.A., 2003. Thermal and mechanical characterization of linear low-density polyethylene/wood flour composites. J. Appl. Polym. Sci. 90, 2775–2784. https://doi.org/10.1002/app.12934

Menyhárd, A., Menczel, J.D., Abraham, T., 2020. Polypropylene fibers, in: Thermal Analysis of Textiles and Fibers. Elsevier, pp. 205–222. https://doi.org/10.1016/B978-0-08-100572-9.00012-4

Mohammed, L., Ansari, M.N.M., Pua, G., Jawaid, M., Islam, M.S., 2015. A Review on Natural Fiber Reinforced Polymer Composite and Its Applications. International Journal of Polymer Science 2015, e243947. https://doi.org/10.1155/2015/243947

Momeni, S., Safder, M., Khondoker, M.A.H., Elias, A.L., 2021. Valorization of Hemp Hurds as Bio-Sourced Additives in PLA-Based Biocomposites. Polymers 13, 3786. https://doi.org/10.3390/polym13213786

Morselli, N., Puglia, M., Pedrazzi, S., Tartarini, P., Allesina, G., 2021. Domestic Heating: Can Hemp-Hurd Derived Pellet Be an Alternative? IJDNE 16, 1–8. https://doi.org/10.18280/ijdne.160101

Mostafa, M.E., Hu, S., Wang, Y., Su, S., Hu, X., Elsayed, S.A., Xiang, J., 2019. The significance of pelletization operating conditions: An analysis of physical and mechanical characteristics as well as energy consumption of biomass pellets. Renewable and Sustainable Energy Reviews 105, 332–348. https://doi.org/10.1016/j.rser.2019.01.053

Murr, L.E., 2015. Handbook of Materials Structures, Properties, Processing and Performance. Springer International Publishing, Cham. https://doi.org/10.1007/978-3-319-01815-7

Mwaikambo, L.Y., Ansell, M.P., 2002. Chemical modification of hemp, sisal, jute, and kapok fibers by alkalization. J. Appl. Polym. Sci. 84, 2222–2234. https://doi.org/10.1002/app.10460

Nam, T.H., Ogihara, S., Tung, N.H., Kobayashi, S., 2011. Effect of alkali treatment on interfacial and mechanical properties of coir fiber reinforced poly(butylene succinate) biodegradable composites. Composites Part B: Engineering 42, 1648–1656. https://doi.org/10.1016/j.compositesb.2011.04.001

Nourbakhsh, A., Kokta, B.V., Ashori, A., Jahan-Latibari, A., 2008. Effect of a Novel Coupling Agent, Polybutadiene Isocyanate, on Mechanical Properties of Wood-Fiber Polypropylene Composites. Journal of Reinforced Plastics and Composites 27, 1679–1687. https://doi.org/10.1177/0731684407087377

Owen, M.M., Ogunleye, C.O., Achukwu, E.O., 2015. MECHANICAL PROPERTIES OF SISAL FIBRE-REINFORCED EPOXY COMPOSITES- EFFECT OF ALKALI CONCENTRATIONS.

P Chinna, R., K S C, C., Y Madhusudan, R., 2011. A_Review_on_Bioadhesive_Buccal_Drug_Delivery_Ssyst.pdf.

Panthapulakkal, S., Sain, M., 2007. Injection-molded short hemp fiber/glass fiber-reinforced polypropylene hybrid composites—Mechanical, water absorption and thermal properties. J. Appl. Polym. Sci. 103, 2432–2441. https://doi.org/10.1002/app.25486

Paredes-Rojas, J.C., Torres San Miguel, C.R., Flores Vela, A.I., Bravo-Díaz, B., De La Cruz Alejo, C., Ramírez, D.P., 2020. Design Proposal of a Prototype for Sawdust Pellet Manufacturing through Simulation. Advances in Materials Science and Engineering 2020, 1–10. https://doi.org/10.1155/2020/9565394

Park, S.-J., Seo, M.-K., 2011. Types of Composites, in: Interface Science and Technology. Elsevier, pp. 501–629. https://doi.org/10.1016/B978-0-12-375049-5.00007-4

Patil, A., Patel, A., Purohit, R., 2017. An overview of Polymeric Materials for Automotive Applications. Materials Today: Proceedings 4, 3807–3815. https://doi.org/10.1016/j.matpr.2017.02.278

Paul, R., Dai, L., 2018. Interfacial aspects of carbon composites. Composite Interfaces 25, 539–605. https://doi.org/10.1080/09276440.2018.1439632

Pavlík, Z., Pavlíková, M., Záleská, M., 2019. Properties of concrete with plastic polypropylene aggregates, in: Use of Recycled Plastics in Eco-Efficient Concrete. Elsevier, pp. 189–213. https://doi.org/10.1016/B978-0-08-102676-2.00009-8

Peacock, A.J., Calhoun, A., 2006. Polymer Chemistry: Properties and Application. Carl Hanser Verlag GmbH & Co. KG, München. https://doi.org/10.3139/9783446433434

Poletto, M., 2017. Assessment of the thermal behavior of lignins from softwood and hardwood species. Maderas. Ciencia y tecnología 19. https://doi.org/10.4067/S0718-221X2017005000006

Pradhan, P., Mahajani, S.M., Arora, A., 2021. Pilot scale production of fuel pellets from waste biomass leaves: Effect of milling size on pelletization process and pellet quality. Fuel 285, 119145. https://doi.org/10.1016/j.fuel.2020.119145

Purohit, V., Orzel, R.A., 1988. Polypropylene: A Literature Review of the Thermal Decomposition Products and Toxicity. Journal of the American College of Toxicology 7, 221–242. https://doi.org/10.3109/10915818809014521

Rahman, N.A., Hassan, A., Yahya, R., Lafia-Araga, R.A., 2013a. Impact properties of glass-fiber/polypropylene composites: The influence of fiber loading, specimen geometry and test temperature. Fibers Polym 14, 1877–1885. https://doi.org/10.1007/s12221-013-1877-6

Rahman, N.A., Hassan, A., Yahya, R., Lafia-Araga, R.A., 2013b. Impact properties of glass-fiber/polypropylene composites: The influence of fiber loading, specimen geometry and test temperature. Fibers Polym 14, 1877–1885. https://doi.org/10.1007/s12221-013-1877-6

Ramesh, M., 2018. Hemp, jute, banana, kenaf, ramie, sisal fibers, in: Handbook of Properties of Textile and Technical Fibres. Elsevier, pp. 301–325. https://doi.org/10.1016/B978-0-08-101272-7.00009-2

Rosa, N., Moura, M.F.S.F., Olhero, S., Simoes, R., Magalhães, F.D., Marques, A.T., Ferreira, J.P.S., Reis, A.R., Carvalho, M., Parente, M., 2022. Bone: An Outstanding Composite Material. Applied Sciences 12, 3381. https://doi.org/10.3390/app12073381

Sajin, J.B., Christu Paul, R., Binoj, J.S., Brailson Mansingh, B., Gerald Arul Selvan, M., Goh, K.L., Rimal Isaac, R.S., Senthil Saravanan, M.S., 2022. Impact of fiber length on mechanical, morphological and thermal analysis of chemical treated jute fiber polymer composites for sustainable applications. Current Research in Green and Sustainable Chemistry 5, 100241. https://doi.org/10.1016/j.crgsc.2021.100241

Sankar, P.H., Reddy, Y.V.M., Reddy, K.H., Kumar, M.A., Ramesh, A., 2014. The Effect of Fiber Length on Tensile Properties of Polyester Resin Composites Reinforced by the Fibers of Sansevieria trifasciata. International Letters of Natural Sciences.

Sarkar, B., Megharaj, M., Xi, Y., Naidu, R., 2011. Structural characterisation of Arquad® 2HT-75 organobentonites: Surface charge characteristics and environmental application. Journal of Hazardous Materials 195, 155–161. https://doi.org/10.1016/j.jhazmat.2011.08.016

Sen, T., Reddy, H.N.J., 2011. Various Industrial Applications of Hemp, Kinaf, Flax and Ramie Natural Fibres. International Journal of Innovation 2.

Soleimani, M., Tabil, L., Panigrahi, S., Opoku, A., 2008. The Effect of Fiber Pretreatment and Compatibilizer on Mechanical and Physical Properties of Flax Fiber-Polypropylene Composites. J Polym Environ 16, 74–82. https://doi.org/10.1007/s10924-008-0102-y

Stelte, W., Holm, J.K., Sanadi, A.R., Barsberg, S., Ahrenfeldt, J., Henriksen, U.B., 2011. A study of bonding and failure mechanisms in fuel pellets from different biomass resources. Biomass and Bioenergy 35, 910–918. https://doi.org/10.1016/j.biombioe.2010.11.003

Stelte, W., Sanadi, A.R., Shang, L., Holm, J.K., Ahrenfeldt, J., Henriksen, U.B., 2012. RECENT DEVELOPMENTS IN BIOMASS PELLETIZATION – A REVIEW.

Stevulova, N., Cigasova, J., Estokova, A., Terpakova, E., Geffert, A., Kacik, F., Singovszka, E., Holub, M., 2014. Properties Characterization of Chemically Modified Hemp Hurds. Materials 7, 8131–8150. https://doi.org/10.3390/ma7128131

Stevulova, N., Kidalova, L., Cigasova, J., Junak, J., Sicakova, A., Terpakova, E., 2013. Lightweight Composites Containing Hemp Hurds. Procedia Engineering 65, 69–74. https://doi.org/10.1016/j.proeng.2013.09.013

Stulpinaite, U., Tilvikiene, V., Zvicevicius, E., 2023. Co-pelletization of Hemp Residues and Agricultural Biomass: Effect on Pellet Quality and Stability. Energies 16, 5900. https://doi.org/10.3390/en16165900

Su, S., Gao, Y., Zhou, X., Xiong, X., Wang, Y., Lyu, L., 2022. Structure of Waste Hemp Stalks and Their Sound Absorbing Properties. Polymers 14, 4844. https://doi.org/10.3390/polym14224844

Sullins, T., Pillay, S., Komus, A., Ning, H., 2017a. Hemp fiber reinforced polypropylene composites: The effects of material treatments. Composites Part B: Engineering 114, 15–22. https://doi.org/10.1016/j.compositesb.2017.02.001

Sullins, T., Pillay, S., Komus, A., Ning, H., 2017b. Hemp fiber reinforced polypropylene composites: The effects of material treatments. Composites Part B: Engineering 114, 15–22. https://doi.org/10.1016/j.compositesb.2017.02.001

Sun, Z., 2018. Progress in the research and applications of natural fiber-reinforced polymer matrix composites. Science and Engineering of Composite Materials 25, 835–846. https://doi.org/10.1515/secm-2016-0072

Svečko, R., Kusić, D., Kek, T., Sarjaš, A., Hančič, A., Grum, J., 2013. Acoustic Emission Detection of Macro-Cracks on Engraving Tool Steel Inserts during the Injection Molding Cycle Using PZT Sensors. Sensors 13, 6365–6379. https://doi.org/10.3390/s130506365

Tabil, L.G., Sokhansanj, S., Tyler, R.T., 1997. Performance of different binders during alfalfa pelleting. CANADIAN AGRICULTURAL ENGINEERING.

Takagi, H., Ichihara, Y., 2004. Effect of Fiber Length on Mechanical Properties of “Green” Composites Using a Starch-Based Resin and Short Bamboo Fibers. JSME Int. J., Ser. A 47, 551–555. https://doi.org/10.1299/jsmea.47.551

Theerarattananoon, K., Xu, F., Wilson, J., Ballard, R., Mckinney, L., Staggenborg, S., Vadlani, P., Pei, Z.J., Wang, D., 2011. Physical properties of pellets made from sorghum stalk, corn stover, wheat straw, and big bluestem. Industrial Crops and Products 33, 325–332. https://doi.org/10.1016/j.indcrop.2010.11.014

Wan Mohamed, W.Z., Baharum, A., Ahmad, I., Abdullah, I., Zakaria, N.E., 2018. Effects of Fiber Size and Fiber Content on Mechanical and Physical Properties of Mengkuang Reinforced Thermoplastic Natural Rubber Composites. BioResources 13, 2945–2959. https://doi.org/10.15376/biores.13.2.2945-2959

Wang, Y., Ural, A., 2019. A finite element study evaluating the influence of mineralization distribution and content on the tensile mechanical response of mineralized collagen fibril networks. Journal of the Mechanical Behavior of Biomedical Materials 100, 103361. https://doi.org/10.1016/j.jmbbm.2019.07.019

Williams, O., Taylor, S., Lester, E., Kingman, S., Giddings, D., Eastwick, C., 2018. Applicability of Mechanical Tests for Biomass Pellet Characterisation for Bioenergy Applications. Materials (Basel) 11, 1329. https://doi.org/10.3390/ma11081329

Xiao, X., Chevali, V.S., Song, P., He, D., Wang, H., 2019. Polylactide/hemp hurd biocomposites as sustainable 3D printing feedstock. Composites Science and Technology 184, 107887. https://doi.org/10.1016/j.compscitech.2019.107887

Yoo, Y., Spencer, M.W., Paul, D.R., 2011. Morphology and mechanical properties of glass fiber reinforced Nylon 6 nanocomposites. Polymer 52, 180–190. https://doi.org/10.1016/j.polymer.2010.10.059

Younis, M., Alnouri, S.Y., Abu Tarboush, B.J., Ahmad, M.N., 2018. Renewable biofuel production from biomass: a review for biomass pelletization, characterization, and thermal conversion techniques. International Journal of Green Energy 15, 837–863. https://doi.org/10.1080/15435075.2018.1529581

Zabava, B.-S., Voicu, G., Dinca, M.-N., Ungureanu, N., Ferdes, M., 2018. Durability of pellets obtained from energy plants: review. Presented at the 17th International Scientific Conference Engineering for Rural Development. https://doi.org/10.22616/ERDev2018.17.N419

Zafari, A., Kianmehr, M.H., 2014. Factors affecting mechanical properties of biomass pellet from compost. Environmental Technology 35, 478–486. https://doi.org/10.1080/09593330.2013.833639

Zhai, Y., Wang, T., Zhu, Y., Peng, C., Wang, B., Li, X., Li, C., Zeng, G., 2018. Production of fuel pellets via hydrothermal carbonization of food waste using molasses as a binder. Waste Management 77, 185–194. https://doi.org/10.1016/j.wasman.2018.05.022

Zhai, Z., Gröschel, C., Drummer, D., 2016. Tensile behavior of quasi-unidirectional glass fiber/polypropylene composites at room and elevated temperatures. Polymer Testing 54, 126–133. https://doi.org/10.1016/j.polymertesting.2016.07.003

Zhang, D., He, M., Qin, S., Yu, J., 2017. Effect of fiber length and dispersion on properties of long glass fiber reinforced thermoplastic composites based on poly(butylene terephthalate). RSC Adv. 7, 15439–15454. https://doi.org/10.1039/C7RA00686A

Zweben, C., 2015. Composite Materials, in: Kutz, M. (Ed.), Mechanical Engineers' Handbook. John Wiley & Sons, Inc., Hoboken, NJ, USA, pp. 1–37. https://doi.org/10.1002/9781118985960.meh110